The Interaction between Vitamin D and Extracellular Calcium on Osteogenic Differentiation

Dongqing Yang

B.Sc, M.Biotechnology

Thesis submitted in fulfilment of the requirements for the degree of

Doctor of Philosophy

October, 2014

The Discipline of Medicine

School of Medicine

Faculty of Health Sciences

The University of Adelaide

South Australia

Australia

TABLE OF CONTENTS

Thesis abstract ..... **I**

Declaration ..... **III**

Acknowledgements ..... **IV**

Publications and Presentations ..... **VI**

Chapter 1 Literature review: The interaction between vitamin D and extracellular calcium in osteogenic differentiation **1**

1.1 Osteoblast biology **2**

1.1.1 Bone formation by osteoblasts *2*

1.1.2 Differentiation of osteoblasts *3*

a) From mesenchymal stem cells to pre-osteoblasts *4*

b) Pre-osteoblasts to immature osteoblasts *6*

c) Mineralisation by mature osteoblasts and the transition to early osteocytes *6*

d) The final stage of osteoblast differentiation: mature osteocytes *9*

1.1.3 Skeletal site differences *12*

1.2 Nutritional factors interacting with osteoblasts **13**

1.2.1 Vitamin D *13*

a) Vitamin D biology *14*

b) The endocrine role of vitamin D *16*

c) Non-classical actions of vitamin D *18*

d) Vitamin D inhibits osteoblast proliferation *21*

e) Vitamin D activity and osteoblast differentiation *22*

1.2.2 Extracellular calcium concentration *23*

1.3 Conclusions and proposal for study **25**

Aim of study *26*

Hypotheses *26*

Approaches *26*

Chapter 2 Materials and Methods **28**

2.1 Materials **28**

2.1.1 Chemicals and reagents *28*

2.1.2 Molecular biology reagents *28*

2.1.3 Animals *28*

2.2 Nucleotide preparations **29**

2.2.1 DNA extraction *29*

2.2.2 RNA extraction *30*

2.2.3 cDNA synthesis *30*

2.2.4 Conventional PCR (polymerase Chain Reaction) *31*

2.2.5 Real-time PCR *32*

2.3 Isolation of osteoblasts **32**

2.3.1 Osteogenic growth media *32*

2.3.2 Osteogenic differentiation media *37*

2.3.3 Isolation of osteoblast-like cells from neonatal mouse calvarial bones *37*

2.3.4 Cryopreservation and thawing of cells *38*

2.4 Histochemical staining **38**

2.4.1 Alizarin Red staining *38*

2.4.2 Von Kossa staining *39*

2.5 Osteoblast proliferation assay **40**

2.6 Osteoblast differentiation and mineralisation assay **40**

Chapter 3 Differential effects of 1,25-dihydroxyvitamin D on mineralisation and differentiation in two different types of osteoblast-like cultures **42**

Abstract **46**

3.1 Introduction **46**

3.2 Materials and methods **47**

3.2.1 Isolation of osteoblasts from juvenile mouse cortical bones *47*

3.2.2 Isolation of osteoblasts from mouse neonatal calvarial bones *47*

3.2.3 Differentiation assays *47*

3.2.4 Statistics *49*

3.3 Results **49**

3.3.1 Characterisation of cells *49*

3.3.2 In vitro mineralisation and response to 1,25D *50*

3.3.3 1,25D effects on gene expression *50*

3.4 Discussion **50**

References **50**

Erratum **51**

Chapter 4 The regulation of osteogenic differentiation of calvaria-derived osteoblasts in response to 1,25D and calcium, and the influence of the level of VDR expression **52**

4.1 Introduction **52**

4.2 Experimental methods **54**

4.3 Results **60**

4.3.1 Vdr/VDR status and 1,25D metabolism in VDRKO, WT and OSVDR cells ... *60*

4.3.2 Comparison of gene expression profiles of WT and VDRKO cells *63*

4.3.3 Comparison of gene expression profiles of WT and OSVDR cells *72*

4.3.4 Expression levels of osteogenic differentiation-related genes under acute and chronic 1,25D treatments at day 24 of WT and OSVDR cell cultures *72*

4.3.5 Effect of chronic 1,25D treatment on in vitro mineral deposition by VDRKO, WT and OSVDR cells under conditions of total extracellular calcium at either 1.8 mM or 2.8 mM *77*

4.4 Discussion **81**

4.5 Conclusion **90**

Chapter 5 Vitamin D metabolites and extracellular calcium promote mineral deposition by a mature osteoblast cell line MLO-A5 91

Abstract 95

5.1 Introduction 96

5.2 Materials and methods 97

5.2.1 Cell culture 97

5.2.2 Proliferation assay 97

5.2.3 Differentiation/mineralisation assay 97

5.2.4 Statistics analyses 98

5.3 Results 99

5.3.1 Vitamin D receptor activity and vitamin D metabolism in MLO-A5 cells 99

5.3.2 Acute Cyp24a1 induction within 72 hours and 1,25D levels from media supernatants of 25D and 1,25D treated cultures 99

5.3.3 Vitamin D inhibition of MLO-A5 proliferation 100

5.3.4 Vitamin D metabolites enhance mineral deposition by MLO-A5 100

5.3.5 Effects of vitamin D metabolites and extracellular calcium on mRNA levels of genes related to osteogenic differentiation and mineral deposition 101

5.4 Discussion 102

Acknowledgements 105

References 106

Chapter 6 Conclusion remarks 122

References 129

Appendix I 151

Appendix II 156

Appendix III 170

Thesis abstract

While the role of vitamin D in the prevention of rickets in children and osteomalacia in adults has been well demonstrated, its benefit in the treatment of osteoporosis is subject to controversy. Clinical trials of vitamin D supplementation to prevent fractures have been conducted with mixed results and some meta-analyses have indicated limited benefit in reducing fracture risk. The most consistent beneficial effects of vitamin D have been obtained when combined with calcium supplements. 1,25-dihydroxyvitamin D acts on the three major types of bone cells (osteoblasts, osteoclasts and osteocytes) to initiate either catabolic or anabolic actions on bone. To elucidating the potential benefits of vitamin D to bone health, this study examined direct actions of vitamin D metabolites on bone cells focussing on stimulation of *in vitro* osteogenic differentiation. Two cell culture models, representing immature and mature stage of osteoblasts, were employed to investigate the role of vitamin D on osteogenic differentiation. The regulation of a variety of gene expressions and modulation of mineral deposition by these cells, were used as key readouts.

In chapter 3, vitamin D was observed to play an inhibitory role on mineral deposition by the immature calvarial bone-derived osteoblast-like cells (Calvarial cells) but did not exert any suppressive effect on the mature osteoblast/early osteocyte cell line, MLO-A5. Thus the actions of vitamin D appear to be dependent on either the stage of cell maturation or their skeletal origin.

The studies using Calvarial cells were expanded in chapter 4 by utilising cells derived from genetically modified mouse lines, including the global vitamin D receptor (VDR) knockout (VDRKO) and the over-expression of VDR in osteocalcin-expressing cells (OSVDR), in comparison to cells derived from wild-type animals. The active hormone form, 1α,25-dihydroxyvitamin D_3 (1,25D), promoted a mature cell phenotype at

physiological levels (around 30 pM) dependent on the level of *Vdr* mRNA. However, in OSVDR cells with high levels of VDR, a pharmacological concentration of 1,25D (1 nM) appeared to stimulate de-differentiation of the osteoblast phenotype by down-regulating the expression of mature osteoblast/osteocyte genes. *Enpp1* and *Tnap* were identified as key genes to modulate mineral deposition in these models.

In chapter 5, the cell line MLO-A5 was again utilised, here for studying the interaction between vitamin D and extracellular calcium on osteoblasts. Both endogenous and exogenous sources of 1,25D, either alone or interacting with extracellular calcium, increased mineral deposition and the expressions of maturation-related genes. Extracellular calcium altered vitamin D metabolism by MLO-A5 cells. Again, key genes associated with mineral deposition were *Enpp1* and *Tnap*.

Data from this study confirm the stimulatory actions of vitamin D on osteogenic differentiation and identified an interaction with extracellular calcium levels. Mineral deposition was found to be dependent on 1,25D modulation of *Enpp1* and *Tnap* expressions. A highly novel finding was that the extracellular calcium concentration modulates the metabolism of vitamin D and the maturation of these cells. These data help to address the controversy on the actions of vitamin D on osteoblast differentiation and mineralisation and improve our understanding of their biology.

Declaration

I certify that this work contains no material which has been accepted for the award of any other degree or diploma in my name in any university or other tertiary institution and, to the best of my knowledge and belief, contains no material previously published or written by another person, except where due reference has been made in the text. In addition, I certify that no part of this work will, in the future, be used in a submission in my name for any other degree or diploma in any university or other tertiary institution without the prior approval of the University of Adelaide and where applicable, any partner institution responsible for the joint award of this degree.

I give consent to this copy of my thesis when deposited in the University Library, being made available for loan and photocopying, subject to the provisions of the Copyright Act 1968.

The author acknowledges that copyright of published works contained within this thesis resides with the copyright holder (s) of those works.

I also give permission for the digital version of my thesis to be made available on the web, via the University's digital research repository, The Library Search and also through web search engines, unless permission has been granted by the University to restrict access for a period of time.

Signature: Date: 04/02/2015

Dongqing Yang

Acknowledgements

Firstly, I would like to thank my supervisors Professor Howard Morris and Associate Professor Gerald Atkins. Back to the time I was looking for a PhD position, it was very lucky that Howard kindly offered me the chance to study in his laboratory and also Gerald agreed to be my co-supervisor to guide me in the cell biology works. During the study period, both Howard and Gerald made available an incredible amount of intelligent, effort and time to discuss my project, inspire my scientific thinking and improve my academic writing skill. Also, only with their continuous encouragement, could I deal with the difficulty and frustration I encountered during scientific research, enabling me to reach the completion of my PhD study.

Secondly, I would like to forward my acknowledgement to Associate Professor Paul Anderson and Dr Andrew Turner in the Musculoskeletal Biology Research Laboratory, the University of South Australia. Without their patience on teaching me and answering my numerous questions, I would never have been able to accomplish my project. I also would like to thank Ms Rebecca Sawyer and Dr Nga Lam in the Musculoskeletal Biology Research Laboratory, the University of South Australia, as well as Dr Asiri Wijenayaka, Miss Renee Ormsby, Dr Masakazu Kogawa, Dr Nobuaki Ito and Dr Matt Prideaux, from Bone Cell Biology Group, the University of Adelaide, for their kindly guidance on the daily bench work from time to time.

I gratefully acknowledge Professor Lynda Bonewald, University of Missouri, Kansas City, MO, USA, for the provision of the MLO-A5 cell line, made available to Associate Professor Gerald Atkins through a pre-existing collaboration. Especially, I would like to give my acknowledgement to Professor Hong Zhou from the ANZAC Research Institute, Concord, NSW, Australia, for accepting me into her laboratory and generously teaching

me the skill of establishing osteoblast-like culture from neonatal mouse skull bone, which was a very important *in vitro* model in my project.

I am giving my most special thankfulness to my wife Jiangqin Wei for her unconditional understanding, forgiveness and encouragement every single day during this period. Without her love and support both physically and mentally, it would have been absolutely impossible for me to finish my study and make this achievement. Last but not least, I also would like to forward my gratefulness to all of our family members in China for their constant encouragement and support for us both.

Publications and Presentations

Yang D, Atkins GJ, Turner AG, Anderson PH, Morris HA. Differential effects of 1,25-dihydroxyvitamin D on mineralisation and differentiation in two different types of osteoblast-like cultures. *Journal of Steroid Biochemistry and Molecular Biology*. 2013;136:166-70.

[With Erratum to "Differential effects of 1,25-dihydroxyvitamin D on mineralisation and differentiation in two different types of osteoblast-like cultures" J. Steroid Biochem. Mol. Biol. 136 (2013) 166–170]

Yang D, Turner A, Anderson PH, Morris HA, Atkins GJ. Vitamin D metabolites and extracellular calcium promote mineral deposition by the mature osteoblast cell line MLO-A5. (Submitted for publication).

Published Abstracts:

Yang D, Atkins GJ, Anderson PH, Welldon KJ, Morris HA (2011) The role of vitamin D in the proliferation and differentiation of osteoblasts in vitro. *Osteoporosis International* 22, Suppl 4, 268.

Yang D, Atkins GJ, Turner A, Anderson P, Morris HA (2012) Differential effects of 1,25-dihydroxyvitmain D on in vitro mineral deposition: interaction between osteoblast stage and culture medium calcium concentration. Presented at the American Society for Bone and Mineral Research (ASBMR) Annual General Meeting, 2012, Minneapolis, MN, USA. *Journal of Bone and Mineral Research* 27, suppl. 1, S175.

Oral Presentations:

Yang D. The role Vitamin D in the proliferation and differentiation of osteoblasts. The 6th (2010) Clare Valley Bone Meeting, Clare, SA, Australia.

Yang D. The role of calcitrol in the differentiation of osteoblasts *in vitro*. The 7th (2012) Clare Valley Bone Meeting, Clare, SA, Australia.

Yang D. Differential effects of 1,25-dihydroxyvitamin D (1,25D) on *in vitro* mineral deposition: Interaction between osteoblast stage of maturation and culture medium calcium concentration, Australian Society for Medical Research (ASMR) Scientific Meeting, 2012, Adelaide, SA, Australia.

Poster Presentations:

Yang D, Atkins GJ, Anderson PH, Welldon KJ, Morris HA. The role of vitamin D in the proliferation and differentiation of osteoblasts. The 20th Australian and New Zealand Bone and Mineral Society (ANZBMS) Annual Scientific Meeting, 2010, Adelaide, Australia.

Yang D, Atkins GJ, Anderson PH, Welldon KJ, Morris HA. The role of vitamin D in the proliferation and differentiation of osteoblasts *in vitro*. The IOF Regionals 2nd Asia-Pacific Osteoporosis and Bone Meeting, 21st ANZBMS Annual Scientific Meeting combined with the Japanese Society of Bone & Mineral Research, 2011, Gold Coast, QLD Australia.

Yang D, Atkins GJ, Turner AG, Anderson PH, Morris HA. The role of calcitriol in the differentiation of osteoblast *in vitro*. The 15th Workshop on Vitamin D, June 20 – 22, 2012, Houston, TX, USA.

Chapter 1: Literature Review

The interaction between vitamin D and extracellular calcium in osteogenic differentiation

This literature review gives a summary of the biological effects of vitamin D and extracellular calcium separately and in combination (their interaction) on osteogenic differentiation, involving the three major bone cell types: osteoblast, osteoclast and osteocyte. These latter two factors have been demonstrated to play multiple important roles in the modulation of gene expression in bone cell types, and hence influence bone homeostasis in various *in vitro* and *in vivo* models. However, the controversy that the role of vitamin D on osteogenic differentiation can either be anabolic or catabolic, has persisted for years, in part due to an insufficient understanding of the molecular and cellular actions of this steroid hormone. Calcium has also been described as a factor that enhances the maturation of osteoblasts, but the effects and mechanism involved is have not been fully elucidated. This literature review briefly updates the current status of the research progress on vitamin D/calcium regulation of bone cell activities in cell culture models and various genetically modified mouse models, and therefore guides the research activities conducted in this PhD project.

Chapter 1: Literature Review

1.1 Osteoblast biology

1.1.1 Bone formation by osteoblasts

There are two different biological processes, by which new bone is formed: intramembranous ossification and endochondral ossification. Intramembranous ossification requires the migration of mesenchymal stem cells (MSCs) to the bone formation sites and their direct differentiation into osteoblasts, but without the formation of intermediate cartilage (1). Intramembranous ossification is usually related to the formation of the 'flat' bone tissues, such as the skull and facial bones, and also in the process of fracture healing. In contrast, endochondral ossification is associated with the formation of axial or appendicular bone tissues in the skeleton, including the long bones and vertebrae. In the process of endochondral tissue formation, MSCs migrate to the appropriate anatomical sites and initially differentiate into chondrocytes to form cartilage tissue. These chondrocytes firstly proliferate to elongate the bone and then undergo hypertrophy, which is the final cell fate of chondrocytes. A large proportion of hypertrophic chondrocytes undergo apoptosis and release collagen type X matrix, which is the environment for osteoprogenitor cells to populate. At the same time, osteoprogenitor cells differentiated from MSCs migrate into the hypertrophic cartilage and produce bone matrix to provide an environment suitable for osteoblast differentiation. These progenitors then undergo osteogenic differentiation to form mineralised bone tissue and replace the intermediate cartilage (2-4).

A third skeletal metabolism event, distinct from intramembranous and endochondral ossification, is bone remodelling. This takes place in the existing bone tissue and occurs continuously to resorb and form bone in the dynamic balance of bone homeostasis. Bone remodelling requires the coordinated activities of the three major bone cell types,

osteoblast-, osteoclast-lineage cells and osteocytes, together with specialised capillaries and cells that form the canopy, which together are termed the basic multicellular unit (BMU) (5-7). On remodelling site, the BMUs adapt to environmental changes, such as mechanical loading, through bone remodelling by modulating the activities of gaining bone by osteoblasts or losing bone by osteoclast resorption accordingly. In the event of bone remodelling, calcium phosphate can be released from bone into the circulation or precipitated from the circulation into the bone matrix. This mechanism of maintaining the calcium homeostasis ensures the optimal function of the endocrine neural systems (8).

In the bone forming activities discussed above, osteoblast differentiation is involved. Hence, there has been much research interest for the comprehensive understanding of the mechanism of osteoblast differentiation and the factors that regulate this process. An intimate knowledge of osteoblast differentiation is important for guiding us to understand the requirements for optimal bone health and to inform us of potential therapies for bone-related disease.

1.1.2 Differentiation of osteoblasts

The term osteoblast derives from ‘osteo’ Greek for ‘bone’ and ‘blast’ Greek for ‘gem’ or ‘embryonic’ such that osteoblast is the term for ‘to make bone’. Under osteogenic regulatory conditions, MSCs are directed to undergo bone cell differentiation. As these cells pass through the various stages from MSCs to cells capable of forming bone tissue, they exhibit phenotypically distinct properties at each of the different stages. Regulation of gene expression varies across the cell differentiation process and dysregulation of this process can give rise to bone-related diseases, such as osteoporosis if bone formation is reduced, or osteopetrosis if bone formation is overly increased.

a) From mesenchymal stem cells to pre-osteoblasts

MSCs are multi-potential cells that can differentiate into different mesenchymal cell types that form a range of specific tissues, including adipocytes to form fat tissue, chondrocytes to form cartilage, myoblasts to form muscle and osteoblasts to form bone. Different potential destinies of MSC differentiation are briefly described in figure 1.1.2A. In early MSC differentiation, cells have the capability to differentiate along different lineages under specific transcriptional signals. The sex-determining gene on the Y chromosome (SRY)-related high-mobility-group box (SOX) family of transcriptional factors (SOX9, SOX5, SOX6) direct chondrogenesis; myogenic differentiation (MyoD) transcriptional factors direct myogenesis; CCAAT/enhancer binding protein (C/EBP) family and peroxisome proliferator-activated receptor gamma (PPARγ) transcriptional factors direct adipogenesis; while the runt-related transcription factor 2 (RUNX2) and wingless integration (Wnt)/β-catenin signalling pathway is critical to ensure that progenitor cells are directed to the osteoblast lineage (9).With the proper activation of β-catenin protein as a result of Wnt signalling, the dephosphorylated β-catenin complex is capable of regulating the transcription factors necessary for the expression of early osteoblast phenotypic-related genes such as bone sialoprotein (BSP) and osteopontin (OPN) (10). Ablation of the β-catenin gene (*Ctnnb*) in a genetically-modified mouse model demonstrated decreased trabecular bone volume as a result of MSCs being switched from the osteoblast to the adipogenic pathway, with concomitant increased fat tissue formation (11). RUNX2, also known as core-binding factor subunit alpha-1 (CBFA1), is a master transcription factor that regulates Wnt/β-catenin signalling and therefore directs progenitor cells to the pre-osteoblast pathway (12). Ablation of RUNX2 markedly compromises bone formation because of the inability to generate osteoblasts in skeletal tissue under this condition (13).

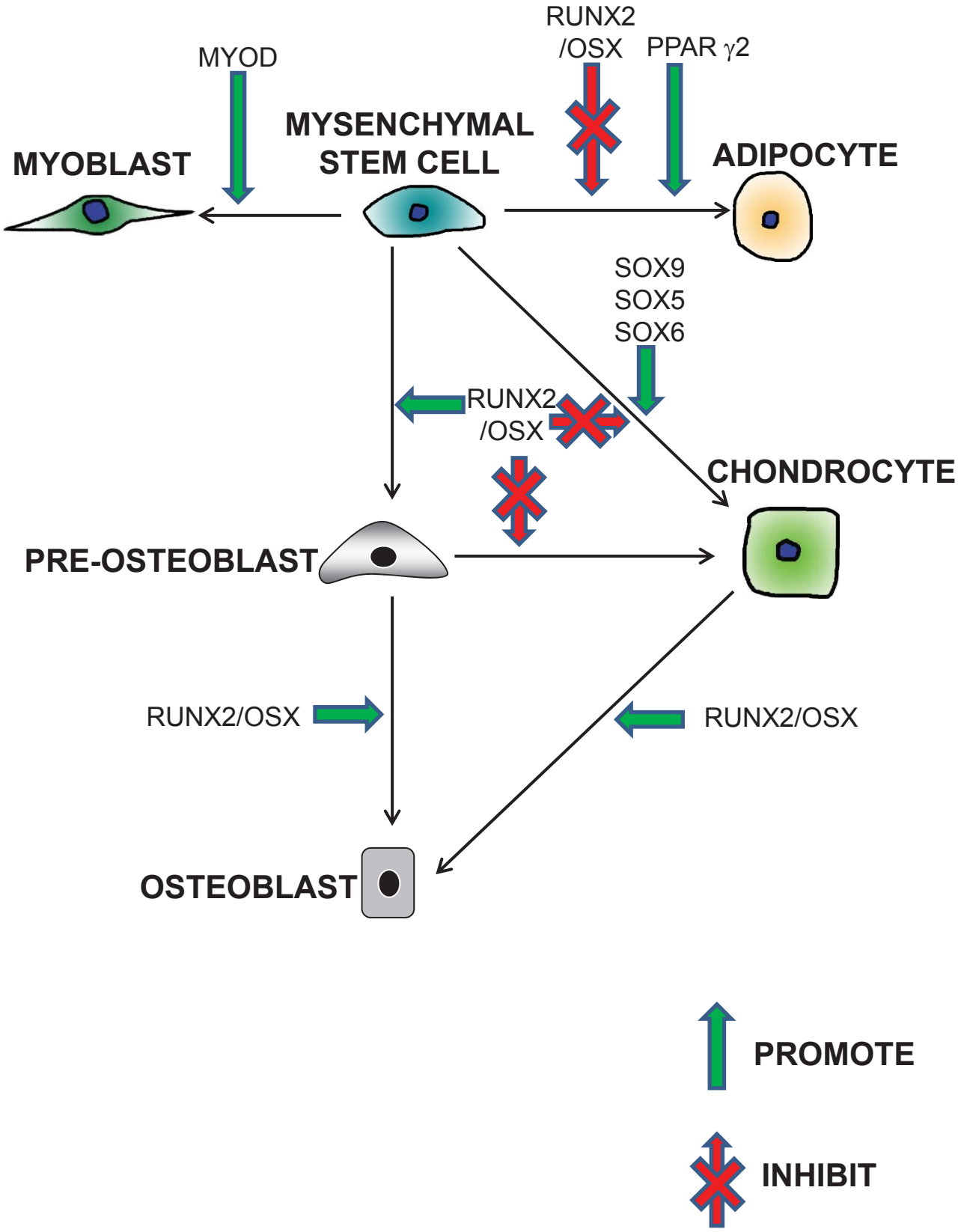

Figure 1.1.2 A **Different destinies of MSC differentiation**

b) Pre-osteoblasts to immature osteoblasts

At the beginning of the bone formation process, pre-osteoblasts transfer to the modelling surface and proliferate (14). At this stage, bone extracellular matrix is starting to be synthesised. The bone extracellular matrix is composed of 90% collagenous proteins and 10% other bone specific products such as BSP, OPN, bone morphogenetic proteins 2 and 7 (BMP-2, BMP-7) and dentin matrix protein 1 (DMP1). The extracellular matrix is not only important as a substrate for mineralisation, but is also essential for directing pre-osteoblasts to adhere to the specific site where modelling is required and is suitable for their further differentiation into osteoblasts. However the osteoblast pathway is not the only differentiation fate for pre-osteoblasts. At this point, if the expression of either SOX9, SOX5 or SOX6 is stimulated, pre-osteoblasts are driven to become chondroblasts and then chondrocytes, to form cartilage tissue, which is the connective tissue at various anatomical sites but particularly at bone joints. A high level of RUNX2 is essential to suppress the expression of SOX family transcription factors and ensure the differentiation along the osteoblast pathway; in conjunction with another secondary master transcriptional factor, osterix (OSX/SP7). OSX is under the positive control of RUNX2 in pre-osteoblasts and it plays the role of regulating bone proteins and the appropriate development of the osteoblast phenotype (15). However, the interrelationship between RUNX2 and OSX is still poorly understood. A mouse *Osx* gene knockout study has confirmed that with normal expression of RUNX2 but ablation of OSX, the normal formation of chondrocyte and bone osteoid occurs, but bone mineralisation is compromised because of the failure of normal osteoblast differentiation and maturation (16).

c) Mineralisation by mature osteoblasts and the transition to early osteocytes

The processes of differentiation and mineralisation by osteoblast and the transition of osteoblast to osteocyte are depicted in figure 1.1.2C. At the beginning of the

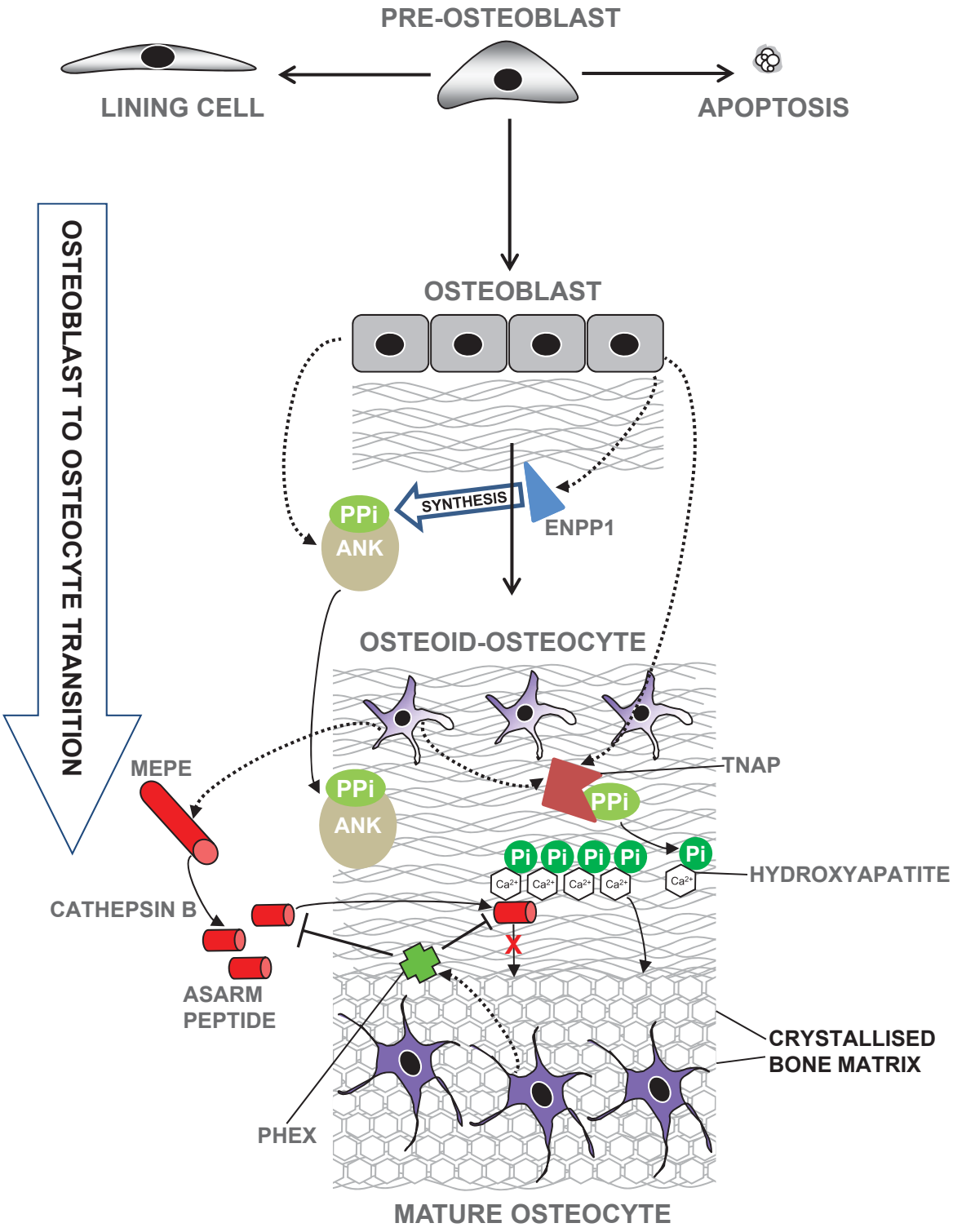

Figure 1.1.2 C **Osteoblast differentiation and mineralisation**

mineralisation process, immature osteoblasts begin synthesising organic bone extracellular matrix, termed osteoid. Osteoid provides the growth environment for cells to proliferate and develop their osteoblastic phenotype. Furthermore, the orientation and structure of mineral deposition are precisely directed by both the cells embedded in osteoid and the extracellular matrix itself (17). As osteoblasts mature, one of the important phenotypic properties is the high level expression of the bone/liver/kidney, or tissue non-specific, isoform of alkaline phosphatase (ALPL/TNAP), which is an essential enzyme for promotion of the deposition of calcium phosphate. Inorganic pyrophosphate (PPi), generated by the enzyme ecto-nucleotide pyrophosphatase/phosphodiesterase-1 (ENPP1) and transported by ankloysis protein (ANK), is a powerful and ubiquitous inhibitor of mineralisation. The presentation of sufficient level of PPi ensures the normal morphology of those soft tissues where mineralisation is not supposed to be deposited. However, in bone tissues, where ENPP1 and TNAP activities co-exist, TNAP degrades PPi to inorganic phosphate (Pi). Therefore the ratio of PPi/Pi is reduced to enable the precise volume of the calcium and phosphate mass being deposited to the bone formation sites to form the hydroxyapatite-like bone mineral. The regulation of Pi homeostasis is a vital function performed by the actions of osteoblasts and osteocytes. The mineralisation of type I collagen begins in cell-associated vesicles termed calcospherulites. In this step, if the enzyme activity of TNAP is absent or low, PPi will be transferred into the intracellular compartment and cell-mediated mineralisation is blocked in response to PPi accumulation (18-20). The activity balance between inhibitors ENPP1/ANK and the mineralisation promoter TNAP ensures that mineral is not deposited in the type I collagen present throughout the soft tissues and occurs only in the bone mineralising sites where bone formation is required (21).

As mineralisation proceeds, nearly 70% of osteoblasts undergo apoptosis and only 30% remain viable and embedded in the mineralising osteoid, and at this stage are termed

osteoid-, immature- or pre-osteocytes (22). The mechanism of how individual osteoblasts are selected to survive or apoptose is not yet clear. Matrix mineralisation promotes the expression of a transmembrane glycoprotein, E11, otherwise known as podoplanin, by mature osteoblasts or pre-osteocytes (23). E11 has been described as the first known marker of the early osteocyte and plays a role in transition to the osteocytic phenotype, of which the development of numerous, elongated cell processes is a prominent feature (24). When osteoblast differentiation proceeds to the early osteocyte stage, osteocytes produce MEPE (matrix extracellular phosphoglycoprotein) and PHEX (phosphate regulating endopeptidase homolog, X-linked) to ensure to regulate the mineralisation process. MEPE is a small peptide that contains a so-called acidic, serine-, and aspartic acid-rich MEPE-associated (ASARM) motif. The MEPE-ASARM peptide was previously shown to be a potent mineralisation inhibitor by the binding to nascent mineral crystals and inhibiting further mineral deposition (25-27). MEPE-ASARM peptide has been shown to be cleaved by the osteocyte produced enzyme, PHEX: MEPE-ASRAM peptide mediated mineralisation inhibition was shown to be rescued by adding PHEX enzyme to *in vitro* osteoblast cultures (28). The ratio of MEPE/PHEX expression has been postulated to regulate correct bone mineralisation (29). In a recent study, our group reported that the *MEPE*/*PHEX* ratio at the mRNA level appeared to explain the mineralisation response of osteocyte-like cells to extracellular calcium (30).

d) The final stage of osteoblast differentiation: mature osteocytes

Following the embedding of mature osteoblasts and the differentiation of a proportion of cells into the pre-osteocyte stage, further differentiation into mature osteocytes occurs. These cells change their morphology and phenotype markedly with the development of numerous, long dendritic cell processes that interconnect for communication between each other and with other cell types, such as surface osteoblasts/lining cells, with shrinkage of the cytoplasm resulting in a dramatic increase in the cell surface

area/cytoplasm ratio (31,32). The cellular composition of bone tissue is approximately 90% osteocytes and the life span of these mineral-embedded cells can be more than 10 years, up to a lifetime, in humans. One important marker expressed by osteocytes as they mature is dentin matrix protein 1 (DMP1). In skeletal development, DMP1 is expressed by osteoblasts during an embryonic stage of development as evidenced by the immunostaining of DMP1 protein in embryonic tissues. Furthermore, DMP1 is most abundant in osteocytes and is especially condensed in the cell processes of osteocytes in postnatal animals (33). The *Dmp1*-null mouse model demonstrated normal embryonic growth, suggesting that there may be redundancy with other genes able to compensate for DMP1 function in the developing skeleton (34). However, pups with *Dmp1* ablated, showed strong postnatal abnormalities including delay and defects in mineralisation, enlargement of the growth plate and failure of cortical bone formation (35). Furthermore, osteocytes in *Dmp1*-null mice display an immature phenotype suggesting that DMP1 is essential for osteocyte maturation (35). *In vitro* studies of DMP1 function have proven its promotional role for the formation of bone mineral (36). There is also an interaction between DMP1 and the cell-surface receptor, CD44, which activates osteogenesis in the bone modelling/remodelling loop (37). Hence, DMP1 is essential for the development of the fully functional skeleton in terms of promoting mineralisation and the control of the proper growth of bone tissues.

One specialist activity of osteocytes is their ability to sense the mechanical loading experienced by the skeleton and regulate bone mineral homeostasis to adapt to such environmental changes. For performing these functions, osteocytes actively communicate with their extracellular environment including circulating fluid, extracellular matrix and other bone cell types such as osteoblasts and osteoclasts. On the osteocyte plasma membrane, six molecules of connexin 43 (CX43/GJA1) (38) form a structure termed a connexon or hemichannel, and this allows signalling molecules of small molecular mass

(less than ~1.3 kDa) to be secreted from the cell. The conjunction of two hemichannels from separate cells allows intercellular communication between osteocytes; this type of paired connexon/hemichannel complex is termed a gap junction (39). Osteocytes also communicate with osteoblasts and osteoclasts through GJA1 composed gap-junctions, which allow the intercellular transportation of small signalling molecules (up to 1.3 kDa), such as amino acids, cAMP, nitric oxide (NO) and prostaglandin E2 (PGE_2) (40). Other than the gap junction, the unpaired hemichannel on the osteocyte cell surface has also been demonstrated to play important roles in bone regulation, particularly in responding to fluid flow shear, the changes in calcium concentration, pH modulation and membrane potential (39). In the response to mechanical loading, physical stimuli are translated into chemical or electrical signals. For example, PGE_2 is secreted by osteocytes through hemichannels when sensing skeletal loading and then transported to neighbouring osteocytes and other bone cell types by passing through the gap-junction network (41). Previous data showed that the long term administration of PGE_2 *in vivo* induced bone loss because of the increased osteoclast activity; however, intermittent PGE_2 treatment enhanced osteoblast activity and hence bone formation (42). In another study (43), osteocyte-like MLO-Y4 cells were seeded at low density in culture to limit the physical interactions between cells *via* gap junctions, to test the unopposed hemichannel function. In that study, after the knockdown of *Gja1* using antisense oligodeoxynucleotide, the release of PGE_2 was found to be significantly reduced compared to the untreated control culture. This study indicated the importance of the unpaired hemichannel in transmitting cell signals, implying the existence of communication between osteocytes and their extracellular environment. A recent review (44) summarised the interactions between osteocyte plasma membrane potential and extracellular calcium levels with osteocytes configured in either an isolated or networked manner, indicating the important role of the two distinct hemichannel based communication mechanisms.

An important factor secreted by osteocytes to regulate the activities of both osteoblasts and osteoclasts to maintain bone homeostasis is sclerostin. Mature osteocytes produce a high level of the sclerostin protein through the expression of the *SOST/Sost* gene. Since sclerostin has a molecular mass between 28-30 kDa, this molecule is unlikely to be transported though gap junction. Sclerostin is suggested to be secreted by osteocytes and then transported to other osteocytes, or osteobalsts and osteoclasts by extracellular fluid (45). Sclerostin inhibits bone formation by inhibiting the Wnt/β-catenin signalling pathway to reduce osteoblast activities (27,46) and it has also been suggested to be a pro-catabolic factor by activating osteoclastogenesis through up-regulating the expression of the osteoclast activator, receptor activator of nuclear factor kappa-B ligand (RANKL) (47). More recently, our group demonstrated that sclerostin induced the production of catabolic mediators in osteocytes and promoted osteocyte-mediated release of calcium in a manner consistent with osteocytic osteolysis (48).

1.1.3 Skeletal site differences

As discussed above, the skeleton is comprised of a variety of bone structures and bone formation varies between these anatomical sites. Although osteoblasts within these sites are all differentiated from mesenchymal progenitor cells, osteoblasts demonstrate different cell phenotypes not only related to the differentiation stage, but also to the skeletal site from which they originated. Cell culture studies have shown that human bone cells derived from mandibular bone exhibit decreased osteoblastic activities compared to cells derived from iliac crest bone as evidenced by lower production of TNAP, osteocalcin (OCN/bone γ-carboxylate (Gla) protein (BGLAP) and a smaller response to mitogenic stimulation in the mandibular bone cell group (49). A more recent study compared the properties of trabecular bone from human iliac crest and lumbar spine, which are different skeletal sites experiencing low and high levels of mechanical loading, respectively. The authors reported that the osteoblast gene expression of *COL1A*, *RUNX2*

and *BMP2*, and osteocyte-specific genes including *MEPE*, *SOST*, *DMP1* and *FGF23*, were all higher in lumbar spine than iliac crest (50). Additionally, *VDR* mRNA expression was found to be 5-fold higher in the skull than in long bones of limbs, which could be one of the reasons that bone from different skeletal sites responds differentially to vitamin D (51). Such evidence suggests that different bone environments may contribute to differential bone cell phenotypes amongst osteoblasts, however it is as yet unclear how such phenotypic differences could be related to bone physiology or health.

1.2 Nutritional factors interacting with osteoblasts

1.2.1 Vitamin D

Vitamin D is critical for human health because of its important endocrine actions to regulate plasma calcium and phosphate homeostasis (52). Previously, it was reported that the deficiency of vitamin D is associated with higher risk of hip fracture in the elderly (53) resulted from decreased bone mineral density (54). Vitamin D-related clinical studies suggested also that the risk of non-vertebral fracture in the elderly was reduced by the daily supplementation of vitamin D (55,56).

At the cellular level, numerous studies have also demonstrated that vitamin D exerts a wide range of activities in various tissues including bone. Vitamin D can modulate bone cell differentiation by regulating gene expression during bone modelling and remodelling as well as directly regulate bone cell gene expression (52). In turn, bone cells, including osteoblasts and osteoclasts, further regulate this process through the variation in expression of vitamin D metabolising enzymes at various stages of their differentiation (57) including synthesis or catabolism of the active form of vitamin D, 1α,25-dihydroxyvitamin D (1,25D). However, the precise mechanisms, by which vitamin D regulates osteoblast differentiation are yet to be fully elucidated.

a) Vitamin D biology

The chemical structures in each step of vitamin D_3 metabolism are shown in figure 1.2.1A. The biosynthesis of vitamin D_3, the form of vitamin D synthesised *in vivo* in animals, occurs in keratinocytes and dermal fibroblasts following exposure to Ultraviolet B (UVB, λ 280-320nm) radiation present in sunlight; vitamin D_3 is synthesised from 7-dehydrocholesterol within the plasma membranes of these cells. With exposure to sunlight, 7-dehydrocholesterol absorbs the energy from UVB causing a carbon ring rearrangement to form pre-vitamin D_3. Pre-vitamin D_3 is then transferred across the membrane and undergoes a further rearrangement into vitamin D_3, which is thermodynamically stable (58). Besides the production in keratinocytes, the other important source of vitamin D is intake from foods, such as fatty fish and vitamin D supplements. This source of vitamin D is especially important for aged people whose synthesis of vitamin D in the skin is not as efficient as that in younger people (59).

The metabolism of vitamin D_3 involves the initial hydroxylation on carbon atom 25 by the liver, giving rise to 25-hydroxyvitamin D_3 (25D), which is the most abundant metabolite of vitamin D_3 in the circulation (59,60). The bioactive form of vitamin D_3, 1,25D, is formed following hydroxylation in position 1 of 25D. This reaction is catalysed by the cytochrome P450 enzyme, 25-hydroxyvitamin D-1-alpha-hydroxylase, encoded by the gene *CYP27B1* (60). 1,25D catabolism first involves C24-hydroxylation by the 25-hydroxyvitamin D 24-hydroxylase (CYP24A1) to form 1α,24,25-trihydroxyvitamin D_3, which is then modified through a series of further intermediates to calcitroic acid by the same enzyme (60,61).

1,25D regulates gene expression through the binding of nuclear vitamin D receptor (VDR). The 1,25D/VDR complex further interacts with specific DNA motifs termed vitamin D response elements (VDREs) located either upstream or downstream of the

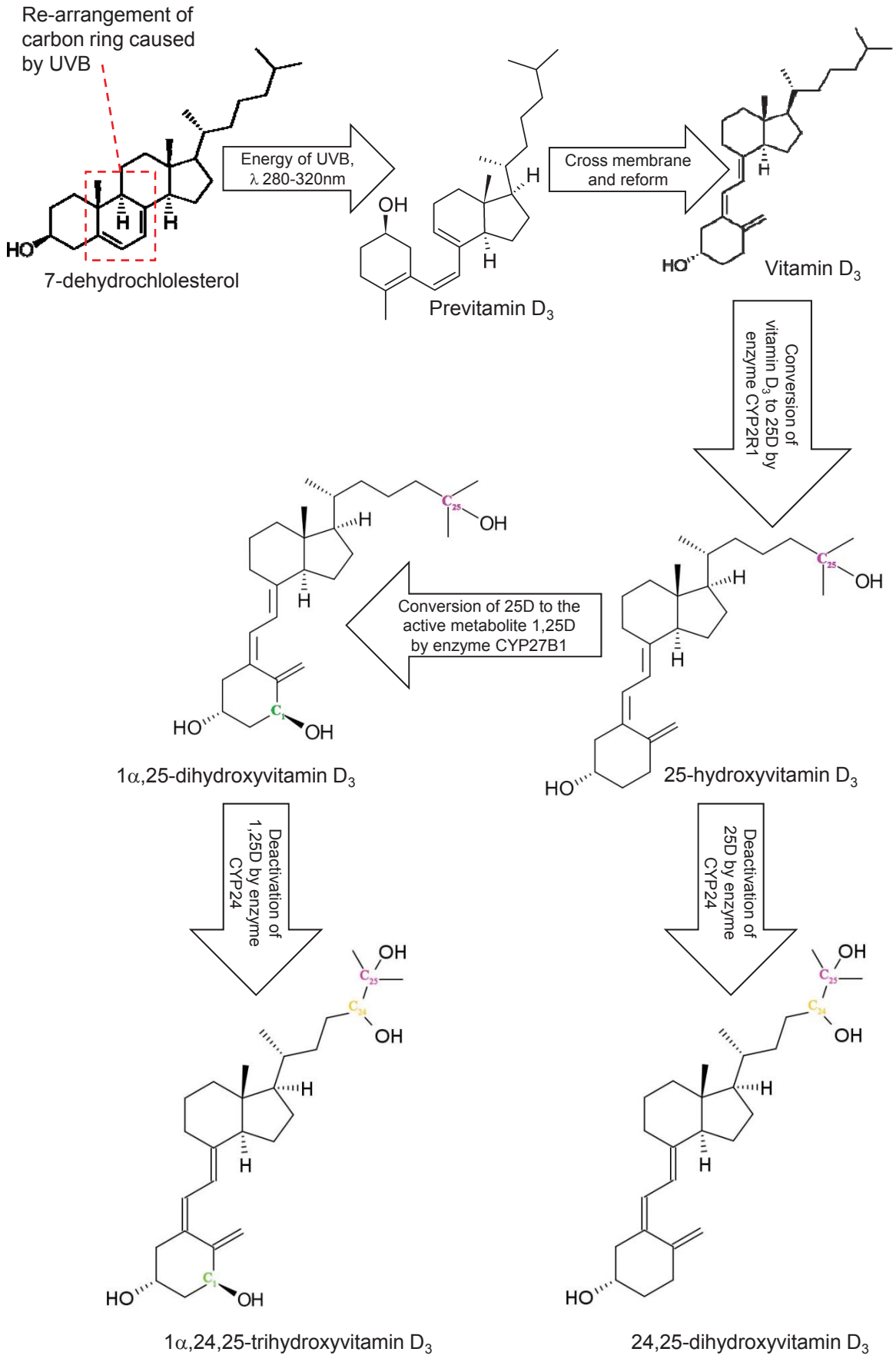

Figure 1.2.1 A **Vitamin D_3 metabolism**

C_{25} and C_1 indicate the activation hydroxylation of vitamin D_3;

C_{24} indicates the inactivation hydroxylation of vitamin D_3.

promoter regions of vitamin D responsive gene and exerts enhancing or inhibitory effects on the transcription of the target gene (62,63). Besides genomic regulation, 1,25D is also thought to exert non-genomic effects on cells through the binding with VDR in plasma membrane in a rapid responsive manner. This rapid response to 1,25D is thought to mainly influence calcium channels within the plasma membrane (64) and suppress mitogen-activated protein kinase (MAPK) pathways to modulate cell proliferation (65).

b) The endocrine role of vitamin D

Under healthy physiological conditions, the production from kidney is considered to be the only source of circulating 1,25D. In the well-studied classical vitamin D endocrine system, calcium and phosphate homeostasis is maintained by the endocrine activities of circulating 1,25D. This complex interaction primarily involves the coordination of actions of vitamin D and other calciotropic hormones on intestine, kidney, parathyroid glands and bone (66). In the intestine, 1,25D is the principal factor controlling calcium and phosphate absorption. The interaction of 1,25D with intestinal VDR directly induces the expression of calcium binding proteins such as Calbindin 9K, which is the calcium transcellular transport agent in the intestine; this captures calcium ions (Ca^{2+}) by physically binding them and then transfers them through the enterocyte cytoplasm. At the same time, it acts as a cytosolic buffer to protect the intestinal cells from the toxicity of the increasing calcium level (67,68). In the kidney, the mechanism of calcium reabsorption is similar to the 1,25D/VDR mediated process in the intestine, except that the calcium transport protein involved is Calbindin 28K, whose expression is also up-regulated by 1,25D (69).

Circulating 1,25D plays a role in regulating renal CYP27B1 and CYP24A1 activity in a negative feedback loop. Within the renal tubule epithelium, 1,25D inhibits *CYP27B1* transcription by a VDR-mediated mechanism through a previously identified vitamin D

interacting repressor (VDIR) in the human *CYP27B1* gene promoter (70). Furthermore, 1,25D dramatically induces the expression of CYP24A1 through multiple and powerful positive VDREs which have been characterised in the *CYP24A1* gene promoters in different species including rat, mouse and human (71-73). Through these negative feedback responses on both *CYP27B1* and *CYP24A1* gene expression, the production and inactivation of 1,25D are coordinated to regulate circulating 1,25D levels and avoid the toxicity of high levels of 1,25D (74,75).

In the endocrine system, circulating 1,25D levels are increased by the action of parathyroid hormone (PTH) on the proximal tubular renal cells under the condition of hypocalcaemia. PTH is the key hormone that centrally regulates the extracellular calcium level. In the parathyroid gland, the calcium sensing receptor (CaR) detects the calcium concentration in extracellular fluid (ECF). When the calcium level decreases, PTH is secreted and acts at the kidney to stimulate renal *CYP27B1* expression by enhancing its promoter activity through the cyclic AMP (cAMP) pathway (76). Correspondingly, 1,25D production is increased because of the increased levels of the CYP27B1 enzyme, following which 1,25D acts to normalise blood calcium levels. At the same time, 1,25D has a negative feedback response in the parathyroid gland by inhibiting the PTH synthesis through acting on the negative VDRE in the *PTH* gene promoter (77).

1,25D is delivered to target tissues *via* the circulation to exert its endocrine actions. 1,25D acts on osteoblasts to directly up-regulate the expression of RANKL through a VDR mediated mechanism (78), apparently more so in immature osteoblasts (79). It should be noted here that this information is based on an early study by our group (79) that examined the 1,25D response in a human bone-derived population of primary cells, termed NHBC, and the expression by these cells of the stromal marker, STRO-1 (80). Our recently acquired knowledge of NHBC implies that they mostly derive from de-differentiated

osteocytes and actually retain properties of pre-osteocytes, such as high levels of the marker E11 (Dr. Gerald Atkins, University of Adelaide, unpublished data). Nevertheless, these cells have been demonstrated to have mesenchymal progenitor-like properties (81) but they may not be representative of a true bone marrow derived mesenchymal stem cell, from which the most immature osteoblast arises. Thus the term 'immature osteoblast' in this context should be considered in terms of the underlying plasticity of the osteoblast/osteocyte lineage. However, at this 'immature stage' of osteoblast differentiation, the factor responsible for suppression of the formation of osteoclasts, osteoprotegerin (OPG), is unaffected by 1,25D (79). Hence, in response to the elevated level of 1,25D, the decrease in the OPG/RANKL ratio activates osteoclast formation and maturation by RANKL, arising from osteoblasts, binding to the receptor activator of nuclear factor kappa-B (RANK) on the surface of immature osteoclasts (82). This mechanism would seem to be particularly important when calcium intake is low and the blood calcium level needs to be restored to the normal level. At this point, PTH is also secreted to stimulate the synthesis of 1,25D in the kidney, further activating osteoclastogenesis and enhancing bone resorption (52).

c) Non-classical actions of vitamin D

Although vitamin D has been defined as an important factor associated with the maintenance of bone mineral density and reducing the risk of non-vertebral fractures particularly in the elderly, the actual circulating vitamin D metabolite responsible for these effects appears to be 25D and not the blood level of 1,25D (57). Results of studies in 30 week-old rats found that with circulating levels of 25D between 20-115 nM, the trabecular bone volume was positively related to circulating 25D concentration; but there was no relationship between trabecular bone volume and either circulating 1,25D or PTH (83). 25D has been demonstrated to directly activate the VDR only at the concentrations of 500 nM or above (84). Such evidence suggests that the circulating 25D is essential for

regulating bone remodelling by firstly being converted to 1,25D *in situ* to work through the VDR ligand system. This concept links to the hypothesis that bone cells play a key role in utilising and metabolising circulating 25D to synthesise 1,25D within bone tissue *in situ*, regulating the bone remodelling process, which may include mineralisation.

There are considerable data confirming that the three major bone cell types, osteoblasts, osteocytes and also osteoclasts, have the capability of catalysing the conversion of 25D to 1,25D by the expression of CYP27B1 (85-97). The locally synthesised 1,25D was claimed to interact with cells through autocrine (when 1,25D works within the cell that generates the hormone) or paracrine (when 1,25D is released to the surrounding cells that produces the hormone) activities (98). 25D has been shown to inhibit proliferation and promote differentiation of bone marrow stromal cells (92) and a human osteosarcoma cell line (85) through the conversion of 25D to 1,25D by CYP27B1. The ability of bone cells to locally synthesise 1,25D and regulate cell differentiation suggests that vitamin D activities within osteoblasts and osteoclasts could have intrinsic, direct effects, independent of levels of exogenous 1,25D. A recent study suggests that a sufficient level of 25D plays an important role to maintain normal osteoblast activity in chronic kidney disease patient even when renal 1,25D synthesis is severely compromised (99). The same group also claimed that 25D treatment restored the osteogenic potential of human MSCs isolated from the elderly where osteogenic activities generally decline with aging. This restoration of osteogenic activity also operates through the local conversion of 25D to 1,25D by MSCs (100). A large body of evidence indicates that the local production of 1,25D by osteoblasts could be essential in specific circumstance when circulating 1,25D is insufficient. However, the exact physiological conditions and mechanisms, by which the 1,25D/VDR system regulates the differentiation and maturation of osteoblasts in an autocrine/paracrine manner remains to be fully elucidated (101).

Studies on the global *Vdr* gene knockout (VDRKO) mouse as a model of ablation of the 1,25D activities through the VDR ligand system have supported the view that vitamin D activity within bone cells or bone tissues is important. In VDRKO mice, the syndromes of hypocalcaemia and hyperparathyroidism can be rescued and plasma calcium levels normalised by feeding a 'rescue diet' containing 2% calcium, 1.25% phosphorus, 20% lactose, and 2.2 units/g vitamin D (102).The VDRKO study by Panda and colleagues on older mice at 4-months of age, demonstrated that although the femur length of these mice was restored to that of wild-type mice by feeding the 'rescue diet', the mutant mice still suffered significant loss of tibial trabecular bone volume. Moreover, bone marrow cells from those 4-month old wild-type and mutant mice demonstrated in culture that the number of mineral colony forming nodules by cells from mutant mice was markedly reduced compared to that from wild-type osteoblasts (103). In that study, exogenous 1,25D was unable to restore the bone loss in mutant animals. To summarise, their data suggest that VDR activity is important for normal osteoblastogenesis and also for the maintenance of bone formation. However, in the global *Vdr* knockout model, it was unclear whether the globally-deleted VDR activity responsible for the bone loss was in the bone organ or in other, non-osseous organs. These authors finally suggested that a tissue-specific knockout model would be preferable in order to uncover the possible autocrine/paracrine role of vitamin D in the bone formation process (103).

Vitamin D activities in bone cells have also been demonstrated to regulate bone cell biology using other animal models. A transgenic mouse model that over-expresses the human *VDR* gene specifically in osteocalcin-expressing cells (OSVDR), which are considered to be mature osteoblasts, demonstrated that with increased VDR activity in osteoblasts, transgenic pups showed increased tibial bone volume and bone strength, by a mechanism of increased bone formation and decreased bone resorption (104). A second transgenic mouse model, in which the human *CYP27B1* gene is over-expressed in

osteocalcin-expressing cells (OSC) has been developed by Drs. Andrew Turner, Paul Anderson and Howard Morris in SA Pathology and the University of South Australia, Adelaide, Australia. The mature osteoblasts in this model are expected to have an increased capacity to convert 25D to the active form 1,25D. OSC mice also feature increased bone volume in tibia and vertebrae (105). However, the detailed mechanisms, by which these bone phenotypes arise in these two transgenic models are still not fully understood.

Thus, there is a considerable amount of data to indicate that besides the traditional endocrine effect, 1,25D also plays autocrine/paracrine role in the skeletal system and that the autocrine/paracrine role of vitamin D is important for the regulation of bone cell proliferation and differentiation (106). Further research into the autocrine/paracrine action of vitamin D in bone cells is, however, required to characterise its role in bone remodelling and requirements for an adequate vitamin D status necessary to maintain bone health.

d) Vitamin D inhibits osteoblast proliferation

Following the initiation of bone remodelling by osteoclasts, osteoblasts migrate to the bone remodelling surface and pass through a proliferation phase, as outlined previously (see Section 1.2). 1,25D has been demonstrated to exert an anti-proliferative effect on osteoblasts derived from foetal rat calvaria (107). Subsequently, a study using a human osteosarcoma cell line showed that 1,25D inhibited this proliferative activity by suppressing the mitogen activated protein kinase (MAPK) pathway via VDR signalling (65). In a breast cancer cell line derived by induction of a tumour in the mammary gland from VDRKO mice, it was confirmed that those cells did not respond to 1,25D in terms of an effect on cell growth (108). A later study, however, claimed that in the human breast cancer cell line, MCF7, the suppressive effect of 1,25D on proliferation was still active

after the significant knockdown of *VDR* expression using short-interfering RNA (siRNA) technology (109). Evidence in this area leads to the conclusion that 1,25D plays a role to arrest growth of cells, including osteoblasts, acting *via* the VDR; however, how 1,25D inhibits proliferation independent from VDR, is yet to be determined.

e) Vitamin D activity and osteoblast differentiation

Recently, new functions of 1,25D in the skeletal system have been uncovered. It has been suggested that the vitamin D hormone modulates the expression of a very large number of genes *in vivo* (possibly 10% of the genome) including genes involved in osteoblast differentiation (110). As outlined above, 1,25D accelerates and enhances the process of osteogenic differentiation. 1,25D treated human bone marrow-derived MSCs demonstrate enhanced osteogenic activities as indicated by expressing higher RUNX2 transcriptional activity and higher levels of TNAP and BSP (92). This activity of vitamin D on osteoblasts has been confirmed by studies indicating that 1,25D enhances osteoblast differentiation with up-regulation of mineralisation-related genes *TNAP* and *OCN/BGLAP* (111) and increasing the production of bone extracellular matrix vesicles (112). However, vitamin D has also been suggested to exert an inhibitory effect on osteoblasts *in vitro* and *in vivo*. One study showed that in avian osteoblast cultures, 1,25D inhibited the production of *Col1a1*, *Opn*, *Bglap*, in a dose-responsive manner (113). Another *in vitro* study, using the mouse osteoblastic cell line MC3T3-E1, showed that with continuous exposure to 1,25D, mineral deposition was dramatically inhibited and this was associated with a decrease in *Tnap* expression (114).

These contrasting data suggest that 1,25D is capable of playing both a promotional or inhibitory role in osteoblast activity. Notably, the studies discussed above showing a positive effect of 1,25D on osteogenesis utilised MSCs or pre-osteoblasts in their experiments; however, other reports demonstrating negative effects of 1,25D, utilised

immature osteoblasts or osteoblastic cell line experimental models. Thus, there is the possibility that 1,25D can exert different effects depending on the stage of osteoblast differentiation. However, the detailed mechanisms, by which 1,25D interacts with osteoblasts at any of their various stages is not fully understood.

A further complexity may be the skeletal site origin of osteoblasts, which may also influence the effects 1,25D on osteoblasts. For example, when osteoblasts derived from human trabecular bone from the proximal femur or tibia were cultured and treated with 1,25D, the expression of OCN in cells from the tibia was double the level compared to the expression in cells derived from the hip (115). Later, the same group showed that not only was the OCN response to 1,25D treatment related to the anatomical origin of the cells, but the level of VDR expression was also different, such that cells from the tibia expressed a higher level of VDR compared cells from the femur (116). These data suggest that vitamin D responsiveness may differ from one anatomical site compared to another. However, this needs to be confirmed by further studies. Also, the mechanisms by which 1,25D may act differently in osteoblasts depending on their stage of maturation or anatomical site of derivation are unclear.

1.2.2 Extracellular calcium concentration

Besides vitamin D, extracellular calcium has been suggested to play an independent or co-regulating role in the differentiation of osteoblasts. In 2004, experiments using osteoblastic cells isolated from either foetal rat calvaria or using the mouse osteoblastic cell line 2T3, suggested that changes in extracellular calcium concentration directly altered the differentiation of osteoblast-like cells as evidenced by changes in cell proliferation, *Tnap* expression and mineral deposition by the cultured cells (117). They further demonstrated that the calcium sensing receptor (CaR) is expressed in osteoblasts and is functional but with a different protein structure to the CaR in kidney. The osteoblast

CaR is documented as being extremely sensitive to subtle changes in the extracellular calcium concentration (117). Experimentation with MSCs showed an optimal calcium concentration (1.8 mM) in culture media, for cells to demonstrate the highest levels of TNAP enzyme activity and *in vitro* mineral deposition, compared to either lower or higher calcium levels in media (118). A recent study also reported that increased calcium concentration in human MSCs culture up-regulated the expression of the anti-apoptotic factor, survivin and as a result promoted the differentiation of osteoblasts (119). A mutant mouse model, in which the kidney *CaR* is globally ablated ($CaR^{-/-}$) has been developed (120). These knockout mice exhibit neonatal hyperparathyroidism, high blood calcium levels and severely reduced bone mineral density, as well as growth retardation. A further study claimed that these $CaR^{-/-}$ mice demonstrated a bone phenotype of excessive amount of un-mineralised osteoid in both trabecular and cortical bones and delayed mineralisation in the growth plate. However, the formation of facial bones in knockout pups was unaffected compared to wild-type littermates (121). Examination of CaR expression in various tissues in wild-type pups revealed that the kidney CaR was also expressed at the mRNA level in bone marrow and slightly in cartilage, but was not detectable at a high level in OCN-expressing, mineralising bone tissues (121).

More recently, a tissue-specific *CaR* ablated mouse model was generated, in which only cells expressing type I collagen were affected, to further investigate the relationship between CaR and osteoblast function. The mutation strategy in that model was to excise exon 7 of *CaR*, which would compromise both kidney and bone CaR protein activity. The osteoblast-specific $CaR^{-/-}$ mice were shown to exhibit severe retardation of skeletal development and impaired bone mineralisation. Gene expression analysis of the knockout mice was consistent with poor mineral deposition and the decreased expression of osteoblast differentiation genes, *Osx*, *Col1a1, Tnap*, *Bglap*, *Dmp1* and *Sost* (122). The same group extended their study by culturing osteoblasts from the osteoblast-specific

CaR mutant mice. *In vitro* cultured osteoblasts from calvariae of one week-old mice showed attenuated mineral nodule formation and decreased levels of differentiation markers *Col1a1*, *Bglap* and *Dmp1*(123).

These findings confirm that an appropriate circulating calcium level, sensed by CaR, is critical for endochondral bone formation during skeletal development involving osteoblast differentiation. Extracellular calcium regulation of osteoblast differentiation could also be dependent on particular anatomical sites within the skeleton or the differentiation stage of the osteoblast. However, detailed information regarding the mechanism of regulation of osteogenesis by extracellular calcium remains to be elucidated, as does any interaction with vitamin D.

1.3 Conclusions and proposal for study

The data reviewed in this chapter demonstrate that vitamin D is capable of promoting osteoblast differentiation *in vitro* and maintaining bone mass *in vivo*. As well, under alternate conditions, vitamin D is capable of inducing bone loss and inhibiting mineral formation by osteoblasts. These inhibitory actions have been proposed under conditions where plasma levels of 1,25D are increased, which maximises the flow of calcium into the plasma compartment from the intestine, the kidney, as well as the skeleton.

In vitro extracellular calcium alone also enhances osteogenesis by promoting the differentiation process. However, it is unclear whether there is an interrelationship between the effects of vitamin D and calcium on osteoblast differentiation. Furthermore, osteoblasts of different skeletal origins demonstrate slightly different phenotypes and different levels of responsiveness to vitamin D. How such variations contribute to the overall osteoblast response to the vitamin D and extracellular calcium levels in combination *in vivo* is intriguing. The generation of data that can address such questions

and attempt to fill in such knowledge gaps will help to improve our understanding of osteoblast biology and the molecular and cellular basis of bone-related diseases.

Aim of study:

The studies described in this thesis were undertaken to contribute to elucidating the mechanisms, by which vitamin D and extracellular calcium modulate osteoblast proliferation and differentiation and mineral deposition using *in vitro* cell culture systems.

Hypotheses:

These studies were based on the hypotheses that 1) vitamin D has differential effects on osteoblast differentiation dependent on the level of VDR activity in cells and also the stage of cell differentiation, and 2) calcium plays an enhancing role in osteoblast differentiation either independently or in combination with vitamin D.

Approaches:

In vitro cell cultures: Cultures using cells derived from both calvaria and long bones were set up to investigate the cell phenotype differences related to their differentiation stage and skeletal origin. These cell cultures were also treated with vitamin D and calcium combinations to investigate the effects of these two factors on osteogenic differentiation at the molecular level. To confirm the dependency of the vitamin D effect on expression of the *VDR*, cells derived from transgenic mouse models with *VDR* activity globally knocked out (VDRKO) and mice with increased *VDR* activity in osteoblasts (OSVDR) were employed. In both cases, cells from transgenic animals were compared to their wild-type counterparts. To investigate the possible autocrine/paracrine role of 1,25D on osteoblast differentiation, the cells from transgenic mice with overexpressed *CYP27B1* in osteocalcin expressing cells (OSC) were also compared to wild-type cells. As an

endogenous source of the active hormone (1,25D), pre-hormone 25D was provided to OSC cells.

Experimental readouts: Gene expression over an extensive time-course of osteoblast differentiation and maturation was investigated to elucidate the effects of vitamin D metabolism in the cell models and the effects of exogenous 1,25D on cell differentiation. Gene analysis includes vitamin D metabolism/response genes, *Cyp27b1*, *Cyp24* and *Vdr*; osteoblast differentiation genes, *Runx2*, *Osx*, *Col-1α1*, *Tnap*, *Gja1*, *Opg*, *Rankl*, *Ocn*, *E11*, *Mepe*, *Phex*, *Dmp1*, *Sost* and *Fgf23*. *In vitro* mineralisation assays were also performed as a direct readout of osteoblast activity.

Chapter 2: Materials and Methods

2.1 Materials

2.1.1 Chemicals and reagents

SYBR Gold, Carboxyfluorescein succinimidyl ester (CFSE) dye, 10% buffered formalin and Triton X 100 were sourced from Life Technologies (Mulgrave, VIC, Australia). Acetic acid, alizarin red S dye, ammonia hydroxide, ascorbic acid, ascorbate-2-phosphate, calcium chloride, dimethyl sulfoxide (DMSO), ethylenediaminetetraacetic acid (EDTA), glycerol, paraformaldehyde, potassium hydroxide, silver nitrite, sodium chloride, sodium thiosulphate were purchased from Sigma-Aldrich (St. Louis, MO, USA). Calcitriol (1α,25-Dihydroxyvitamin D_3; 1,25D) and Calcifediol (25-Hydroxyvitamin D_3; 25D) were sourced from Wako Pure Chemicals (Osaka, Japan).

2.1.2 Molecular biology reagents

iQ CYBR Green Supermix was sourced from Bio-Rad (Gladesville, NSW, Australia). Oligo-dT nucleotide primers (designed in-house) and dNTPs for the synthesis of complementary DNA (cDNA) were sourced from Geneworks (Thebarton, SA, Australia). TRIzol reagent, DEPC-treated water, Proteinase K, Agarose powder, Polymerase Chain Reaction kit (including polymerase, 10X buffer, $MgCl_2$) and Superscript-III kit (including 0.1M DTT, 5X buffer, Superscript-III enzyme) were sourced from Life Technologies.

2.1.3 Animals

All mice used in this project were backcrossed at least 6 times to pure C57BL/6 genetic background. Genetically modified models including VDRKO (Vitamin D receptor global knockout) (124) and OSVDR (Vitamin D receptor overexpressed in osteocalcin expressing cells) (104) were compared to wild-type controls. VDRKO mice were sourced from Jackson Laboratory, Bar Harbor, ME, USA. OSVDR mice were generously

provided by Professor Edith Gardiner from Garvan Institute for Medical Research, Sydney, NSW, Australia. All animals used were maintained in the animal facility of SA Pathology. All usage of animals was approved by both the SA Pathology and The University of Adelaide animal research ethics committees.

2.2 Nucleotide preparations

2.2.1 DNA extraction

Genomic DNA was extracted from both animal tissues and cultured cells. One piece of soft tissue (approximately 5 mm^3) or a minimum 1 x 10^6 cultured cells was required for DNA extraction. DNA extraction lysis buffer (consisted 20mM Hepes-KOH (pH 7.9), 25% Glycerol, 420mM NaCl, 1.5mM MgCl2, 0.2mM EDTA, 0.5mM Dithiothreitol and 0.2mM PMSF) (500 µl) and proteinase K (final concentration of 200 µg/ml) were added to soft tissue or cells to produce a lysate that contained released DNA. Soft tissue was digested by proteinase K with an overnight incubation at 55^{o}C and cultured cells were digested for 10 minutes at 55^{o}C to release DNA. Lysates were centrifuged at 12,000g for 10 minutes at room temperature to pellet debris. Supernatants were transferred to fresh 2 ml reaction tubes (Eppendorf, North Ryde, NSW, Australia) and mixed with of isopropanol (500 µl) to precipitate DNA. DNA was pelleted by centrifuging at 8000g for 5 minutes at room temperature. Supernatants were then decanted and 70% ethanol (1 ml) was added to each tube to wash DNA followed by centrifugation at 8,000g for 5 minutes at room temperature. Washed DNA was dissolved in an appropriate volume (adjusted DNA concentration to around 200 ng/µl) of TE buffer (consisted 10mM Tris-HCl (pH 7.5), 0.1mM EDTA) and then quantified using a Nanodrop 2000 Spectrophotometer (Thermo Scientific). Purified DNA samples were stored at 4^{o}C for short term and preserved at -20^{o}C over long term to avoid DNA denaturing.

2.2.2 RNA extraction

A minimum of 1 x 10^6 cultured cells were preserved in 1ml of TRIZOL reagent (Life Technologies) to generate a lysate containing released RNA. Cell lysates in TRIZOL were frozen at -80^{o}C for at least 30 minutes and then thawed to room temperature to ensure complete lysis. Chloroform (1/5 of lysate volume) was added to each thawed lysate and the solution mixed by gently inverting tubes. Samples were then centrifuged at 12,000g at 4^{o}C for 15 minutes to separate RNA from debris and genomic DNA. After centrifugation, 300 µl of the upper phase liquid was transferred to fresh tubes and mixed thoroughly with 600 µl of isopropanol. Glycogen (4 µg/sample) was added to promote precipitation and the samples were then snap frozen at -80^{o}C for at least 30 minutes to precipitate RNA. The mixtures were thawed and centrifuged at 12000g at 4^{o}C for 10 minutes to pellet RNA. RNA pellets were washed by adding 1ml of 70% ethanol and then centrifugation at 12000g at 4^{o}C for 5 minutes. Resulting RNA pellets were then air-dried and dissolved in an appropriate (adjusted DNA concentration to around 200 ng/µl) volume of DEPC-treated water. Dissolved RNA samples were stored at -80^{o}C and always kept on ice when thawed for experimentation.

2.2.3 cDNA synthesis

Reverse transcription (RT) reactions using purified total RNA as the template were performed to synthesise cDNA. RNA samples were pre-quantified by Nanodrop 2000 Spectrophotometer. A standard amount of RNA from all samples was added to each RT reaction (1 µg of RNA/20 µl volume of RT reaction). cDNA was synthesised in two steps followed as per manufacturer's instruction:

Step one: Identical amounts of RNA from each sample were separately combined with 1 µl oligo-dT primer (1 µg/µl) and 1 µl 10 mM dNTP. Then the volume of each mixture was adjusted to a total volume of 16 µl with DEPC water in 200µl reaction tubes.

Mixtures were pulse-centrifuged to ensure the liquid was at the bottom of the tubes and incubated at 65ºC for 15 minutes to denature the RNA and allow access of the oligo dT primers. Immediately after the programme finished, all tubes were rapidly cooled to 4ºC to promote primer-RNA annealing.

Step two: While the above reaction was running, master-mix for the RT step was prepared using Superscript-III kit (Life Technologies). Each single aliquot of master-mix contained 4 µl of 5X Superscript buffer, 1 µl of 0.1M DTT and 1 µl of Superscript-III (200 units/µl) enzyme. Master-mix (6 µl) was added to each reaction from step one and the mixture was then allowed to react in a thermocycler with extension at 55ºC for 60 minutes, denaturation at 70ºC for 15 minutes and rapidly cooled to 4ºC. Synthesised cDNA samples were stored at -20ºC until used for PCR.

2.2.4 Conventional PCR (Polymerase Chain Reaction)

Conventional PCR reactions followed by gel electrophoresis separation were used for the genotype determination of VDRKO animals. Each single PCR reaction mixture contained 1X PCR buffer, 2 mM $MgCl_2$, 40 nM dNTPs, 250 nM forward and reverse primers (if more than two primers were required, each primer concentration were identical), 5U of polymerase and 40ng of DNA template. All the reaction mixtures were adjusted to a total volume of 25µl by DEPC-water. PCR reactions followed a programme consisting of denaturation at 94ºC for 5 minutes, followed by 35 cycles of 94ºC for 1 minute, annealing at a temperature according to each pair of primers used for 30 seconds, and extension at 70ºC for 30 seconds, ending with a final extension at 70ºC for 5 minutes and cooling to 10ºC. PCR products were loaded onto 1% w/v agarose gels casted by TBE buffer (consisted 90mM Tris, 90mM Boric acid and 2.5 mM EDTA (pH 8.3)) and electrophoresed at 110V for 30 minutes. Gels were stained with SYBR Gold dye for 15 minutes and DNA products visualised under UV light.

2.2.5 Real-time PCR

Real-time RT-PCR reactions were performed to determine the copy number of a specific mRNA species within the cell transcriptome. The mRNA level of the gene of interest was normalised to that of the housekeeping gene β-actin, which was predicted to be relatively constant in cells. Each of the real-time PCR reactions contained 5μl of iQ CYBR Green Supermix (2X), 250nM forward primer and 250nM reverse primer, 1μl of cDNA template directly from each of the RT reaction. All the reagents were added to 100μl PCR tubes and each of the mixtures were to a 10μl total volume. Amplification was performed in a Rotor-Gene 2000 thermocycler (Corbett Research) using the programme of 95ºC for 5 minutes, [35 cycles of 95ºC for 1 minute, annealing temperature (60ºC for all the real-time PCR primer sets used in this study) for 30 seconds, 70ºC for 30 seconds], 70ºC for 5 minutes, melt curve analysis. The primer sequences and related information for real-time PCRs are listed in table 2.2.5

Data were analysed using the ΔCT method (125) formula of 2^-(CT gene of interest)/2^-(CT β-actin), where the CT value represented the cycle threshold number, being the cycle, at which log-linear amplification was achieved.

2.3 Isolation of osteoblasts

2.3.1 Osteogenic growth media

Media supporting cell growth without cell differentiation, consisted of α-Minimal Essential Medium (α-MEM) plus 10% v/v fetal bovine serum (FBS) (Thermo Scientific, Scoresby, VIC, Australia), tissue culture additives (100 U/ml penicillin, 100 mg/ml streptomycin and L-glutamine (2 mM), manufactured by SA Pathology media production unit).

Table 2.2.5

Primer sets used for real-time PCR analysis of gene expression in mRNA level (specific for mouse transcriptome)			
Gene	**Sequence (5'to 3')**	**Gene bank accession number**	**Amplicon size (bp)**
β-Actin	Forward: AGGGTGTGATGGTGGGAAT Reverse: GCTGGGGTGTTGAAGGTCT	NM_007393.3	271
Vdr	Forward: CTGAATGAAGAAGGCTCCGAT Reverse: AAGCAGGACAATCTGGTCATCA	NM_009504.4	171
Cyp27b1	Forward: GACCTTGTGCGACGACTAA Reverse: TCTGTGTCAGGAGGGACTTCA	NM_010009.2	167
Cyp24a1	Forward: TTGAAAGCATCTGCCTTGTGT Reverse: GTCACCATCATCTTCCCAAAT	NM_009996.3	130

Runx2	Forward: CACAAGGACAGAGTCAGATTACAGAT Reverse: CGTGGTGGAGTGGATGGAT	NM_001146038.2 (isoform 1) NM_001145920.2 (isoform 2) NM_001271630.1 (isoform 3) NM_001271631.1 (isoform 4)	122
Osx	Forward: GCGTCCTCTCTGCTTGAGG Reverse: GGCTTCTTTGTGCCTCCTTTC	NM_130458.3	137
Tnap	Forward: TCCTGACCAAAAACCTCAAAGG Reverse: TGCTTCATGCAGAGCCTGC	NM_007431.2	101
Col-1α1	Forward: AGGCATAAAGGGTCATCGTG Reverse: CGTTGAGTCCGTCTTTGCCA	NM_007742.3	155
Ank	Forward: TCGCTGACGCTCTGTTTTGT Reverse: GGCAAAGTCCACTCCAATGATAT	NM_020332.4	84
Enpp1	Forward: AAGCGCTTACACTTCGCTAAAAG Reverse: TGATGGATTCAACGCAAGTTG	NM_008813.3	87

Opg	Forward: GTCCCTTGCCCTGACCACT Reverse: GGTAACGCCCTTCCTCACAC	NM_008764.3	151
Rankl	Forward: TGAAGACACACTACCTGACTCCTG Reverse: CTGGCAGCATTGATGGTGAG	NM_011613.3	198
Ocn	Forward: AGACCTAGCAGACACCATGA Reverse: GAAGGCTTTGTCAGACTCAG	NM_031368.4 (osteocalcin related protein) NM_001037939.1 (osteocalcin isoform 1) NM_007541.2 (osteocalcin isoform 2)	118
Cx43	Forward: AAGTGAAAGAGAGGTGCCCA Reverse: GTGGAGTAGGCTTGGACCTT	NM_010288.3	79
E11	Forward: AAACGCAGACAACAGATAAGAAAGAT Reverse: GTTCTGTTTAGCTCTTTAGGGCGA	NM_010329.2	158
Sost	Forward: CCACCATCCCTATGACGCCAA Reverse: TGTCAGGAAGCGGGTGTAGT	NM_024449.5	73
Fgf23	Forward: GGAAGCCTGACCCACCTGT Reverse: CGGCGTCCTCTGATGTAATC	NM_022657.3	133

Phex	Forward: GAAAAGCTGTTCCCAAAACAGAG Reverse: TAGCACCATAACTCAGGGATCG	NM_011077.2	156
Mepe	Forward: CCTGAAGGTGAATGACGCCAGA Reverse: TGCTCCTGTCTTCATTCGGCATT	NM_053172.2	111
Dmp1	Forward: GAAAGCTCTGAAGAGAGGACGGG Reverse: TGTCCGTGTGGTCACTATTTGCCT	NM_016779.2	121

2.3.2 Osteogenic differentiation media

Media supporting osteogenic differentiation consisted of α-MEM plus 10% v/v FBS (for differentiation of calvaria-derived cells) or 2% v/v FBS (for differentiation of MLO-A5), antibiotics (100 U/ml penicillin and 100 mg/ml streptomycin), L-glutamine (2 mM), 10 mM β-glycerol phosphate and 50 μg/ml ascorbic acid.

2.3.3 Isolation of osteoblast-like cells from neonatal mouse calvarial bones

One to three day old mice were used for acquiring primary osteoblast-like cells from mouse neonatal calvaria following a method kindly provided by Dr. Hong Zhou (ANZAC Institute, Concord, NSW, Australia). Two pieces of calvariae from the top of the skull were dissected and gently cleaned by scalpel. Calvariae from 4-7 pups aged 1-3 days of the same mouse genotype were pooled to perform 6 sequential enzymatic digestions in a 50 ml polypropylene reaction tube, in digestion fluid consisting of 1 mg/ml Collagenase-I (Life Technologies) plus 2 mg/ml Dispase (Life Technologies) in PBS. The liquid fractions from each digestion containing released osteoblasts were labelled F1-F6, and were collected by the following protocol:

Digestion 1: 3ml of digestion fluid was added to calvarial bones in each of the 50 ml tube. Tubes were incubated in a 37^{o}C shaking water bath at 200 rpm for 5 minutes. Cells released in F1 are mostly fibroblastic cells associated with the bone surface and hence F1 was discarded.

Digestion 2-6: Further 3ml volumes of digestion fluid were added to bones in each of the Falcon tubes. Tubes were incubated as above, whereupon the supernatants were collected and stored on ice until the procedure was completed. This step was repeated 5 times. Fractions F2-F6 were considered the fractions containing osteoblastic cells.

Fractions F2-6 were pooled and washed 3 times with PBS and centrifugation at 300g for 5 minutes to completely remove the enzyme solution. Resulting primary osteoblast-like cells were seeded in 24-well plates at a density of 1 x 10^4 cells/well or for 6-well plates, at a density of 5 x 10^4 cells/well, in 0.5 ml and 1 ml/well, respectively, of osteogenic growth media. Calvarial osteoblast-like cells were used for experimentation without passaging to avoid any major changes of cell phenotype.

2.3.4 Cryopreservation and thawing of cells

Cells were frozen for preservation over the long term in liquid nitrogen. Aliquots of 1 x 10^6 cells were resuspended in 1 ml α-MEM containing 20% v/v FBS and 10% v/v DMSO at 4ºC and distributed into 2 ml cryopreservation ampoules (Thermo Scientific). Ampoules were placed in a plastic rack at ambient temperature enclosed in a polystyrene box, which was then placed in a -80ºC freezer, an in-house designed protocol which effectively 'rate froze' the cells. For long-term storage, cells were then transferred to liquid nitrogen. When frozen cells were required for experimentation, a frozen vial was rapidly thawed in 37ºC water bath. Cells were then gently supplied drop-wise with 1 ml of α-MEM containing 2% v/v FBS and incubated at room temperature for 5 minutes. The volume of cell suspension was then doubled by PBS drop-wisely. The cell mixture was washed by PBS 3 times with cells harvested by centrifugation at 300g for 5 minutes to remove DMSO at each wash. Washed cells were cultured in fresh osteogenic growth media for experimentation.

2.4 Histochemical staining

2.4.1 Alizarin Red staining

For the analysis of calcium incorporation into the extracellular matrix, Alizarin Red staining was used. For this, cells in each well of a 24-well plate were washed by PBS

once, and then fixed at room temperature for 1 hour by 200 µl of 10% v/v buffered formalin. Formalin was then removed by washing with PBS. Following this, 250 µl of 2% w/v Alizarin Red S solution was added to each well to stain for calcium ions over 5 minutes. Excess dye was removed by washing with water, following which the plates were photographed. The amount of mineral deposited in each well was quantified by measuring the level of Alizarin Red staining. For this, 500 µl of 10% v/v acetic acid was added to each well for 30 minutes at room temperature to dissolve the stain. Supernatant from each well was transferred to fresh 1.5 ml reaction tubes. Cell debris was pelleted by centrifugation at 20,000g at 4ºC for 15 minutes. Each cleared supernatant was adjusted to pH 4.1-4.5 using 10% v/v ammonia hydroxide (usually 150 µl of Alizarin Red in 10% v/v acetic acid required 30µl of 10% v/v ammonium hydroxide) in flat bottomed 96-well plates. Samples were analysed by a plate spectrophotometer at 405nm. The absorption at 405 nm quantified the Alizarin Red staining for each sample, which represented the level of calcium deposition in each culture (126).

2.4.2 Von Kossa staining

As an additional readout of mineralisation, cultures were stained using a modified Von Kossa protocol to visualise deposited phosphate. For this, cultures were fixed in 200 µl of 10% v/v buffered formalin for 5 minutes. Formalin was then removed by washing three times in RO water. Following this, 250 µl of 1% w/v silver nitrate solution was added to each well to stain phosphate for 1 hour under exposure to strong white light (by placing the plate under a 100 W light bulb). Excess silver nitrite was then removed by gentle rinsing in RO water and then 250 µl of 2.5% w/v sodium thiosulphate was added to each well for 10 minutes to precipitate the silver phosphate complex. All wells were finally rinsed with RO water twice to remove excess staining reagents. The intensity of the silver sulphide precipitation in brown/black was proportional to the degree of phosphate deposition in the cultures (127).

2.5 Osteoblast proliferation assay

In order to assay cell proliferation, a modified CFSE staining technique was used (85), in which daughter cells each contain 50% of the parental level of CFSE stain, which can be assessed by flow cytometry (128). For this up to 1 x 10^7 of MLO-A5 cells were resuspended in a volume of 1 ml PBS containing 0.1% w/v BSA. Note that this reaction is not cell density dependent but rather volume-dependent. CFSE was supplied to the cells at a concentration of 20 μM at 37ºC for 15 minutes. Staining was quenched by rapidly transferring the tubes to wet ice. Excess CFSE was removed by washing in PBS (40 ml) with centrifugation at 300g at room temperature for 5 minutes. Cells were then seeded in osteogenic differentiation media for experimentation. CFSE labelled MLO-A5 cells were cultured under osteogenic differentiation media supplied with 25D or 1,25D treatments, as indicated, for 5 days. 2 x 10^4 cells were seeded into each well of a 12-well plate on Day 1. Fresh media were supplied to all wells on Day 3. On Day 5, media were removed and the cells rinsed in PBS. Cells were detached in 0.1% w/v trypsin with 5 mM EDTA and incubation at 37°C for 5 min. Cells from each well were then washed with PBS and then fixed in of 2% w/v paraformaldehyde (200 μl/well) at 4ºC before flow cytometric analysis (85). 1 x 10^5 unstained cells were fixed directly in 200μl of 2% w/v paraformaldehyde as unstained flow cytometry control. Flow cytometry results were analysed by ModFit 3 software (Verity Software House, Brunswick, ME, USA) to calculate the percentage of proliferation of each treatment group.

2.6 Osteoblast differentiation and mineralisation assays

Osteoblast-like cells were seeded into 6-well plates for differentiation assays for gene expression analysis and into 24-well plates for mineralisation assays. Cells were seeded in growth medium at 50% confluence (5 x 10^4 cells into each well of a 6-well plate in 2 ml or 1 x 10^4 cells into each well on 24-well plate in 0.5 ml) for 3 days to just achieve full

confluence, which was then taken as day 0 of differentiation. At this time, osteogenic differentiation media were supplemented with the appropriate vitamin D treatment (25D or 1,25D) combined with appropriate calcium treatment (1.8mM or 2.8mM total Ca^{2+}). All cultures were supplied with fresh media every 72 hours until Day 24. On Days 3, 9, 15 and 24, cultures in 6-well plates were treated with TRIZOL reagent to preserve mRNA; cultures in 24-well plates were used to perform Alizarin Red and Von Kossa staining to visualise mineral deposition.

Chapter 3

Differential effects of 1,25-dihydroxyvitamin D on mineralisation and differentiation in two different types of osteoblast-like cultures

As published in the Journal *of Steroid Biochemistry & Molecular Biology*, 2013

With the erratum to "Differential effects of 1,25-dihydroxyvitamin D on mineralisation and differentiation in two different types of osteoblast-like cultures" [J. Steroid Biochem. Mol. Biol. 136 (2013) 166–170]

The aim of this chapter was to identify osteoblast culture models that can respond to 1,25D treatment and to address the controversy on the different and apparently contradictory cellular actions of vitamin D on osteoblasts. The rationale behind this study was that at least some of the controversy in the field may be due to the different cell models used in particular studies. Thus, the approach here was to attempt to compare the response to vitamin D metabolites in both primary calvarial osteoblasts and primary cortical bone derived osteoblasts. The neonatal calvarial osteoblast model is well established and the Candidate learned the technique in the laboratory of Prof. Hong Zhou, ANZAC Research Institute, Concord, NSW, Australia. The long (cortical) bone osteoblast model was developed in-house by the Candidate, and studies were performed and the results published in good faith with the assumption that the cortical bone cells were actually primary long bone osteoblasts. These latter cells were further investigated by the Candidate and it was noticed that despite possessing the property of differentiation and *in vitro* mineralisation, they displayed qualities of a cell line, in that they could be repeatedly passaged. It should be noted that human bone-derived primary osteoblasts can also be passaged as many as 7-10 times without markedly changing their phenotype (G. Atkins, unpublished observations). Subsequent investigations however, outlined in

Appendix I, confirmed that the cells in question were MLO-A5 cells. The findings and interpretation of the study were considered still valid, since MLO-A5 cells were originally also isolated from a long bone pool of cortical osteoblasts. After consultation with the Editor-in-Chief of the Journal of Steroid Biochemistry and Molecular Biology, an erratum was submitted and subsequently published by the journal. The finding of a differential role of 1,25D on osteogenic differentiation is presented here in published format with the correction to clarify the termed “Cortical cells” in this study is the cell line MLO-A5, as shown in Appendix I.

Statement of authorship

Differential effects of 1,25-dihydroxyvitamin D on mineralisation and differentiation in two different types of osteoblast-like cultures. The Journal of Steroid Biochemistry and Molecular Biology. 2013;136:166-70

With the erratum to "Differential effects of 1,25-dihydroxyvitamin D on mineralisation and differentiation in two different types of osteoblast-like cultures" [J. Steroid Biochem. Mol. Biol. 136 (2013) 166–170]

D. Yang

First author. Generated data and analysed results; reviewed literature; preparation of figures and preparation of sections of the manuscript.

I hereby certify that the statement of contribution is accurate:

Sign: Date: 28/10/2014

G.J. Atkins

Planned and supervised research work, helped with data interpretation and manuscript preparation.

I hereby certify that the statement of contribution is accurate:

Sign: Date: 28/10/2014

A.G. Turner

Helped with data interpretation and manuscript evaluation.

I hereby certify that the statement of contribution is accurate

Sign: Date: 28/10/2014

P.H. Anderson

Helped with data interpretation and manuscript evaluation.

I hereby certify that the statement of contribution is accurate

Sign: Date: 29.10.14

H.A. Morris

Planned and supervised research work, helped with data interpretation and manuscript preparation. Senior author.

I hereby certify that the statement of contribution is accurate:

Sign: Date: 29/10/14

Journal of Steroid Biochemistry & Molecular Biology 136 (2013) 166–170

Contents lists available at SciVerse ScienceDirect

Journal of Steroid Biochemistry and Molecular Biology

journal homepage: www.elsevier.com/locate/jsbmb

Review

Differential effects of 1,25-dihydroxyvitamin D on mineralisation and differentiation in two different types of osteoblast-like cultures

D. Yang[a,b,c,*], G.J. Atkins[c], A.G. Turner[b,d], P.H. Anderson[b,d], H.A. Morris[a,b,d]

[a] Discipline of Medicine, University of Adelaide, Adelaide, SA 5005, Australia
[b] Endocrine Bone Research, Chemical Pathology, SA Pathology, Adelaide, SA 5000, Australia
[c] Bone Cell Biology Group, Discipline of Orthopaedics and Trauma, University of Adelaide, Adelaide, SA 5005, Australia
[d] Musculoskeletal Biology Research, School of Pharmacy and Medical Sciences, University of South Australia, Adelaide, SA 5000, Australia

ARTICLE INFO

Article history:
Received 5 July 2012
Received in revised form 6 November 2012
Accepted 28 November 2012

Keywords:
Osteogenesis
1,25-Dihydroxyvitamin D
Osteoblast differentiation
Mineralisation

ABSTRACT

In osteoblast cultures, 1,25-dihydroxyvitamin D (1,25D) has been shown to play either catabolic or anabolic roles on differentiation and mineralisation. We have employed osteoblast-like cells extracted from neonatal mouse calvariae and cells derived from juvenile mouse long bones to compare the biological effects of 1,25D on differentiation and mineralisation *in vitro*. 1,25D exerts differential effects on osteoblast-like cells depending on their stage of maturation and possibly their skeletal origin.

This article is part of a Special Issue entitled 'Vitamin D Workshop'.

Contents

1. Introduction 166
2. Materials and methods 167
   2.1. Isolation of osteoblasts from juvenile mouse cortical bones 167
   2.2. Isolation of osteoblast from mouse neonatal calvarial bones 167
   2.3. Differentiation assays 167
   2.4. Statistics 169
3. Results 169
   3.1. Characterisation of cells 169
   3.2. *In vitro* mineralisation and response to 1,25D 170
   3.3. 1,25D effects on gene expression 170
4. Discussion 170
   References 170

1. Introduction

Osteoblastogenesis is essential for bone formation requiring a sequential process of cell proliferation and maturation [1]. Immature osteoblasts are capable of proliferating and expressing genes required for synthesis of extracellular matrix compared to mature osteoblasts which exhibit activities required for mineral deposition. A proportion of these mature cells will become embedded in the matrix, forming an osteoid- or pre-osteocyte, and finally differentiate into mature osteocytes embedded in mineral. Understanding the process of osteoblast differentiation and mineralisation is important for elucidating the cellular activities required for bone health and a number of *in vitro* models have been utilised [2].

Numerous studies have demonstrated an interaction between vitamin D activity and osteoblast differentiation with the expression of a multitude of osteoblast genes directly regulated by 1,25-dihydroxyvitamin D(1,25D) [3]. However there remains considerable controversy regarding whether the overall activity of 1,25D is catabolic or anabolic for bone. 1,25D was reported to inhibit proliferation and enhance differentiation of osteoblasts isolated

* Corresponding author at: Endocrine Bone Research, Chemical Pathology, SA Pathology, Box 14 Rundle Mall PO, Adelaide, SA 5000, Australia. Tel.: +61 882223514; fax: +61 882223518.
E-mail addresses: dongqing.yang@health.sa.gov.au, dongqing.yang@adelaide.edu.au (D. Yang).

0960-0760/$ – see front matter © 2012 Elsevier Ltd. All rights reserved.
http://dx.doi.org/10.1016/j.jsbmb.2012.11.016

Table 1
Primer sets used for real-time PCR for gene amplification.

Gene	Sequence (5′–3′)
TNAP	Forward: TCCTGACCAAAAACCTCAAAGG Reverse: TGCTTCATGCAGAGCCTGC
β-Actin	Forward: AGGGTGTGATGGTGGGAAT Reverse: GCTGGGGTGTTGAAGGTCT
Col-IA1	Forward: AGGCATAAAGGGTCATCGTG Reverse: CGTTGAGTCCGTCTTTGCCA
MEPE	Forward: CCTGAAGGTGAATGACGCCAGA Reverse: TGCTCCTGTCTTCATTCGGCATT
OCN	Forward: AGACCTAGCAGACACCATGA Reverse: GAAGGCTTTGTCAGACTCAG
OSX	Forward: GCGTCCTCTCTGCTTGAGG Reverse: GGCTTCTTTGTGCCTCCTTTC
RANKL	Forward: TGAAGACACACTACCTGACTCCTG Reverse: CTGGCAGCATTGATGGTGAG
RUNX2	Forward: CACAAGGACAGAGTCAGATTACAGAT Reverse: CGTGGTGGAGTGGATGGAT
VDR	Forward: CTGAATGAAGAAGGCTCCGAT Reverse: AAGCAGGACAATCTGGTCATCA

from rat calvaria in the early 1990s [4]. The response of osteoblasts to 1,25D appears to depend on the stage of osteoblast maturation, with preferential induction of the catabolic factor, receptor activator of nuclear factor kappa B ligand (RANKL), in osteoblast cultures related to an immature phenotype rather than a mature phenotype [5]. In the osteoblastic cell line MC3T3-E1, 1,25D had pro-anabolic activity by enhancing the production of matrix vesicles and mineral deposition [6]. Osteogenesis, as measured by mineral deposition *in vitro*, is a critical readout of osteoblast differentiation and maturation. *In vitro* mineralisation by *VDR-null* mouse primary calvarial cells was enhanced compared to wild type cells [7], while mineral nodule formation by primary bone marrow cells was reduced by the ablation of vitamin D activity [8]. To address the controversy around the role of vitamin D activity on *in vitro* osteogenesis, we examined the effects of 1,25D on two types of mouse primary osteoblast-like cells either extracted from neonatal calvariae or derived from pre-pubertal mouse cortical bone. We report here that 1,25D acts on these two types of osteoblast populations distinctly, including effects on mineral deposition and gene expression.

2. Materials and methods

2.1. Isolation of osteoblasts from juvenile mouse cortical bones

Explant cultures of osteoblast-like cells were derived from mouse long bones [9]. Femora and tibiae from 4-week old C57BL/6 mice were excised and all connected soft tissue removed with a scalpel. Bone marrow was removed by flushing with PBS through a syringe after removal of growth plate regions. Diaphyseal cortical bone was then minced into ~1 mm^3 pieces and digested by 2 mg/ml of collagenase-I (Invitrogen, Australia) at 37 °C for 1 h. Cortical bone chips were incubated in α-Minimal Essential Medium (αMEM) (Invitrogen, Australia) with 10% Foetal Calf Serum (FCS) (Hyclone, Australia), antibiotics and L-glutamine. The osteoblast-like cells which grew from the bone chips were passaged to provide sufficient cells for experimentation.

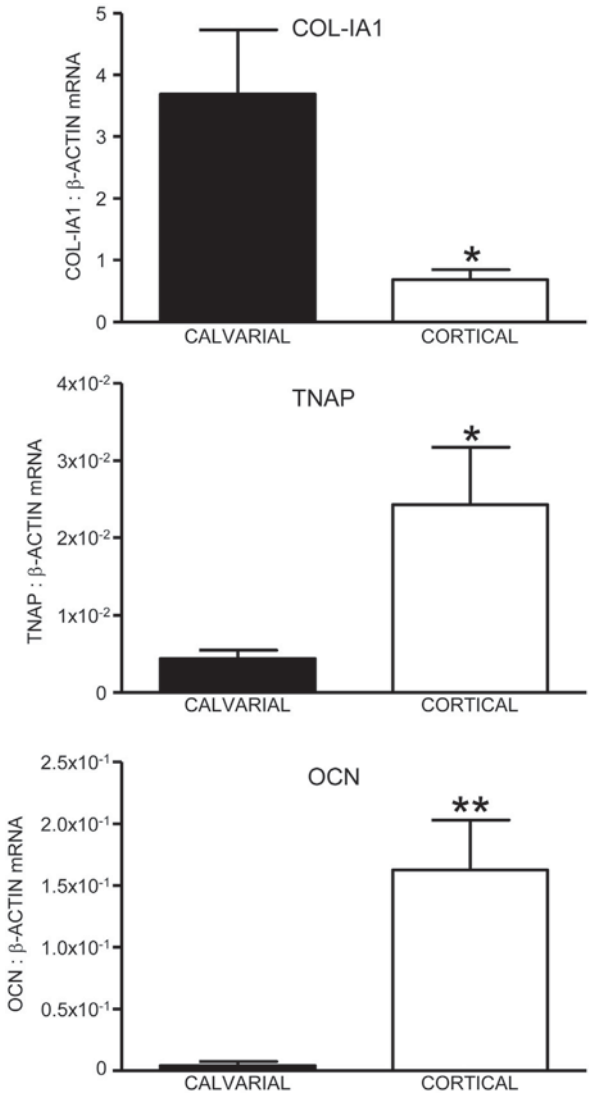

Fig. 1. Calvarial cells express a gene profile consistent with an immature osteoblast phenotype compared to cortical cells. Ratios of Col-IA1, TNAP and OCN mRNA species to β-actin mRNA from calvarial cells (closed bar) and cortical cells (open bar) (mean ± SEM, $n = 3$; $^{*}p < 0.05$; $^{**}p < 0.01$).

2.2. Isolation of osteoblast from mouse neonatal calvarial bones

Calvaria were dissected from 1 to 3 day old C57BL/6 mouse pups and carefully cleaned with a scalpel [10]. Multiple calvariae were pooled and subjected to sequential enzymatic digestion using collagenase-I (1 mg/ml) and dispase (2 mg/ml) (Invitrogen, Australia) for 10 min at 37 °C in a shaking water bath. After this time, cells were collected and the digestion protocol repeated 6 times in total. Cells pooled from digests 2–6 were used as primary cultures.

2.3. Differentiation assays

Cells were seeded into 24-well plates at a density of 3×10^4 cells/well and cultured in growth media, comprising of αMEM (Invitrogen) with 10% FCS (Hyclone), antibiotics and L-glutamine, for 3 days to reach 100% confluence. Cells were then cultured in differentiation media comprising growth media containing 50 mg/ml ascorbic acid (Sigma–Aldrich, St Louis, MO, USA) and 10 mM β-glycerol phosphate (Sigma). Fresh differentiation medium was supplied to cultures every 72 h with either 1,25D

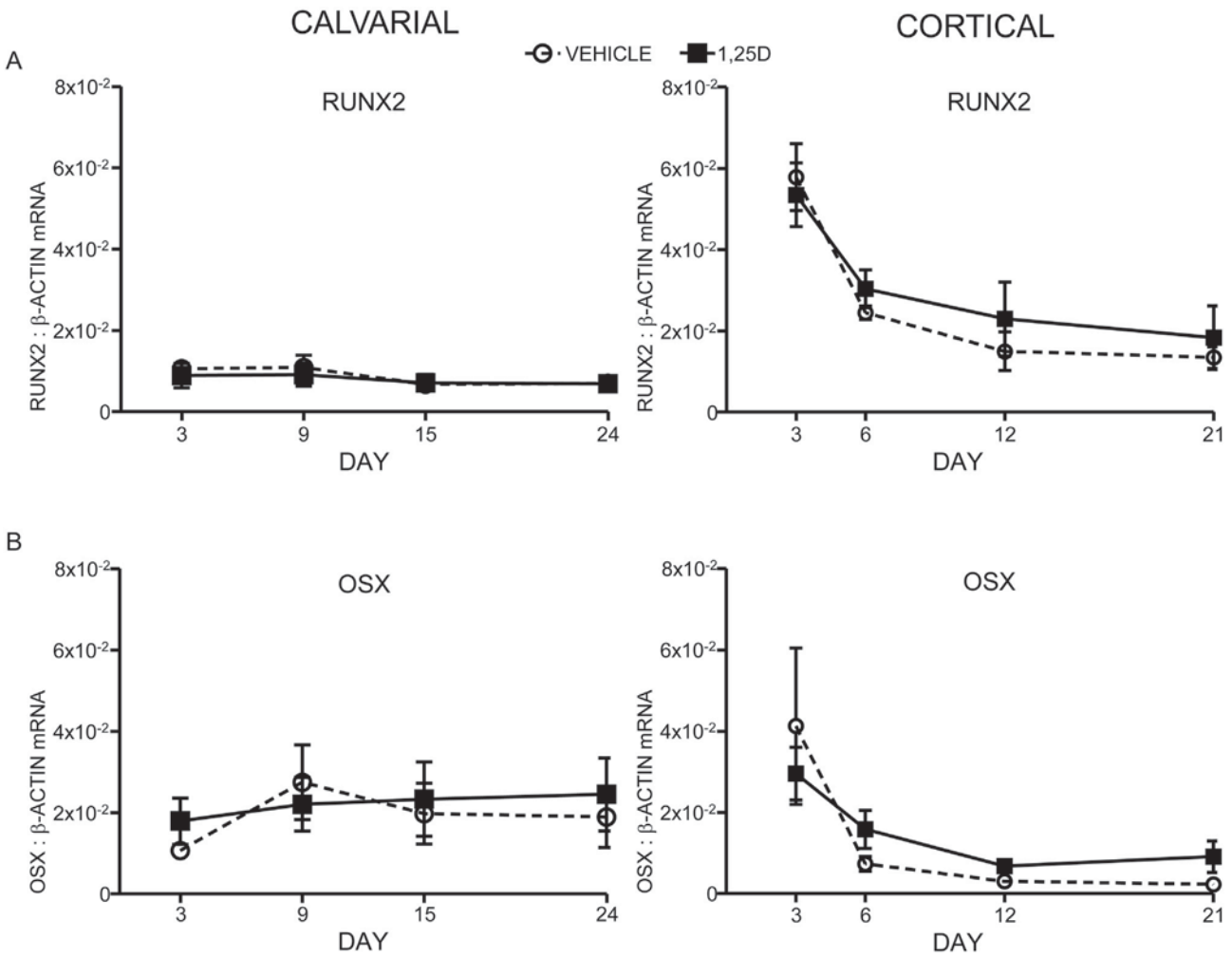

Fig. 2. mRNA expression of RUNX2 (A) and OSX (B) by calvarial cells (left column) and cortical cells (right column) treated with vehicle (broken line) and 1 nM 1,25D (solid line) (mean ± SEM, $n = 3$).

(1 nM, Wako, Japan) or vehicle (0.1% ethanol final concentration) added at each media change. *In vitro* mineralisation was visualised by staining with Alizarin Red. The alizarin–calcium complex was dissolved in acetic acid, neutralised to pH 4.2 with ammonium hydroxide, and quantified by measuring absorption at 405 nm in a spectrophotometer.

Total RNA was extracted from the cell cultures using the trizol method (Invitrogen) and cDNA synthesised (superscript III) to

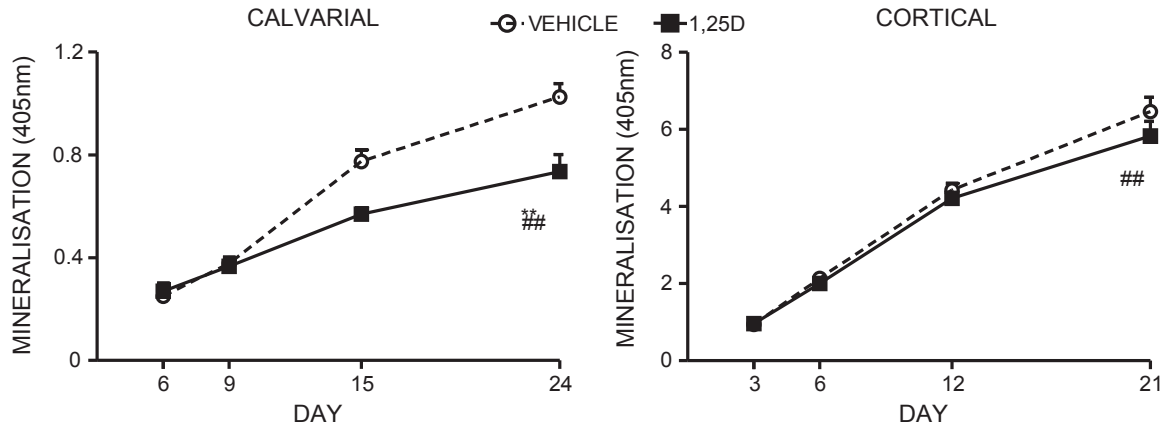

Fig. 3. Calvarial cells deposit less mineral, which is further reduced with 1,25D treatment, compared with cortical cells. *In vitro* mineralisation by calvarial cells (left) and cortical cells (right) treated with vehicle (broken line) and 1 nM 1,25D (solid line) (mean ± SEM, $n = 3$; effect of 1,25D treatment: $^{**}p < 0.01$; effect of time: $^{\#\#}p < 0.01$).

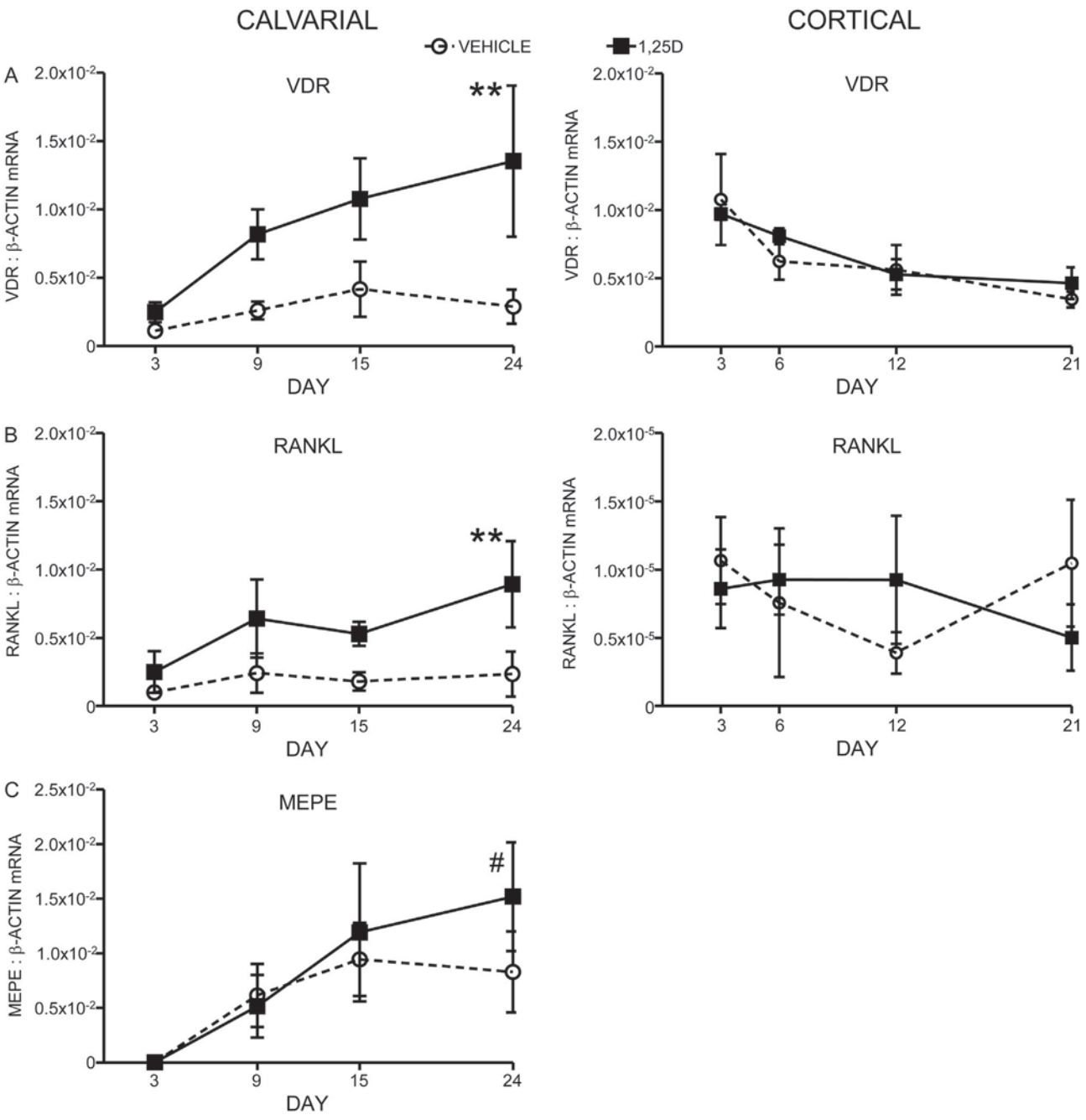

Fig. 4. Differential effects of 1,25D on mRNA levels in calvarial and cortical cells. Ratios of VDR (A), RANKL (B) and MEPE (C) mRNA to β-actin mRNA from calvarial cells (left column) and cortical cells (right column) treated with vehicle (broken line) and 1 nM 1,25D (solid line) (mean ± SEM, $n = 3$; MEPE mRNA levels were undetectable in cortical cells (data not shown). Effect of 1,25D treatment: $^{**}p < 0.01$; effect of time: $^{\#}p < 0.05$).

measure the expression of genes of interest using real-time PCR. The primer sets for each gene are listed in Table 1. Each experiment was conducted in triplicate and repeated on three occasions. Gene expression was normalised to that of the housekeeping gene, β-actin.

2.4. Statistics

All data were analysed by GraphPadPrism 5.04 (Graphpad Software, San Diego, USA). *t*-Tests were used to analyse data from single time point experiments. Two-way ANOVA, followed by Bonferroni post-tests, were used to assess the effect of 1,25D treatment in long-term cultures.

3. Results

3.1. Characterisation of cells

At 100% confluence, the relative mRNA level of type-I collagen alpha 1 (Col-IA1) in calvarial cells was 3-fold higher than in cortical cells ($p < 0.05$), whereas the expression of tissue non-specific alkaline phosphatase (TNAP) and osteocalcin (OCN) in cortical cells was 5-fold ($p < 0.05$) and 30-fold ($p < 0.01$) higher, respectively, than in calvarial cells (Fig. 1).

Expression levels of early osteoblast transcriptional factors RUNX2 and OSX were initially relatively high in cortical cells and reduced with time, whereas levels in calvarial cultures remained

unchanged. The expression of RUNX2 and OSX mRNA was unaffected by 1,25D (1 nM) treatment in both cell types (Fig. 2A and B).

3.2. In vitro mineralisation and response to 1,25D

The level of mineralisation in cortical cell cultures over 21 days was 6-fold greater than in calvarial cell cultures after 24 days. Moreover, the mineralisation in cortical cell cultures was not significantly impacted by 1,25D treatment while mineral deposition in calvarial cell cultures was inhibited by 1,25D ($p < 0.01$), and by day 24 was reduced by 28% ($p < 0.01$) (Fig. 3).

3.3. 1,25D effects on gene expression

In calvarial cell cultures, relative mRNA levels of matrix extracellular phosphoglycoprotein (MEPE) showed a significant increase over time ($p < 0.05$) while VDR showed a trend to increase over time ($p = 0.082$). Relative RANKL mRNA levels did not change with time ($p = 0.23$). VDR and RANKL mRNAs were further significantly induced by 1,25D treatment ($p < 0.01$) while MEPE mRNA was unchanged ($p = 0.13$ at 24 days) (Fig. 4A–C). Notably, the relative level of RANKL mRNA expression in calvarial cultures was 1000-fold higher than in cortical cells (Fig. 4B).

In cortical cell cultures, the mRNA levels of VDR and RANKL were detectable but unaffected by incubation with 1,25D (Fig. 4A and B). The expression of MEPE was undetectable in cortical cultures (data not shown) in the presence or absence of 1,25D.

4. Discussion

Our results show that two different mouse primary osteoblast preparations used in this study had different properties prior to *in vitro* differentiation, suggesting that the calvarial preparation represents a more immature osteoblast phenotype than the cortical preparation. Compared to calvarial cells, cortical cells expressed less Col-IA1 but more TNAP and OCN mRNA. At early stages of differentiation, osteoblasts express more Col-IA1 mRNA synthesising extracellular matrix than in the post-matrix producing period, when the expression of TNAP, an enzyme that degrades the potent mineralisation inhibitor pyrophosphate, is increased enabling mineralisation to proceed [11]. OCN is defined as a mature osteoblast marker [12,13]. The ability of cortical cells to deposit mineral *in vitro* was significantly enhanced compared to calvarial cells consistent with the difference in their apparent stage of maturation. Moreover, the ability of the pro-catabolic gene RANKL to be induced by 1,25D in calvarial cultures is also consistent with these cells representing a more immature osteoblast model than the cortical cells [5].

The osteoblast gene product MEPE, which increased with time in the calvarial cell cultures, exerts a post-translational, inhibitory role on osteoblast mineralisation [14,15]. Furthermore when cultures were treated with 1,25D, the levels of VDR and RANKL mRNAs were increased in calvarial cells but not in cortical cells. This pro-catabolic, anti-anabolic gene expression profile in calvarial cultures is consistent with the overall lower levels of mineral deposition by these cells and the inhibitory effect of 1,25D compared with the 6-fold greater level of mineral deposition and the absence of a 1,25D effect in cortical cells.

Our findings suggest that the interpretation of data from *in vitro* osteoblast models requires characterisation of the maturation stage of the cell preparations under study. Each culture type displays a particular differentiation potential and phenotypic profile. Furthermore 1,25D, an important regulator of osteoblast activity, also has distinct effects at different stages of osteoblast differentiation. Thus, interpretation of data related to the activities of 1,25D on bone cells must also be made in the context of the maturation stage of the osteoblasts. It is possible that at least some of the differential response to 1,25D was due to the different skeletal sites from which the cultures originated. It is interesting from this point of view that the skull is protected from the age-related bone loss observed in the axial skeleton; it will be of interest in future studies to compare directly the effect of vitamin D on cranial and axial skeletal bone mass. The findings presented here suggest that the choice of osteoblast model is critical to the outcome of studies into osteoblast differentiation and their response to 1,25D.

References

[1] G.S. Stein, J.B. Lian, Molecular mechanisms mediating proliferation/differentiation interrelationships during progressive development of the osteoblast phenotype, Endocrine Reviews 14 (4) (1993) 424–442.
[2] V. Kartsogiannis, K.W. Ng, Cell lines and primary cell cultures in the study of bone cell biology, Molecular and Cellular Endocrinology 228 (1–2) (2004) 79–102.
[3] G.J. Atkins, D.M. Findlay, P.H. Anderson, H.A. Morris, Target genes: bone proteins, in: D. Feldman, J.W. Pike, J.S. Adams (Eds.), Vitamin D, 3rd edition, Elsevier, San Diego, 2011.
[4] T.A. Owen, et al., Pleiotropic effects of vitamin D on osteoblast gene expression are related to the proliferative and differentiated state of the bone cell phenotype: dependency upon basal levels of gene expression, duration of exposure, and bone matrix competency in normal rat osteoblast cultures, Endocrinology 128 (3) (1991) 1496–1504.
[5] G.J. Atkins, et al., RANKL expression is related to the differentiation state of human osteoblasts, Journal of Bone and Mineral Research 18 (6) (2003) 1088–1098.
[6] V.J. Woeckel, et al., 1Alpha,25-(OH)2D3 acts in the early phase of osteoblast differentiation to enhance mineralization via accelerated production of mature matrix vesicles, Journal of Cellular Physiology 225 (2) (2010) 593–600.
[7] K. Sooy, Y. Sabbagh, M.B. Demay, Osteoblasts lacking the vitamin D receptor display enhanced osteogenic potential in vitro, Journal of Cellular Biochemistry 94 (1) (2005) 81–87.
[8] D.K. Panda, et al., Inactivation of the 25-hydroxyvitamin D 1alpha-hydroxylase and vitamin D receptor demonstrates independent and interdependent effects of calcium and vitamin D on skeletal and mineral homeostasis, Journal of Biological Chemistry 279 (16) (2004) 16754–16766.
[9] A. Bakker, J. Klein-Nulend, Osteoblast isolation from murine calvariae and long bones, Methods in Molecular Medicine 80 (2003) 19–28.
[10] H. Zhou, et al., Osteoblasts directly control lineage commitment of mesenchymal progenitor cells through Wnt signaling, Journal of Biological Chemistry 283 (4) (2008) 1936–1945.
[11] L.D. Quarles, et al., Distinct proliferative and differentiated stages of murine MC3T3-E1 cells in culture: an in vitro model of osteoblast development, Journal of Bone and Mineral Research 7 (6) (1992) 683–692.
[12] M. Morike, et al., Expression of osteoblastic markers in cultured human bone and fracture callus cells, Journal of Molecular Medicine (Berlin) 73 (11) (1995) 571–575.
[13] R. Yamamoto, et al., 1alpha,25-dihydroxyvitamin D3 acts predominately in mature osteoblasts under conditions of high extracellular phosphate to increase fibroblast growth factor 23 production in vitro, Journal of Endocrinology 206 (3) (2010) 279–286.
[14] W.N. Addison, et al., MEPE-ASARM peptides control extracellular matrix mineralization by binding to hydroxyapatite: an inhibition regulated by PHEX cleavage of ASARM, Journal of Bone and Mineral Research 23 (10) (2008) 1638–1649.
[15] G.J. Atkins, et al., Sclerostin is a locally acting regulator of late-osteoblast/preosteocyte differentiation and regulates mineralization through a MEPE-ASARM-dependent mechanism, Journal of Bone and Mineral Research 26 (7) (2011) 1425–1436.

Journal of Steroid Biochemistry & Molecular Biology xxx (2014) exxx

Contents lists available at ScienceDirect

Journal of Steroid Biochemistry & Molecular Biology

journal homepage: www.elsevier.com/locate/jsbmb

Erratum

Erratum to "Differential effects of 1,25-dihydroxyvitamin D on mineralisation and differentiation in two different types of osteoblast-like cultures" [J. Steroid Biochem. Mol. Biol. 136 (2013) 166–170]

D. Yang [a,b,c,*], G.J. Atkins [c], A.G. Turner [b,d], P.H. Anderson [b,d], H.A. Morris [a,b,d]

[a] Discipline of Medicine, University of Adelaide, Adelaide, SA 5005, Australia
[b] Endocrine Bone Research, Chemical Pathology, SA Pathology, Adelaide, SA 5000, Australia
[c] Bone Cell Biology Group, Discipline of Orthopaedics and Trauma, University of Adelaide, Adelaide, SA 5005, Australia
[d] Musculoskeletal Biology research, School of Pharmacy and Medical Sciences, University of South Australia, Adelaide, SA 5000, Australia

The authors regret that there was an error in this article describing cortical cells as primary cells isolated from juvenile mouse long bones. Our subsequent analysis has demonstrated unequivocally that the cortical cells used in this study were the well-characterised MLO-A5 cells as described by Kato et al., J. Bone Miner. Res. 16 (2001) 1622–1633. The MLO-A5 cell line was isolated as a single colony cultured from the long bones of juvenile mice expressing the osteocalcin promoter-driven T-antigen as a transgene (Kato et al., J. Bone Miner. Res. 12 (1997) 2014–2023). As such, this study should be considered a comparison between murine calvarium derived osteoblasts and a murine long bone derived osteoblast cell line. The authors do not wish to change the presentation or interpretation of the data related to this study.

Section 2.1 should be replaced by the following paragraph:

2.1 MLO-A5 cells as a model of cortical bone cells

The MLO-A5 cell line, utilised as a model of cortical postosteoblast/preosteocyte cells, was generously provided by Prof. Lynda Bonewald (University of Missouri–Kansas City, MO, USA) and cultured as previously described (Kato et al., J. Bone Miner. Res. 16 (2001) 1622–1633).

DOI of original article: http://dx.doi.org/10.1016/j.jsbmb.2012.11.016
* Corresponding author.

http://dx.doi.org/10.1016/j.jsbmb.2014.07.006

Please cite this article in press as: D. Yang, et al., Erratum to "Differential effects of 1,25-dihydroxyvitamin D on mineralisation and differentiation in two different types of osteoblast-like cultures" [J. Steroid Biochem. Mol. Biol. 136 (2013) 166–170], J. Steroid Biochem. Mol. Biol. (2014), http://dx.doi.org/10.1016/j.jsbmb.2014.07.006

Chapter 4: The regulation of osteogenic differentiation of calvaria-derived osteoblasts in response to 1,25D and calcium, and the influence of the level of VDR expression

4.1 Introduction

As described in Chapter 3, neonatal calvarial-derived osteoblast-like cells (Calvarial cells) respond to chronic 1,25D treatment in a catabolic manner, as indicated by inhibition of mineral deposition and increased *Rankl* mRNA expression. In this chapter, data are reported on the effects of VDR activated by physiological and pharmacological levels of 1,25D on the ability of Calvarial cells to differentiate and deposit mineral under the standard extracellular calcium concentration (1.8 mM) included in the culture medium generally used for osteogenesis assays, and media with increased extracellular calcium (2.8 mM) levels.

Also in this study, Calvarial cells were isolated and examined from two genetically-modified mouse models, the global VDR knockout (VDRKO) and another mouse strain, designated OSVDR, in which the human *VDR* gene is over-expressed under the control of the human osteocalcin gene promoter.

In VDRKO mice, the *Vdr* gene, and therefore VDR activity, is globally ablated. Data from two independent research groups, each of whom contributed to the generation of one distinct mouse line of this model, confirmed that mice lacking VDR activity developed osteomalacia after weaning at 3-weeks of age (124,129). At slightly older ages these mice also developed alopecia. Amling *et al.*, demonstrated that by feeding animals a 'rescue diet' containing 2% calcium, 1.25% phosphorus, 20% lactose, and 2.2 units/g vitamin D from weaning until 10 weeks of age, the bone phenotype, including bone volume and strength, was 'rescued' to the level of wild-type littermate controls. This

rescue was achieved as a result of normalisation of circulating calcium and phosphate levels (130). Osteoblasts derived from the calvariae of 3-day old VDRKO mice demonstrated a higher level of osteogenic differentiation and formation of mineral nodules *in vitro*, compared to cells from wild-type mice (131). Bone marrow cells from 18-day old VDRKO and wild-type mice were shown to have a similar capacity for osteogenesis *in vitro*, with similar levels of alkaline phosphatase enzyme activity and gene expression of *Opn*, *Bsp* and *Ocn* (132). However, an earlier study by Panda *et al.* (103) reported that formation of mineral nodules by bone marrow cells from 4-month old VDRKO mice was significantly decreased compared to cells from wild-type littermates. They suggested that VDR activity may be particularly important to bone in older animals. The controversy surrounding the role of VDR activity in osteoblast differentiation has continued since discordance between these publications remains unresolved.

The characterisation of the OSVDR mouse model was first published in 2000 (104).This transgenic model was created in mice with the *FVBN* genetic background. OCN was suggested to be a marker of the differentiation and maturation of osteoblasts (133) and human *OCN* promoter activity was previously shown to be enhanced by 1,25D stimulation, acting via a classical VDRE (134). As such, the over-expression of human VDR in the OSVDR model is presumably restricted to mature osteoblasts and osteocytes, and the expression is expected to be further up-regulated by 1,25D treatment. Phenotypically, this model features increased bone volume at cortical and trabecular bones sites, as well as increased cortical bone strength (104). The*in vivo* data for this model suggested that the bone phenotype at cortical sites was associated with an elevated periosteal mineral apposition rate that was contributed by the activity of mature osteoblasts. The transgene was found to be expressed in cuboidal osteoblasts, osteocytes and lining cells in OSVDR mice. The enhanced VDR production in osteoblasts and/or osteocytes was proposed to be the factor that altered the attributes of the cortical bone in

this transgenic model (104). However, in contrast, the trabecular bone phenotype was attributed to a reduction in osteoclast surface and bone resorption, but with bone formation rate unchanged in trabecular sites (104). Recently, the OSVDR model has been characterised by our group on a second genetic background, C57BL/6, and the original skeletal phenotype has been confirmed (135). This important finding reinforces the concept that increased VDR activity in mature osteoblasts is responsible for the increased bone mineral phenotype. Further characterisation of the OSVDR mouse on the original *FVBN* genetic background has demonstrated that osteoblasts from OSVDR mice exhibit reduced capability to support osteoclastogenesis when co-cultured with human monocytes, compared with wild-type osteoblasts *in vitro*; in addition, osteoclast activity was reduced in OSVDR bone *in vivo*. These observations were attributed to the maintenance of OPG expression in the face of increased VDR signalling in this model (136). However, in both previous OSVDR studies, the cellular mechanism, by which increased VDR activity in osteoblasts modified the osteoblast phenotype was not elucidated.

In this study, primary, calvaria-derived osteoblast cultures from WT, VDRKO and OSVDR mouse models, representing normal, depleted and increased levels of *Vdr* gene expression, respectively, were utilised to examine the interaction between the 1,25D/VDR system and osteoblast differentiation. This approach offered the ability to collect data from each model simultaneously, thus eliminating some of the potentially confounding technical influences (e.g. sample preparation, observer error, variation due to specific cell culture conditions) on experimental outcomes.

4.2 Experimental methods

The VDRKO mouse line on the C57BL/6 genetic background was fed the ‘rescue diet’, discussed above, after weaning in the animal facility of SA Pathology (Adelaide, SA,

Australia). This mouse line was maintained by mating homozygous VDRKO ($Vdr^{-/-}$) males with heterozygous knockout ($Vdr^{+/-}$) females. This breeding strategy resulted in generation of pups only of the $Vdr^{-/-}$and $Vdr^{+/-}$genotypes. The genotype of the pups was determined by a conventional PCR followed by electrophoresis gel visualisation, as described in Section 2.2.4.

The following three PCR primers were added to PCR reactions:

1) 5′-CTCCATCCCCATGTGTCTTT-3′

2) 5′-TTCTTCAGTGGCCAGCTCTT-3′

3) 5′-CACGAGACTAGTGAGACGTG-3′

Primers 1) and 2) targeted the intact *Vdr* genomic DNA sequence by producing an amplicon of 382 bp. Primers 2) and 3) targeted the mutated *Vdr* DNA sequence by producing an amplicon of 500 bp, which included part of the replacement cassette of exon 3 in the *Vdr* gene. PCR reactions with a single amplicon of 500 bp indicated the $Vdr^{-/-}$ genotype, as only the mutated *Vdr* gene sequence was present; PCR reactions with both 500 bp and 382 bp amplicons indicated the $Vdr^{+/-}$ genotype, as each of the mutant and intact alleles of *Vdr* gene were present (Fig. 4.2A). In addition, $Vdr^{-/-}$ males and females were mated for the breeding of pure $Vdr^{-/-}$ litters, which were used for calvarial cell isolation.

The OSVDR mouse line on the C57/BL6 background was bred in the same animal facility (SA Pathology), during which time they were fed a standard chow diet. The mouse line was maintained by breeding hemizygous ($Osvdr^{+/-}$) transgenic male mice with WT (i.e. $Osvdr^{-/-}$) females. This breeding strategy produced only WT and $Osvdr^{+/-}$ pups. The genotypes of the pups were determined by the absence or presence, respectively, of human *VDR* mRNA, which was detected by species-specific RT-PCR amplification, using the oligonucleotide primers 5′-CTCCCTCCACCATCATTCACA-3′ (forward) and 5′-GGACGCCCACCATAAGACCTA-3′ (reverse) (Figure 4.2 B). In this study, all

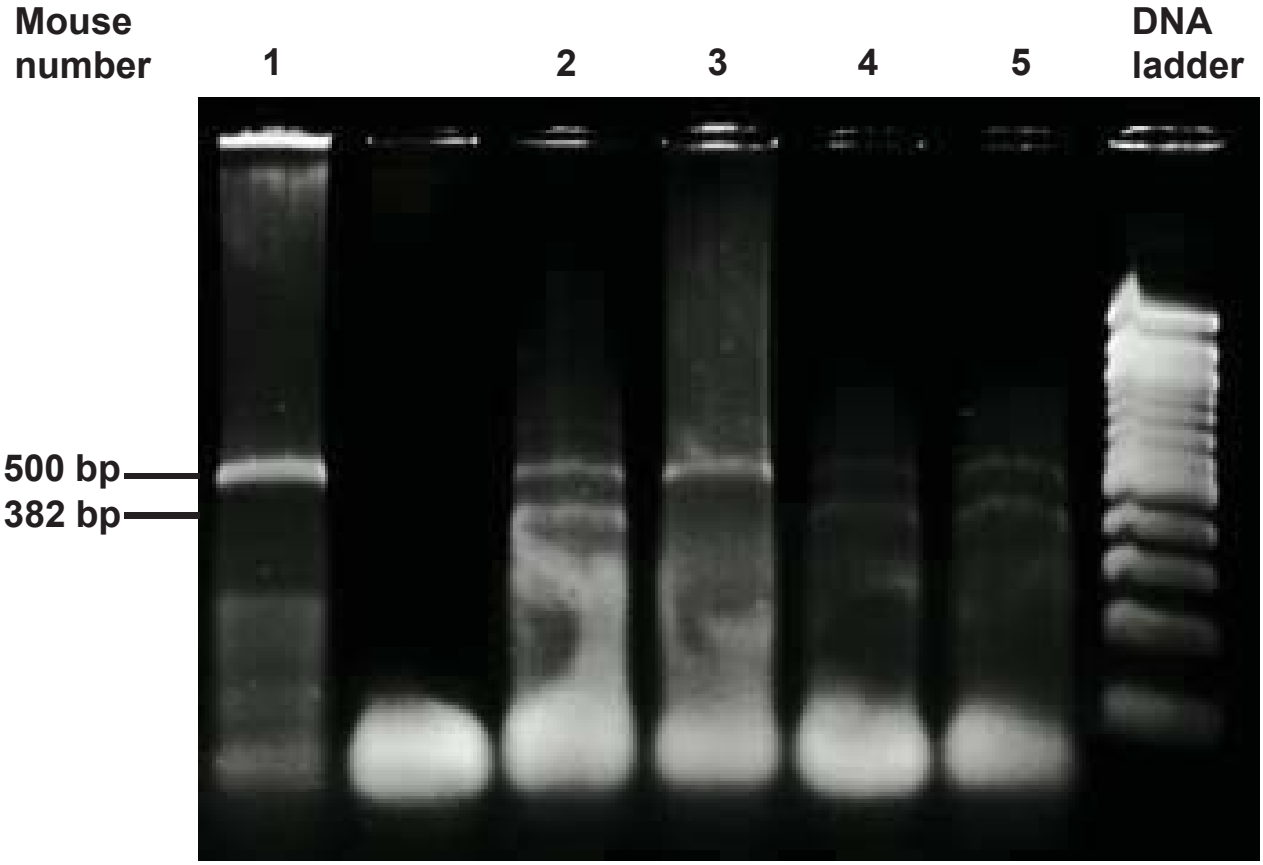

Figure 4.2 A **Genotype determination of *Vdr*$^{-/-}$ and *Vdr*$^{+/-}$ mice**

PCRs represented mouse number of 1 and 3 generated 500 bp amplicon only which was a part of the mutant vitamin D receptor (*Vdr*) gene sequence. Hence mice 1 and 3 were confirmed as homologous knockout (*Vdr*$^{-/-}$).

PCRs represented mouse number of 2, 4, 5 generated both 500 bp and 382 bp amplicons which were a part of the mutant and intact *Vdr* gene sequence respectively. Hence mice 2, 4, 5 were confirmed as heterozygous knockout (*Vdr*$^{+/-}$).

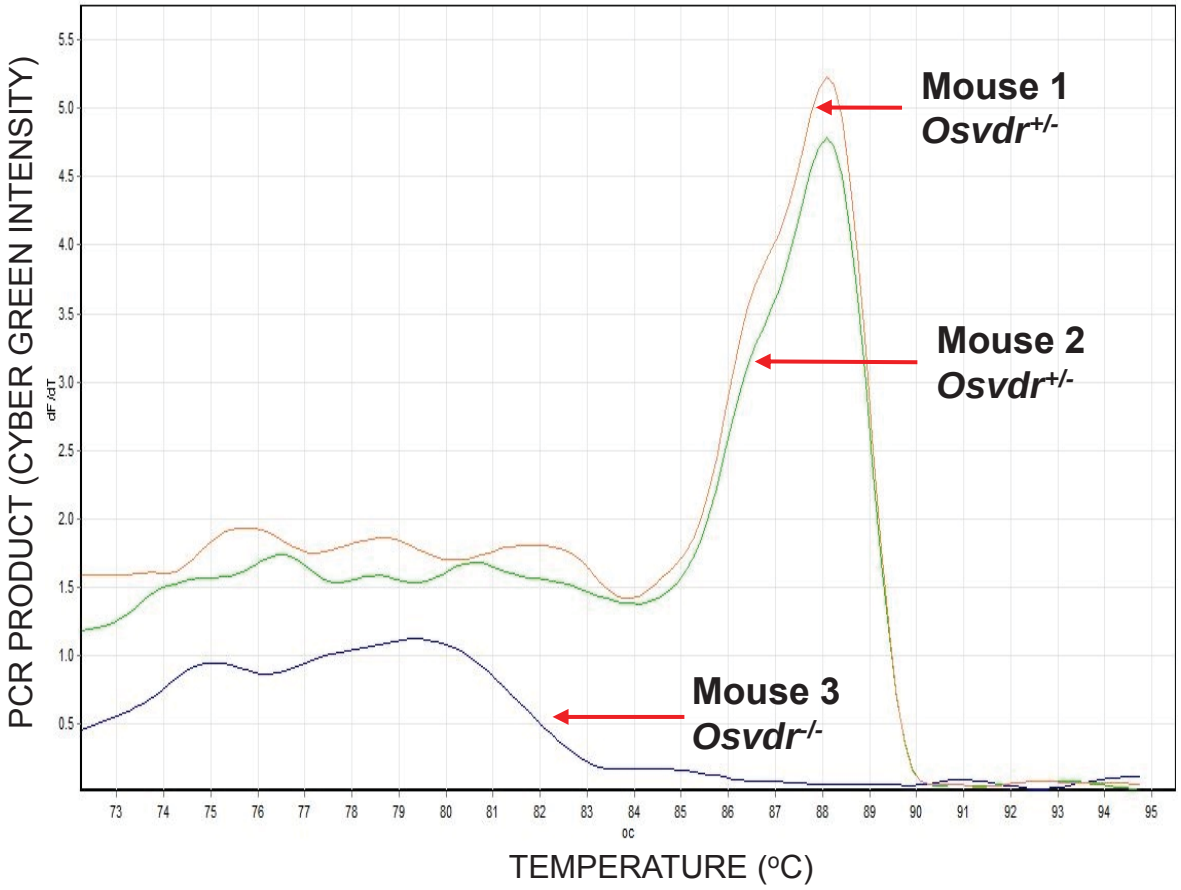

Figure 4.2 B **Genotype determination of *Osvdr*$^{-/-}$ and *Osvdr*$^{+/-}$ mice**

PCRs represented mouse number of 1 and 2 generated a single genuine amplicon which was a part of the human vitamin D receptor (*hVDR*) gene sequence. Hence mice 1 and 2 were confirmed as hemizygous transgenic (*Osvdr*$^{+/-}$).

PCR represented mouse number 3 did not generate any amplicon. Hence mouse number 3 was confirmed as wild type (*Osvdr*$^{-/-}$).

OSVDR transgenic pups used for experiments were hemizygous (i.e.*Osvdr*$^{+/-}$) with only one chromosome containing the transgene combining with the other chromosome unchanged from wild type.

Using the neonatal calvarial bone-derived cell preparation method described in Section 2.3.3, osteoblast-like cells were isolated from WT, VDRKO and OSVDR pups for mRNA samples and *in vitro* mineralisation assay. Cells were seeded in cell culture plates for 3 days in growth media to allow proliferation followed by 24 days culture in differentiation media (for detailed methods see sections 2.3.1, 2.3.2 and 2.6). The treatments of vehicle (0.1% v/v ethanol) and chronic 1,25D (1 nM) were supplied to cell cultures every 72 hours in fresh media throughout the 24-day culture period. Note that a concentration of 30 pM 1,25D was measured in batches of culture media containing FCS used in our laboratories (personal communication from Dr. Andrew Turner), thus 'vehicle' treatments used in this study actually represent a low physiological concentration of 1,25D. A concentration of 1 nM, on the other hand, represents a pharmacological dose of 1,25D, since this is approximately 6 – 20x higher than the normal physiological range detected in human plasma of approximately 48 – 155 pM (137). Samples of total RNA for each time point (days 0, 3, 9, 15 and 24) and for each treatment from all three cell genotypes, were extracted from the cell lysates of two individual culture wells. Each RNA sampling time point was at the end of one 72-hour media change cycle. All RNA samples were quantified to ensure that identical quantities of RNA were added to each cDNA synthesis reaction. The expression of genes of interest was measured by qPCR using primer sets listed in table 2.2.5. Each gene amplification was normalised for the housekeeping gene β-Actin, as described in section 2.2.5.

WT and OSVDR calvarial cells were also assessed following acute 1,25D (1 nM) treatment, which only exposed cells to 1,25D for 24 hours prior to the harvest of RNA.

This strategy was utilised to identify direct effects of 1,25D due to the modulation of gene expression by 1,25D-VDR activity acting through a VDRE, as opposed to possible indirect effects of 1,25D on mRNA levels resulting from modulation of osteoblast maturation. In contrast, the chronic 1,25D treatment would measure the combined direct and indirect effects on gene expression.

Mineralisation assays including vehicle and chronic 1,25D treatments were conducted for each cell genotype. Mineralisation was visualised by both Alizarin Red staining of calcium, producing a red stain, and Von Kossa staining of phosphate, which produces a brown/black colour, on days 6, 9, 15 and 24. The Alizarin Red level was quantified by light absorption at 405_{nm} (Section 2.4.1).

In addition to measuring effects of acute and chronic 1,25D treatment, experiments were also performed under conditions of standard (1.8 mM) and elevated (2.8 mM) total calcium concentration in the culture media. This variation was based on our group's observation that calcium enhances *in vitro* mineralisation by osteoblasts (30), suggesting that calcium levels in standard culture media are limiting, and also the fact that the major endocrine function of 1,25D is the maintenance of calcium homeostasis, and as such it was predicted that the 1,25D response may be modulated by the prevailing concentration of calcium.

Each cell culture study was carried out in triplicate for 3 independent experiments. The error bars in gene expression graphs represented the standard errors of the mean (SEM) of data combined from the 3 experiments. The error bars in mineralisation graphs represented the SEM of triplicate culture wells within one representative experiment. Statistical analyses were performed using GraphPad Prism (version 6.05) software using

two-way ANOVA, followed by a Bonferroni post-hoc test. A value for *p* less than 0.05 was considered significant.

4.3 Results

4.3.1 Vdr/VDR status and 1,25D metabolism in VDRKO, WT and OSVDR cells

Neither *Vdr* (*mVdr)* nor *Cyp24a1*mRNA expression was detectable in VDRKO cells, determined by the lack of the respective qPCR products after 35 amplification cycles. Consistent with the complete lack of a functional VDR in this genotype, chronic 1,25D treatment of VDRKO cells had no discernible effect compared to vehicle treatment (see Appendix II).

In vehicle treated WT and OSVDR cells, endogenous *Vdr* mRNA expression was similar. In WT cells, the *Vdr* mRNA level was transiently increased 2-fold by acute 1,25D treatment at 9 days before returning to control levels at 24 days. Chronic 1,25D treatment resulted in the increased *Vdr* mRNA levels being maintained up to day 24 (Fig. 4.3.1A). In OSVDR cells, endogenous *Vdr* mRNA expression was also induced by acute 1,25D treatment 2-fold, but was unchanged in response to chronic 1,25D treatment (Fig. 4.3.1B). In vehicle treated OSVDR cells, the mRNA level of human *VDR* was on average approximately 6-fold higher than mouse *Vdr,* based on relative cycle threshold (C_T) values. Acute 1,25D treatment further increased human *VDR* expression 2-fold over those in chronically-treated cells and these levels persisted until 24 days in culture. Interestingly, chronic 1,25D treatment induced a peak of total *VDR* mRNA (mouse + human) between days 9 and 15 of culture (Fig. 4.3.1 C).

Cyp24a1 mRNA expression was elevated by chronic 1,25D treatment in both WT and OSVDR cells to similar levels. With acute 1,25D treatment, the induction of *Cyp24a1* mRNA levels in both cell types was markedly increased (>10-fold) compared with levels

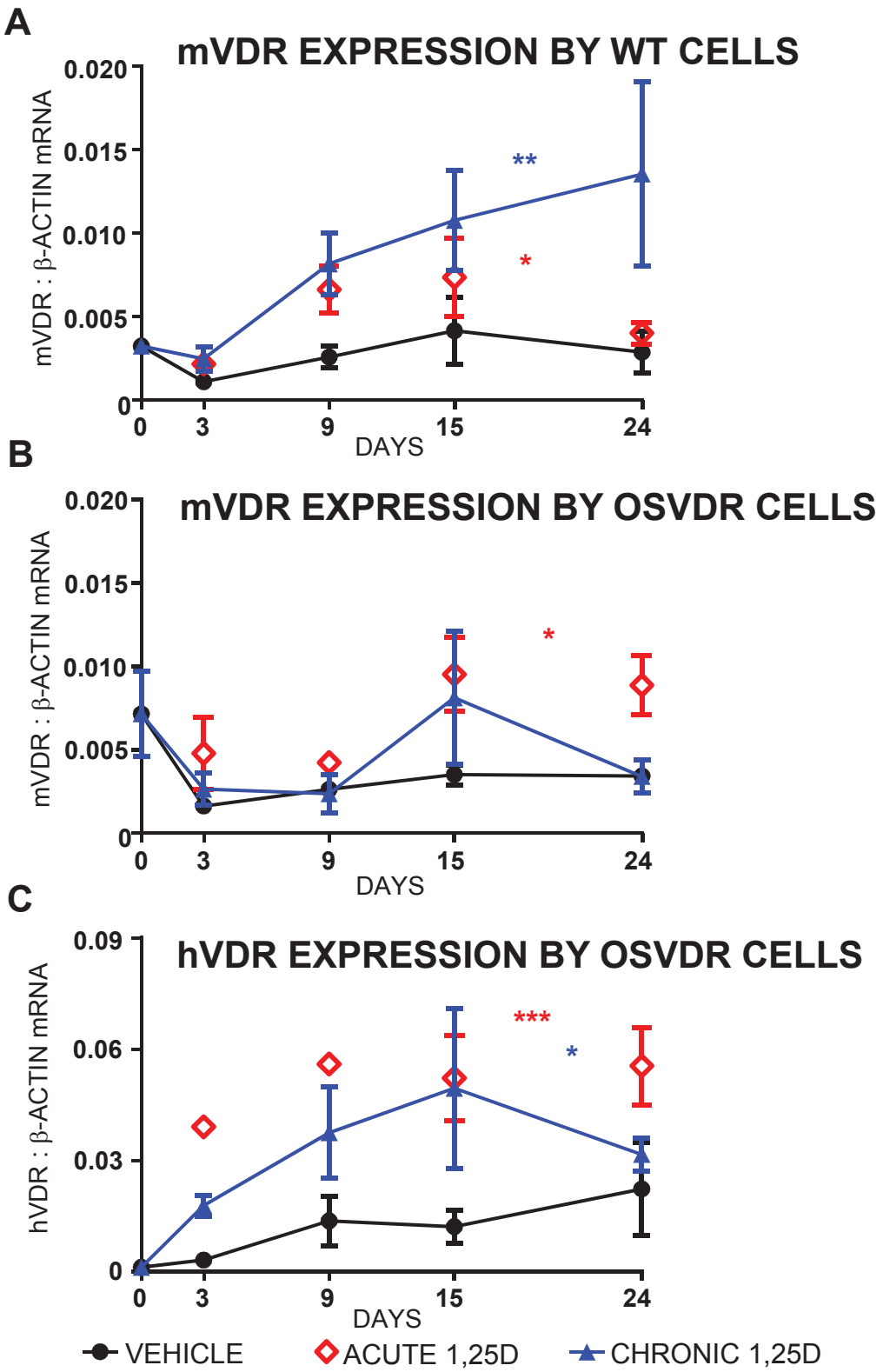

Figure 4.3.1 A-C **Vitamin D receptor status in WT and OSVDR cells**

The mRNA ratios of mouse vitamin D receptor (mVDR) to *β-Actin* by WT (A) and OSVDR (B) cells and the mRNA ratio of human vitamin D receptor (hVDR) to *β-Actin* by OSVDR cells only (C), with vehicle (black line), acute 1,25D (1 nM) (red dots) and chronic 1,25D (1 nM) (blue line) treatments in standard osteogenic differentiation media (1.8 mM total calcium). Three independent experiments for gene expression analyses were carried out and the error bars on graphs represent the standard errors of mean data collected from the three experiments (mean±SEM, n = 3; * indicates the effects of 1,25D treatments matching with the color of treatment groups, actue 1,25D (red), or chronic 1,25D (blue); * $p < 0.05$; ** $p < 0.01$; *** $p < 0.001$).

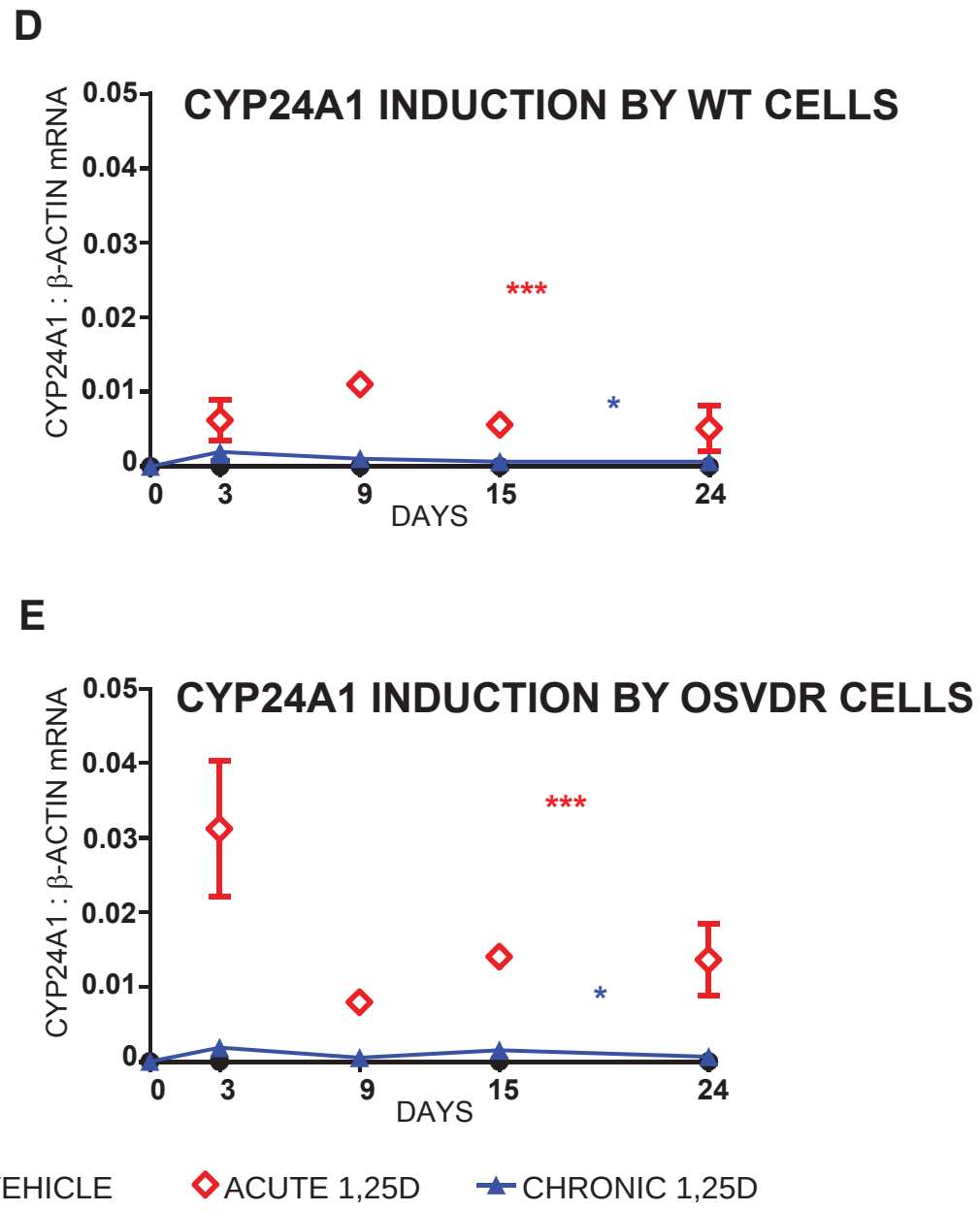

Figure 4.3.1 D and E ***Cyp24a1*** **induction in WT and OSVDR cells by 1,25D treatments**

The mRNA ratios of 25-hydroxyvitamin D 24-hydroxylase (*Cyp24a1*) to *β-Actin* by WT (D) and OSVDR (E) cells, with vehicle (black line), acute 1,25D (1 nM) (red dots) and chronic 1,25D (1 nM) (blue line) treatments in standard osteogenic differentiation media (1.8 mM total calcium). Three independent experiments for gene expression analyses were carried out and the error bars on graphs represent the standard errors of mean data collected from the three experiments (mean±SEM, n = 3; * indicates the effects of 1,25D treatments matching with the color of treatment groups, actue 1,25D (red), or chronic 1,25D (blue); * $p < 0.05$; ** $p < 0.01$; *** $p < 0.001$).

evident with chronic treatment. In OSVDR cells, which express approximately 6-fold more (total) *VDR* mRNA than WT cells, the induction of *Cyp24a1* mRNA by acute 1,25D treatment was on average 2-fold higher than in WT cells (Fig. 4.3.1D &E). Although *Cyp27b1* mRNA levels were detectable in both WT and OSVDR cells, 25D (100 nM) had no discernible biological effect on either cell type, as determined by gene expression and *in vitro* mineral deposition analyses (data not shown). Also, *Cyp24a1* was not induced in either cell type with 25D treatment during the 24-day culture period (data not shown). Thus, the treatment with the pro-hormone 25D, at least at the concentration of 100 nM, was demonstrated to be identical to vehicle treatment, presumably because the substrate was not converted to reactive levels of 1,25D.

4.3.2 Comparison of gene expression profiles of WT and VDRKO cells

Under standard osteogenic differentiation conditions, i.e. with 1.8 mM Ca^{2+} (discussed in Section 2.3.2), over 24 days of culture in the presence of vehicle, the expression of genes associated with differentiation of osteoblasts and the presence of osteocytes in WT and VDRKO cells was measured by qPCR, normalised to the expression of the housekeeping gene *β-actin*. The mRNA levels of *Col1a1* (type-I collagen), *Tnap* (tissue non-specific alkaline phosphatase), *Ank* (ankylosis protein), *Enpp1* (ecto-nucleotide pyrophosphatase/phosphodiesterase-1), *Ocn* (osteocalcin), *E11* (gp38), *Phex* (phosphate regulating endopeptidase homolog, X-linked), *Fgf23* (fibroblast growth factor 23), *Opg* (osteoprotegerin), *Runx2* (runt-related transcription factor) and *Osx* (osterix), were not different between WT and VDRKO cells (Fig. 4.3.2A-G and J, M, O, P), strongly implying that the starting populations of calvarial cells were identical in nature between genotypes. However, mRNA levels for *Mepe* (matrix extracellular phosphoglycoprotein) (Fig. 4.3.2H, $p < 0.05$), *Dmp1* (dentin matrix protein 1) (Figure 4.3.2K, $p < 0.01$) and *Rankl* (receptor activator of NF-kappa-B ligand) (Figure 4.3.2L, $p < 0.05$), were

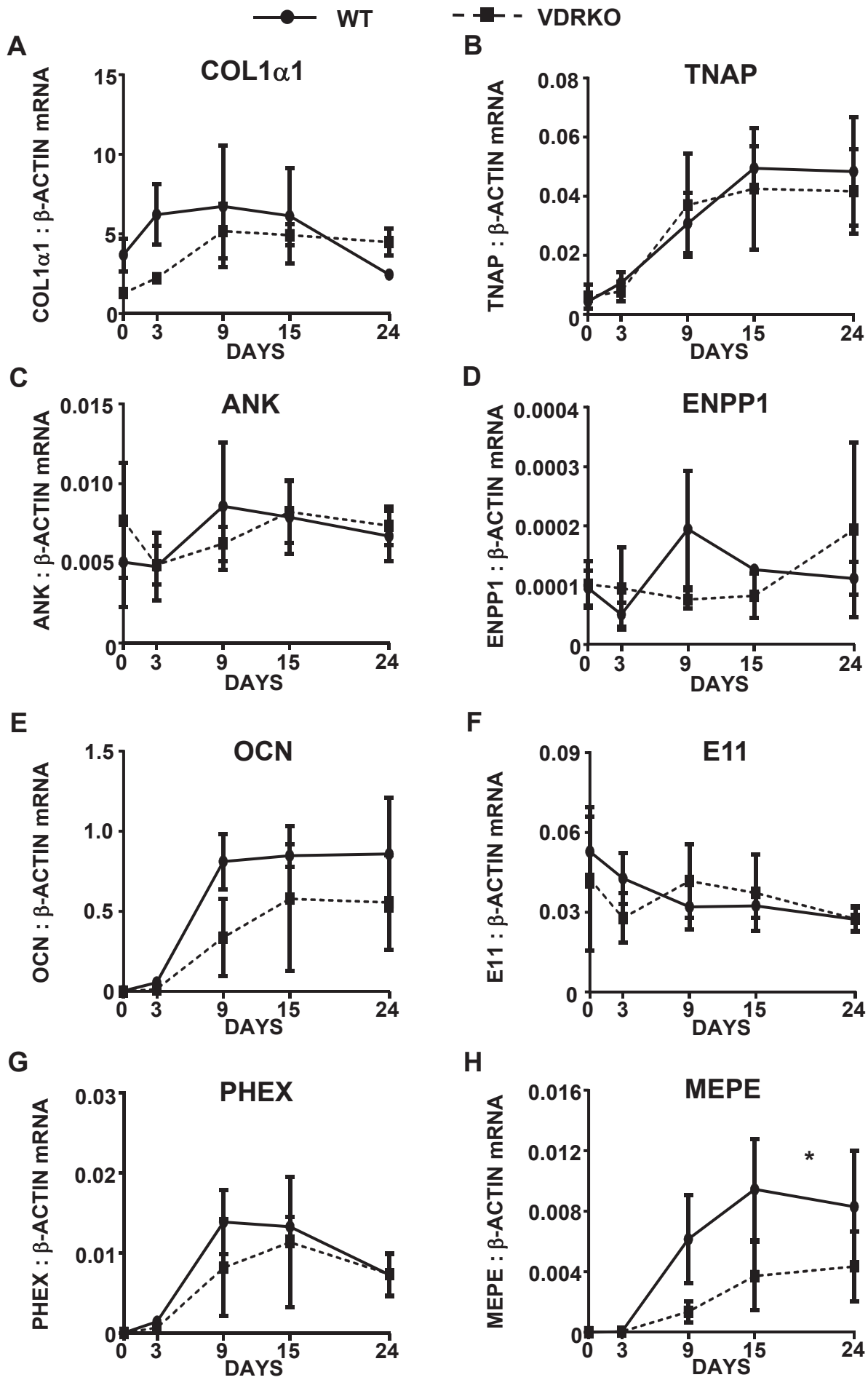
WT
VDRKO
A
COL1α1
COL1α1 : β-ACTIN mRNA
15
10
5
0
0 3 9 15 24
DAYS
B
TNAP
TNAP : β-ACTIN mRNA
0.08
0.06
0.04
0.02
0
0 3 9 15 24
DAYS
C
ANK
ANK : β-ACTIN mRNA
0.015
0.010
0.005
0
0 3 9 15 24
DAYS
D
ENPP1
ENPP1 : β-ACTIN mRNA
0.0004
0.0003
0.0002
0.0001
0
0 3 9 15 24
DAYS
E
OCN
OCN : β-ACTIN mRNA
1.5
1.0
0.5
0
0 3 9 15 24
DAYS
F
E11
E11 : β-ACTIN mRNA
0.09
0.06
0.03
0
0 3 9 15 24
DAYS
G
PHEX
PHEX : β-ACTIN mRNA
0.03
0.02
0.01
0
0 3 9 15 24
DAYS
H
MEPE
MEPE : β-ACTIN mRNA
0.016
0.012
0.008
0.004
0
*
0 3 9 15 24
DAYS

Figure 4.3.2 A-H **Comparison of gene expression profile of WT and VDRKO cells**

Relative gene expression by wild type (WT) (solid line) and vitamin D receptor knockout (VDRKO) (broken line) cells over the 24-day culture with standard osteogenic differentiation media supplied (1.8 mM total calcium). Three independent experiments for gene expression analyses were carried out and the error bars on graphs represent the standard errors of mean data collected from the three experiments (mean±SEM, n = 3).

A: *Col1α1* (type-I collagen)

B: *Tnap* (tissue nonspecific alkaline phosphatase)

C: *Ank* (ankloysis protein)

D: *Enpp1* (ecto-nucleotide pyrophosphatase/phosphodiesterase-1)

E: *Ocn* (osteocalcin)

F: *E11* (gp38)

G: *Phex* (phosphate regulating endopeptidase homolog, X-linked)

H: *Mepe* (matrix extracellular phosphoglycoprotein)

* $p<0.05$

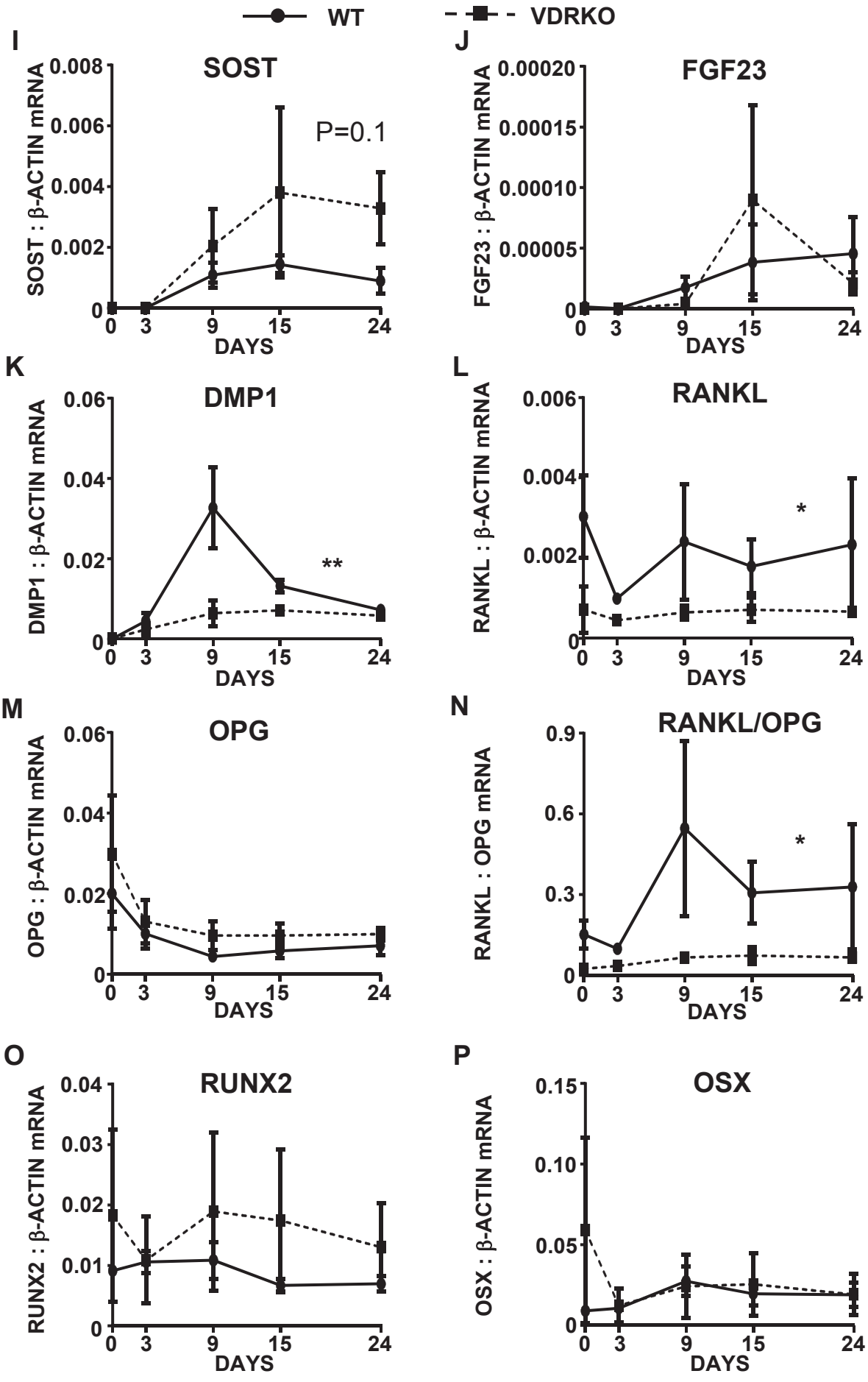
WT
VDRKO
I
SOST
P=0.1
SOST : β-ACTIN mRNA
0.008
0.006
0.004
0.002
0
0 3 9 15 24
DAYS
J
FGF23
FGF23 : β-ACTIN mRNA
0.00020
0.00015
0.00010
0.00005
0
0 3 9 15 24
DAYS
K
DMP1
DMP1 : β-ACTIN mRNA
0.06
0.04
0.02
0
**
0 3 9 15 24
DAYS
L
RANKL
RANKL : β-ACTIN mRNA
0.006
0.004
0.002
0
*
0 3 9 15 24
DAYS
M
OPG
OPG : β-ACTIN mRNA
0.06
0.04
0.02
0
0 3 9 15 24
DAYS
N
RANKL/OPG
RANKL : OPG mRNA
0.9
0.6
0.3
0
*
0 3 9 15 24
DAYS
O
RUNX2
RUNX2 : β-ACTIN mRNA
0.04
0.03
0.02
0.01
0
0 3 9 15 24
DAYS
P
OSX
OSX : β-ACTIN mRNA
0.15
0.10
0.05
0
0 3 9 15 24
DAYS

Figure 4.3.2 I-P **Comparison of gene expression profile of WT and VDRKO cells**

Relative gene expression by wild type (WT) (solid line) and vitamin D receptor knockout (VDRKO) (broken line) cells over the 24-day culture with standard osteogenic differentiation media supplied (1.8 mM total calcium). Three independent experiments for gene expression analyses were carried out and the error bars on graphs represent the standard errors of mean data collected from the three experiments (mean±SEM, n = 3).

I: ***Sost*** (sclerostin)

J: ***Fgf23*** (fibroblast growth factor 23)

K: ***Dmp1*** (dentin matrix protein 1)

L: ***Rankl*** (receptor activator of NF-kappa-B ligand)

M: ***Opg*** (osteoprotegerin)

N: ***Rankl/Opg***

O: ***Runx2*** (runt-related transcription factor)

P: ***Osx*** (osterix)

* $p<0.05$, ** $p<0.01$

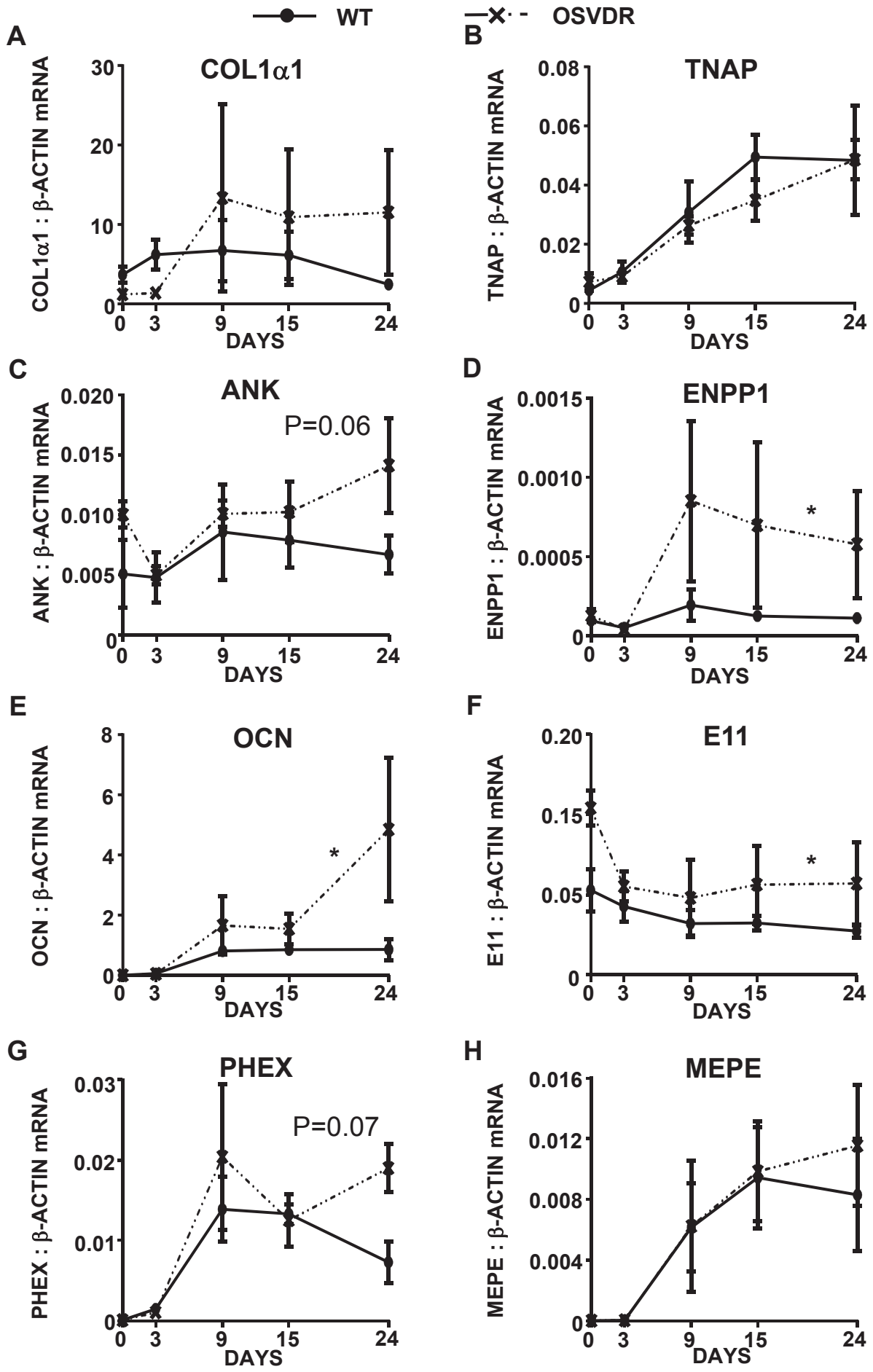
WT
OSVDR
A
COL1α1
COL1α1 : β-ACTIN mRNA
DAYS
B
TNAP
TNAP : β-ACTIN mRNA
DAYS
C
ANK
P=0.06
ANK : β-ACTIN mRNA
DAYS
D
ENPP1
ENPP1 : β-ACTIN mRNA
*
DAYS
E
OCN
OCN : β-ACTIN mRNA
*
DAYS
F
E11
E11 : β-ACTIN mRNA
*
DAYS
G
PHEX
P=0.07
PHEX : β-ACTIN mRNA
DAYS
H
MEPE
MEPE : β-ACTIN mRNA
DAYS

Figure 4.3.3 A-H **Comparison of gene expression profile of WT and OSVDR cells**

Relative gene expression by wild type (WT) (solid line) and over-expressed vitamin D receptor in osteocalcin expressing (OSVDR) (broken line) cells over the 24-day culture with standard osteogenic differentiation media supplied (1.8 mM total calcium). Three independent experiments for gene expression analyses were carried out and the error bars on graphs represent the standard errors of mean data collected from the three experiments (mean±SEM, n = 3).

A: *Col1α1* (type-I collagen)

B: *Tnap* (tissue nonspecific alkaline phosphatase)

C: *Ank* (ankloysis protein)

D: *Enpp1* (ecto-nucleotide pyrophosphatase/phosphodiesterase-1)

E: *Ocn* (osteocalcin)

F: *E11* (gp38)

G: *Phex* (phosphate regulating endopeptidase homolog, X-linked)

H: *Mepe* (matrix extracellular phosphoglycoprotein)

* $p < 0.05$

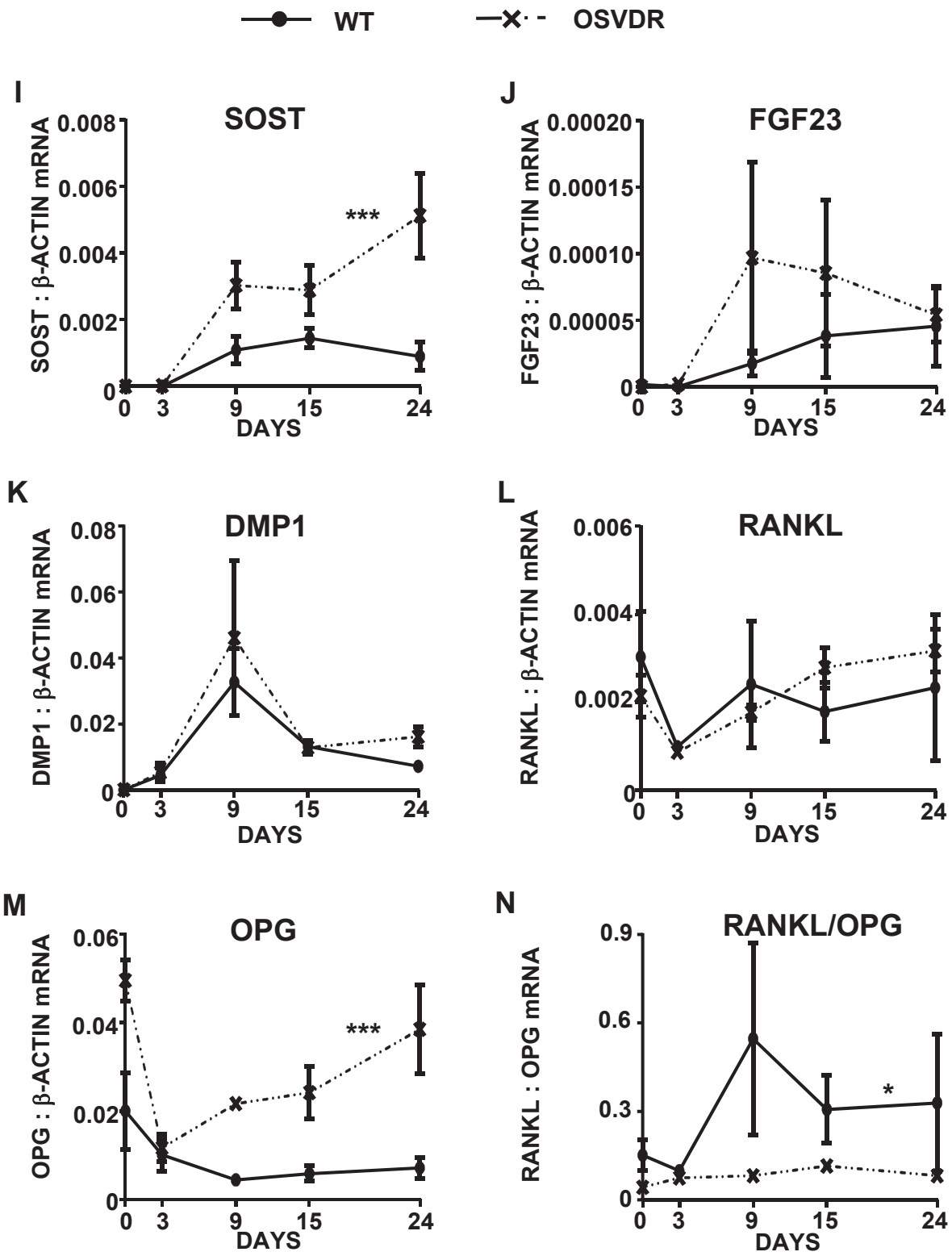
WT
OSVDR
I
SOST
SOST : β-ACTIN mRNA
0.008
0.006
0.004
0.002
0
***
0 3 9 15 24
DAYS
J
FGF23
FGF23 : β-ACTIN mRNA
0.00020
0.00015
0.00010
0.00005
0
0 3 9 15 24
DAYS
K
DMP1
DMP1 : β-ACTIN mRNA
0.08
0.06
0.04
0.02
0
0 3 9 15 24
DAYS
L
RANKL
RANKL : β-ACTIN mRNA
0.006
0.004
0.002
0
0 3 9 15 24
DAYS
M
OPG
OPG : β-ACTIN mRNA
0.06
0.04
0.02
0
***
0 3 9 15 24
DAYS
N
RANKL/OPG
RANKL : OPG mRNA
0.9
0.6
0.3
0
*
0 3 9 15 24
DAYS

Figure 4.3.3 I-N **Comparison of gene expression profile of WT and OSVDR cells**

Relative gene expression by wild type (WT) (solid line) and over-expressed vitamin D receptor in osteocalcin expressing (OSVDR) (broken line) cells over the 24-day culture with standard osteogenic differentiation media supplied (1.8 mM total calcium). Three independent experiments for gene expression analyses were carried out and the error bars on graphs represent the standard errors of mean data collected from the three experiments (mean ± SEM, n = 3).

I: *Sost* (sclerostin)

J: *Fgf23* (fibroblast growth factor 23)

K: *Dmp1* (dentin matrix protein 1)

L: *Rankl* (receptor activator of NF-kappa-B ligand)

M: *Opg* (osteoprotegerin)

N: *Rankl/Opg*

* $p < 0.05$, *** $p < 0.001$

significantly lower in VDRKO cells, as was the ratio of *Rankl/Opg* mRNA (Fig. 4.3.2N, $p < 0.05$). There was a trend for increased expression of *Sost* (sclerostin) mRNA levels in VDRKO cells, however this did not reach statistical significance (Fig. 4.3.2I, $p = 0.1$).

4.3.3 Comparison of gene expression profiles of WT and OSVDR cells

A similar comparison to that above was made between WT and OSVDR cells grown under standard osteogenic differentiation conditions in the presence of vehicle for 24 days in culture. As with WT and VDRKO cultures, the normalised mRNA levels of *Col1α1*, *Tnap* and *Fgf23* were not statistically different between WT and OSVDR cells (Fig. 4.3.2 A, B, J and Fig. 4.3.3 A, B, J). Unlike the WT/VDRKO comparison, however, *Mepe, Dmp1* and *Rankl* mRNA levels were also not different between WT and OSVDR (Fig. 4.3.2 H, K, L and Fig.4.3.3 H, K, L). The expression of *Enpp1* (Figure 4.3.3D, $p < 0.05$), *Ocn* (Fig. 4.3.3E, $p < 0.05$), *E11* (Figure 4.3.3F, $p < 0.05$), *Sost* (Fig. 4.3.3I, $p < 0.001$) and *Opg* (Fig. 4.3.3M, $p < 0.001$), were all significantly increased in OSVDR cells relative to WT. Also, the expression of *Ank* (Fig. 4.3.3C, $p = 0.06$) and *Phex* (Fig. 4.3.3G, $p = 0.07$), demonstrated a strong trend to be higher in OSVDR cells. Interestingly, as was the case with VDRKO cultures, the ratio of *Rankl/Opg* mRNA was significantly decreased in OSVDR cells (Fig. 4.3.3N, $p < 0.05$).

4.3.4 Expression levels of osteogenic differentiation-related genes under acute and chronic 1,25D treatments at day 24 of WT and OSVDR cell cultures

The pattern of gene expression in either WT or OSVDR cultures differentiated for 24 days treated acutely or chronically with 1,25D is summarised in Table 4.3.4. Following culture in standard differentiation media (1.8 mM Ca^{2+}), WT cell cultures at day 24 expressed genes *Col1a1 ,Tnap, E11, Mepe,* and *Opg* that were not altered by either acute or chronic 1,25D treatment (Fig. 4.3.4 A, B, F, H, M). The mRNA levels of *Ank, Enpp1, Ocn, Phex, Sost* and *Fgf23* were also not changed by acute 1,25D but were increased by

Gene	WT		OSVDR	
	ACUTE 1,25D	CHRONIC 1,25D	ACUTE 1,25D	CHRONIC 1,25D
Col-1α1	---	---	---	---
Tnap	---	---	↓	↓↓
Ank	---	↑	---	---
Enpp1	---	↑	↑	---
Ocn	---	↑	↓	↓
E11	---	---	---	---
Phex	---	↑	↓	↓
Mepe	---	---	↓	↓
Sost	---	↑	↓	↓↓
Fgf23	---	↑↑	---	↑↑
Dmp1	↓	---	↓	---
Rankl	↑	↑	↑↑	---
Opg	---	---	↓	↓
Rankl/Opg	---	---	↑↑	---

Table 4.3.4. In comparison of vehicle treatment and acute 1,25D or chronic 1,25D treatments, '---' indicates the mRNA level of gene of interest not changed; '↓' indicates the mRNA level of gene of interest decreased ; '↑' indicates the mRNA level of gene of interest increased. The numbers of '↓' or '↑' indicate the proportion of decrease or increase of the mRNA levels, respectively.

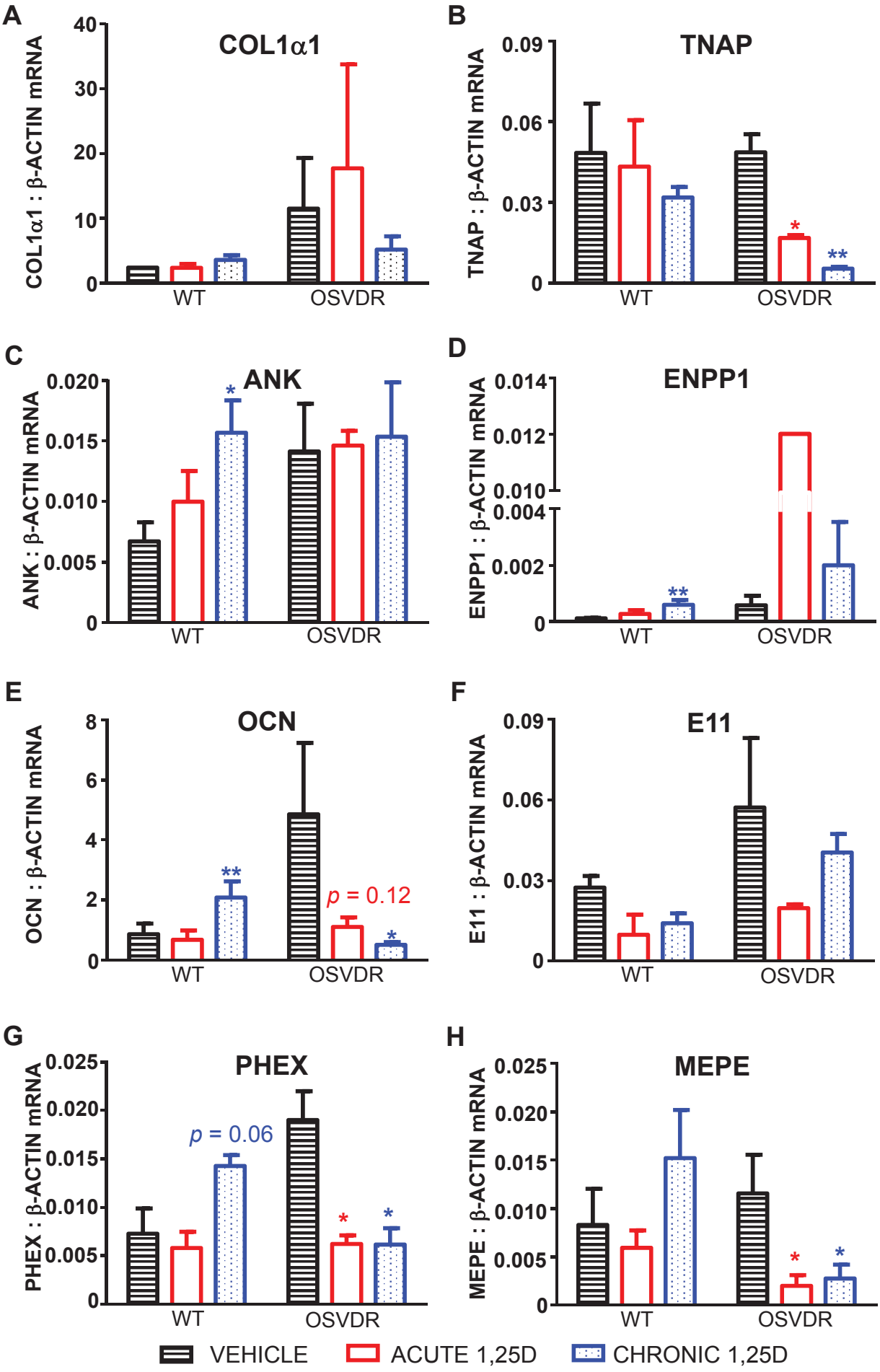
A
COL1α1
COL1α1 : β-ACTIN mRNA
40
30
20
10
0
WT
OSVDR
B
TNAP
TNAP : β-ACTIN mRNA
0.09
0.06
0.03
0
*
**
C
ANK
ANK : β-ACTIN mRNA
0.020
0.015
0.010
0.005
D
ENPP1
ENPP1 : β-ACTIN mRNA
0.014
0.012
0.010
0.004
0.002
E
OCN
OCN : β-ACTIN mRNA
8
6
4
2
p = 0.12
F
E11
E11 : β-ACTIN mRNA
G
PHEX
PHEX : β-ACTIN mRNA
0.025
p = 0.06
H
MEPE
MEPE : β-ACTIN mRNA
VEHICLE
ACUTE 1,25D
CHRONIC 1,25D

Figure 4.3.4 A-F **Osteogenic differentiation related gene expressions under acute and chronic 1,25D treatments by Day-24 WT and OSVDR cell cultures**

The mRNA ratios of osteogenic differentiation related genes, *Col1α1* (A), *Tnap* (B), *Ank* (C), *Enpp1* (D), *Ocn* (E), *E11* (F), *Phex* (G), *Mepe* (H) to *β-Actin* by Day-24 of WT and OSVDR cell cultures, with vehicle (black bar), acute 1,25D (1nM) (red bar) and chronic 1,25D (1nM) (blue bar) treatments in standard osteogenic differentiation media (1.8 mM total calcium). Three independent experiments for gene expression analyses were carried out and the error bars on graphs represent the standard errors of mean data collected from the three experiments. (mean±SEM, n = 3; * indicates the effects of 1,25D treatments matching with the color of treatment groups, actue 1,25D (red), or chronic 1,25D (blue); * $p < 0.05$; ** $p < 0.01$; *** $p < 0.001$)

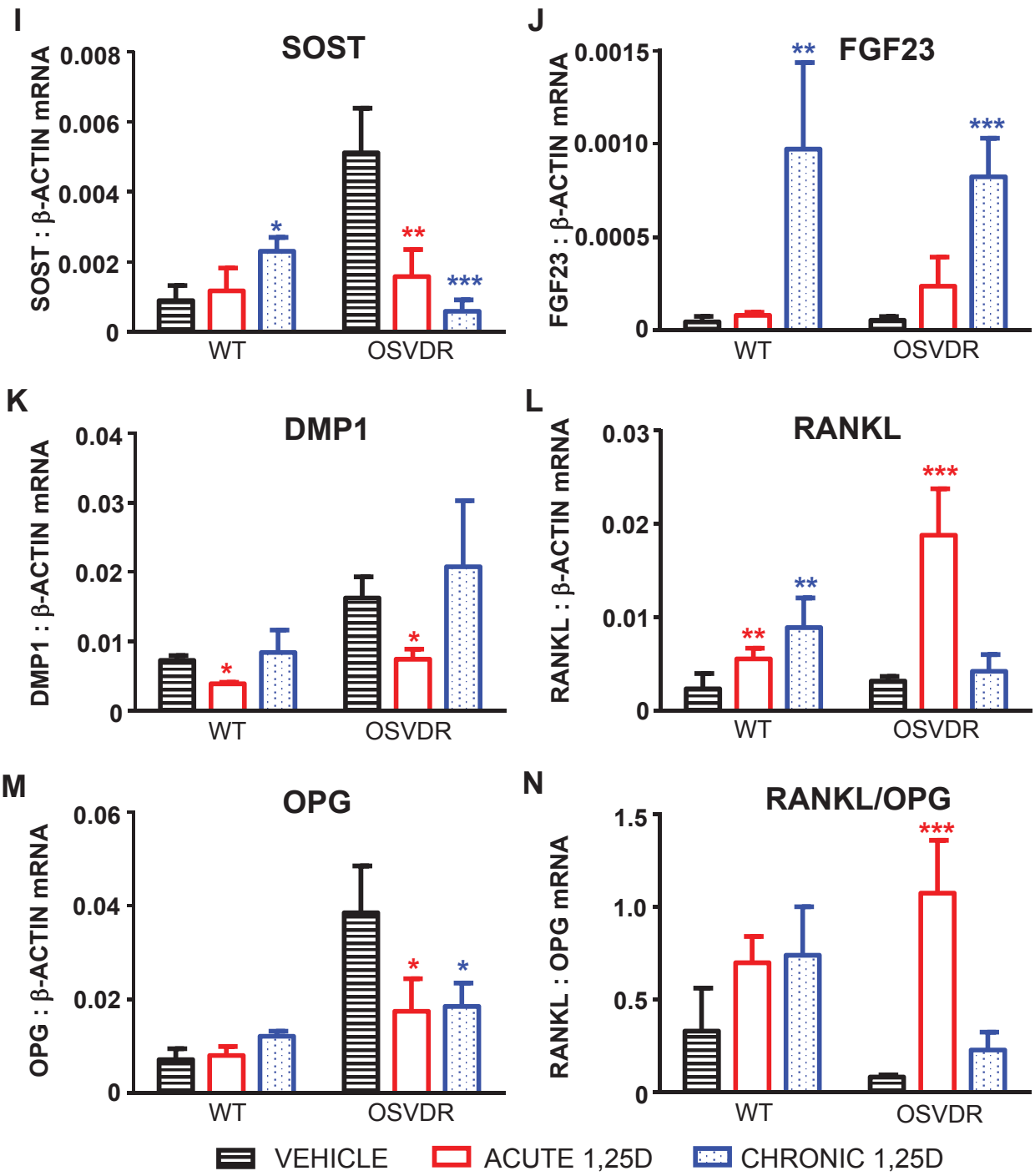

Figure 4.3.4 I-N **Osteogenic differentiation related gene expressions under acute and chronic 1,25D treatments by Day-24 WT and OSVDR cell cultures**

The mRNA ratios of osteogenic differentiation related genes, *Sost* (I), *Fgf23* (J), *Dmp1* (K), *Rankl* (L), *Opg* (M) to *β-Actin* and *Rankl/Opg* (N), by Day-24 of WT and OSVDR cell cultures, with vehicle (black bar), acute 1,25D (1nM) (red bar) and chronic 1,25D (1nM) (blue bar) treatments in standard osteogenic differentiation media (1.8 mM total calcium). Three independent experiments for gene expression analyses were carried out and the error bars on graphs represent the standard errors of mean data collected from the three experiments. (mean±SEM, n = 3; * indicates the effects of 1,25D treatments matching with the color of treatment groups, actue 1,25D (red), or chronic 1,25D (blue); * $p < 0.05$; ** $p < 0.01$; *** $p < 0.001$)

chronic 1,25D treatment (Fig. 4.3.4 C, D, E, G, I, J); the mRNA level of *Dmp1* was decreased by acute 1,25D treatment but not changed by chronic 1,25D (Fig 4.3.4 K); the mRNA level of *Rankl* was increased by both 1,25D treatments (Fig. 4.3.4 L).

In OSVDR cell cultures after 24 days of differentiation, the mRNA level *Dmp1* was inhibited by acute 1,25D treatment, however unaffected under chronic 1,25D treatment (Fig. 4.3.4 K). The mRNA levels of *Tnap*, *Ocn*, *Phex*, *Mepe*, *Sost* and *Opg* were inhibited by both acute and chronic 1,25D treatments (Fig. 4.3.4 B, E, G, H, I, M). Interestingly, the mRNA expression of *Fgf23* was greatly induced by chronic 1,25D treatment only (Fig. 4.3.4 J). Conversely, the mRNA levels of *Enpp1* and *Rankl* were increased by acute 1,25D only but unchanged by chronic 1,25D (Fig. 4.3.4 D and L). Finally, the mRNA levels of *Col1a1, Ank* and *E11* remained unchanged by either acute or chronic 1,25D treatments (Fig. 4.3.4 A, C, F).

4.3.5 Effect of chronic 1,25D treatment on in vitro mineral deposition by VDRKO, WT and OSVDR cells under conditions of total extracellular calcium at either 1.8 mM or 2.8 mM

Next, the effect of 1,25D on *in vitro* mineralisation by calvarial-derived cells from WT, OSVDR and VDRKO mice, was analysed. Since the mineralised matrix is relatively slow to develop, it was presumed that acute 1,25D treatments would not yield measurable changes, therefore only the effects of chronic 1,25D treatment were measured, The degree of *in vitro* mineralisation by VDRKO, WT and OSVDR cells was visualised by both Alizarin Red (calcium) and Von Kossa (phosphate) staining, and representative images of stained day 15 and day 24 cultures are shown in figures 4.3.5A and 4.3.5B. Increasing the extracellular calcium concentration to 2.8 mM enhanced the mineral deposition compared to wells containing 1.8 mM. 1,25D treatment inhibited mineral deposition by both WT and OSVDR cells in the presence of 1.8 mM extracellular calcium but had no

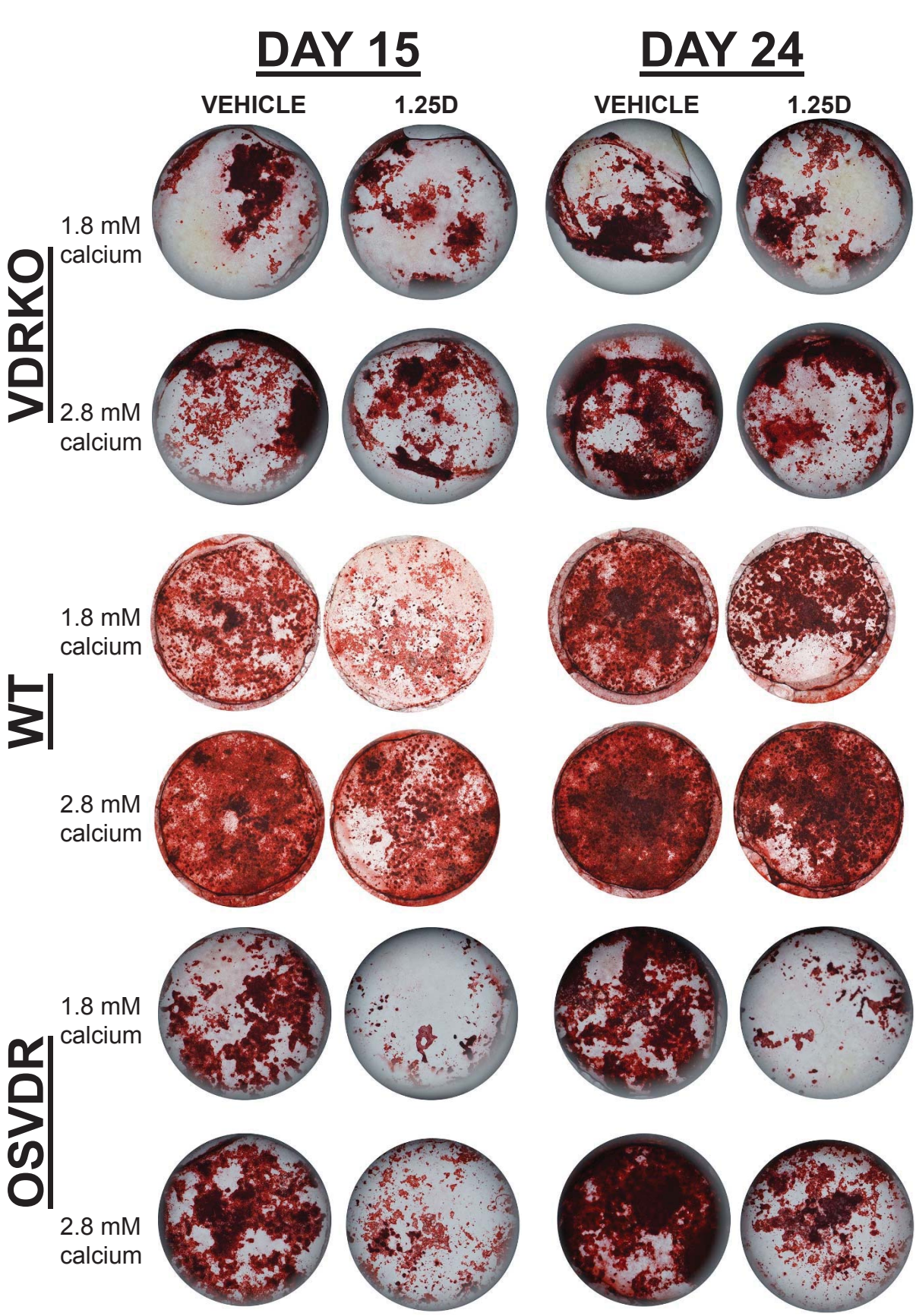

Figure 4.3.5 A **Alizarin red staining of mineralisation assay by VDRKO, WT and OSVDR cells**

Visualisation of mineralisation assay of Day 15 and Day 24 cultures of VDRKO, WT and OSVDR cells with vehicle and chronic 1,25D (1 nM) treatments with 1.8 and 2.8 mM total calcium presented in culture media, by Alizarin Red staining on calcium in red colour. Three independent experiments were carried out and a representative experiment is shown. All the treatment groups showed the similar biological effects within these three experiments.

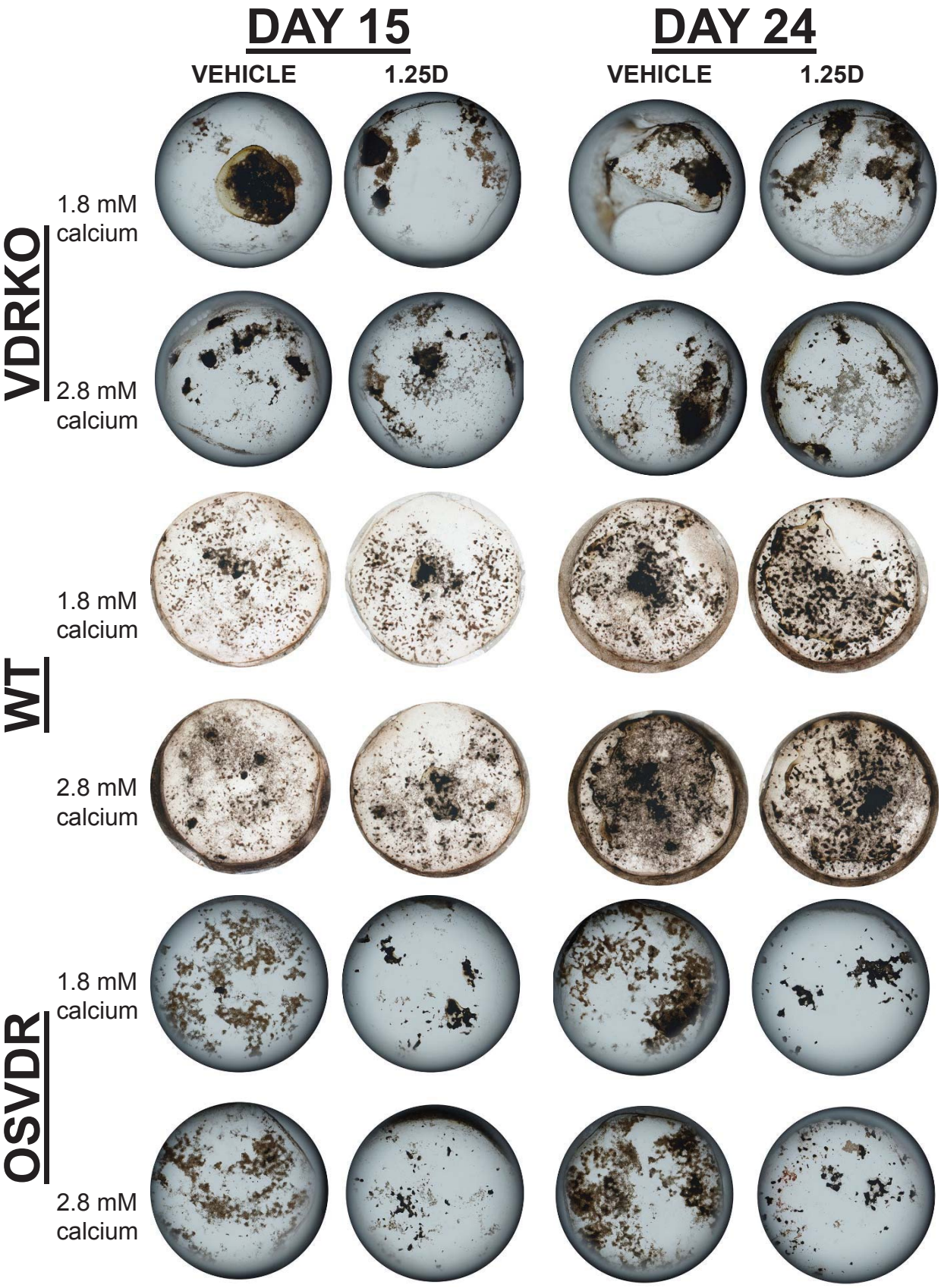

Figure 4.3.5 B **Von Kossa staining of mineralisation assay by VDRKO, WT and OSVDR cells** Visualisation of mineralisation assay of Day 15 and Day 24 cultures of VDRKO, WT and OSVDR cells with vehicle and chronic 1,25D (1 nM) treatments with 1.8 and 2.8 mM total calcium presented in culture media, by Von Kossa staining on phosphate in black/brown colour. Three independent experiments were carried out and a representative experiment is shown. All the treatment groups showed the similar biological effects within these three experiments.

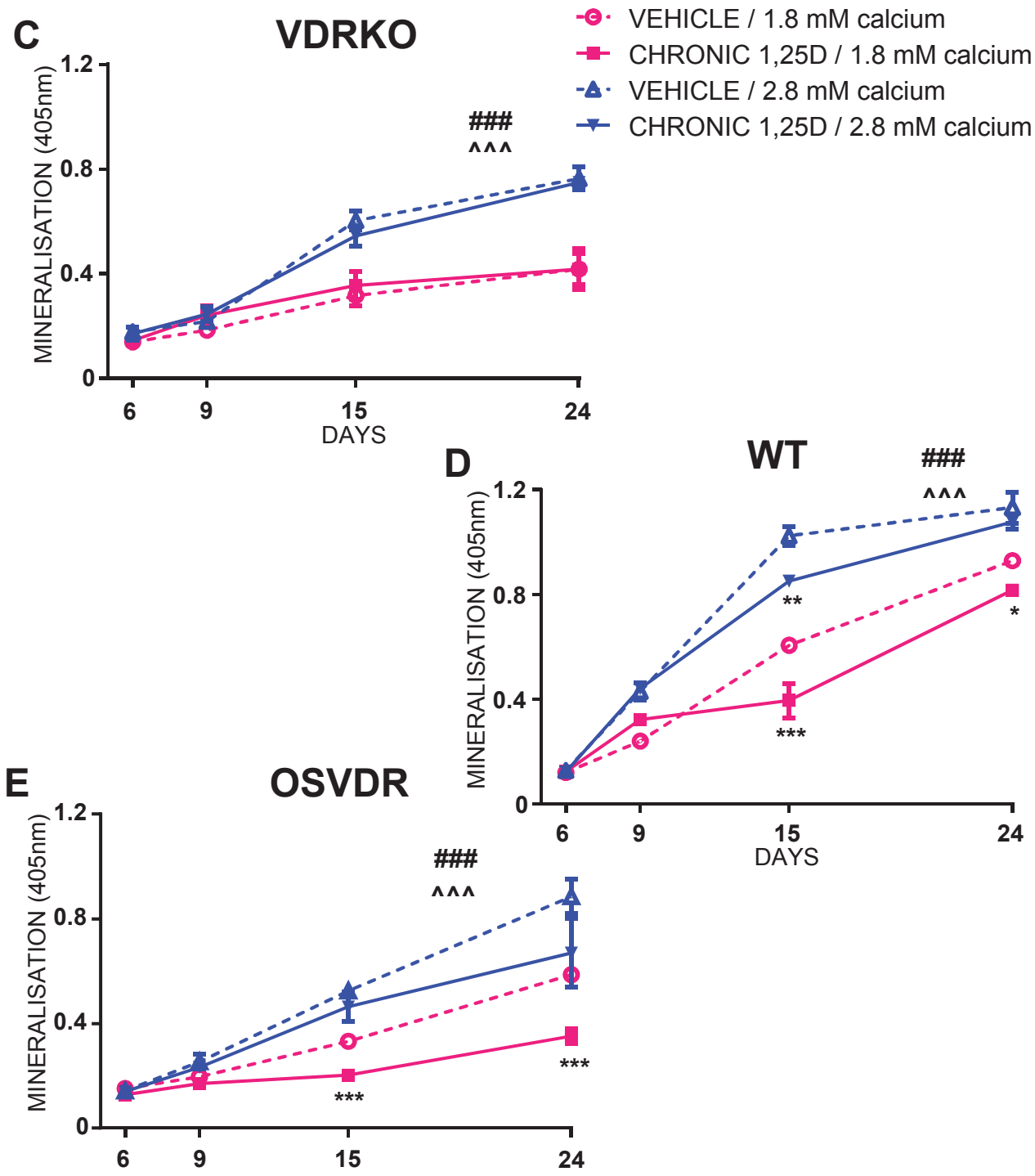

Figure 4.3.5 C-E ***In vitro*** **mineralisation curve by the quantification of Alizarin Red staining on mineralisation assays of VDRKO, WT and OSVDR cells**

In vitro mineralisation curve by VDRKO (C), WT (D) and OSVDR (E) cells with vehicle (broken lines) and chronic 1,25D (1nM) (solid lines) treatments with 1.8 mM total calcium (pink) and 2.8 mM total calcium (blue) presented in culture media reflected by the quantification of Alizarin Red staining on mineralisation assays. Three independent experiments were carried out and a representative experiment is shown. The error bars on the graphs represented 4 replicates of cell culture wells for each treatment group. All the treatment groups showed the similar biological effects within these three experiments (Effect of 1,25D: *** $p < 0.001$, ** $p < 0.01$, * $p < 0.05$; Effect of calcium: ^^^ $p < 0.001$; Effect of time: ### $p < 0.001$).

effect on VDRKO cells. This inhibition of mineral deposition was apparently reduced when the extracellular calcium concentration was increased to 2.8 mM (Fig. 4.3.5A&B).

The deposited mineral as detected by Alizarin Red stains was quantified following solubilisation and subsequent measurement of light absorption at 405_{nm}. Mineral deposition by VDRKO, WT and OSVDR cells increased over the 24-day culture ($p < 0.001$). However, there were no significant differences between the three genotypes with respect to relative the levels of mineral deposited overall. The elevated calcium level of 2.8 mM generally enhanced mineral deposition in cell of all three genotypes compared to 1.8 mM ($p < 0.001$). As expected, in VDRKO cultures, 1,25D treatment had no effect mineral deposition regardless of the calcium concentration in media (Fig. 4.3.5 C). In WT cultures, with 1.8 mM Ca^{2+}, 1,25D treatment inhibited mineralisation by 20% ($p < 0.001$) at day 15 and by 10% ($p < 0.05$) at day 24. With 2.8 mM Ca^{2+} in the culture media, 1,25D treatment inhibited mineralisation on day 15 by 17% ($p < 0.01$) but no effect was observed at day 24 (Fig. 4.3.5 D). At the standard calcium concentration (1.8 mM), OSVDR cultures responded to 1,25D in a fashion indistinguishable from WT cells, with inhibition of mineralisation by 18% ($p < 0.001$) at day 15 and by 20% ($p < 0.001$) on Day 24. Similarly, with 2.8 mM Ca^{2+} in the culture media, the deposited mineral levels between vehicle and 1,25D treatments were not statistically different (Fig. 4.3.5 E).

4.4 Discussion

In this study, the role of VDR in osteoblast differentiation was investigated by exposing primary osteoblast cultures derived from the calvariae of WT, VDRKO and OSVDR mice to a pharmacological concentration of 1,25D (1 nM) compared with vehicle treatment. Cells isolated from these mouse strains expressing different levels of *Vdr* mRNA presumably express different levels of VDR protein, as was demonstrated by Demay *et al.* for the VDRKO cells (124) and Gardiner *et al.* for the OSVDR mouse line *in vivo*

(104). In each of the cell culture experiments in which WT, VDRKO and OSVDR cells were cultured under vehicle treatment, 10% v/v foetal bovine serum (FBS) was supplied in the osteogenic differentiation media for normal cell growth and development, which constituted a 'treatment' of approximately 30 pM 1,25D, measurable by a commercial assay (personal communication from Dr. Andrew Turner). It was previously reported that 1,25D at a concentration of less than 100 pM was able to enhance osteogenesis (138). Hence, in this context, even under the vehicle treatment, cells would be exposed to a basal level of 1,25D within the physiological range. Thus, effectively in this study, 1,25D concentrations within the low physiological range were compared to a pharmacological level of 1,25D (1 nM) for their effects on osteoblast differentiation.

Based on real-time PCR quantification targeting the functional motif within mouse *Vdr* and human *VDR* gene sequences (specifically for the OSVDR model), the total *Vdr* mRNA level was confirmed to be ablated in VDRKO cells and dramatically elevated (at least 6-fold based on the comparison of relative mRNA levels) in OSVDR cells compared to WT cells. The cell properties of the mutant model VDRKO and transgenic model OSVDR were compared to those of WT cells separately, under vehicle treatment (with a low physiological concentration of 1,25D). VDRKO cells exhibited a similar capability for osteoblast differentiation and mineral deposition as WT cells, as evidenced by similar mRNA levels of osteoblast specific transcriptional factors (*Runx2* and *Osx*), similar mRNA levels of mineralisation related genes (*Col1a1*, *Tnap*, *Ank* and *Enpp1*), and similar mRNA levels of a number of genes related to osteoblast differentiation (*Opg*, *Ocn*, *Cx43*, *E11*, *Fgf23* and *Phex*). These data suggest that VDR is not essential for osteoblastogenesis and the ability of these cells to deposit mineral. However, the levels of the important osteocyte marker *Dmp1* (35) were markedly lower in VDRKO cells, particularly on Day 9. Messenger RNA levels for the osteoclast differentiation and activation factor *Rankl* were also significantly lower in VDRKO cells. These data are consistent with previous

studies demonstrating that *Dmp1* and *Rankl* are directly upregulated by 1,25D, acting through VDRE's in the respective gene promoter regions (139,140), and endogenous 1,25D present in the culture medium driving the basal expression of these genes. The lower mRNA levels of *Dmp1* and *Rankl* in VDRKO cultures suggest that VDR activity may contribute to achieving a mature and normal osteocyte phenotype (35) capable of supporting osteoclast formation (141). Further, the mineralisation modulating gene, *Mepe*, was more lowly expressed in VDRKO cells. *Mepe* expression has been demonstrated to be either up- or down regulated by 1,25D under different circumstances. For example, in a study that utilised the osteocyte-like cell line IDG-SW3 (142), *Mepe* mRNA expression was shown to be up-regulated by 1,25D (143). However, in other studies using mouse osteoblasts and the immature osteoblast-like cell line MC3T3-E1, *Mepe* expression was shown to be decreased by 1,25D (144) and a markedly increased *Mepe* mRNA expression level was reported in VDRKO mouse calvarial cell cultures compared to WT (145). However, the exact mechanism, by which 1,25D regulates *Mepe* is not understood and therefore further study is required to elucidate why *Mepe* mRNA levels were lower in VDRKO calvarial cultures in this study.

In OSVDR cells, in which human *VDR* is over-expressed, phenotypic differences were also observed compared to WT cells. Although the mRNA levels of pro-anabolic factors for mineralisation, *Col1a1* and *Tnap* were not different between the genotypes, the expression of the mineralisation inhibitors, *Ank* and *Enpp1* was increased in OSVDR cells. This pattern of gene expression was observed under conditions, in which mineral deposition was equivalent between WT and OSVDR cells. This implies that mRNA levels of *Ank* and *Enpp1* are increased during differentiation of OSVDR osteoblasts in order to maintain an 'appropriate' level of mineral deposition, perhaps acting as a brake under a condition where mineral deposition is enhanced by the over-expression of *VDR*. The mRNA level of *Dmp1* rose transiently up on Day 9 in OSVDR cultures in a similar pattern

to that seen in WT cultures. This pattern of mRNA expression again suggests that the increase in expression of *Dmp1* during mineralisation and differentiation requires basal VDR activity. Previous *in vivo* data suggested that trabecular bone volume (%BV/TV) in OSVDR transgenic mice increased because of the reduction in the *Rankl/Opg* mRNA ratio, in which the *Opg* level was unchanged and *Rankl* expression was reduced (136). In the current study, the lower *Rankl/Opg* mRNA ratio in OSVDR cells was confirmed by mRNA measurement, although this was as a result of a markedly increased *Opg* level with an unchanged *Rankl* mRNA level. Thus OSVDR osteoblasts are once again characterised as less capable of supporting osteoclastogenesis in response to 1,25D within the physiological range. However, the basis for a different mechanism in the reduction of the *Rankl/Opg* mRNA ratio in the two studies requires further investigation. While it is widely accepted that 1,25D induces *Rankl* mRNA expression and inhibits that of *Opg* in mouse osteoblasts (146), it may be that these genes are co-ordinately regulated and that ultimately it is the ratio between them that delivers the important functional outcome. For example, it was previously shown that while *RANKL* and *OPG* mRNA levels were not different between osteoporotic and non-osteoporotic women, the ratio of *RANKL*:*OPG* mRNA was different (147).

The expression of the mature osteoblast and osteocyte products, *Ocn*, *Phex* and *Sost* were found to be increased in OSVDR cells. This finding suggested that by exposing cells to physiological level of 1,25D, OSVDR cells achieved a more mature differentiation stage within the timeframe of the experiment compared to WT cells, by virtue of their increased *VDR* expression. Intriguingly, the expression of *Sost* mRNA in both VDRKO and OSVDR cells was higher than was seen in WT cells. These data suggest that 1,25D modulates the expression of *Sost* indirectly through other factors. One candidate factor may be RUNX2; an important RUNX2 responsive element in the *Sost* gene promoter has been identified (148) and RUNX2 protein has been reported to interact with VDR to

enhance the nuclear transcriptional capability of 1,25D (149). Alternatively, *Sost* expression is induced by BMP4 (bone morphogenetic protein 4) and the induction is further enhanced in combination with 1,25D (150). However, the exact mechanism, either direct or indirect, by which 1,25D regulates the *Sost* gene is not defined. Our data here indicate that *Sost* mRNA expression can be up-regulated when 1,25D activity is either ablated or elevated. Further study is required to elucidate the molecular basis of 1,25D regulation of *Sost* expression.

Cultures of osteoblasts from WT, VDRKO and OSVDR mice were also exposed to a pharmacological level of 1,25D (1 nM) either acutely for 24 hours, to assess the direct regulation through VDREs over a short period, or chronically throughout the 24 day culture period, to assess the combination of direct regulation and indirect effects resulting from osteoblast cell maturation. In VDRKO cultures, there was no detectable induction of *Cyp24a1* mRNA expression by 1,25D treatment. Also, when VDRKO cell cultures were treated chronically with 1,25D, no biological effects were seen in terms of either osteogenesis-related gene expression (shown in Appendix II) or mineral deposition. These data confirm that the expression of 1,25D-responsive genes, including *Cyp24a1*, is highly dependent on VDR and therefore the effects of 1,25D reported here on osteoblast differentiation and mineral deposition in WT and OSVDR cells can all be assumed to be dependent on VDR.

When the total (i.e. both endogenous and transgenic) *VDR* mRNA level was markedly increased in OSVDR cells compared to WT cells, *Cyp24a1* mRNA induction following 24-hour (acute) stimulation by pharmacological levels of 1,25D was around 2-fold higher in OSVDR cells. This finding indicates, perhaps not surprisingly, that when 1,25D is present in marked excess, catabolism of 1,25D by osteoblasts is dependent on the level of VDR. The *Cyp24a1* mRNA expression by both cell types dropped to a similar level by

the end of a 72-hour period (i.e. chronic treatment) presumably because the 1,25D was catabolised, following which transcriptional activity was reduced. To fully elucidate the metabolism of 1,25D in WT and OSVDR cells, a more detailed time course within the 72 hour period would be required to enable the course of *Cyp24a1* mRNA and protein expression to be closely mapped. The 1,25D residual concentration in culture media at each of the time points would also be a useful and critical readout as to the metabolic status of the hormone.

Data describing mRNA levels of target genes associated with differentiation of osteoblasts at day 24 of culture in both WT and OSVDR cells under acute and chronic 1,25D treatments are presented here as a snapshot of the whole differentiation process for clarity. The detailed mRNA levels throughout the 24-day time course were consistent with the day 24 patterns (shown in Appendices II & III). As discussed previously, the acute 1,25D treatment most likely represents direct regulation of the transcriptional activities of 1,25D/VDR acting via VDREs. The chronic 1,25D treatment represents a combination of direct regulation of transcriptional activity (both primary and downstream responsive genes) and net effects of 1,25D on cell differentiation, i.e. effects due to induced phenotypic changes in the responding cells.

In WT cells, the levels of a panel of differentiation-related genes including *Ocn*, *Ank*, *Opg*, *Sost*, *Fgf23* and *Phex*, were elevated by chronic but not acute 1,25D treatments. The mRNA level of *Rankl* was increased by both 1,25D treatments. These findings support the proposal that prolonged exposure of WT cells to a pharmacological level of 1,25D promotes osteoblast differentiation and maturation. However, most of the effects of 1,25D were not observed following acute exposure, indicating that prolonged exposure is required, which in turn suggests that the effective intracellular level of 1,25D is maintained at a low level due to the high level of *Cyp24a1* induction and the efficient

catabolic activity the CYP24 enzyme. The promoting role of 1,25D on WT cells could therefore be the combination of direct effects on VDREs on some of the key genes (yet to be identified) in the differentiation process and then the enhancement of the cellular maturation process by 1,25D.

In contrast to effects in WT cultures, acute 1,25D treatment had inhibitory effects on mRNA expression of *Tnap*, *Ocn*, *Phex*, *Mepe*, *Sost*, *Dmp1* and *Opg* in OSVDR cells. Inhibitory effects on mRNA levels of *Tnap*, *Ocn*, *Phex*, *Mepe*, *Sost* and *Opg* were also seen with chronic 1,25D treatment in OSVDR cultures. Furthermore, OSVDR exhibited elevated expression of differentiation related genes in response to vehicle (see Section 4.3.3), which contains a physiological 1,25D dose. A possible interpretation of the difference between OSVDR and WT cultures is that with elevated total VDR expression (i.e. as in OSVDR), sensitivity to physiological (vehicle) 1,25D levels is enhanced and a positive effect of these low 1,25D levels on osteoblast differentiation is seen basally. Under stimulation with pharmacological 1,25D levels however, negative regulation of gene expression occurs in an attempt by the cells to regulate the differentiation process in OSVDR cells. These inhibitory effects of 1,25D on gene expression are presumably working through VDREs directly since effects were seen with acute 1,25D treatment. The data presented here invokes the concept that VDR in osteoblasts plays the role of modulating osteoblast activities by either promoting or inhibiting osteogenesis, depending on the levels of both VDR and 1,25D in the cells.

The genes *Enpp1*, *Rankl* and *Fgf23* were all up-regulated in both WT and OSVDR cells by exogenous 1,25D treatment. In WT cells, *Enpp1* and *Rankl* trended to increase in response to acute exposure but were significantly up-regulated by chronic 1,25D treatment. Consistent with their elevated expression of VDR, the levels of *Enpp1* and *Rankl* in OSVDR cultures were greatly induced by acute 1,25D treatment, but were not

changed by chronic 1,25D exposure, presumably because of the enhanced rate of CYP24-mediated 1,25D catabolism under these conditions. The finding of *Rankl* mRNA induction by 1,25D stimulation here is consistent with previously reported data that *RANKL*/*Rankl* was up-regulated by 1,25D through the multiple VDREs in its promoter (140). We further propose that the regulation of *Rankl* expression by 1,25D is tightly related to the level of VDR activity. However, to our knowledge, there are no available published data reporting the mechanism of 1,25D regulation of *Enpp1* expression. Based on our findings here, the pattern of *Enpp1* induction under acute 1,25D treatment in WT and OSVDR cells appears very similar to that of *Rankl* induction, suggesting that 1,25D also acts though potential VDREs within the *Enpp1* promoter; future molecular studies will be needed to test this hypothesis.

The mRNA expression of *Fgf23* in both WT and OSVDR cells was not changed by acute 1,25D treatment but was up-regulated 10-fold by chronic 1,25D treatment. FGF23 was previously shown to be up-regulated by 1,25D through a VDRE-mediated mechanism (151). Our data indicate that at the concentration of 1 nM, the up-regulation of *Fgf23* expression by 1,25D stimulation requires more than 24 hours. Moreover, the proportion of *Fgf23* induction by chronic 1,25D increased by culture time course (referred to Appendix II. J). This finding also suggests that the up-regulation of *Fgf23* expression by 1,25D is related to cell differentiation.

Mineralisation assays were employed in this study as a functional readout of osteoblast differentiation. With respect to gene expression, the presence of 2.8 mM Ca^{2+} in the culture media had no apparent effect compared to 1.8 mM (see Appendices II & III). This was surprising given that a previous study from our group showed a gene expression effect of calcium in human primary osteoblasts, with calcium up-regulating the expression of genes such as *SOST*, *OCN* and *OPG*. However, these were human adult

trabecular bone-derived cells (30) rather than neonatal mouse calvarial cells , and it is possible that there are species, age and site-specific differences in the osteoblast response to calcium. In the current study, the elevated calcium concentration significantly increased mineral deposition by all three genotypes of osteoblasts, including VDRKO. This observation suggests that calcium plays an independent role in osteoblast differentiation to that of vitamin D activity in this commonly used model. However, further studies are required to investigate why gene expression is not changed in this cell model by an increased calcium concentration and yet mineral deposition is enhanced. In WT cells, chronic 1,25D treatment inhibited mineralisation under both concentrations of media calcium. This could be related to the gene expression data from WT cells, that the mineralisation promoter *Tnap* was not changed by chronic 1,25D treatment, but mineralisation inhibitors *Ank* and *Sost* (27) and the catabolic factor *Rankl*, were increased. Chronic 1,25D treatment also inhibited the mineralisation level in OSVDR cells. Interestingly, in OSVDR cells, *Tnap* expression was markedly reduced and the differentiation process measured at the level of gene expression was apparently inhibited by chronic exposure to 1,25D. However, we did not observe a corresponding inhibitory effect of 1,25D on mineralisation in OSVDR cultures. It is possible that direct comparisons of mineralisation *per se* as performed here, combined from multiple independent experiments, are of limited value perhaps because of excessive inter-experimental variation. An observation in this study was that the measurements of mineralisation in response to multiple treatments was only useful within each individual experiment. The experimental variation was likely due to the variation in calvarial cell isolation and the rates of cell growth. In further studies, the mineralisation could be normalised for the amount of extracellular matrix production or cell number, to enable better comparisons to be made. It is also possible that mineralisation as commonly measured, i.e. total levels of deposited calcium and phosphate, is a relatively early event and does not capture more subtle, but potentially biologically important, effects on

mineral composition and quality. Instead, mineralisation *per se* may not be the most important feature of osteoblast differentiation and is thus poorly regulated; it may be that phenotypic effects of 1,25D on the resulting differentiated cells in these cultures are more important, giving rise to cells (i.e. osteocytes) with various functional capabilities. This area is worthy of further investigation since osteocytes constitute the majority of all bone cells and perform many vital functions, functions which are becoming increasingly elucidated. Of great interest is the ability of mature osteocytes once formed to regulate their mineralised environment (31) and perform diverse functions such as control of phosphate homeostasis (152).

4.5 Conclusion

In conclusion, the calvarial osteoblast cell culture model has provided evidence that the early stage of osteoblast differentiation and mineral deposition are independent of the 1,25D/VDR system. However, VDR could be particularly important at the late stages of osteoblast/osteocyte differentiation evidenced by the inability to increase mature osteocyte marker expression in long-term cultures of VDRKO cells and the development of a more mature cell phenotype in OSVDR cells. VDR is also known to be important for osteoblast and osteocyte support of osteoclastogenesis (141,153). Whether the 1,25D/VDR system plays a promoting or inhibitory role in osteoblast differentiation presumably depends on the level of VDR in osteoblasts. Consistent with studies in human osteoblasts (30), an increased calcium concentration in culture media enhances mouse calvarial osteoblast mineralisation. Further studies are warranted to elucidate the mechanism of the calcium effect.

Chapter 5

Vitamin D Metabolites and Extracellular Calcium Promote Mineral Deposition by a Mature Osteoblast Cell Line MLO-A5

Manuscript submitted for publication

The findings in this chapter, presented as a manuscript for publication, describe the anabolic effects of both endogenous and exogenous sources of vitamin D on osteogenic differentiation and mineralisation, with an interaction with extracellular calcium. The use of a cell line was warranted for this study for the purposes of inter- and intra-experimental reproducibility. The well characterised mouse cell line MLO-A5 was chosen for these studies because our group has shown that it is capable of metabolising 25D into 1,25D, and for its ability to differentiate under osteogenic conditions and mineralise its matrix in a manner equivalent to bone *in vivo*. The findings indicate that extracellular calcium concentration alone is an important factor that regulates osteogenic differentiation. The cell line MLO-A5 could be a useful model to further investigate the calcium sensing mechanism during osteogenic differentiation process.

Statement of authorship

Vitamin D Metabolites and Extracellular Calcium Promote Mineral Deposition by a Mature Osteoblast Cell Line MLO-A5

D. Yang

First author. Generated data and analysed results; reviewed literature; preparation of figures and preparation of sections of the manuscript.

I hereby certify that the statement of contribution is accurate:

Sign: Date: 28/10/2014

A.G. Turner

Helped with data interpretation and manuscript evaluation.

I hereby certify that the statement of contribution is accurate

Sign: Date: 28/10/2014

P.H. Anderson

Helped with data interpretation and manuscript evaluation.

I hereby certify that the statement of contribution is accurate

Sign: Date: 29.10.14

H.A. Morris

Planned and supervised research work, helped with data interpretation and manuscript preparation. Equal senior author.

I hereby certify that the statement of contribution is accurate:

Sign: Date: 29/10/14

G.J. Atkins

Planned and supervised research work, helped with data interpretation and manuscript preparation. Equal senior author.

I hereby certify that the statement of contribution is accurate:

Sign: Date: 28/10/2014

Vitamin D Metabolites and Extracellular Calcium Promote Mineral Deposition by a Mature Osteoblast Cell Line MLO-A5

D.Yang[1,3], A.G.Turner[2,4], P.H.Anderson[2,4], H.A.Morris[1,2,4]* and G.J.Atkins[3]*†

[1]Discipline of Medicine, University of Adelaide, Adelaide, SA, Australia 5005

[2]Endocrine Bone Research, Chemical Pathology, SA Pathology, Adelaide, SA, Australia 5000

[3]Bone Cell Biology Group, Centre for Orthopaedic and Trauma Research, University of Adelaide, Adelaide, SA, Australia, 5005

[4]Musculoskeletal Biology Research, School of Pharmacy and Medical Sciences, University of South Australia, Adelaide, SA, Australia, 5000

*Equal senior authors

†Corresponding Author

Abbreviated Title: Vitamin D and calcium promote mineral deposition

Key terms: Osteoblast differentiation, Mineralisation, Vitamin D, Extracellular calcium

Word count: 3497

Number of figures and tables: 7 figures and 1 table

Corresponding author and person to whom reprint requests should be addressed:

Assoc. Professor Gerald J. Atkins, PhD

Bone Cell Biology Group, Centre for Orthopaedic & Trauma Research

University of Adelaide

Adelaide SA 5005

Australia

Phone: + 618 8222 3107

Mobile: +61 402 841063

Fax: +618 8232 3065

E-mail: Gerald.atkins@adelaide.edu.au

Disclosure Statement: The authors have nothing to disclose.

Abstract

An adequate level of the circulating prohormone form of vitamin D_3, 25-hydroxyvitamin D (25D), is important for both calcium homeostasis and optimal bone health. In order to maintain plasma calcium homeostasis vitamin D has both catabolic and anabolic effects on bone mineral status. A current controversy involves vitamin D actions to improve bone mineral status. The mature osteoblast/pre-osteocyte cell line, MLO-A5 was utilised to investigate the effects of both endogenous active vitamin D hormone, 1,25-dihydroxyvitamin D_3(1,25D)synthesised from 25Dand exogenously supplied 1,25D at two levels of extracellular calcium on osteoblast differentiation and mineral deposition. Both 25D and 1,25Dinhibited cell proliferation and enhanced differentiation and matrix mineralisation in this cell model. Vitamin D dependent-differentiation and mineral deposition were markedly enhanced at the higher level of extracellular calcium (ionised calcium 1.5 mM). Mineral deposition was related to the level of mRNA for the gene coding for nucleotide pyrophosphatase phosphodiesterase 1 (*Enpp1)* induced by 1,25D. Endogenous and exogenous sources of 1,25D demonstrated differential pharmacokinetics and pharmacodynamics for mRNA levels of genes coding for 25-hydroxyvitamin D-1α-hydroxylase and 25-hydroxyvitamin D-24-hydroxylase but not for other genes. These data demonstrate vitamin D stimulation of osteoblast differentiation and mineral deposition, interacting with extracellular calcium and acting through regulation of expression of genes for *Enpp1* and tissue non-specific alkaline phosphatase.

1 Introduction

Combined vitamin D and calcium supplementation is a common approach in the elderly to treat age-related bone loss and reduce the risk of fractures (1). The physiological mechanism, by which this treatment achieves this outcome, is unclear. Importantly, in both human clinical trials (2) and rodent pre-clinical studies (3), it is the circulating pro-hormone form, 25-hydroxyvitamin D_3 (25D) that is associated with the increase in bone mineral density (BMD) and reduction in fracture risk rather than the circulating levels of the active hormone, 1,25-dihydroxyvitamin D_3 (1,25D). The effects of 25D on bone metabolism are dependent on conversion to 1,25D locally in bone (4). Hence, the local production of 1,25D in bone is proposed to be physiologically important and independent from circulating 1,25D, which is derived from and regulated by renal tissue via an endocrine pathway (5).

Osteoblastogenesis is essential for bone formation requiring a sequential process of cell proliferation and maturation. Over the last 20 years or so, multiple cellular and animal model studies have demonstrated that 1,25D can exert both inhibitory and enhancing effects on osteoblast differentiation and mineral deposition (6-12). To date, the regulation of these various actions of 1,25D remains unclear. Current data suggest that the stage of osteoblast maturation is an important determinant. For example 1,25D stimulates a catabolic action on bone as a result of induction of the osteoclastogenic cytokine receptor activator of nuclear factor kappa-B ligand (RANKL) in immature osteoblast-like cells but not in more mature cells (13,14). Extracellular calcium also promotes osteogenic differentiation in human primary osteoblasts (15).

In the current study, the late osteoblast/early osteocyte cell line MLO-A5 (16,17), was used to investigate the effects of vitamin D metabolites and their interaction with extracellular calcium levels on the differentiation of mature osteoblast-like cells and *in vitro* mineral deposition. Recent data have confirmed that MLO-A5 cells have the capacity to convert 25D to 1,25D through the expression of the gene encoding the 25-hydroxyvitamin D 1α-hydroxylase (CYP27B1) (18). In order to compare the effects of both endogenous and exogenous sources of 1,25D, both 25D and 1,25D metabolites were investigated, representing endogenous and exogenous sources of the hormone respectively. Furthermore, the interactions between extracellular calcium levels and

vitamin D metabolites on osteoblast differentiation were investigated utilising two levels of culture media total calcium concentrations, 1.8 mM, the basal level in α-MEM culture media, and an elevated level at 2.8 mM total calcium.

2 Methods and Materials

2.1 Cell culture

The MLO-A5 cell line was generously provided by Professor Lynda Bonewald (University of Missouri-Kansas City, MO, USA) and cultured as previously described (16). For differentiation experiments, cells were cultured in osteogenic differentiation media consisting of 2% v/v foetal bovine serum (Thermo Fisher Scientific, Scoresby, VIC, Australia), 10 mM β-glycerol-2-phosphate (Sigma-Aldrich, St. Louis, MO, USA), 100 μM ascorbate-2-phosphate (Sigma-Aldrich) and α-MEM (Life Technologies, Grand Island, NY, USA) with and without the treatments of 25D (100 and 200 nM; Wako Pure Chemicals, Osaka, Japan), 1,25D (0.1 and 1 nM; Wako Pure Chemicals) or vehicle (0.1% v/v ethanol), as indicated. Culture medium containing total calcium concentration at 2.8 mM was prepared by adding 0.1% v/v of 1 M calcium chloride (Sigma-Aldrich) to α-MEM.

2.2 Proliferation assay

Cells for the proliferation assay were pre-labelled with carboxyfluorescein succinimidyl ester (CFSE) by intracellular staining as described previously (4). Fluorescent labelled cells were cultured in osteogenic differentiation media, as described above, for 5 days. Cells were seeded at the density of 3×10^4 cells per well in 1 ml media, in 12-well plates. On day 5, 0.1% w/v trypsin was added to cultures to harvest cells for flow cytometric analysis of CFSE intensity (4).The cell cycle generations were calculated using ModFit LT 3 (Verity Software House, ME, USA) by judging the distribution of CFSE dye in each cell cycle.

2.3 Differentiation/mineralisation assay

Cells for differentiation/mineralisation assays were seeded at 3×10^4 cells per well in 0.5 ml media, in 24-well plates and cultures were allowed to proliferate to 100% confluence. At confluence,

differentiation media plus 25D (100 nM), 1,25D (1 nM) or vehicle (0.1% v/v ethanol) at two concentrations of total calcium (1.8 and 2.8 mM) were supplied to cultures every 72 hours until day 21. Measurement of the ionised calcium concentrations in these media preparations (Siemens RAPIDLAB 1265 system, Munich, Germany), revealed corresponding levels of 1.1 and 1.5 mM, respectively. On days 3, 6, 12 and 21 (for long term culturing experiment) and 12, 24 and 72 hours (for investigating the acute induction of the gene coding for 25-hydroxyvitamin D-24-hydroxylase (*Cyp24a1*)), total RNA was extracted from triplicate culture wells of 24-well plates with TRIZOL reagent (Life Technologies) according to manufacturer's instructions. cDNA against the total RNA template was synthesised by Superscript-III kit (Life Technologies). The mRNA expression of genes of interest was then measured using real-time PCR by iQ SYBR Green Supermix (Bio-Rad Laboratories, Hercules, USA), as per the manufacturer's instructions. Oligonucleotide primer sets targeting *Cyp27b1*, *Cyp24a1*, *Gja1*, *Dmp1*, *Ank*, *Enpp1*, *E11* and *Phex* gene sequences are listed in Table 1. Primer sets for other genes were described previously (14). The specificity of primer binding was confirmed by melt-curve analysis after the PCR reactions. For quantification, gene expression was normalised to that of the housekeeping gene *β-Actin*. The levels of 1,25D in media supernatants were measured by the iSYS-1,25D immunoassay (Immuno Diagnostic Systems, Boldon, UK) in triplicate for each treatment group.

In vitro mineral deposition on days 3, 6, 12 and 21were visualised by Alizarin Red staining of cultures in 24-well plates. The Alizarin Red-calcium complexes were dissolved in 10% v/v acetic acid, neutralised to pH 4.2 by 10% v/v ammonium hydroxide and quantified by measuring light absorption at 405_{nm} (19). The chemical composition of the mineral deposited by these cultures was investigated by analysing the ratio of elemental calcium to phosphorus using energy dispersive spectroscopy (EDS) analysis, as described previously (20).

2.4 Statistical analyses

One-way ANOVA followed by a Bonferroni post-test was performed to analyse the effects of vitamin D metabolites on cell proliferation and two-way ANOVA followed by a Bonferroni post-test were performed to analyse the effects of vitamin D metabolites and extracellular calcium on

differentiation/mineralisation studies including mRNA levels, using GraphPad Prism 6.05 (GraphPad Software, La Jolla, CA, USA).

3 Results

3.1 Vitamin D receptor activity and vitamin D metabolism in MLO-A5 cells

Vitamin D receptor (*Vdr*) mRNA levels reduced with time in all cultures with 1.1 mM Ca^{2+} ($p < 0.02$), but not 1.5 mM Ca^{2+} and were enhanced with 25D treatment only with 1.1 mM Ca^{2+} ($p < 0.05$) (Fig. 1A). mRNA levels of *Cyp27b1*were significantly suppressed by 25D treatment at both 1.1 and 1.5 mM Ca^{2+} ($p < 0.05$) and tended to be suppressed by 1,25D with 1.1 mM Ca^{2+} ($p = 0.07$) (Fig. 1B). On days 3, 6, 12, and 21, mRNA levels of the gene *Cyp24a1*were at the limits of detection with vehicle treatment (Fig. 1C). These time points were the end of 72-hour media feeding cycles, *Cyp24a1*mRNA expression was markedly induced by 1,25D and 25D ($p < 0.01$), with on average 10-fold higher levels with 25D than with 1,25D. Induction of *Cyp24a1* mRNA by 1,25D was greater in the presence of 1.5 mM Ca^{2+} compared to 1.1 mM Ca^{2+}($p < 0.05$). The inactive vitamin D metabolite 24,25-dihydroxyvitamin D did not demonstrate any induction of *Cyp24a1* (data not shown).

3.2 Acute Cyp24a1 induction within 72 hours and 1,25D levels from media supernatants of 25D and 1,25D treated cultures

The lower induction of *Cyp24a1* mRNA levels over the 21 day cultures with 1,25D compared with 25D treatment raised the question as to whether exogenous 1,25D demonstrates differential pharmacodynamics compared with endogenous 1,25D. Therefore the effects of these vitamin D metabolites on *Cyp24a1* mRNA and media 1,25D levels were investigated at earlier time points than 3 days (72h). After 12h stimulation, *Cyp24a1* mRNA expression was elevated in response to 1,25D (1 nM) reaching a maximum at 24h and subsequently declining by 72h (Fig. 2A). There was no effect of Ca^{2+} on this induction over the shorter time period. *Cyp24a1* mRNA induction by 25D (100 nM) was delayed, consistent with endogenous synthesis of 1,25D, and continued to increase up to 72h.Consistent with data shown in figure 1C, *Cyp24a1* mRNA expression was elevated in response to 25D (100 nM) and 1.5 mM Ca^{2+} (Fig 2A) only at 72h ($p < 0.001$). With vehicle treatment *Cyp24a1* mRNA levels were very low, similar to levels in figure 1C (data not

shown). Measurement of 1,25D in the culture supernatant confirmed that endogenous and exogenous sources of 1,25D demonstrate marked differences in pharmacokinetics. Hormone levels in cultures supplied with exogenous 1,25D decreased from the initial level of 1000 pM to 600 pM by 72h (Fig. 2C), indicative of robust induction of CYP24A1 activity unaffected by the calcium concentration. Treatment with 100 nM 25D produced some 40 pM 1,25D concentrations, which were maintained over the 72 hour period (Fig. 2D). Treatment with 500 nM 25D increased1, 25D levels to 100 pM at 72hours (Fig. 2E). Media 1,25D levels with 25D treatment demonstrated a trend for reduced levels at 1.5 mM $Ca^{2+}$with 500 nM treatment ($p = 0.07$ at 72h), consistent with increased induction of *Cyp24a1* mRNA with this treatment.

3.3 Vitamin D inhibition of MLO-A5 proliferation

The percentage of cells which had passed through at least one division by day 5 was significantly lower with 200 nM 25D and 1 nM 1,25D treatment compared to vehicle group ($p<0.001$) (Fig. 3A); the percentage of cells that proliferated more than 4 generations was significantly lower in all vitamin D treatment groups compared to vehicle group ($p < 0.001$) (Fig. 3B). These findings indicate that both 25D and 1,25D exert inhibitory effects on the proliferation of MLO-A5 cells. The inhibition was dose-dependent with stronger arrest of cell cycling at 200 nM 25D and 1 nM 1,25D treatments compared to 100nM 25D and 0.1 nM 1,25D respectively ($p<0.001$). This inhibition of proliferation by vitamin D metabolites was independent of ionised media calcium concentrations (data not shown). The inactive vitamin D metabolite 24,25-dihydroxyvitamin D did not demonstrate any inhibition of proliferation (data not shown), suggesting that CYP27B1 activity, rather than CYP24A1, was responsible for the observed effects with 25D.

3.4 Vitamin D metabolites enhance mineral deposition by MLO-A5

Mineral deposition was assessed by Alizarin Red stain (Fig. 4A), which was quantified at 4 time points over the 21-day culture period (Fig. 4B). EDS analyses indicated that the Ca/P ratio of this deposited mineral ranged between 1.65 to 1.8, which is similar to the Ca/P ratio (around 1.67) of *in vivo* bone mineral, hydroxyapatite ($Ca_5(PO_4)_3(OH)$). During this time period the level of mineral deposition increased with 1.5 mM Ca^{2+} in the culture media compared with 1.1 mM Ca^{2+} ($p < 0.01$). The addition of 1,25D (1nM) to medium that contained 1.1 mM Ca^{2+} was associated

with a slight but significant increase in mineral deposition ($p < 0.001$). In the presence of 25D, mineral deposition was only increased at day 21 ($p < 0.001$). With 1.5 mM Ca^{2+} in the media both vitamin D metabolites (25D at 100 nM; 1,25D at 1 nM) significantly increased mineral deposition over vehicle treatment by 30% at day 21 ($p < 0.001$). The increased mineral deposition induced by each vitamin D metabolite was also significantly greater in the presence 1.5 mM Ca^{2+} than 1.1 mM Ca^{2+} ($p < 0.001$).

3.5 Effects of vitamin D metabolites and extracellular calcium on mRNA levels of genes related to osteogenic differentiation and mineral deposition

Expression of the osteoblast maturation-associated gene osteocalcin (*Ocn*) at 1.1 mM Ca^{2+} was induced by both vitamin D metabolites ($p < 0.01$) (Fig. 5A). When media ionised calcium concentrations were elevated to 1.5 mM, the enhancing effects of 25D and 1,25D on *Ocn* mRNA were significantly reduced ($p < 0.05$). mRNA levels of *Gja1*, encoding gap junction protein alpha 1/connexin 43, a principal protein component for functional hemi-channels and gap junctions and a marker of mature osteoblasts and osteocytes (21), was increased by 1.5 mM Ca^{2+} ($p < 0.01$) suggesting a maturation effect of elevated extracellular calcium alone. *Gja1* mRNA levels were enhanced by both 25D ($p<0.01$) and 1,25D ($p < 0.001$) treatments with 1.1 mM Ca^{2+} in culture media (Fig. 5B) but were no different from vehicle with 1.5 mM Ca^{2+}. Gene expression of the osteocyte marker, dentin matrix acidic phosphoprotein 1 (*Dmp1*) demonstrated a trend for increased mRNA levels with elevated calcium alone ($p = 0.08$) while 25D and 1,25D treatment groups showed no effects (Fig. 5C).

Levels of tissue non-specific alkaline phosphatase (*Tnap*) mRNA, encoding the enzyme critical for the initiation of bone mineralisation by degrading pyrophosphate (PPi), decreased with time with 1.1 mM Ca^{2+} ($p < 0.05$) and were increased by both 25D ($p < 0.02$) and 1,25D ($p < 0.01$) on day 3 (Fig. 6A). When media ionised calcium was elevated to 1.5 mM, *Tnap* mRNA levels were similar to the basal levels with vehicle treatment at 1.1 mM Ca^{2+} regardless of vitamin D metabolite treatments. The mRNA level of ankylosis protein (*Ank*), which is responsible for transporting PPi into the extracellular fluid, was unaffected by either vitamin D metabolite or calcium concentration variations (Fig. 6B). The mRNA level of ecto-nucleotide

pyrophosphatase/phosphodiesterase-1 (*Enpp1*), the enzyme responsible for synthesis of PPi, with 1.1 mM Ca^{2+} was increased slightly but significantly by both 25D ($p < 0.01$) and 1,25D ($p < 0.001$) treatments from a low baseline level and increased with time by 1,25D ($p < 0.05$). The elevated ionised calcium concentration increased the basal level of *Enpp1* mRNA to a minor extent compared to that with 1.1 mM Ca^{2+} ($p < 0.05$). However with 25D and 1,25D treatments there were greater than 2-fold increases in *Enpp1* mRNA levels compared with vehicle at 1.5 mM Ca^{2+} ($p < 0.02$) and increases compared to 25D and 1,25D treatment levels with 1.1 mM Ca^{2+} ($p < 0.01$) (Fig. 6C).

Messenger RNA levels of type I collagen alpha chain 1 (*Col1α1*), the major component of bone organic matrix, *E11,* the early osteocyte transition related gene, and phosphate regulating endopeptidase homolog, X-linked (*Phex*) the osteocyte marker that promotes mineralisation, were all highly detectable but unaffected by either vitamin D metabolites or the ionised calcium concentration (supplementary Fig. 1A-C).

4 Discussion

Using the late osteoblast/early osteocyte cell line MLO-A5, we examined the effects of vitamin D metabolites 25D and 1,25D at two levels of total extracellular calcium concentration (1.8 mM and 2.8 mM) on *in vitro* proliferation, osteogenic differentiation and mineral deposition. These differentiation conditions contained ionised calcium concentrations at 1.1 and 1.5 mM respectively spanning the physiological range from normal to hypercalcaemia (22).These cells contain the machinery necessary for vitamin D activity arising from either exogenous or endogenous sources with expression of *Vdr,* essential for biological activity of 1,25D (23) and *Cyp27b1* required for conversion of 25D to 1,25D. The addition of 25D reduced*Cyp27b1* mRNA levels confirming a previous report of 1,25D reducing *Cyp27b1* mRNA at 2-days post treatment (18). This is a most interesting observation as a proposed inhibitory mechanism reported in the renal cell line MCT (24) is currently under active discussion. *In vivo* data indicate that *Cyp27b1* mRNA levels in bone are regulated independently of renal *Cyp27b1* mRNA levels (5). Therefore MLO-A5cells are potentially a reproducible model to investigate this mechanism.

Cyp24a1 mRNA levels were induced by both 25D and 1,25D. However over the 21 day culture period, induction by 25D was on average 10-fold higher than 1,25D. Maximum levels with 1 nM 1,25D were reached at 24 hours followed by a marked reduction at 72 hours despite maintaining high 1,25D levels (600 pM) in the medium. In contrast, with 25D treatment, *Cyp24a1* mRNA levels were maintained or rose over the 72 hour period while the media 1,25D level was markedly lower. Interestingly, at the 72-hour time point, the levels of *Cyp24a1* mRNA levels in 25D (100 nM) and 1,25D (1 nM) treatment groups were similar, whereas the media 1,25D concentrations in 1,25D-treated cultures were still 15-fold higher than 25D-treated cultures. These data indicate differences between endogenous and exogenous sources of 1,25D in terms of pharmacodynamics and pharmacokinetics of intracellular 1,25D with effects on the expression of genes coding for two vitamin D metabolising enzymes, *Cyp24a1* and *Cyp27b1*. 1,25D induction of *Cyp24a1* expression is complex with synergism between two vitamin D response elements in the proximal promoter dependent on levels of 1,25D (25). A novel finding is the effect of extracellular calcium on *Cyp24a1* mRNA levels. With 1.5 mM Ca^{2+}, the acute induction level of *Cyp24a1* mRNA with 25D treatment was significantly higher than that with basal Ca^{2+} (1.1 mM) and the measured 1,25D at the higher Ca^{2+} levels tended to be lower. Similar observations were seen with 1,25D induction of *Cyp24a1* mRNA at 12 and 21 days suggesting an interaction between extracellular calcium and vitamin D metabolites with regard to induction of *Cyp24a1* expression with higher extracellular calcium increasing the clearance of 1,25D.

25D showed similar biological effects to 1,25D on proliferation and differentiation of these cells. Both 25D and 1,25D dose-dependently inhibited cell proliferation consistent with our previous report of vitamin D inhibiting the proliferation of human osteoblasts (4). Notably, the inhibitory effect of 25D at 100 nM was similar to that of 1,25D at 0.1 nM, representing physiological plasma levels for these metabolites. Both 25D and 1,25D enhanced osteogenic differentiation as evidenced by the elevated mRNA levels of maturation related genes, osteocalcin (*Ocn*) (26) and gap junction protein alpha 1/connexin 43 (*Gja1*) (27).These vitamin D metabolites equally promoted mineral deposition by some 30% when combined with 1.5 mM $Ca^{2+}$and small but statistically significant effects were detected at 1.1 mM Ca^{2+}. These observations are in contrast

to our finding that 1,25D inhibited *in vitro* mineral deposition by neonatal calvarial bone-derived osteoblast-like cultures (14).

To investigate a possible mechanism for such effects of these vitamin D metabolites on vitamin D-induced mineral deposition, the levels of mRNA for three genes (*Tnap*, *Ank* and *Enpp1*) involved in synthesis and metabolism of pyrophosphate and mineralisation were assessed. Nucleotide pyrophosphatase phosphodiesterase 1 (NPP1), the enzyme coded by *ENPP1*/*Enpp1* is responsible for synthesis of inorganic pyrophosphate (PPi) (28). Progressive ankylosis protein (ANK) is responsible for transporting PPi (29). In soft tissues *ENPP1*/*Enpp1* and *ANK*/*Ank* activities ensure the appropriate extracellular level of PPi to prevent pathological calcification. In the bone environment, tissue non-specific alkaline phosphatase (TNAP) is co-expressed together with NPP1 and ANK, metabolising PPi into inorganic phosphate (Pi), a key component of bone mineral hydroxyapatite. Thus when PPi is transported to the extracellular space, the action of TNAP generates Pi necessary to initiate the mineralisation process along type I collagen fibrils (30). In MLO-A5 cell cultures, *Enpp1* mRNA levels were slightly up-regulated by the elevated extracellular Ca^{2+} (1.5 mM) and with 25D and 1,25D treatments when combined with 1.1 mM Ca^{2+}. mRNA levels were markedly stimulated by each of the vitamin D metabolites with 1.5 mM Ca^{2+}, consistent with previous data (31). This study has demonstrated a relationship between *ENPP1*/*Enpp1* mRNA levels and vitamin D-induced levels of *in vitro* mineral deposition. mRNA levels for *Tnap* and *Ank* remained detectable and constant under these culture conditions suggesting adequate levels for mineralisation. Consequently in these cultures, NPP1 appears to be enhancing mineral deposition by providing the substrate (PPi) for TNAP to generate Pi, thus promoting mineralisation. NPP1 can also act as an inhibitor of mineral deposition but when TNAP enzyme is added to such cultures this inhibition of mineral deposition is abrogated (31).

When the ionised calcium level in the media was elevated to 1.5 mM, we found not only an increase in mineral deposition but an increase in mRNA levels of *Gja1*and *Enpp1* and a trend for increased *Dmp1* mRNA levels, independently of vitamin D treatments. Each of these genes is related to osteogenic differentiation and therefore it appears that 1.5 mCa^{2+} can mimic the effects of vitamin D metabolites to promote differentiation to a more mature phenotype, consistent

with findings with human osteoblasts (15). Presumably, such calcium effects are mediated through the calcium-sensing receptor (32) and the interplay with the vitamin D response represents an interesting area of future research. These data provide evidence for a mechanism by which the calciotropic effects of 1,25D can directly modulate bone mineral status through an interaction with extracellular calcium by varying the relative activities of two osteoblastic enzymes, nucleotide pyrophosphatase phosphodiesterase 1 and tissue non-specific alkaline phosphatase. While the higher level of ionised calcium used in these experiments represents hypercalcaemia in humans, we have no knowledge at this time of the minimal level of extracellular ionised calcium necessary to achieve such stimulation of vitamin D induction of mineral deposition by osteoblasts.

Acknowledgements

The authors wish to thank Prof. L. Bonewald (University of Missouri Kansas City, Kansas City, MO, USA) for provision of the MLO-A5 cell line; and also forward our thankfulness to Adelaide Microscopy service (The University of Adelaide, Australia) for the EDS analysis. This study was supported by funding from the National Health and Medical Research Council of Australia (NHMRC), Grant No. APP102992.

References

1. Bischoff-Ferrari HA, Willett WC, Orav EJ, Lips P, Meunier PJ, Lyons RA, Flicker L, Wark J, Jackson RD, Cauley JA, Meyer HE, Pfeifer M, Sanders KM, Stahelin HB, Theiler R, Dawson-Hughes B. A pooled analysis of vitamin D dose requirements for fracture prevention. *The New England journal of medicine.* 2012;367(1):40-49.

2. Bischoff-Ferrari HA, Dietrich T, Orav EJ, Dawson-Hughes B. Positive association between 25-hydroxy vitamin D levels and bone mineral density: a population-based study of younger and older adults. *The American journal of medicine.* 2004;116(9):634-639.

3. Anderson PH, Sawyer RK, Moore AJ, May BK, O'Loughlin PD, Morris HA. Vitamin D depletion induces RANKL-mediated osteoclastogenesis and bone loss in a rodent model. *Journal of bone and mineral research : the official journal of the American Society for Bone and Mineral Research.* 2008;23(11):1789-1797.

4. Atkins GJ, Anderson PH, Findlay DM, Welldon KJ, Vincent C, Zannettino AC, O'Loughlin PD, Morris HA. Metabolism of vitamin D3 in human osteoblasts: evidence for autocrine and paracrine activities of 1 alpha,25-dihydroxyvitamin D3. *Bone.* 2007;40(6):1517-1528.

5. Anderson PH, O'Loughlin PD, May BK, Morris HA. Modulation of CYP27B1 and CYP24 mRNA expression in bone is independent of circulating 1,25(OH)2D3 levels. *Bone.* 2005;36(4):654-662.

6. Khanna-Jain R, Vuorinen A, Sandor GK, Suuronen R, Miettinen S. Vitamin D(3) metabolites induce osteogenic differentiation in human dental pulp and human dental follicle cells. *The Journal of steroid biochemistry and molecular biology.* 2010;122(4):133-141.

7. Woeckel VJ, Alves RD, Swagemakers SM, Eijken M, Chiba H, van der Eerden BC, van Leeuwen JP. 1Alpha,25-(OH)2D3 acts in the early phase of osteoblast

differentiation to enhance mineralization via accelerated production of mature matrix vesicles. *J Cell Physiol.* 2010;225(2):593-600.

8. Matsumoto T, Igarashi C, Takeuchi Y, Harada S, Kikuchi T, Yamato H, Ogata E. Stimulation by 1,25-dihydroxyvitamin D3 of in vitro mineralization induced by osteoblast-like MC3T3-E1 cells. *Bone.* 1991;12(1):27-32.

9. Owen TA, Aronow MS, Barone LM, Bettencourt B, Stein GS, Lian JB. Pleiotropic effects of vitamin D on osteoblast gene expression are related to the proliferative and differentiated state of the bone cell phenotype: dependency upon basal levels of gene expression, duration of exposure, and bone matrix competency in normal rat osteoblast cultures. *Endocrinology.* 1991;128(3):1496-1504.

10. Yamamoto Y, Yoshizawa T, Fukuda T, Shirode-Fukuda Y, Yu T, Sekine K, Sato T, Kawano H, Aihara K, Nakamichi Y, Watanabe T, Shindo M, Inoue K, Inoue E, Tsuji N, Hoshino M, Karsenty G, Metzger D, Chambon P, Kato S, Imai Y. Vitamin D receptor in osteoblasts is a negative regulator of bone mass control. *Endocrinology.* 2013;154(3):1008-1020.

11. Yamaguchi M, Weitzmann MN. High dose 1,25(OH)2D3 inhibits osteoblast mineralization in vitro. *International journal of molecular medicine.* 2012;29(5):934-938.

12. Chen YC, Ninomiya T, Hosoya A, Hiraga T, Miyazawa H, Nakamura H. 1alpha,25-Dihydroxyvitamin D3 inhibits osteoblastic differentiation of mouse periodontal fibroblasts. *Archives of oral biology.* 2012;57(5):453-459.

13. Atkins GJ, Kostakis P, Pan B, Farrugia A, Gronthos S, Evdokiou A, Harrison K, Findlay DM, Zannettino AC. RANKL expression is related to the differentiation state of human osteoblasts. *Journal of bone and mineral research : the official journal of the American Society for Bone and Mineral Research.* 2003;18(6):1088-1098.

14. Yang D, Atkins GJ, Turner AG, Anderson PH, Morris HA. Differential effects of 1,25-dihydroxyvitamin D on mineralisation and differentiation in two different types of osteoblast-like cultures. *J Steroid Biochem Mol Biol.* 2013;136:166-170.

15. Welldon KJ, Findlay DM, Evdokiou A, Ormsby RT, Atkins GJ. Calcium induces pro-anabolic effects on human primary osteoblasts associated with acquisition of mature osteocyte markers. *Molecular and cellular endocrinology.* 2013;376(1-2):85-92.

16. Kato Y, Boskey A, Spevak L, Dallas M, Hori M, Bonewald LF. Establishment of an osteoid preosteocyte-like cell MLO-A5 that spontaneously mineralizes in culture. *Journal of bone and mineral research : the official journal of the American Society for Bone and Mineral Research.* 2001;16(9):1622-1633.

17. Barragan-Adjemian C, Nicolella D, Dusevich V, Dallas MR, Eick JD, Bonewald LF. Mechanism by which MLO-A5 late osteoblasts/early osteocytes mineralize in culture: similarities with mineralization of lamellar bone. *Calcified tissue international.* 2006;79(5):340-353.

18. Turner AG, Hanrath MA, Morris HA, Atkins GJ, Anderson PH. The local production of 1,25(OH)2D3 promotes osteoblast and osteocyte maturation. *The Journal of steroid biochemistry and molecular biology.* 2014;144 Pt A:114-118.

19. Gregory CA, Gunn WG, Peister A, Prockop DJ. An Alizarin red-based assay of mineralization by adherent cells in culture: comparison with cetylpyridinium chloride extraction. *Analytical biochemistry.* 2004;329(1):77-84.

20. Kumarasinghe DD, Sullivan T, Kuliwaba JS, Fazzalari NL, Atkins GJ. Evidence for the dysregulated expression of TWIST1, TGFbeta1 and SMAD3 in differentiating osteoblasts from primary hip osteoarthritis patients. *Osteoarthritis and cartilage / OARS, Osteoarthritis Research Society.* 2012;20(11):1357-1366.

21. Yellowley CE, Li Z, Zhou Z, Jacobs CR, Donahue HJ. Functional gap junctions between osteocytic and osteoblastic cells. *Journal of bone and mineral research :*

the official journal of the American Society for Bone and Mineral Research. 2000;15(2):209-217.

22. Larsson L, Ohman S. Serum ionized calcium and corrected total calcium in borderline hyperparathyroidism. *Clinical chemistry.* 1978;24(11):1962-1965.

23. Kim S, Shevde NK, Pike JW. 1,25-Dihydroxyvitamin D3 stimulates cyclic vitamin D receptor/retinoid X receptor DNA-binding, co-activator recruitment, and histone acetylation in intact osteoblasts. *Journal of bone and mineral research : the official journal of the American Society for Bone and Mineral Research.* 2005;20(2):305-317.

24. Murayama A, Kim MS, Yanagisawa J, Takeyama K, Kato S. Transrepression by a liganded nuclear receptor via a bHLH activator through co-regulator switching. *The EMBO journal.* 2004;23(7):1598-1608.

25. Kerry DM, Dwivedi PP, Hahn CN, Morris HA, Omdahl JL, May BK. Transcriptional synergism between vitamin D-responsive elements in the rat 25-hydroxyvitamin D3 24-hydroxylase (CYP24) promoter. *The Journal of biological chemistry.* 1996;271(47):29715-29721.

26. Ducy P. Cbfa1: a molecular switch in osteoblast biology. *Developmental dynamics : an official publication of the American Association of Anatomists.* 2000;219(4):461-471.

27. Batra N, Kar R, Jiang JX. Gap junctions and hemichannels in signal transmission, function and development of bone. *Biochimica et biophysica acta.* 2012;1818(8):1909-1918.

28. Harmey D, Hessle L, Narisawa S, Johnson KA, Terkeltaub R, Millan JL. Concerted regulation of inorganic pyrophosphate and osteopontin by akp2, enpp1, and ank: an integrated model of the pathogenesis of mineralization disorders. *The American journal of pathology.* 2004;164(4):1199-1209.

29. Ho AM, Johnson MD, Kingsley DM. Role of the mouse ank gene in control of tissue calcification and arthritis. *Science.* 2000;289(5477):265-270.

30. Addison WN, Azari F, Sorensen ES, Kaartinen MT, McKee MD. Pyrophosphate inhibits mineralization of osteoblast cultures by binding to mineral, up-regulating osteopontin, and inhibiting alkaline phosphatase activity. *The Journal of biological chemistry.* 2007;282(21):15872-15883.

31. Lieben L, Masuyama R, Torrekens S, Van Looveren R, Schrooten J, Baatsen P, Lafage-Proust MH, Dresselaers T, Feng JQ, Bonewald LF, Meyer MB, Pike JW, Bouillon R, Carmeliet G. Normocalcemia is maintained in mice under conditions of calcium malabsorption by vitamin D-induced inhibition of bone mineralization. *J Clin Invest.* 2012;122(5):1803-1815.

32. Caudarella R, Vescini F, Buffa A, Rizzoli E, Ceccoli L, Francucci CM. Role of calcium-sensing receptor in bone biology. *Journal of endocrinological investigation.* 2011;34(7 Suppl):13-17.

Figure legends

Figure 1: Effects of vitamin D metabolites and extracellular calcium on genes coding for vitamin D receptor and vitamin D metabolising enzymes. The mRNA ratios of *Vdr* (A), *Cyp27b1* (B) and *Cyp24a1* (C) to *β-Actin* in MLO-A5, with vehicle (—●—), 25D (100 nM) (·····□·····), or 1,25D (1 nM) (- - ✕ - -) treatments with media containing 1.1 (left) or 1.5 (right) mM Ca^{2+} (mean ± SEM, n = 3); * and † indicate effects of 25D and 1,25D respectively compared to vehicle for specific time points; one symbol indicates $p < 0.05$ and two symbols indicate $p < 0.01$. Three independent experiments for gene expression analyses were carried out and the error bars on graphs represent the standard errors of mean data collected from the three experiments.

Figure 2: Short term effects on induction of *Cyp24a1* mRNA levels: The mRNA ratios of *Cyp24a1* to *β-Actin* in MLO-A5 within the first 72 hours of differentiation assay with 1.1 (—●—) or 1.5 (- - □ - -) mM Ca^{2+}in culture media combined with the treatments of 1 nM 1,25D (A) or 100 nM 25D (B); 1,25D concentrations from the cell culture supernatants with 1.1 (■) or 1.5 (■) mM Ca^{2+}in culture media combined with the treatments of 1 nM 1,25D (C), 100 nM 25D (D) or 500 nM 25D (E) (mean ± SEM, n = 3); *** indicates the effect of calcium concentration on 100 nM 25D treatment group with $p < 0.001$ at 72h. Three independent experiments for gene expression analyses were carried out and the error bars on graphs represent the standard errors of mean data collected from the three experiments.

Figure 3: Effects of vitamin D metabolites on cell proliferation: The percentage of divided cells (A) and cells that proliferated more than 4 generations (B),at day 5 MLO-A5 cultures with the treatments of vehicle, 25D (100 and 200 nM) and 1,25D (0.1 and 1 nM) with 1.1 mM Ca^{2+} in culture media (mean ± SEM, n = 4; *** indicates $p < 0.001$). Three independent experiments were carried out and a representative experiment is shown. The error bars on the graphs represented 4 replicates of cell culture wells for each treatment group. All the treatment groups showed the similar biological effects within these three experiments.

Figure 4: Effects of vitamin D metabolites and extracellular calcium on mineral deposition: A: Day 12 snapshot of the mineralisation assay stained with Alizarin Red on the cell culture with the treatments of vehicle, 100 nM 25D and 1 nM 1,25D combined with 1.1 (left panel) and 1.5 (right panel) mM Ca^{2+} in media. B: The level of *in vitro* mineralisation by MLO-A5 under the treatments of vehicle (—●—), 25D (100 nM) (·····□·····), or 1,25D (1 nM) (- - ✖ - -) combined with 1.1 (left) and 1.5 (right) mM Ca^{2+} in media (mean ± SEM, n = 3); * and † indicate the effect of 25D and 1,25D respectively, compared to vehicle at specific time points and three symbols indicate $p <$ 0.001. Three independent experiments were carried out and one experiment was chosen to present in the graph. The error bars on the graphs represented 3 replicates of cell culture wells for each treatment group. All the treatment groups showed the similar biological effects within these three experiments.

Figure 5: Effects of vitamin D metabolites and extracellular calcium on mRNA levels for genes associated with osteogenic differentiation: The mRNA ratios of *Ocn* (A), *Gja1* (B) and *Dmp1* (C) to *β-Actin* in MLO-A5, with vehicle (—●—), 25D (100nM) (·····□·····), or 1,25D (1nM) (- - ✖ - -) treatments with media containing 1.1 (left) or 1.5 (right) mM Ca^{2+} (mean ± SEM, n = 3); * indicates the effect of 25D at specific time points compared to vehicle and two symbols indicate $p < 0.01$. Three independent experiments for gene expression analyses were carried out and the error bars on graphs represent the standard errors of mean data collected from the three experiments.

Figure 6: Effects of vitamin D metabolites and extracellular calcium on mRNA levels for genes required for pyrophosphate metabolism: The mRNA ratios of *Tnap* (A), *Ank* (B) and*Enpp1* (C) to *β-Actin* in MLO-A5, with vehicle (—●—), 25D (100nM) (·····□·····), or 1,25D (1nM) (- - ✖ - -) treatments with media containing 1.1 (left) or 1.5 (right) mM Ca^{2+} (mean ± SEM, n = 3); * and † indicate the effect of 25D and 1,25D respectively at specific time points compared to vehicle; one symbol indicates $p < 0.05$ and two symbols indicate $p < 0.01$. Three independent experiments for gene expression analyses were carried out and the error bars on graphs represent the standard errors of mean data collected from the three experiments.

Supplementary Figure 1: Effects of vitamin D metabolites and extracellular calcium on mRNA levels of osteoblast and osteocyte genes: The mRNA ratios of *Col1α1* (A), *E11* (B) and*Phex*(C) to *β-Actin* in MLO-A5, with vehicle (—●—), 25D (100nM) (·····□·····), or 1,25D (1nM) (- - ✖ - -) treatments with media containing 1.1 (left) or 1.5 (right) mM Ca^{2+} (mean ± SEM, n = 3). Three independent experiments for gene expression analyses were carried out and the error bars on graphs represent the standard errors of mean data collected from the three experiments.

Table 1. Primer sets used for real-time PCR for gene amplification

Gene	Sequence (5'to 3')	Gene bank accession number	Amplicon (bp)
Cyp27b1	Forward: gaccttgtgcgacgactaa	NM_010009.2	167
	Reverse: tctgtgtcaggagggacttca		
Cyp24a1	Forward: ttgaaagcatctgccttgtgt	NM_009996.3	130
	Reverse: gtcaccatcatcttcccaaat		
Gja1	Forward: aagtgaaagagaggtgccca	NM_010288.3	79
	Reverse: gtggagtaggcttggacctt		
Dmp1	Forward: gaaagctctgaagagaggacggg	NM_016779.2	121
	Reverse: tgtccgtgtggtcactatttgcct		
Ank	Forward: tcgctgacgctctgttttgt	NM_020332.4	84
	Reverse:ggcaaagtccactccaatgatat		
Enpp1	Forward: aagcgcttacacttcgctaaaag	NM_008813.3	87
	Reverse: tgatggattcaacgcaagttg		
E11	Forward: aaacgcagacaacagataagaaagat	NM_010329.2	158
	Reverse: gttctgtttagctctttagggcga		
Phex	Forward: gaaaagctgttcccaaaacagag	NM_011077.2	156
	Reverse: tagcaccataactcagggatcg		

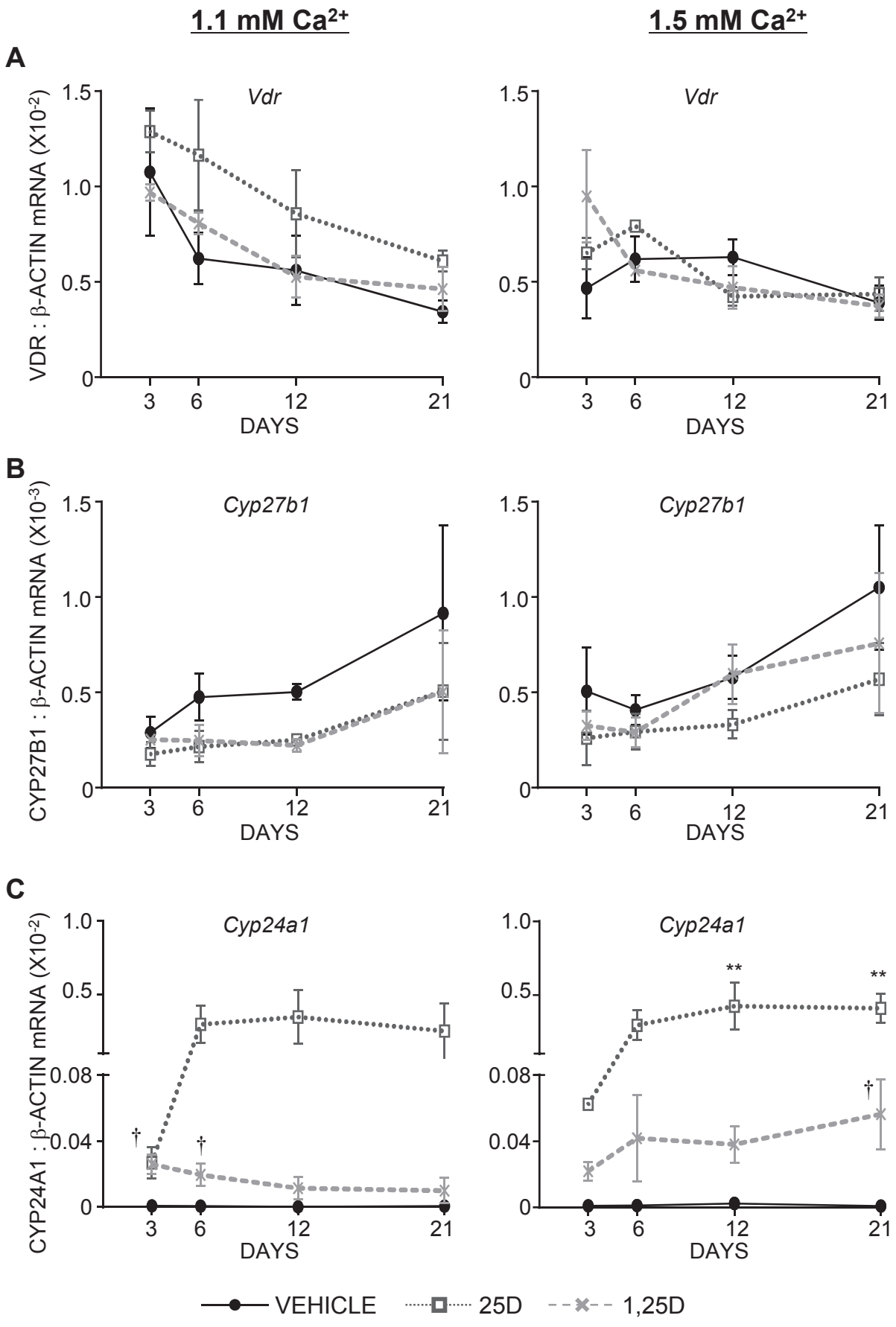
1.1 mM Ca2+
1.5 mM Ca2+
A
Vdr
VDR : β-ACTIN mRNA (X10-2)
DAYS
B
Cyp27b1
CYP27B1 : β-ACTIN mRNA (X10-3)
C
Cyp24a1
CYP24A1 : β-ACTIN mRNA (X10-2)
VEHICLE
25D
1,25D

Figure 1

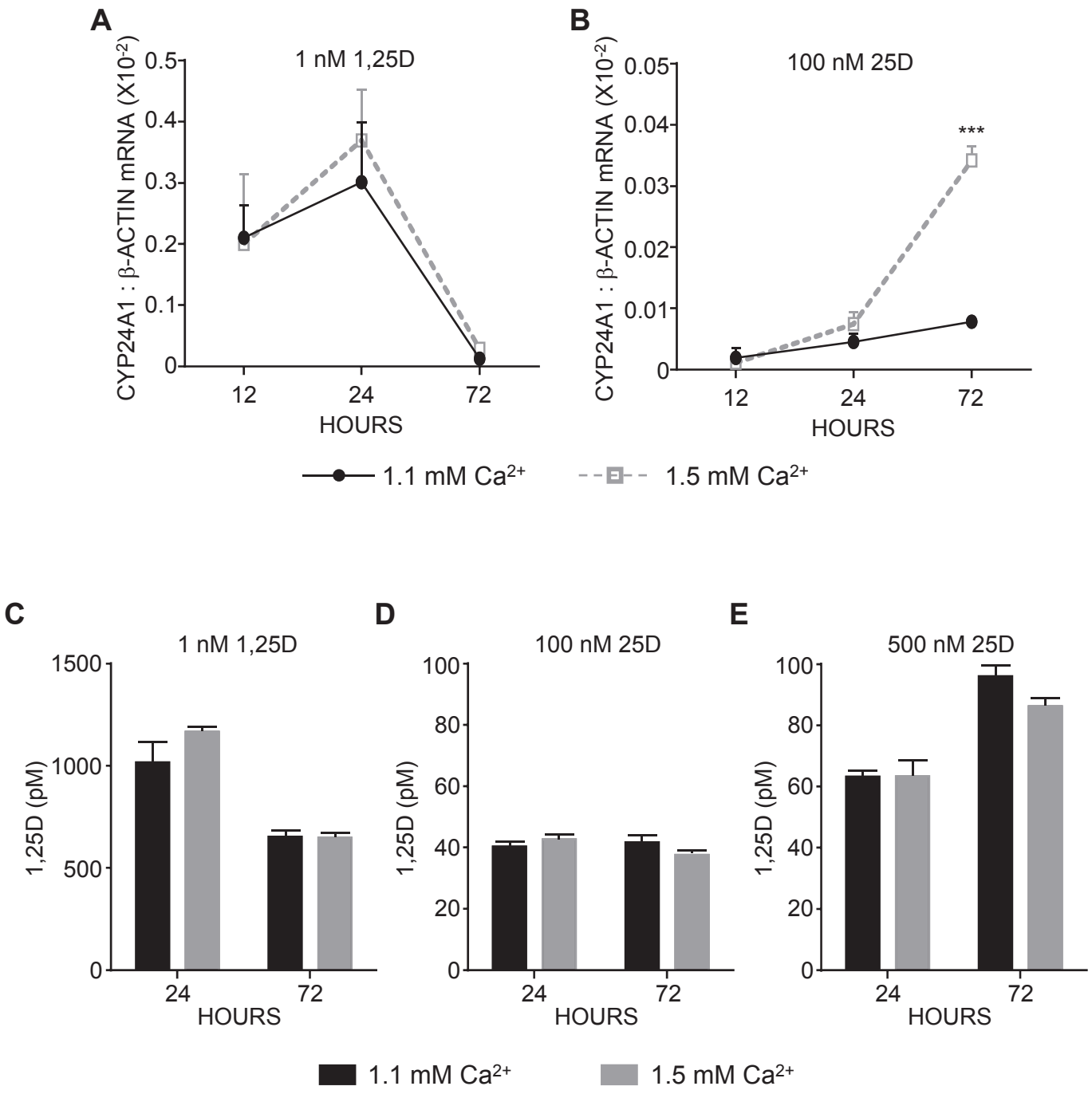
A
1 nM 1,25D
CYP24A1 : β-ACTIN mRNA (X10-2)
0.5
0.4
0.3
0.2
0.1
0
12
24
72
HOURS
B
100 nM 25D
***
0.05
0.04
0.03
0.02
0.01
1.1 mM Ca2+
1.5 mM Ca2+
C
1 nM 1,25D
1,25D (pM)
1500
1000
500
D
100 nM 25D
100
80
60
40
20
E
500 nM 25D

Figure 2

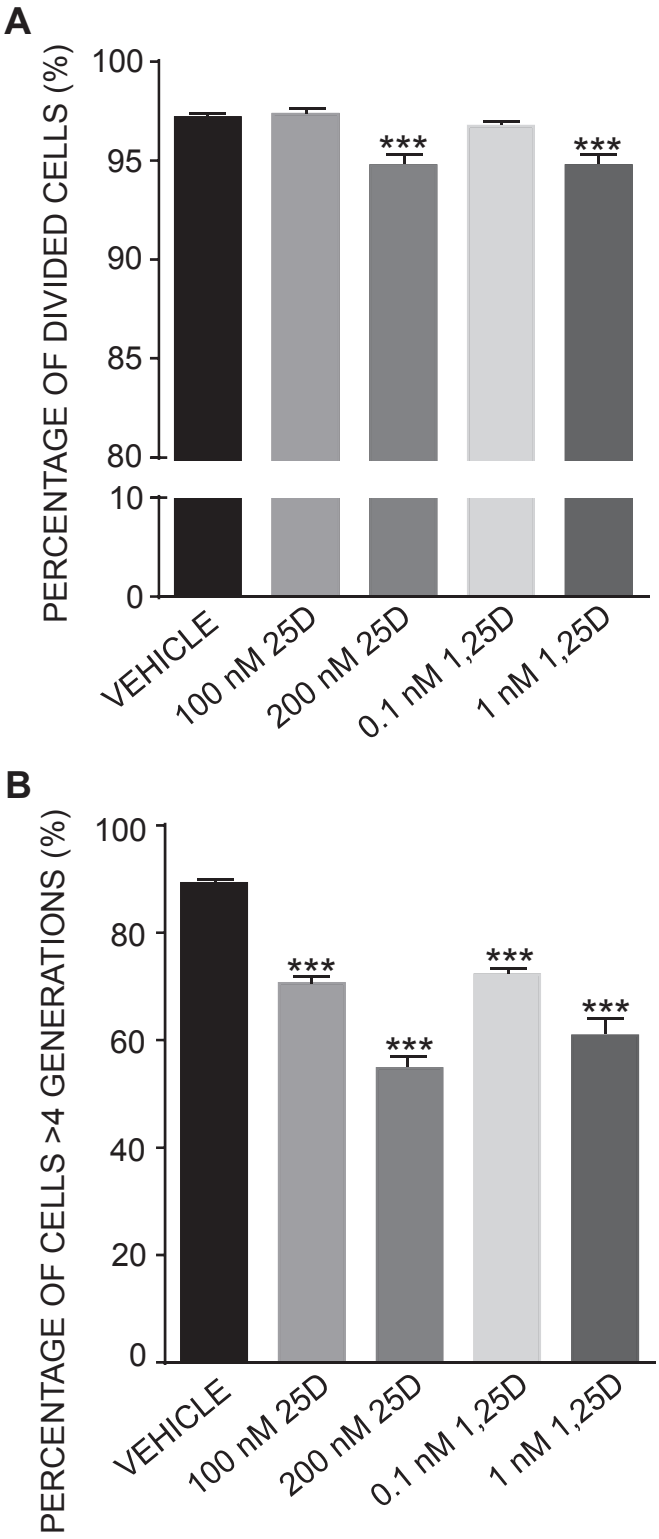
A
PERCENTAGE OF DIVIDED CELLS (%)
100
95
90
85
80
10
0
***
***
VEHICLE
100 nM 25D
200 nM 25D
0.1 nM 1,25D
1 nM 1,25D
B
PERCENTAGE OF CELLS >4 GENERATIONS (%)
100
80
60
40
20
0
***
***
***
***
VEHICLE
100 nM 25D
200 nM 25D
0.1 nM 1,25D
1 nM 1,25D

Figure 3

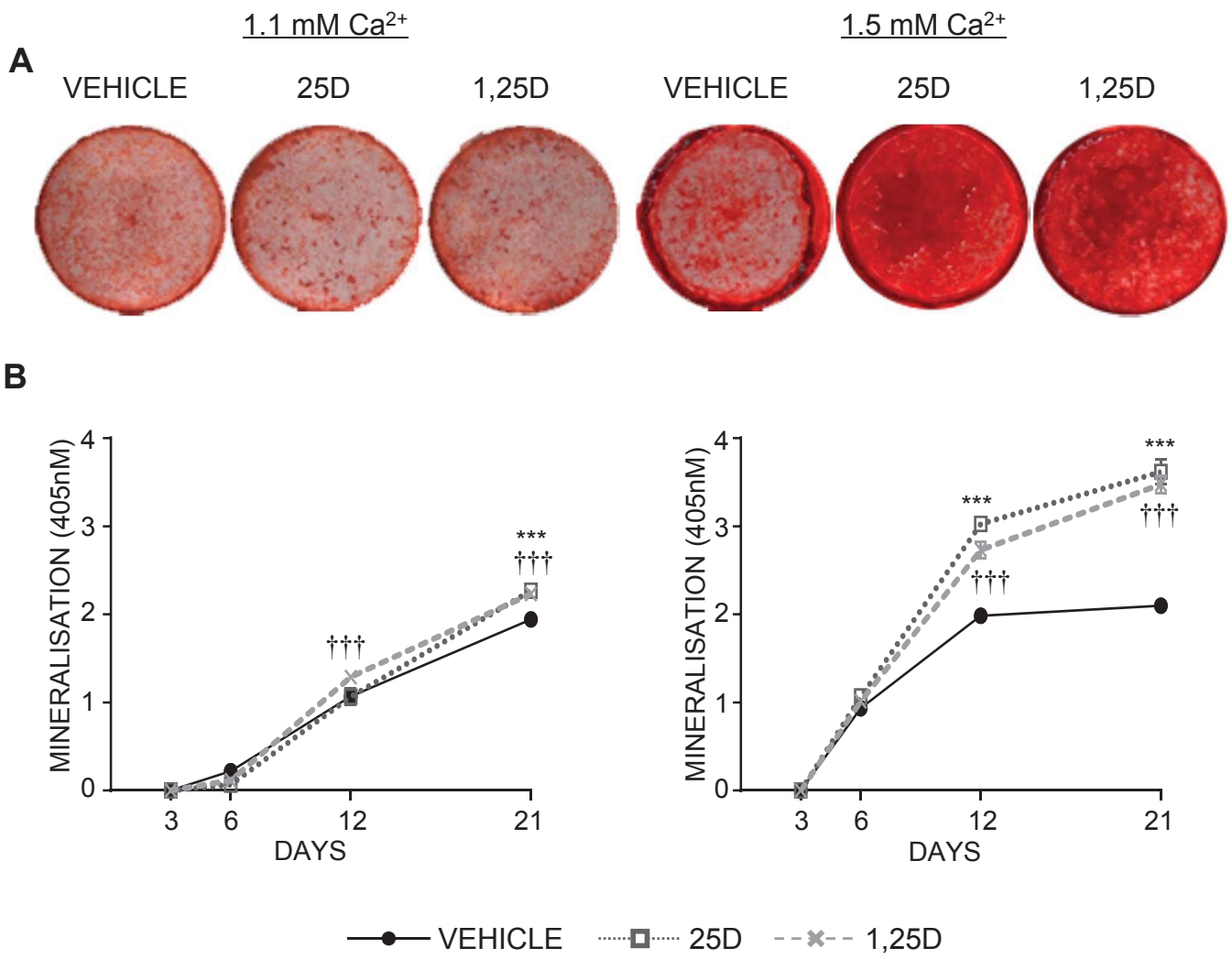
A
1.1 mM Ca2+
1.5 mM Ca2+
VEHICLE
25D
1,25D
VEHICLE
25D
1,25D
B
MINERALISATION (405nM)
DAYS
***
†††
VEHICLE
25D
1,25D

Figure 4

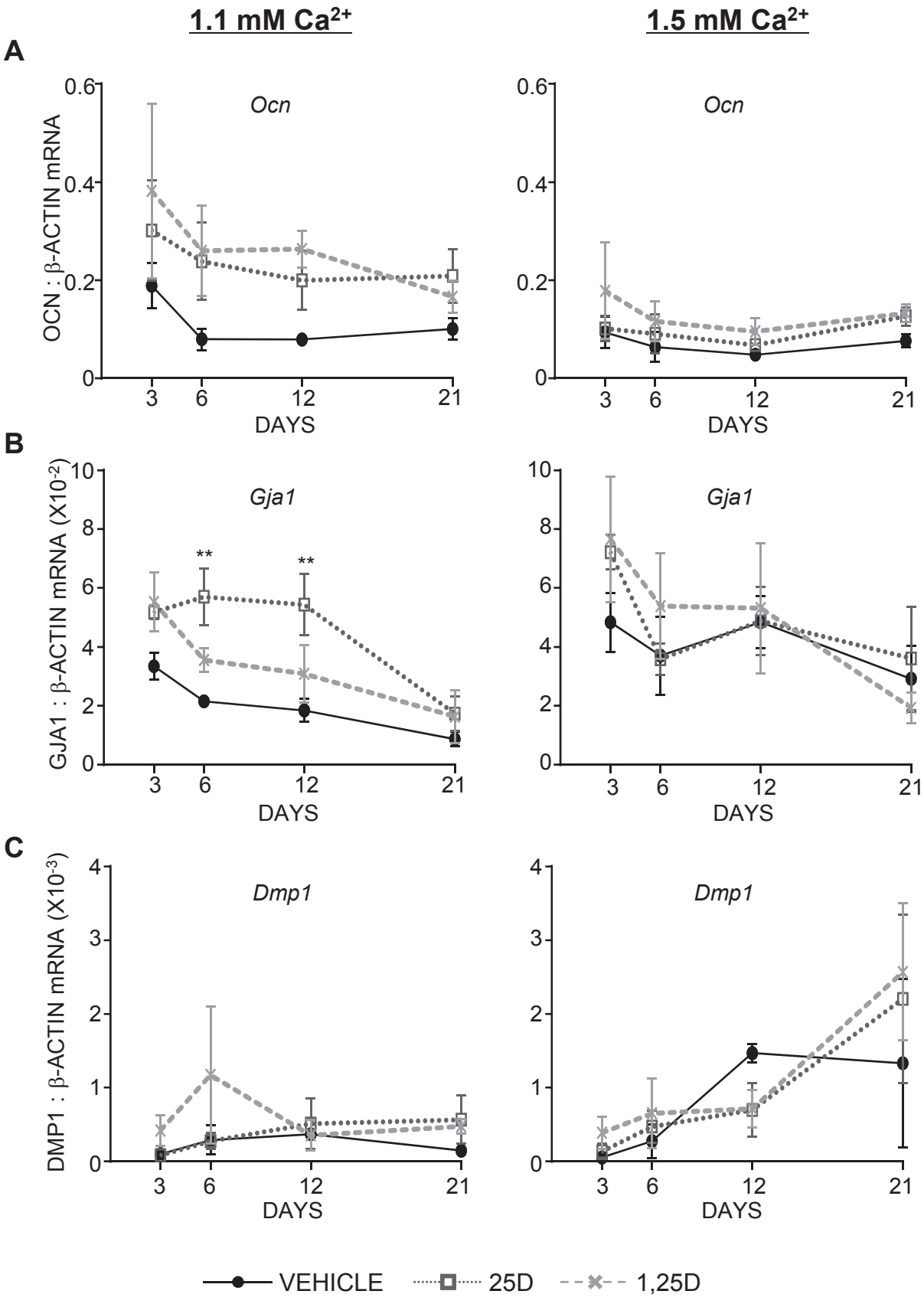
1.1 mM Ca2+
1.5 mM Ca2+
A
Ocn
OCN : β-ACTIN mRNA
0.6
0.4
0.2
0
3
6
12
21
DAYS
B
Gja1
GJA1 : β-ACTIN mRNA (X10-2)
10
8
6
4
2
0
**
**
C
Dmp1
DMP1 : β-ACTIN mRNA (X10-3)
4
3
2
1
0
VEHICLE
25D
1,25D

Figure 5

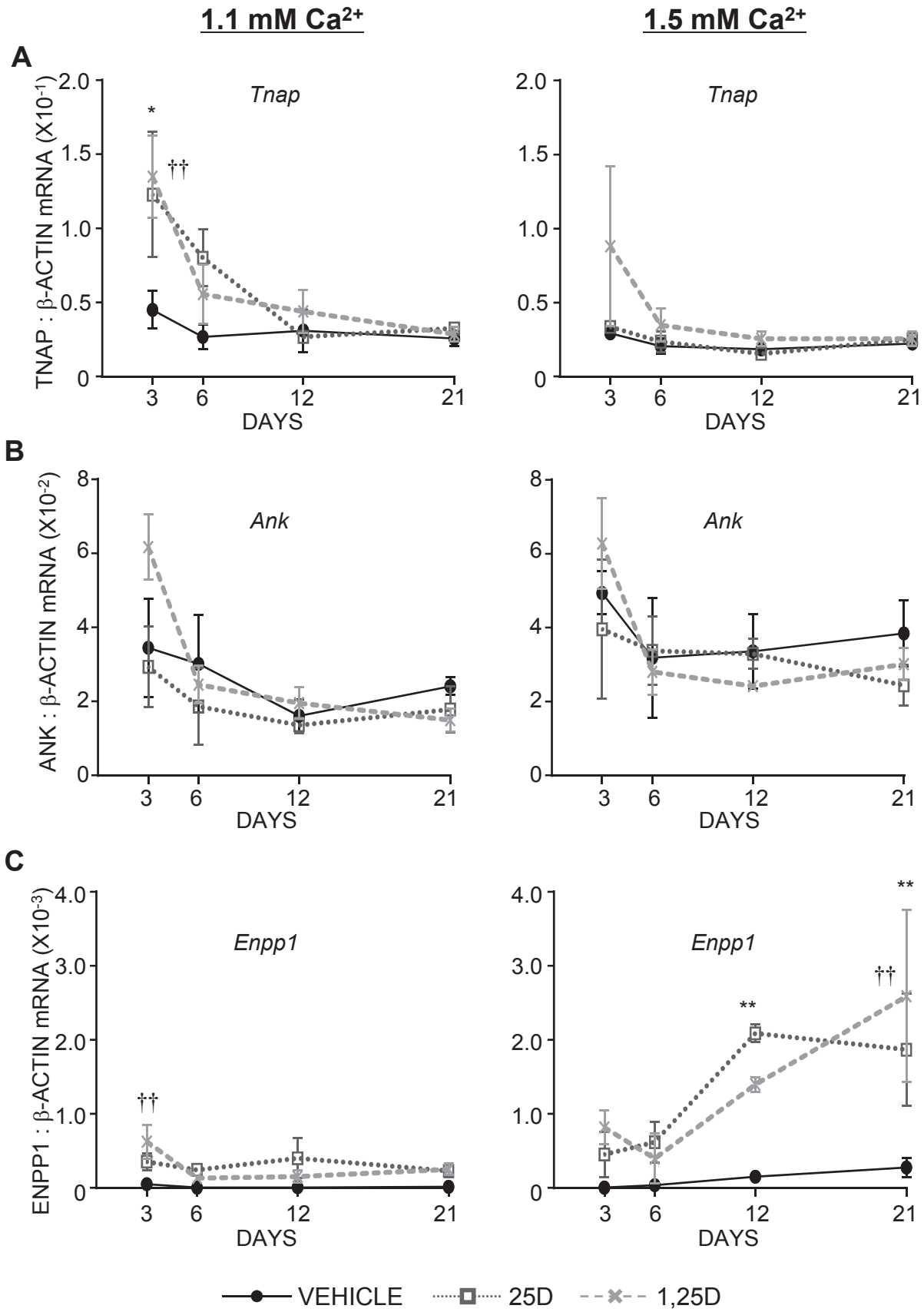
1.1 mM Ca2+
1.5 mM Ca2+
A
Tnap
TNAP : β-ACTIN mRNA (X10-1)
DAYS
B
Ank
ANK : β-ACTIN mRNA (X10-2)
C
Enpp1
ENPP1 : β-ACTIN mRNA (X10-3)
VEHICLE
25D
1,25D

Figure 6

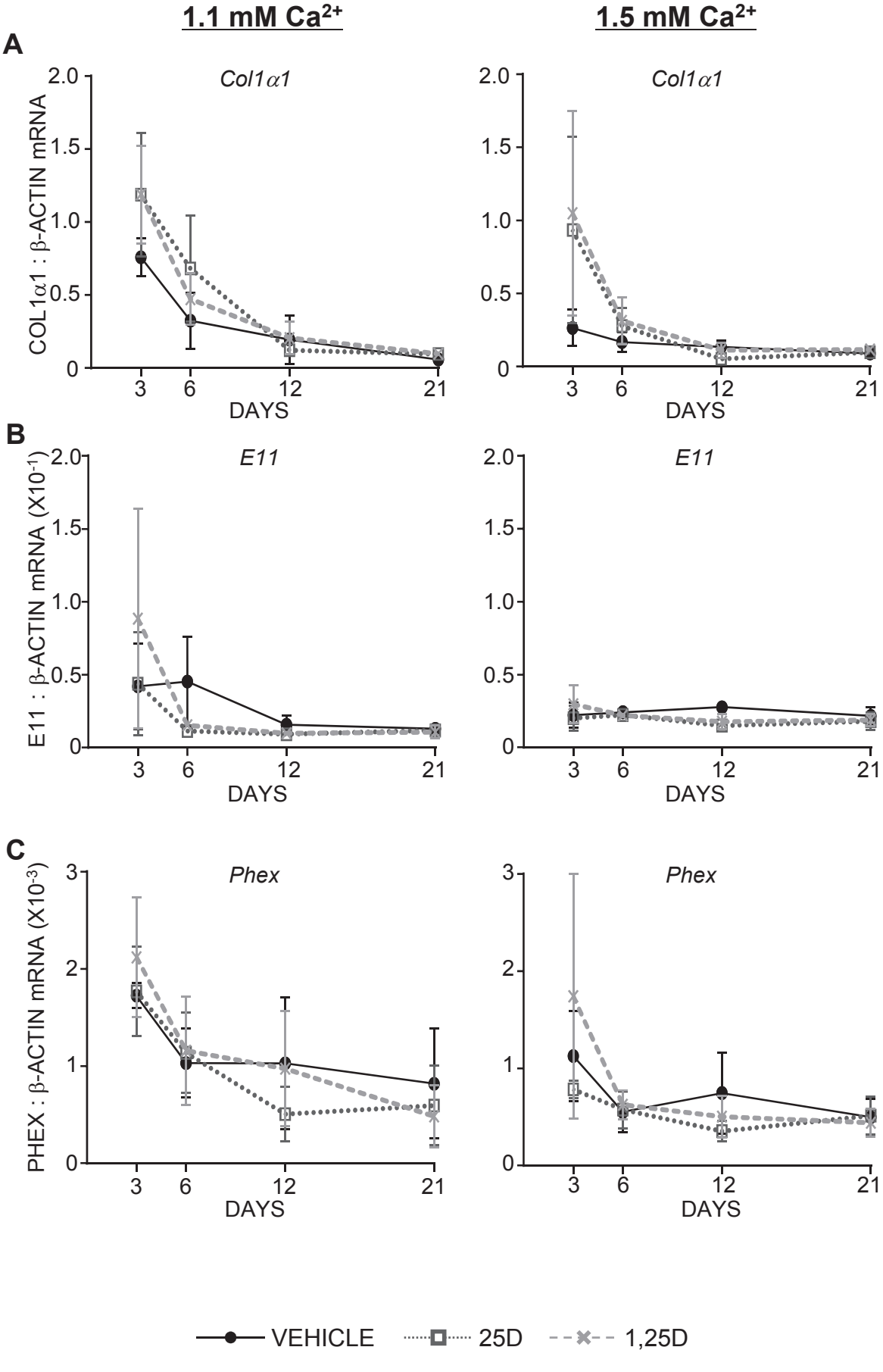

Supplementary Figure 1

Chapter 6: Concluding Remarks

Since the discovery that vitamin D deficiency is more prevalent in hip fracture patients (154), the results of numerous combined vitamin D and calcium supplement trials have suggested a beneficial effect for maintaining bone mineral density, prevention of osteoporosis and reducing the risk of fracture (56). Some investigators have suggested that the benefit arises from the endocrine action of 1,25D to improve intestinal calcium absorption. Despite the reported positive relationship between the circulating 25D level and bone mineral density, a recent review pointed out that the dietary supplement of vitamin D has limited benefit for recovering bone mineral density or for treating osteoporosis (155). Therefore, the actual mechanism of vitamin D effects on bone health is not understood and the threshold level of 25D for obtaining optimal bone health is yet to be determined. The studies reported in this thesis have focussed on the interaction between the vitamin D activities on osteoblast-like cells and osteogenic differentiation. Over the last 20 years or so, multiple vitamin D related studies have demonstrated that 1,25D plays both inhibitory and enhancing effects on osteoblast differentiation by modulating gene expression during osteogenic differentiation and mineral deposition (107,112,156-160). This project has utilised different cell culture models to research the interaction between 1,25D activity and the proliferation and differentiation of osteoblasts. These data again confirm the inhibitory effects of 1,25D on osteoblast proliferation. They also demonstrate an interaction between vitamin D activities (the combination of cellular 1,25D concentration and the level of vitamin D receptor), stage of osteoblast maturation and concentration of extracellular calcium to either enhance or inhibit effects on osteogenic differentiation and *in vitro* mineralisation.

The effects of 1,25D on cell proliferation were assessed using the late osteoblast cell line, MLO-A5. In these cells, the local production of 1,25D was confirmed and therefore, 25D

and 1,25D were added to cultures to identify any distinct effects between exogenous and endogenous 1,25D on these cells. In this cell line model, the biological effects of 25D and 1,25D on cell proliferation and differentiation were found to be identical, as discussed in chapter 5. Of interest, however, is that the physiological level of the pro-hormone (200 nM 25D) inhibits cell proliferation to a similar degree as a pharmacological level of the active hormone (1 nM 1,25D). A possible mechanism to explain this observation is the different pharmacokinetics of 25D and 1,25D being metabolised intracellularly, as demonstrated in chapter 5. We hypothesise that physiological levels of pro-hormone provide a lower and more constant level of locally-produced 1,25D to cells; whereas the pharmacological level of 1,25D initially supplies a high dosage of 1,25D, the availability of which rapidly declines due to catabolism by the induced CYP24 activity. 1,25D induction of *Cyp24a1* gene expression is complex, and involves synergism between two VDRE transcriptional complexes dependent on 1,25D concentrations (161). Consequently, further studies on the differential pharmacodynamics of endogenous and exogenous 1,25D on expression of the genes encoding CYP27B1 and CYP24 would be of great interest to the field. Our data indicate that the MLO-A5 cell line would be a suitable model for such studies.

To further study the relationship between vitamin D activity and osteogenic differentiation, calvarial cells isolated from three mouse lines, two of which were genetically-modified with regard to the VDR, were utilised. The mouse lines were the globally-ablated VDR gene (VDRKO) and the transgenically over-expressed VDR in mature osteoblasts (OSVDR) mouse lines, which were compared with wild-type (WT) mice. Calvarial cell cultures from these different genotypes were examined under culture conditions, in which media containing FCS introduced 1,25D within the physiological range (30 pM final concentration). VDRKO derived calvarial cells demonstrated reduced *Dmp1*, *Mepe* and *Rankl* mRNA expression compared to WT cells suggesting that

inactivation of the VDR delays maturation and reduces the potential support of osteoclast formation. In contrast, OSVDR cells with physiological levels of 1,25D demonstrated increases of mRNA levels for a panel of differentiation-related genes as shown in chapter 4, compared to WT cells. These data suggest that increased vitamin D activity enhances the development of the mature osteoblast phenotype as a result of increased levels of VDR. These observations imply a positive effect of physiological levels of 1,25D acting through the VDR to promote osteoblast maturation.

When cells were treated chronically with exogenous 1,25D (at the pharmacological concentration of 1 nM) every 3 days for 24 days, VDRKO cultures were unaffected, as expected. However, in WT cells, the differentiation-related genes examined were up-regulated, as presented in chapter 4. These data again confirm that the effects of 1,25D act through the VDR to exert effects on osteoblastic differentiation. Interestingly, in OSVDR cell cultures, the levels of differentiation-related genes were down-regulated with 1 nM 1,25D treatment. Based on these findings, we conclude that 1,25D activity at physiological levels and even pharmacological levels with normal VDR expression promotes osteogenic differentiation; however with a pharmacological level of 1,25D in association with a high level of VDR expression, leading to an amplification of VDR activity for a given prevailing concentration of 1,25D, normal osteoblast differentiation is disrupted.

The acute effects of 1,25D treatment were also studied in Calvarial cells by supplying the cells with 1,25D just 24 hours prior to sampling for mRNA preparations. As discussed in chapter 4, the purpose of this acute treatment was to identify the direct effects of 1,25D on target gene mRNA levels as opposed to the combined effects of direct effects on target gene transcription and indirect effects arising from 1,25D effects on osteoblast maturation. Evidence from these acute studies demonstrated that *Rankl* mRNA is significantly

induced within 24 hours of 1,25D treatment in both WT and OSVDR cells (refer to Appendix III L), which is consistent with the previous characterised mechanism that 1,25D acts directly to promote the transcription of *Rankl* through interaction of the 1,25D/VDR complex with VDREs (140). Our results show a very similar transcriptional pattern on *Enpp1* mRNA levels under the acute treatment (refer to Appendix III D). Recently, a mechanism for activating *Enpp1* transcription through the binding of 1,25D/VDR complex to a VDRE located in the adjacent gene, *Enpp3*, has been identified (162). The activation of this VDRE co-activates both *Enpp1* and *Enpp3*. Whether there is an independent regulation cassette within the *Enpp1* gene sequence is yet to be determined. Interestingly, the induction of *Rankl* mRNA by 1,25D was not detectable in the MLO-A5 study, while the baseline level of *Rankl* mRNA in MLO-A5 is around 1000-fold lower than Calvarial osteoblasts. Moreover, a recent study from our group demonstrated that the *Rankl* mRNA level was inhibited by locally synthesised 1,25D in cell line MLO-A5 cultures (90). These findings raise the most interesting question, regarding the molecular mechanism(s) by which the direct regulation of gene expression by 1,25D is modulated by osteoblast cell maturation.

The effects of vitamin D activity on *in vitro* mineral deposition were assessed in cultures of osteoblast-like cells at different stages of maturity, as discussed previously. Both inhibition and promotion of *in vitro* mineralisation by 1,25D have been observed in these studies. In chapter 4, the mineral levels deposited by WT Calvarial cells were reduced by chronic 1,25D treatment. This finding is consistent with published data demonstrating that osteoblasts from wild-type mice produced less mineral nodules *in vitro* compared to osteoblasts derived from VDRKO animals (131). In chapter 5, mineral deposition by the late stage osteoblast cell line, MLO-A5, was enhanced by 1,25D. This finding is consistent with the previous study from our group reporting that 1,25D treatment increased mineral deposition by normal human bone derived osteoblasts (85). To

investigate the molecular basis for the differential effects of 1,25D on *in vitro* mineralisation, two of the mineral regulatory systems (the pyrophosphate metabolism pathway and the PHEX/MEPE pathway) were examined in these cell models. The mineralisation inhibitor *Mepe* (reviewed in chapter 1 as a mineralisation inhibitor secreted by osteoblasts and osteocytes), is detectable in Calvarial cultures but, is non-detectable at the mRNA level in MLO-A5 cultures. We observed that with physiological levels of 1,25D the quantity of mineral deposited by WT Calvarial cells was consistently lower than that by MLO-A5 cells (5-fold on average increase by MLO-A5 cells). The absence of the mineralisation inhibitor MEPE could be an important mechanism enabling the MLO-A5 cells to deposit an increased quantity of mineral compared to WT Calvarial cells. With chronic 1,25D treatment, neither the ratio of *Phex/Mepe* mRNA in WT Calvarial cells nor the *Phex* mRNA level in MLO-A5 cells was significantly changed. On the other hand, the mineralisation inhibitor genes *Ank* and *Enpp1*, which operate on the pyrophosphate metabolism pathway, were up-regulated by chronic 1,25D treatment in WT Calvarial cells. The increased mRNA levels of these genes could be one mechanism, by which 1,25D treatment inhibits mineral deposition by WT Calvarial cell cultures. Related to this, several important observations were made in treated MLO-A5 cultures: the level of *Ank* was unchanged by either of the vitamin D metabolites; the level of *Enpp1* mRNA was increased by both 25D and 1,25D treatments; mRNA levels of the mineralisation promoter *Tnap* in MLO-A5 cultures was increased by both 25D and 1,25D treatments. It is possible that the increase in *Enpp1* mRNA expression in the MLO-A5 cells produces higher enzyme activity of NPP1 and with a higher extracellular production of PPi, which is a substrate for the enzyme TNAP to produce inorganic phosphate (Pi) to promote mineralisation. Thus in MLO-A5 cells, TNAP activity is sufficient, such that *Enpp1* is playing a promotional role to enhance mineral deposition rather than as an inhibitor. Hence, at least in the MLO-A5 cell line model, the anabolic factor(s) promoting mineralisation are presumably dominant over the inhibitors. These results support the

hypothesis that in the two cell models used in this project (WT Calvarial cells and the MLO-A5 cell line), 1,25D exerted differential activities with regard to effects on 1,25D-dependent *in vitro* mineralisation *via* the regulation of the pyrophosphate metabolism pathway. In order to verify this proposal, further studies on these gene products at the level of protein activity and the enzyme kinetics are required.

Increasing culture media calcium concentration enhanced mineral deposition in both WT Calvarial cell and MLO-A5 cultures. However, with WT Calvarial cells, an elevated calcium level in culture media did not significantly change the mRNA levels of the target genes investigated. With the MLO-A5 cell line, some effects were evident, including a reduction of mRNA level of a mature osteoblast marker, *Ocn* and enhancement of mRNA levels of the main component of functional gap junction, *Gja1* and the osteocyte marker and promoter of mineralisation, *Dmp1*. All of these effects of calcium on maturing osteoblasts were independent of vitamin D treatment. This observation is consistent with the recent report from our group, showing that increasing media calcium promotes the maturation of human bone-derived osteoblasts towards a mature osteocyte phenotype (30). The elevated calcium concentration also alters the *Cyp27b1* and *Cyp24a1* mRNA levels and consequently changes the metabolism of 25D and 1,25D, as shown in chapter 5. Our findings indicate a potential mechanism, by which media ionised calcium and the calcium sensing receptor in osteoblasts interact with the cellular vitamin D activities. The further exploration of calcium sensing receptor activities in the MLO-A5 cell line would be useful for investigating the role of calcium on osteoblast differentiation.

In all of the assessments of *in vitro* mineralisation in this study, the quantity of mineral deposited in culture was measured as a function of the level of Alizarin Red dye, which binds calcium ions. Furthermore, the calcium/phosphate ratio as assessed by energy-

dispersive X-ray spectroscopy (EDS) microanalysis was employed and demonstrated that this ratio was identical to that reported for bone hydroxyapatite formed *in vivo*.

The findings from this project suggest several exciting directions to further explore the relationship between vitamin D activity and optimal bone health. Such further studies include the following:

a) Research on the physiological roles for 1,25D arising from either endogenous or exogenous sources can be conducted utilising the cell line MLO-A5.

b) The molecular mechanisms, by which cell phenotype or stage of osteoblast maturation modulates the regulation of 1,25D expression of target genes acting though VDREs can be investigated using Calvarial cells and cell line MLO-A5. The measurements of protein levels using Western blot, ELISA, immunohistochemistry staining, etc., could also be performed to verify the findings by mRNA analysis.

c) These cell models would be suitable for investigating the mechanisms, by which the calcium sensing receptor acts in osteoblast-like cells, the effect of calcium on osteogenic differentiation and the interaction between the calcium sensing receptor and VDR pathways to regulate osteoblast proliferation, maturation and mineral deposition.

d) The role of the *Enpp1* and *Tnap* gene products in mediating the effects of vitamin D in the skeletal system represents another exciting area of future research.

The potential new knowledge from these areas of research would significantly improve understanding of the molecular and cellular basis of the interaction between vitamin D activities and the skeletal system, and has the potential for clinical translation to improve therapies for metabolic bone disease.

References

1. Ornitz DM, Marie PJ. FGF signaling pathways in endochondral and intramembranous bone development and human genetic disease. *Genes & development.* 2002;16(12):1446-1465.

2. Long F, Ornitz DM. Development of the endochondral skeleton. *Cold Spring Harbor perspectives in biology.* 2013;5(1):a008334.

3. Mackie EJ, Ahmed YA, Tatarczuch L, Chen KS, Mirams M. Endochondral ossification: how cartilage is converted into bone in the developing skeleton. *The international journal of biochemistry & cell biology.* 2008;40(1):46-62.

4. Mackie EJ, Tatarczuch L, Mirams M. The skeleton: a multi-functional complex organ: the growth plate chondrocyte and endochondral ossification. *The Journal of endocrinology.* 2011;211(2):109-121.

5. Courpron P, Meunier P, Vignon G. [Dynamics of bone remodeling explained by Harold Frost. Theory of the B. M.U. (basic multicellular unit)]. *La Nouvelle presse medicale.* 1975;4(6):421-424.

6. Kular J, Tickner J, Chim SM, Xu J. An overview of the regulation of bone remodelling at the cellular level. *Clinical biochemistry.* 2012;45(12):863-873.

7. Seeman E. Bone modeling and remodeling. *Critical reviews in eukaryotic gene expression.* 2009;19(3):219-233.

8. Hadjidakis DJ, Androulakis, II. Bone remodeling. *Annals of the New York Academy of Sciences.* 2006;1092:385-396.

9. Komori T. Regulation of osteoblast differentiation by transcription factors. *Journal of cellular biochemistry.* 2006;99(5):1233-1239.

10. Takahashi T, Kato S, Suzuki N, Kawabata N, Takagi M. Autoregulatory mechanism of Runx2 through the expression of transcription factors and bone

matrix proteins in multipotential mesenchymal cell line, ROB-C26. *Journal of oral science.* 2005;47(4):199-207.

11. Song L, Liu M, Ono N, Bringhurst FR, Kronenberg HM, Guo J. Loss of wnt/beta-catenin signaling causes cell fate shift of preosteoblasts from osteoblasts to adipocytes. *Journal of bone and mineral research : the official journal of the American Society for Bone and Mineral Research.* 2012;27(11):2344-2358.

12. Long F. Building strong bones: molecular regulation of the osteoblast lineage. *Nature reviews Molecular cell biology.* 2012;13(1):27-38.

13. Komori T, Yagi H, Nomura S, Yamaguchi A, Sasaki K, Deguchi K, Shimizu Y, Bronson RT, Gao YH, Inada M, Sato M, Okamoto R, Kitamura Y, Yoshiki S, Kishimoto T. Targeted disruption of Cbfa1 results in a complete lack of bone formation owing to maturational arrest of osteoblasts. *Cell.* 1997;89(5):755-764.

14. Anselme K. Osteoblast adhesion on biomaterials. *Biomaterials.* 2000;21(7):667-681.

15. Marie PJ. Transcription factors controlling osteoblastogenesis. *Archives of biochemistry and biophysics.* 2008;473(2):98-105.

16. Nakashima K, Zhou X, Kunkel G, Zhang Z, Deng JM, Behringer RR, de Crombrugghe B. The novel zinc finger-containing transcription factor osterix is required for osteoblast differentiation and bone formation. *Cell.* 2002;108(1):17-29.

17. Veis A. Mineral-matrix interactions in bone and dentin. *Journal of bone and mineral research : the official journal of the American Society for Bone and Mineral Research.* 1993;8 Suppl 2:S493-497.

18. Hessle L, Johnson KA, Anderson HC, Narisawa S, Sali A, Goding JW, Terkeltaub R, Millan JL. Tissue-nonspecific alkaline phosphatase and plasma cell membrane glycoprotein-1 are central antagonistic regulators of bone mineralization.

Proceedings of the National Academy of Sciences of the United States of America. 2002;99(14):9445-9449.

19. Millan JL. The role of phosphatases in the initiation of skeletal mineralization. *Calcified tissue international.* 2013;93(4):299-306.

20. Golub EE, Boesze-Battaglia K. The role of alkaline phosphatase in mineralization. *Current Opinion in Orthopaedics.* 2007;18(5):444-448 410.1097/BCO.1090b1013e3282630851.

21. Addison WN, Azari F, Sorensen ES, Kaartinen MT, McKee MD. Pyrophosphate inhibits mineralization of osteoblast cultures by binding to mineral, up-regulating osteopontin, and inhibiting alkaline phosphatase activity. *The Journal of biological chemistry.* 2007;282(21):15872-15883.

22. Franz-Odendaal TA, Hall BK, Witten PE. Buried alive: how osteoblasts become osteocytes. *Developmental dynamics : an official publication of the American Association of Anatomists.* 2006;235(1):176-190.

23. Prideaux M, Loveridge N, Pitsillides AA, Farquharson C. Extracellular matrix mineralization promotes E11/gp38 glycoprotein expression and drives osteocytic differentiation. *PloS one.* 2012;7(5):e36786.

24. Zhang K, Barragan-Adjemian C, Ye L, Kotha S, Dallas M, Lu Y, Zhao S, Harris M, Harris SE, Feng JQ, Bonewald LF. E11/gp38 selective expression in osteocytes: regulation by mechanical strain and role in dendrite elongation. *Molecular and cellular biology.* 2006;26(12):4539-4552.

25. Rowe PS, Kumagai Y, Gutierrez G, Garrett IR, Blacher R, Rosen D, Cundy J, Navvab S, Chen D, Drezner MK, Quarles LD, Mundy GR. MEPE has the properties of an osteoblastic phosphatonin and minhibin. *Bone.* 2004;34(2):303-319.

26. Addison WN, Nakano Y, Loisel T, Crine P, McKee MD. MEPE-ASARM peptides control extracellular matrix mineralization by binding to hydroxyapatite:

an inhibition regulated by PHEX cleavage of ASARM. *Journal of bone and mineral research : the official journal of the American Society for Bone and Mineral Research.* 2008;23(10):1638-1649.

27. Atkins GJ, Rowe PS, Lim HP, Welldon KJ, Ormsby R, Wijenayaka AR, Zelenchuk L, Evdokiou A, Findlay DM. Sclerostin is a locally acting regulator of late-osteoblast/preosteocyte differentiation and regulates mineralization through a MEPE-ASARM-dependent mechanism. *Journal of bone and mineral research : the official journal of the American Society for Bone and Mineral Research.* 2011;26(7):1425-1436.

28. Addison WN, Masica DL, Gray JJ, McKee MD. Phosphorylation-dependent inhibition of mineralization by osteopontin ASARM peptides is regulated by PHEX cleavage. *Journal of bone and mineral research : the official journal of the American Society for Bone and Mineral Research.* 2010;25(4):695-705.

29. Rowe PS. Regulation of bone-renal mineral and energy metabolism: the PHEX, FGF23, DMP1, MEPE ASARM pathway. *Critical reviews in eukaryotic gene expression.* 2012;22(1):61-86.

30. Welldon KJ, Findlay DM, Evdokiou A, Ormsby RT, Atkins GJ. Calcium induces pro-anabolic effects on human primary osteoblasts associated with acquisition of mature osteocyte markers. *Molecular and cellular endocrinology.* 2013;376(1-2):85-92.

31. Atkins GJ, Findlay DM. Osteocyte regulation of bone mineral: a little give and take. *Osteoporos Int.* 2012;23(8):2067-2079.

32. Bonewald LF. The amazing osteocyte. *Journal of bone and mineral research : the official journal of the American Society for Bone and Mineral Research.* 2011;26(2):229-238.

33. Qin C, D'Souza R, Feng JQ. Dentin matrix protein 1 (DMP1): new and important roles for biomineralization and phosphate homeostasis. *Journal of dental research.* 2007;86(12):1134-1141.

34. Feng JQ, Huang H, Lu Y, Ye L, Xie Y, Tsutsui TW, Kunieda T, Castranio T, Scott G, Bonewald LB, Mishina Y. The Dentin matrix protein 1 (Dmp1) is specifically expressed in mineralized, but not soft, tissues during development. *Journal of dental research.* 2003;82(10):776-780.

35. Feng JQ, Ward LM, Liu S, Lu Y, Xie Y, Yuan B, Yu X, Rauch F, Davis SI, Zhang S, Rios H, Drezner MK, Quarles LD, Bonewald LF, White KE. Loss of DMP1 causes rickets and osteomalacia and identifies a role for osteocytes in mineral metabolism. *Nature genetics.* 2006;38(11):1310-1315.

36. Tartaix PH, Doulaverakis M, George A, Fisher LW, Butler WT, Qin C, Salih E, Tan M, Fujimoto Y, Spevak L, Boskey AL. In vitro effects of dentin matrix protein-1 on hydroxyapatite formation provide insights into in vivo functions. *The Journal of biological chemistry.* 2004;279(18):18115-18120.

37. Wu H, Teng PN, Jayaraman T, Onishi S, Li J, Bannon L, Huang H, Close J, Sfeir C. Dentin matrix protein 1 (DMP1) signals via cell surface integrin. *The Journal of biological chemistry.* 2011;286(34):29462-29469.

38. Loiselle AE, Jiang JX, Donahue HJ. Gap junction and hemichannel functions in osteocytes. *Bone.* 2013;54(2):205-212.

39. Goodenough DA, Paul DL. Beyond the gap: functions of unpaired connexon channels. *Nature reviews Molecular cell biology.* 2003;4(4):285-294.

40. Martinez AD, Hayrapetyan V, Moreno AP, Beyer EC. Connexin43 and connexin45 form heteromeric gap junction channels in which individual components determine permeability and regulation. *Circulation research.* 2002;90(10):1100-1107.

41. Jiang JX, Cheng B. Mechanical stimulation of gap junctions in bone osteocytes is mediated by prostaglandin E2. *Cell communication & adhesion.* 2001;8(4-6):283-288.

42. Tian XY, Zhang Q, Zhao R, Setterberg RB, Zeng QQ, Iturria SJ, Ma YF, Jee WS. Continuous PGE2 leads to net bone loss while intermittent PGE2 leads to net bone gain in lumbar vertebral bodies of adult female rats. *Bone.* 2008;42(5):914-920.

43. Cherian PP, Siller-Jackson AJ, Gu S, Wang X, Bonewald LF, Sprague E, Jiang JX. Mechanical strain opens connexin 43 hemichannels in osteocytes: a novel mechanism for the release of prostaglandin. *Molecular biology of the cell.* 2005;16(7):3100-3106.

44. Fasciani I, Temperan A, Perez-Atencio LF, Escudero A, Martinez-Montero P, Molano J, Gomez-Hernandez JM, Paino CL, Gonzalez-Nieto D, Barrio LC. Regulation of connexin hemichannel activity by membrane potential and the extracellular calcium in health and disease. *Neuropharmacology.* 2013;75:479-490.

45. van Bezooijen RL, Roelen BA, Visser A, van der Wee-Pals L, de Wilt E, Karperien M, Hamersma H, Papapoulos SE, ten Dijke P, Lowik CW. Sclerostin is an osteocyte-expressed negative regulator of bone formation, but not a classical BMP antagonist. *The Journal of experimental medicine.* 2004;199(6):805-814.

46. Galli C, Passeri G, Macaluso GM. Osteocytes and WNT: the mechanical control of bone formation. *Journal of dental research.* 2010;89(4):331-343.

47. Wijenayaka AR, Kogawa M, Lim HP, Bonewald LF, Findlay DM, Atkins GJ. Sclerostin stimulates osteocyte support of osteoclast activity by a RANKL-dependent pathway. *PloS one.* 2011;6(10):e25900.

48. Kogawa M, Wijenayaka AR, Ormsby RT, Thomas GP, Anderson PH, Bonewald LF, Findlay DM, Atkins GJ. Sclerostin regulates release of bone mineral by osteocytes by induction of carbonic anhydrase 2. *Journal of bone and mineral*

research : the official journal of the American Society for Bone and Mineral Research. 2013;28(12):2436-2448.

49. Kasperk C, Wergedal J, Strong D, Farley J, Wangerin K, Gropp H, Ziegler R, Baylink DJ. Human bone cell phenotypes differ depending on their skeletal site of origin. *The Journal of clinical endocrinology and metabolism.* 1995;80(8):2511-2517.

50. Varanasi SS, Olstad OK, Swan DC, Sanderson P, Gautvik VT, Reppe S, Francis RM, Gautvik KM, Datta HK. Skeletal site-related variation in human trabecular bone transcriptome and signaling. *PloS one.* 2010;5(5):e10692.

51. Rawlinson SC, McKay IJ, Ghuman M, Wellmann C, Ryan P, Prajaneh S, Zaman G, Hughes FJ, Kingsmill VJ. Adult rat bones maintain distinct regionalized expression of markers associated with their development. *PloS one.* 2009;4(12):e8358.

52. Anderson PH, Turner AG, Morris HA. Vitamin D actions to regulate calcium and skeletal homeostasis. *Clinical biochemistry.* 2012;45(12):880-886.

53. Baker MR, McDonnell H, Peacock M, Nordin BE. Plasma 25-hydroxy vitamin D concentrations in patients with fractures of the femoral neck. *British medical journal.* 1979;1(6163):589.

54. Heckman GA, Papaioannou A, Sebaldt RJ, Ioannidis G, Petrie A, Goldsmith C, Adachi JD. Effect of vitamin D on bone mineral density of elderly patients with osteoporosis responding poorly to bisphosphonates. *BMC musculoskeletal disorders.* 2002;3:6.

55. Bischoff-Ferrari HA, Willett WC, Wong JB, Stuck AE, Staehelin HB, Orav EJ, Thoma A, Kiel DP, Henschkowski J. Prevention of nonvertebral fractures with oral vitamin D and dose dependency: a meta-analysis of randomized controlled trials. *Archives of internal medicine.* 2009;169(6):551-561.

56. Bischoff-Ferrari HA, Willett WC, Orav EJ, Lips P, Meunier PJ, Lyons RA, Flicker L, Wark J, Jackson RD, Cauley JA, Meyer HE, Pfeifer M, Sanders KM, Stahelin HB, Theiler R, Dawson-Hughes B. A pooled analysis of vitamin D dose requirements for fracture prevention. *The New England journal of medicine.* 2012;367(1):40-49.

57. Morris HA, Turner AG, Anderson PH. Vitamin-D regulation of bone mineralization and remodelling during growth. *Frontiers in bioscience.* 2012;4:677-689.

58. Holick MF, Tian XQ, Allen M. Evolutionary importance for the membrane enhancement of the production of vitamin D3 in the skin of poikilothermic animals. *Proceedings of the National Academy of Sciences of the United States of America.* 1995;92(8):3124-3126.

59. Lips P. Vitamin D physiology. *Progress in biophysics and molecular biology.* 2006;92(1):4-8.

60. Jones G, Strugnell SA, DeLuca HF. Current understanding of the molecular actions of vitamin D. *Physiol Rev.* 1998;78(4):1193-1231.

61. Beckman MJ, Tadikonda P, Werner E, Prahl J, Yamada S, DeLuca HF. Human 25-hydroxyvitamin D3-24-hydroxylase, a multicatalytic enzyme. *Biochemistry.* 1996;35(25):8465-8472.

62. Lian JB, Stein GS. Transcriptional control of vitamin D-regulated proteins. *Journal of cellular biochemistry.* 1992;49(1):37-45.

63. Pike JW, Meyer MB. The vitamin D receptor: new paradigms for the regulation of gene expression by 1,25-dihydroxyvitamin D3. *Rheumatic diseases clinics of North America.* 2012;38(1):13-27.

64. Zanello LP, Norman A. 1alpha,25(OH)2 vitamin D3 actions on ion channels in osteoblasts. *Steroids.* 2006;71(4):291-297.

65. Wu W, Zhang X, Zanello LP. 1alpha,25-Dihydroxyvitamin D(3) antiproliferative actions involve vitamin D receptor-mediated activation of MAPK pathways and AP-1/p21(waf1) upregulation in human osteosarcoma. *Cancer letters.* 2007;254(1):75-86.

66. Anderson PH, May BK, Morris HA. Vitamin D metabolism: new concepts and clinical implications. *The Clinical biochemist.* 2003;24(1):13-26.

67. Bronner F. Mechanisms of intestinal calcium absorption. *Journal of cellular biochemistry.* 2003;88(2):387-393.

68. Bouillon R, Van Cromphaut S, Carmeliet G. Intestinal calcium absorption: Molecular vitamin D mediated mechanisms. *Journal of cellular biochemistry.* 2003;88(2):332-339.

69. Gagnon AM, Simboli-Campbell M, Welsh JE. Induction of calbindin D-28K in Madin-Darby bovine kidney cells by 1,25(OH)2D3. *Kidney international.* 1994;45(1):95-102.

70. Murayama A, Kim MS, Yanagisawa J, Takeyama K, Kato S. Transrepression by a liganded nuclear receptor via a bHLH activator through co-regulator switching. *The EMBO journal.* 2004;23(7):1598-1608.

71. Chen KS, DeLuca HF. Cloning of the human 1 alpha,25-dihydroxyvitamin D-3 24-hydroxylase gene promoter and identification of two vitamin D-responsive elements. *Biochimica et biophysica acta.* 1995;1263(1):1-9.

72. Kim S, Shevde NK, Pike JW. 1,25-Dihydroxyvitamin D3 stimulates cyclic vitamin D receptor/retinoid X receptor DNA-binding, co-activator recruitment, and histone acetylation in intact osteoblasts. *Journal of bone and mineral research : the official journal of the American Society for Bone and Mineral Research.* 2005;20(2):305-317.

73. Ohyama Y, Ozono K, Uchida M, Shinki T, Kato S, Suda T, Yamamoto O, Noshiro M, Kato Y. Identification of a vitamin D-responsive element in the 5'-flanking

region of the rat 25-hydroxyvitamin D3 24-hydroxylase gene. *The Journal of biological chemistry.* 1994;269(14):10545-10550.

74. Akeno N, Saikatsu S, Kawane T, Horiuchi N. Mouse vitamin D-24-hydroxylase: molecular cloning, tissue distribution, and transcriptional regulation by 1alpha,25-dihydroxyvitamin D3. *Endocrinology.* 1997;138(6):2233-2240.

75. Murayama A, Takeyama K, Kitanaka S, Kodera Y, Hosoya T, Kato S. The promoter of the human 25-hydroxyvitamin D3 1 alpha-hydroxylase gene confers positive and negative responsiveness to PTH, calcitonin, and 1 alpha,25(OH)2D3. *Biochem Biophys Res Commun.* 1998;249(1):11-16.

76. Armbrecht HJ, Hodam TL, Boltz MA. Hormonal regulation of 25-hydroxyvitamin D3-1alpha-hydroxylase and 24-hydroxylase gene transcription in opossum kidney cells. *Archives of biochemistry and biophysics.* 2003;409(2):298-304.

77. Delmez JA, Tindira C, Grooms P, Dusso A, Windus DW, Slatopolsky E. Parathyroid hormone suppression by intravenous 1,25-dihydroxyvitamin D. A role for increased sensitivity to calcium. *J Clin Invest.* 1989;83(4):1349-1355.

78. Tang X, Meng H. Osteogenic induction and 1,25-dihydroxyvitamin D3 oppositely regulate the proliferation and expression of RANKL and the vitamin D receptor of human periodontal ligament cells. *Archives of oral biology.* 2009;54(7):625-633.

79. Atkins GJ, Kostakis P, Pan B, Farrugia A, Gronthos S, Evdokiou A, Harrison K, Findlay DM, Zannettino AC. RANKL expression is related to the differentiation state of human osteoblasts. *Journal of bone and mineral research : the official journal of the American Society for Bone and Mineral Research.* 2003;18(6):1088-1098.

80. Simmons PJ, Torok-Storb B. Identification of stromal cell precursors in human bone marrow by a novel monoclonal antibody, STRO-1. *Blood.* 1991;78(1):55-62.

81. Gronthos S, Zannettino AC, Graves SE, Ohta S, Hay SJ, Simmons PJ. Differential cell surface expression of the STRO-1 and alkaline phosphatase antigens on discrete developmental stages in primary cultures of human bone cells. *Journal of bone and mineral research : the official journal of the American Society for Bone and Mineral Research.* 1999;14(1):47-56.

82. Boyle WJ, Simonet WS, Lacey DL. Osteoclast differentiation and activation. *Nature.* 2003;423(6937):337-342.

83. Anderson PH, Sawyer RK, Moore AJ, May BK, O'Loughlin PD, Morris HA. Vitamin D depletion induces RANKL-mediated osteoclastogenesis and bone loss in a rodent model. *Journal of bone and mineral research : the official journal of the American Society for Bone and Mineral Research.* 2008;23(11):1789-1797.

84. Rowling MJ, Gliniak C, Welsh J, Fleet JC. High dietary vitamin D prevents hypocalcemia and osteomalacia in CYP27B1 knockout mice. *The Journal of nutrition.* 2007;137(12):2608-2615.

85. Atkins GJ, Anderson PH, Findlay DM, Welldon KJ, Vincent C, Zannettino AC, O'Loughlin PD, Morris HA. Metabolism of vitamin D3 in human osteoblasts: evidence for autocrine and paracrine activities of 1 alpha,25-dihydroxyvitamin D3. *Bone.* 2007;40(6):1517-1528.

86. Kogawa M, Findlay DM, Anderson PH, Atkins GJ. Modulation of osteoclastic migration by metabolism of 25OH-vitamin D3. *The Journal of steroid biochemistry and molecular biology.* 2013;136:59-61.

87. Kogawa M, Findlay DM, Anderson PH, Ormsby R, Vincent C, Morris HA, Atkins GJ. Osteoclastic metabolism of 25(OH)-vitamin D3: a potential mechanism for optimization of bone resorption. *Endocrinology.* 2010;151(10):4613-4625.

88. Kogawa M, Anderson PH, Findlay DM, Morris HA, Atkins GJ. The metabolism of 25-(OH)vitamin D3 by osteoclasts and their precursors regulates the differentiation of osteoclasts. *The Journal of steroid biochemistry and molecular biology.* 2010;121(1-2):277-280.

89. Ormsby RT, Findlay DM, Kogawa M, Anderson PH, Morris HA, Atkins GJ. Analysis of vitamin D metabolism gene expression in human bone: evidence for autocrine control of bone remodelling. *The Journal of steroid biochemistry and molecular biology.* 2014;144 Pt A:110-113.

90. Turner AG, Hanrath MA, Morris HA, Atkins GJ, Anderson PH. The local production of 1,25(OH)2D3 promotes osteoblast and osteocyte maturation. *The Journal of steroid biochemistry and molecular biology.* 2014;144 Pt A:114-118.

91. Geng S, Zhou S, Bi Z, Glowacki J. Vitamin D metabolism in human bone marrow stromal (mesenchymal stem) cells. *Metabolism: clinical and experimental.* 2013;62(6):768-777.

92. Geng S, Zhou S, Glowacki J. Effects of 25-hydroxyvitamin D(3) on proliferation and osteoblast differentiation of human marrow stromal cells require CYP27B1/1alpha-hydroxylase. *Journal of bone and mineral research : the official journal of the American Society for Bone and Mineral Research.* 2011;26(5):1145-1153.

93. Anderson PH, Iida S, Tyson JH, Turner AG, Morris HA. Bone CYP27B1 gene expression is increased with high dietary calcium and in mineralising osteoblasts. *The Journal of steroid biochemistry and molecular biology.* 2010;121(1-2):71-75.

94. van Driel M, Koedam M, Buurman CJ, Hewison M, Chiba H, Uitterlinden AG, Pols HA, van Leeuwen JP. Evidence for auto/paracrine actions of vitamin D in bone: 1alpha-hydroxylase expression and activity in human bone cells. *FASEB journal : official publication of the Federation of American Societies for Experimental Biology.* 2006;20(13):2417-2419.

95. Somjen D, Katzburg S, Stern N, Kohen F, Sharon O, Limor R, Jaccard N, Hendel D, Weisman Y. 25 hydroxy-vitamin D(3)-1alpha hydroxylase expression and activity in cultured human osteoblasts and their modulation by parathyroid hormone, estrogenic compounds and dihydrotestosterone. *The Journal of steroid biochemistry and molecular biology.* 2007;107(3-5):238-244.

96. Tang WJ, Wang LF, Xu XY, Zhou Y, Jin WF, Wang HF, Gao J. Autocrine/paracrine action of vitamin D on FGF23 expression in cultured rat osteoblasts. *Calcified tissue international.* 2010;86(5):404-410.

97. Ichikawa F, Sato K, Nanjo M, Nishii Y, Shinki T, Takahashi N, Suda T. Mouse primary osteoblasts express vitamin D3 25-hydroxylase mRNA and convert 1 alpha-hydroxyvitamin D3 into 1 alpha,25-dihydroxyvitamin D3. *Bone.* 1995;16(1):129-135.

98. Anderson PH, Atkins GJ. The skeleton as an intracrine organ for vitamin D metabolism. *Molecular aspects of medicine.* 2008;29(6):397-406.

99. Zhou S, Leboff MS, Waikar SS, Glowacki J. Vitamin D metabolism and action in human marrow stromal cells: effects of chronic kidney disease. *The Journal of steroid biochemistry and molecular biology.* 2013;136:342-344.

100. Geng S, Zhou S, Glowacki J. Age-related decline in osteoblastogenesis and 1alpha-hydroxylase/CYP27B1 in human mesenchymal stem cells: stimulation by parathyroid hormone. *Aging cell.* 2011;10(6):962-971.

101. Bouillon R, Carmeliet G, Verlinden L, van Etten E, Verstuyf A, Luderer HF, Lieben L, Mathieu C, Demay M. Vitamin D and human health: lessons from vitamin D receptor null mice. *Endocr Rev.* 2008;29(6):726-776.

102. Li YC, Amling M, Pirro AE, Priemel M, Meuse J, Baron R, Delling G, Demay MB. Normalization of mineral ion homeostasis by dietary means prevents hyperparathyroidism, rickets, and osteomalacia, but not alopecia in vitamin D receptor-ablated mice. *Endocrinology.* 1998;139(10):4391-4396.

103. Panda DK, Miao D, Bolivar I, Li J, Huo R, Hendy GN, Goltzman D. Inactivation of the 25-hydroxyvitamin D 1alpha-hydroxylase and vitamin D receptor demonstrates independent and interdependent effects of calcium and vitamin D on skeletal and mineral homeostasis. *The Journal of biological chemistry.* 2004;279(16):16754-16766.

104. Gardiner EM, Baldock PA, Thomas GP, Sims NA, Henderson NK, Hollis B, White CP, Sunn KL, Morrison NA, Walsh WR, Eisman JA. Increased formation and decreased resorption of bone in mice with elevated vitamin D receptor in mature cells of the osteoblastic lineage. *FASEB journal : official publication of the Federation of American Societies for Experimental Biology.* 2000;14(13):1908-1916.

105. Turner AG, O'loughlin PD, M.Kogawa, Atkins GJ, Anderson PH, Morris HA. INCREASED BONE VOLUME I N THE BONE-SPECIFIC CYP27B1 TRANSGENIC MOUSE. Paper presented at: IOF Regionals ANZBMS Annual Scientific Meeting, held with the JSBMR 2nd Asia-Pacific Osteoporosis and Bone Meeting, Osteoporosis International; 2011/09/01, 2011; Gold Coast, Australia.

106. St-Arnaud R. The direct role of vitamin D on bone homeostasis. *Archives of biochemistry and biophysics.* 2008;473(2):225-230.

107. Owen TA, Aronow MS, Barone LM, Bettencourt B, Stein GS, Lian JB. Pleiotropic effects of vitamin D on osteoblast gene expression are related to the proliferative and differentiated state of the bone cell phenotype: dependency upon basal levels of gene expression, duration of exposure, and bone matrix competency in normal rat osteoblast cultures. *Endocrinology.* 1991;128(3):1496-1504.

108. Zinser GM, McEleney K, Welsh J. Characterization of mammary tumor cell lines from wild type and vitamin D3 receptor knockout mice. *Molecular and cellular endocrinology.* 2003;200(1-2):67-80.

109. Costa JL, Eijk PP, van de Wiel MA, ten Berge D, Schmitt F, Narvaez CJ, Welsh J, Ylstra B. Anti-proliferative action of vitamin D in MCF7 is still active after siRNA-VDR knock-down. *BMC Genomics.* 2009;10:499.

110. Wang TT, Tavera-Mendoza LE, Laperriere D, Libby E, MacLeod NB, Nagai Y, Bourdeau V, Konstorum A, Lallemant B, Zhang R, Mader S, White JH. Large-scale in silico and microarray-based identification of direct 1,25-dihydroxyvitamin D3 target genes. *Mol Endocrinol.* 2005;19(11):2685-2695.

111. Piek E, Sleumer LS, van Someren EP, Heuver L, de Haan JR, de Grijs I, Gilissen C, Hendriks JM, van Ravestein-van Os RI, Bauerschmidt S, Dechering KJ, van Zoelen EJ. Osteo-transcriptomics of human mesenchymal stem cells: accelerated gene expression and osteoblast differentiation induced by vitamin D reveals c-MYC as an enhancer of BMP2-induced osteogenesis. *Bone.* 2010;46(3):613-627.

112. Woeckel VJ, Alves RD, Swagemakers SM, Eijken M, Chiba H, van der Eerden BC, van Leeuwen JP. 1Alpha,25-(OH)2D3 acts in the early phase of osteoblast differentiation to enhance mineralization via accelerated production of mature matrix vesicles. *J Cell Physiol.* 2010;225(2):593-600.

113. Broess M, Riva A, Gerstenfeld LC. Inhibitory effects of 1,25(OH)2 vitamin D3 on collagen type I, osteopontin, and osteocalcin gene expression in chicken osteoblasts. *Journal of cellular biochemistry.* 1995;57(3):440-451.

114. Shi YC, Worton L, Esteban L, Baldock P, Fong C, Eisman JA, Gardiner EM. Effects of continuous activation of vitamin D and Wnt response pathways on osteoblastic proliferation and differentiation. *Bone.* 2007;41(1):87-96.

115. Martinez ME, Medina S, Sanchez M, Del Campo MT, Esbrit P, Rodrigo A, Martinez P, Sanchez-Cabezudo MJ, Moreno I, Garces MV, Munuera L. Influence of skeletal site of origin and donor age on 1,25(OH)2D3-induced response of various osteoblastic markers in human osteoblastic cells. *Bone.* 1999;24(3):203-209.

116. Martinez P, Moreno I, De Miguel F, Vila V, Esbrit P, Martinez ME. Changes in osteocalcin response to 1,25-dihydroxyvitamin D(3) stimulation and basal vitamin D receptor expression in human osteoblastic cells according to donor age and skeletal origin. *Bone.* 2001;29(1):35-41.

117. Dvorak MM, Siddiqua A, Ward DT, Carter DH, Dallas SL, Nemeth EF, Riccardi D. Physiological changes in extracellular calcium concentration directly control osteoblast function in the absence of calciotropic hormones. *Proceedings of the National Academy of Sciences of the United States of America.* 2004;101(14):5140-5145.

118. Liu YK, Lu QZ, Pei R, Ji HJ, Zhou GS, Zhao XL, Tang RK, Zhang M. The effect of extracellular calcium and inorganic phosphate on the growth and osteogenic differentiation of mesenchymal stem cells in vitro: implication for bone tissue engineering. *Biomed Mater.* 2009;4(2):025004.

119. Ortiz J, Chou LL. Calcium upregulated survivin expression and associated osteogenesis of normal human osteoblasts. *Journal of biomedical materials research Part A.* 2012;100(7):1770-1776.

120. Ho C, Conner DA, Pollak MR, Ladd DJ, Kifor O, Warren HB, Brown EM, Seidman JG, Seidman CE. A mouse model of human familial hypocalciuric hypercalcemia and neonatal severe hyperparathyroidism. *Nature genetics.* 1995;11(4):389-394.

121. Garner SC, Pi M, Tu Q, Quarles LD. Rickets in cation-sensing receptor-deficient mice: an unexpected skeletal phenotype. *Endocrinology.* 2001;142(9):3996-4005.

122. Chang W, Tu C, Chen TH, Bikle D, Shoback D. The extracellular calcium-sensing receptor (CaSR) is a critical modulator of skeletal development. *Science signaling.* 2008;1(35):ra1.

123. Dvorak-Ewell MM, Chen TH, Liang N, Garvey C, Liu B, Tu C, Chang W, Bikle DD, Shoback DM. Osteoblast extracellular Ca2+ -sensing receptor regulates bone

development, mineralization, and turnover. *Journal of bone and mineral research : the official journal of the American Society for Bone and Mineral Research.* 2011;26(12):2935-2947.

124. Li YC, Pirro AE, Amling M, Delling G, Baron R, Bronson R, Demay MB. Targeted ablation of the vitamin D receptor: an animal model of vitamin D-dependent rickets type II with alopecia. *Proceedings of the National Academy of Sciences of the United States of America.* 1997;94(18):9831-9835.

125. Nolan T, Hands RE, Bustin SA. Quantification of mRNA using real-time RT-PCR. *Nature protocols.* 2006;1(3):1559-1582.

126. Gregory CA, Gunn WG, Peister A, Prockop DJ. An Alizarin red-based assay of mineralization by adherent cells in culture: comparison with cetylpyridinium chloride extraction. *Analytical biochemistry.* 2004;329(1):77-84.

127. Puchtler H, Meloan SN. Demonstration of phosphates in calcium deposits: a modification of von Kossa's reaction. *Histochemistry.* 1978;56(3-4):177-185.

128. Lyons AB, Parish CR. Determination of lymphocyte division by flow cytometry. *Journal of immunological methods.* 1994;171(1):131-137.

129. Yoshizawa T, Handa Y, Uematsu Y, Takeda S, Sekine K, Yoshihara Y, Kawakami T, Arioka K, Sato H, Uchiyama Y, Masushige S, Fukamizu A, Matsumoto T, Kato S. Mice lacking the vitamin D receptor exhibit impaired bone formation, uterine hypoplasia and growth retardation after weaning. *Nature genetics.* 1997;16(4):391-396.

130. Amling M, Priemel M, Holzmann T, Chapin K, Rueger JM, Baron R, Demay MB. Rescue of the skeletal phenotype of vitamin D receptor-ablated mice in the setting of normal mineral ion homeostasis: formal histomorphometric and biomechanical analyses. *Endocrinology.* 1999;140(11):4982-4987.

131. Sooy K, Sabbagh Y, Demay MB. Osteoblasts lacking the vitamin D receptor display enhanced osteogenic potential in vitro. *Journal of cellular biochemistry.* 2005;94(1):81-87.

132. Cianferotti L, Demay MB. VDR-mediated inhibition of DKK1 and SFRP2 suppresses adipogenic differentiation of murine bone marrow stromal cells. *Journal of cellular biochemistry.* 2007;101(1):80-88.

133. Nakamura A, Dohi Y, Akahane M, Ohgushi H, Nakajima H, Funaoka H, Takakura Y. Osteocalcin secretion as an early marker of in vitro osteogenic differentiation of rat mesenchymal stem cells. *Tissue Eng Part C Methods.* 2009;15(2):169-180.

134. Sims NA, White CP, Sunn KL, Thomas GP, Drummond ML, Morrison NA, Eisman JA, Gardiner EM. Human and murine osteocalcin gene expression: conserved tissue restricted expression and divergent responses to 1,25-dihydroxyvitamin D3 in vivo. *Mol Endocrinol.* 1997;11(11):1695-1708.

135. Triliana R, Lam NN, O'Loughlin PD, Morris HA, Anderson PH. Over-expression of osteoblastic Vitamin D Receptor (VDR) levels in a mouse model mediates anabolic or anti-anabolic activity which is associated with dietary calcium-mediated changes to circulating 1,25D levels. The 22nd Australian and New Zealand Bone and Mineral Society (ANZBMS) Annual Scientific Meeting; 2012; Perth, Australia.

136. Baldock PA, Thomas GP, Hodge JM, Baker SU, Dressel U, O'Loughlin PD, Nicholson GC, Briffa KH, Eisman JA, Gardiner EM. Vitamin D action and regulation of bone remodeling: suppression of osteoclastogenesis by the mature osteoblast. *Journal of bone and mineral research : the official journal of the American Society for Bone and Mineral Research.* 2006;21(10):1618-1626.

137. Fraser WD, Durham BH, Berry JL, Mawer EB. Measurement of plasma 1,25 dihydroxyvitamin D using a novel immunoextraction technique and immunoassay

with iodine labelled vitamin D tracer. *Annals of clinical biochemistry.* 1997;34 (Pt 6):632-637.

138. Dang ZC, Lowik CW. Removal of serum factors by charcoal treatment promotes adipogenesis via a MAPK-dependent pathway. *Molecular and cellular biochemistry.* 2005;268(1-2):159-167.

139. Farrow EG, Davis SI, Ward LM, Summers LJ, Bubbear JS, Keen R, Stamp TC, Baker LR, Bonewald LF, White KE. Molecular analysis of DMP1 mutants causing autosomal recessive hypophosphatemic rickets. *Bone.* 2009;44(2):287-294.

140. Kim S, Yamazaki M, Zella LA, Shevde NK, Pike JW. Activation of receptor activator of NF-kappaB ligand gene expression by 1,25-dihydroxyvitamin D3 is mediated through multiple long-range enhancers. *Molecular and cellular biology.* 2006;26(17):6469-6486.

141. Nakashima T, Hayashi M, Fukunaga T, Kurata K, Oh-Hora M, Feng JQ, Bonewald LF, Kodama T, Wutz A, Wagner EF, Penninger JM, Takayanagi H. Evidence for osteocyte regulation of bone homeostasis through RANKL expression. *Nat Med.* 2011;17(10):1231-1234.

142. Woo SM, Rosser J, Dusevich V, Kalajzic I, Bonewald LF. Cell line IDG-SW3 replicates osteoblast-to-late-osteocyte differentiation in vitro and accelerates bone formation in vivo. *Journal of bone and mineral research : the official journal of the American Society for Bone and Mineral Research.* 2011;26(11):2634-2646.

143. Ito N, Findlay DM, Anderson PH, Bonewald LF, Atkins GJ. Extracellular phosphate modulates the effect of 1alpha,25-dihydroxy vitamin D3 (1,25D) on osteocyte like cells. *The Journal of steroid biochemistry and molecular biology.* 2013;136:183-186.

144. Argiro L, Desbarats M, Glorieux FH, Ecarot B. Mepe, the gene encoding a tumor-secreted protein in oncogenic hypophosphatemic osteomalacia, is expressed in bone. *Genomics.* 2001;74(3):342-351.

145. T O, N T, C H, S K. Functional properties of cultured normal and vitamin D receptor knockout mice calvarial osteoblasts (Abstract). *Journal of bone and mineral research : the official journal of the American Society for Bone and Mineral Research.* 2003;18(Suppl 2):S141.

146. Horwood NJ, Elliott J, Martin TJ, Gillespie MT. Osteotropic agents regulate the expression of osteoclast differentiation factor and osteoprotegerin in osteoblastic stromal cells. *Endocrinology.* 1998;139(11):4743-4746.

147. Tsangari H, Findlay DM, Kuliwaba JS, Atkins GJ, Fazzalari NL. Increased expression of IL-6 and RANK mRNA in human trabecular bone from fragility fracture of the femoral neck. *Bone.* 2004;35(1):334-342.

148. Sevetson B, Taylor S, Pan Y. Cbfa1/RUNX2 directs specific expression of the sclerosteosis gene (SOST). *The Journal of biological chemistry.* 2004;279(14):13849-13858.

149. Paredes R, Arriagada G, Cruzat F, Villagra A, Olate J, Zaidi K, van Wijnen A, Lian JB, Stein GS, Stein JL, Montecino M. Bone-specific transcription factor Runx2 interacts with the 1alpha,25-dihydroxyvitamin D3 receptor to up-regulate rat osteocalcin gene expression in osteoblastic cells. *Molecular and cellular biology.* 2004;24(20):8847-8861.

150. Sutherland MK, Geoghegan JC, Yu C, Winkler DG, Latham JA. Unique regulation of SOST, the sclerosteosis gene, by BMPs and steroid hormones in human osteoblasts. *Bone.* 2004;35(2):448-454.

151. Kolek OI, Hines ER, Jones MD, LeSueur LK, Lipko MA, Kiela PR, Collins JF, Haussler MR, Ghishan FK. 1alpha,25-Dihydroxyvitamin D3 upregulates FGF23 gene expression in bone: the final link in a renal-gastrointestinal-skeletal axis that

controls phosphate transport. *American journal of physiology Gastrointestinal and liver physiology.* 2005;289(6):G1036-1042.

152. Ito N, Findlay DM, Atkins GJ. Osteocyte Communication with the Kidney Via the Production of FGF23: Remote Control of Phosphate Homeostasis. *Clinic Rev Bone Miner Metab.* 2014;12(1):44-58.

153. Xiong J, Onal M, Jilka RL, Weinstein RS, Manolagas SC, O'Brien CA. Matrix-embedded cells control osteoclast formation. *Nat Med.* 2011;17(10):1235-1241.

154. Morris HA, Morrison GW, Burr M, Thomas DW, Nordin BE. Vitamin D and femoral neck fractures in elderly South Australian women. *The Medical journal of Australia.* 1984;140(9):519-521.

155. Reid IR, Bolland MJ, Grey A. Effects of vitamin D supplements on bone mineral density: a systematic review and meta-analysis. *Lancet.* 2014;383(9912):146-155.

156. Khanna-Jain R, Vuorinen A, Sandor GK, Suuronen R, Miettinen S. Vitamin D(3) metabolites induce osteogenic differentiation in human dental pulp and human dental follicle cells. *The Journal of steroid biochemistry and molecular biology.* 2010;122(4):133-141.

157. Matsumoto T, Igarashi C, Takeuchi Y, Harada S, Kikuchi T, Yamato H, Ogata E. Stimulation by 1,25-dihydroxyvitamin D3 of in vitro mineralization induced by osteoblast-like MC3T3-E1 cells. *Bone.* 1991;12(1):27-32.

158. Yamamoto Y, Yoshizawa T, Fukuda T, Shirode-Fukuda Y, Yu T, Sekine K, Sato T, Kawano H, Aihara K, Nakamichi Y, Watanabe T, Shindo M, Inoue K, Inoue E, Tsuji N, Hoshino M, Karsenty G, Metzger D, Chambon P, Kato S, Imai Y. Vitamin D receptor in osteoblasts is a negative regulator of bone mass control. *Endocrinology.* 2013;154(3):1008-1020.

159. Yamaguchi M, Weitzmann MN. High dose 1,25(OH)2D3 inhibits osteoblast mineralization in vitro. *International journal of molecular medicine.* 2012;29(5):934-938.

160. Chen YC, Ninomiya T, Hosoya A, Hiraga T, Miyazawa H, Nakamura H. 1alpha,25-Dihydroxyvitamin D3 inhibits osteoblastic differentiation of mouse periodontal fibroblasts. *Archives of oral biology.* 2012;57(5):453-459.

161. Kerry DM, Dwivedi PP, Hahn CN, Morris HA, Omdahl JL, May BK. Transcriptional synergism between vitamin D-responsive elements in the rat 25-hydroxyvitamin D3 24-hydroxylase (CYP24) promoter. *The Journal of biological chemistry.* 1996;271(47):29715-29721.

162. Lieben L, Masuyama R, Torrekens S, Van Looveren R, Schrooten J, Baatsen P, Lafage-Proust MH, Dresselaers T, Feng JQ, Bonewald LF, Meyer MB, Pike JW, Bouillon R, Carmeliet G. Normocalcemia is maintained in mice under conditions of calcium malabsorption by vitamin D-induced inhibition of bone mineralization. *J Clin Invest.* 2012;122(5):1803-1815.

163. Kato Y, Windle JJ, Koop BA, Mundy GR, Bonewald LF. Establishment of an osteocyte-like cell line, MLO-Y4. *Journal of bone and mineral research : the official journal of the American Society for Bone and Mineral Research.* 1997;12(12):2014-2023.

164. Kato Y, Boskey A, Spevak L, Dallas M, Hori M, Bonewald LF. Establishment of an osteoid preosteocyte-like cell MLO-A5 that spontaneously mineralizes in culture. *Journal of bone and mineral research : the official journal of the American Society for Bone and Mineral Research.* 2001;16(9):1622-1633.

165. Yang D, Atkins GJ, Turner AG, Anderson PH, Morris HA. Erratum to "Differential effects of 1,25-dihydroxyvitamin D on mineralisation and differentiation in two different types of osteoblast-like cultures" [J. Steroid Biochem. Mol. Biol. 136 (2013) 166–170]. *The Journal of steroid biochemistry and molecular biology.* 2014, http://dx.doi.org/10.1016/j.jsbmb.2014.07.006.

Appendix I:

Identification of Cortical cells in Chapter 3 as the cell line MLO-A5

Experimentation:

Using the method of establishing cell cultures from juvenile mouse long bones described in chapter 3, two distinct cell culture types were generated. The initial cultures (Appendix I Fig. 1A) featured a cuboidal cell shape, with strong proliferative activity and was uniform with type I collagen positive cells only. The majority of subsequent preparations yielded cells (Appendix I Fig. 1B) which demonstrated an elongated and dendritic cell shape, reduced ability to proliferate and were heterogeneous in culture with both type I collagen- and the macrophage marker, F4/80-positive cells. Control staining was performed with a negative control rat IgG1 antibody (Appendix I Fig. 1C). All the cells termed "Cortical cells" in experimentation within chapter 3 were the cell population with type I collagen positive only.

At the time of long bone derived cell preparations were being conducted, the immortalised cell line MLO-A5 was also cultured for another study. Hence, for the purpose of investigating whether the Cortical cells used in chapter 3 could be the cell line MLO-A5, suspended Cortical cell cultures were subjected to flow cytometric cell sorting to generate single cell cultures. Seven of the resulting clonal cultures were randomly chosen for expansion and characterisation. Originally, MLO-A5 was established by transfecting cortical bone derived cells with a plasmid construct containing the large and small T antigen cassette from the SV40 virus in front of the rat osteocalcin (*Ocn*) promoter region (163,164). Hence, total DNA samples from the 7 individual cultures were compared to a DNA sample generated from a known MLO-A5 culture and wild-type mouse tail

extracted DNA, in a PCR reaction using primer sets targeting the large T antigen (forward: 5'-CCCTCCAGTGCCCTTTACAT-3'; reverse: 5'-AAGAATGGATGGCTGGAGTTG-3'; amplicon expected to be 287 bp) and the rat *Ocn* promoter (forward: 5'-GCACTGGGTGAATGAGGAC-3'; reverse: 5'-AGGAGATGCTGCCAGGACTA-3'; amplicon expected to be 398 bp). The transcriptomes from the 7 clonal cultures were also screened for large T antigen mRNA level in comparison to both known MLO-A5 culture and Calvarial cells derived from wild-type mice.

Results:

All 7 of the clonal cultures (number 1, 4, 5, 6, 7, 8 and 10), as well as the known MLO-A5 sample, were positive for both large T antigen and rat *Ocn* promoter sequences within their total DNA samples, while the mouse tail extracted DNA samples was negative for both signals (Appendix I Fig. 2). Upon quantification, varied but comparable levels of large T antigen mRNA levels were measured within all the 7 clones and the known MLO-A5 culture, while the same PCR product was not able to be generated from wild-type Calvarial cells (Appendix I Fig. 3).

Conclusion:

The cells termed Cortical cells used in chapter 3 contained all the components featuring of cell line MLO-A5, and hence arose by cross-contamination of primary cultures with the cell line. Hence, the Cortical cells used in chapter 3 study was confirmed to be the established cell line MLO-A5, prompting the erratum published in the Journal of Steroid Biochemistry and Molecular Biology (165).

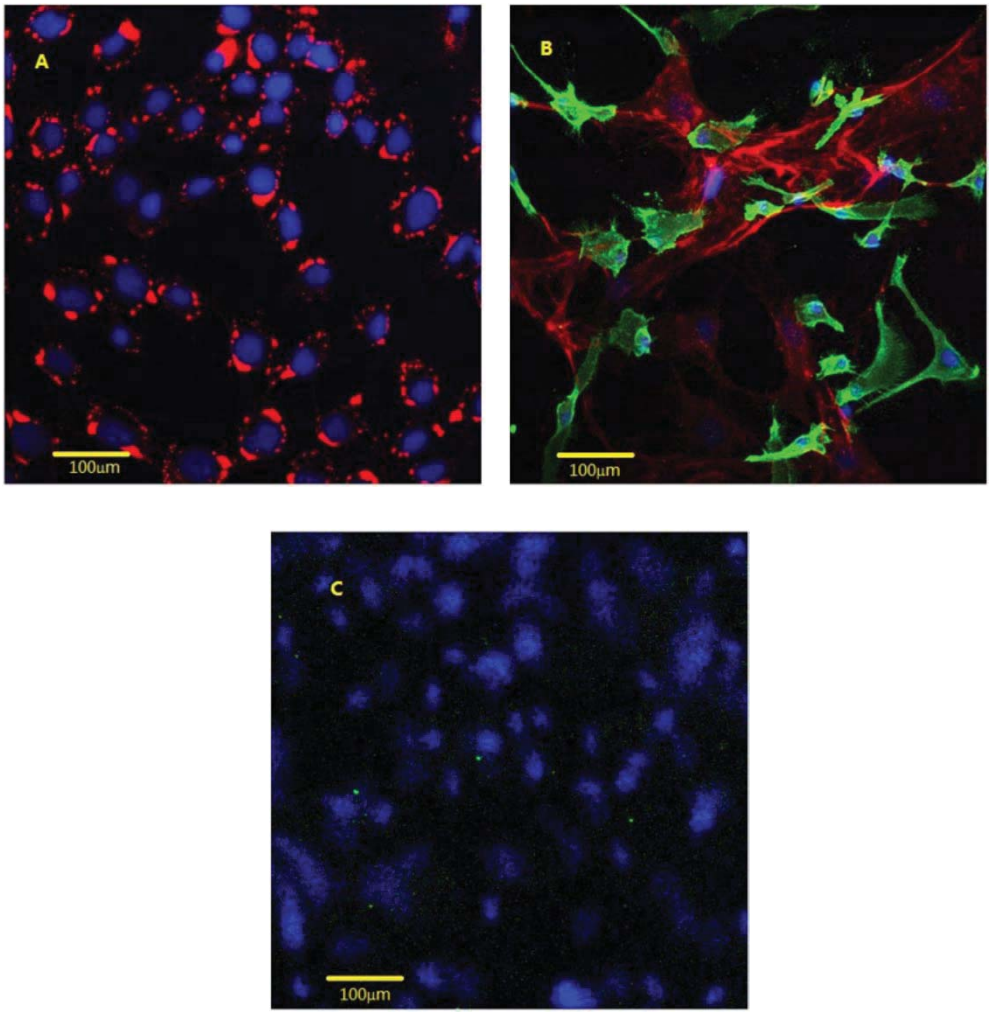

Appendix I figure 1 **Immunostaining for type I collagen and F4/80 antigens**

Cell cultures stained with type I collagen (in red colour) and F4/80 (in green colour) antibodies and DAPI (in blue colour).

A: Collagen-I positive and F4/80 negative cell population

B: Collagen-I and F4/80 positive cell population

C: Control antibody staining on cells

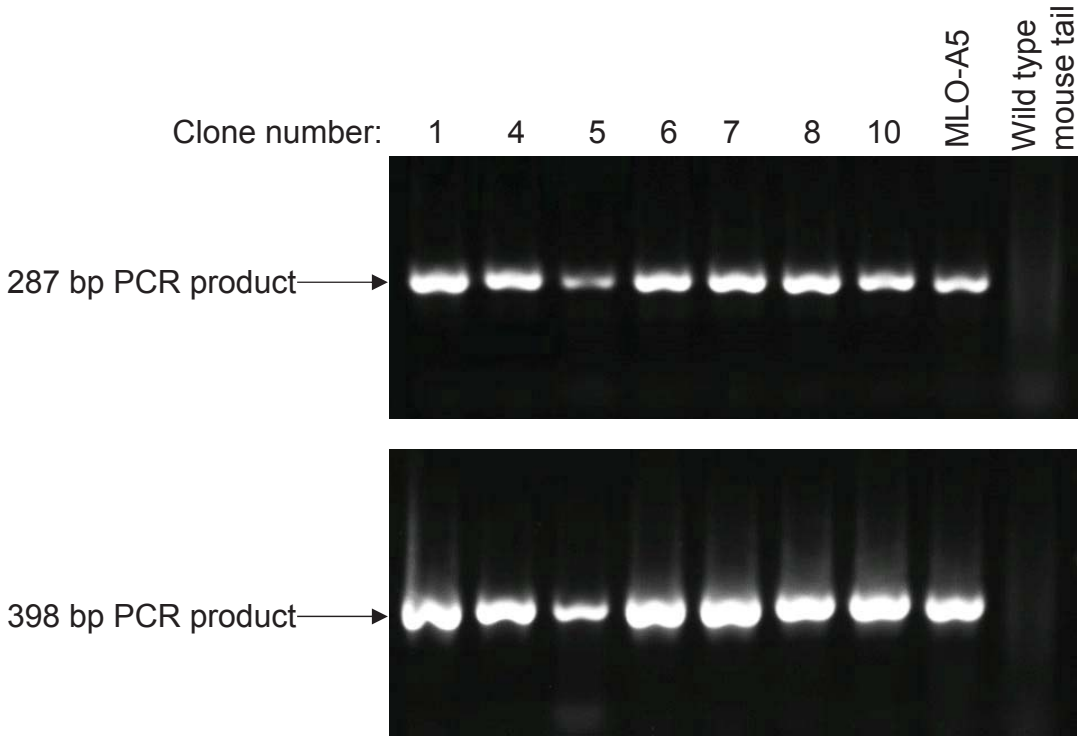

Appendix I figure 2 **PCR products representing Large T antigen sequence and rat *Ocn* promoter region from DNA samples**

PCR reactions using DNA samples from single clonal cultures 1, 4, 5, 6, 7, 8, 10 and a known MLO-A5 culture, generated 287 bp and 398 bp amplicons, representing large T antigen sequence and rat *Ocn* promoter region respectively; both amplicons were not able to be generated using wild-type mouse tail extracted DNA sample. One experiment for gene was conducted and the error bars on graphs represent the standard errors of mean data collected from the three PCR replicates.

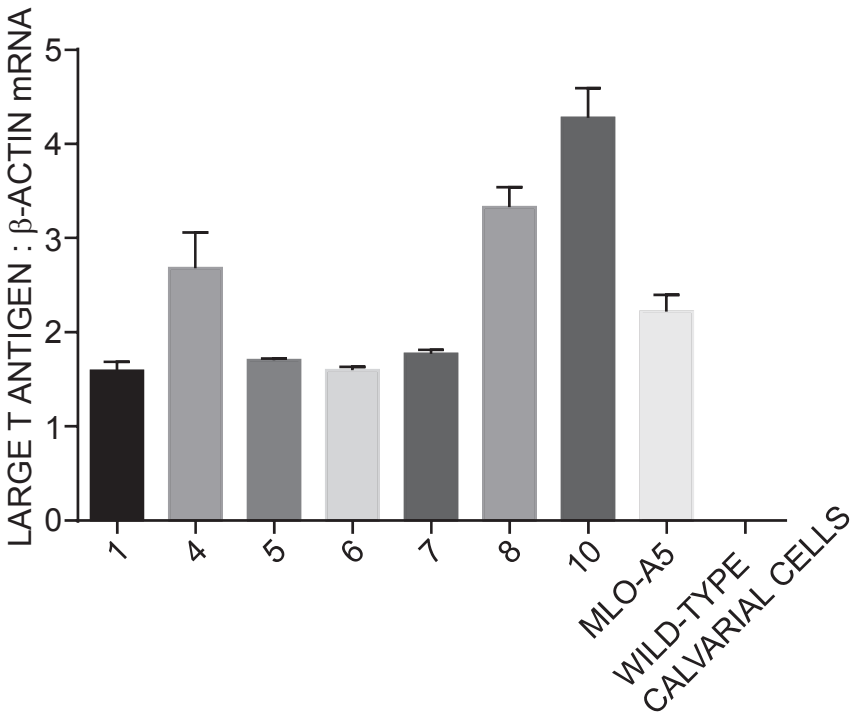

Appendix I figure 3 **Real-time PCR reactions for measuring the mRNA levels of Large T antigen from transcriptomes**

Real-time PCRs confirmed that similar mRNA levels of large T antigen presented in the transcriptomes from single clonal cultures 1, 4, 5, 6, 7, 8, 10 and a known MLO-A5 culture, but large T antigen was absent in transcriptome extracted from wild-type Calvarial cells. One experiment was conducted and the error bars on graphs represent the standard errors of mean data collected three PCR replicates.

Appendix II

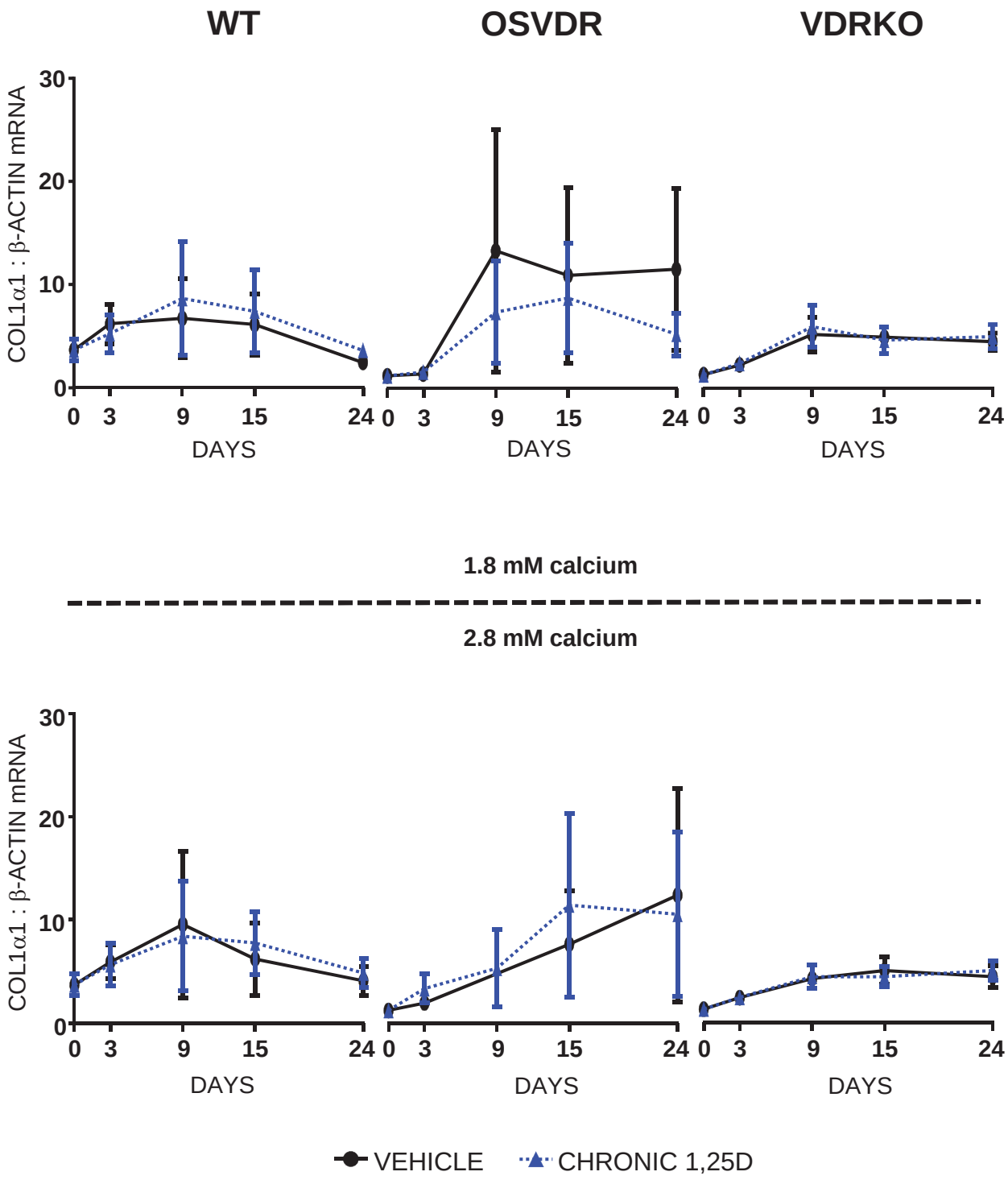

Appendix II. A **mRNA levels of *Col1α1***

The mRNA ratios of *Col1α1* to *β-Actin* by WT (left), OSVDR (middle) and VDRKO (right) cells, with vehicle (solid line) and chronic 1,25D (1nM) (broken line) treatments with 1.8 mM (upper) and 2.8 mM total calcium (lower) presented in culture media. Three independent experiments for gene expression analyses were conducted and the error bars on graphs represent the standard errors of mean data collected from the three experiments (mean±SEM, n = 3).

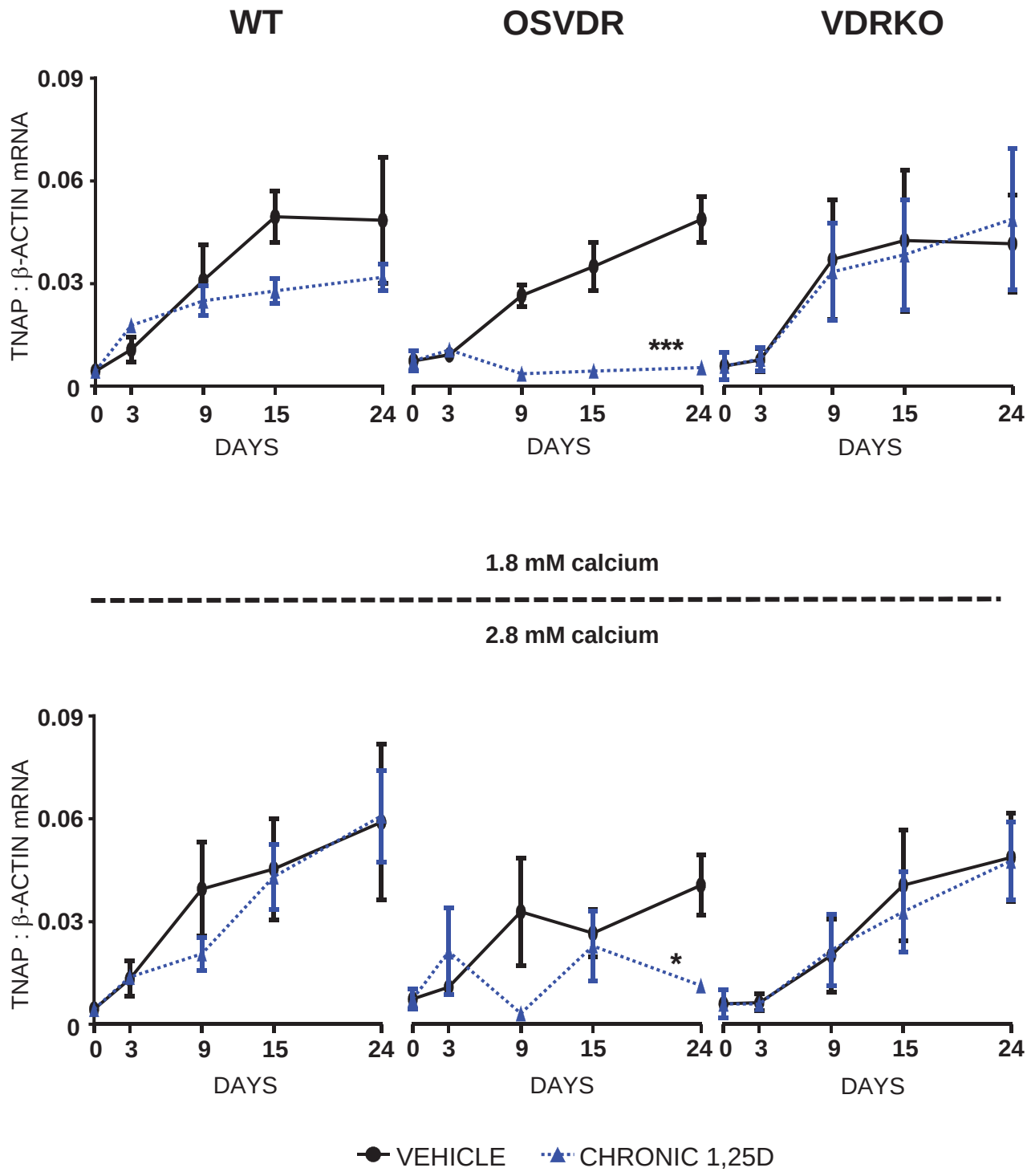

Appendix II. B **mRNA levels of *Tnap***

The mRNA ratios of *Tnap* to *β-Actin* by WT (left), OSVDR (middle) and VDRKO (right) cells, with vehicle (solid line) and chronic 1,25D (1nM) (broken line) treatments with 1.8 mM (upper) and 2.8 mM total calcium (lower) presented in culture media. Three independent experiments for gene expression analyses were conducted and the error bars on graphs represent the standard errors of mean data collected from the three experiments (mean±SEM, n = 3; * $p<0.05$, *** $p<0.001$).

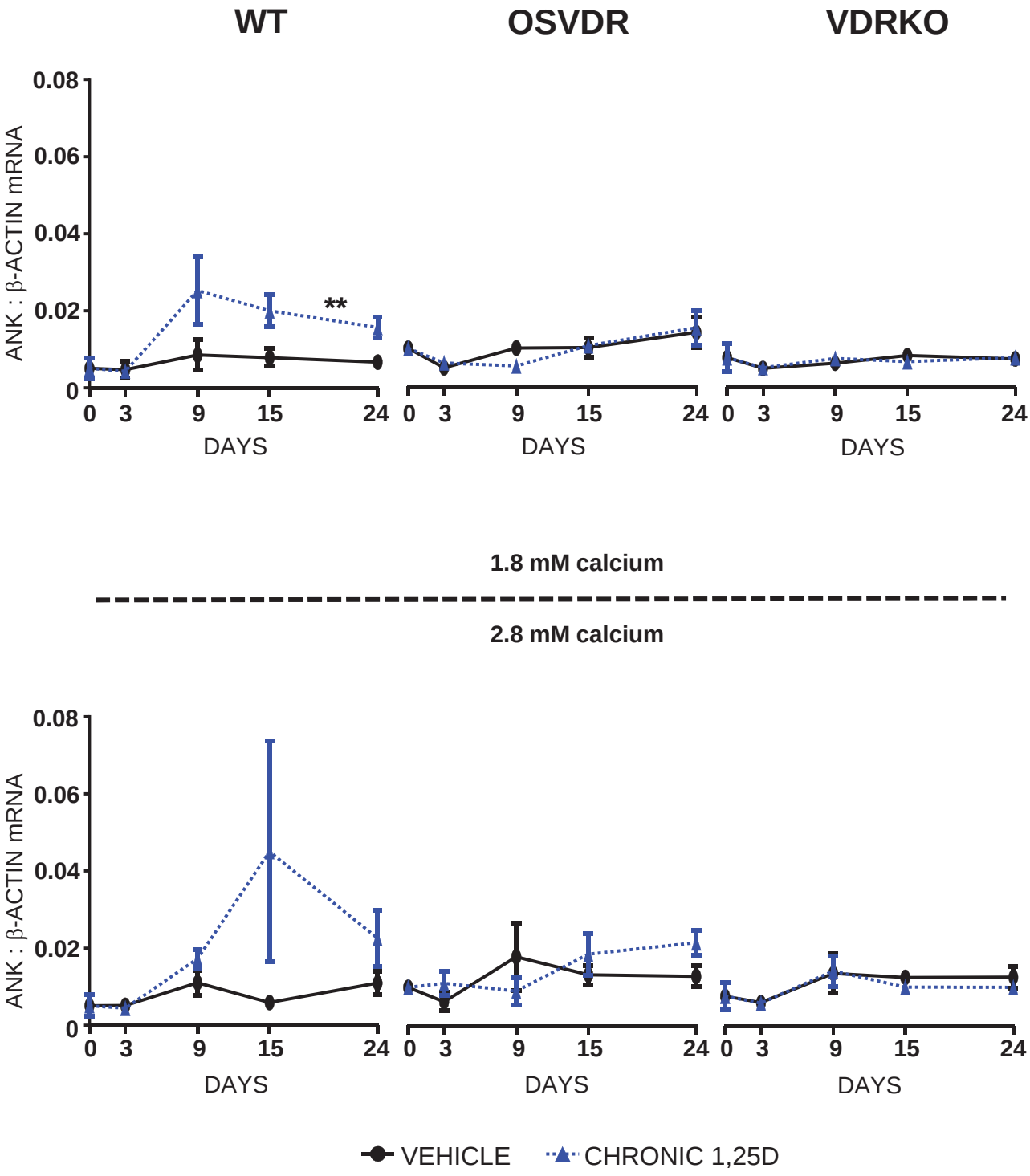

Appendix II. C **mRNA levels of *Ank***

The mRNA ratios of *Ank* to *β-Actin* by WT (left), OSVDR (middle) and VDRKO (right) cells, with vehicle (solid line) and chronic 1,25D (1nM) (broken line) treatments with 1.8 mM (upper) and 2.8 mM total calcium (lower) presented in culture media. Three independent experiments for gene expression analyses were conducted and the error bars on graphs represent the standard errors of mean data collected from the three experiments (mean±SEM, n = 3; ** p<0.01).

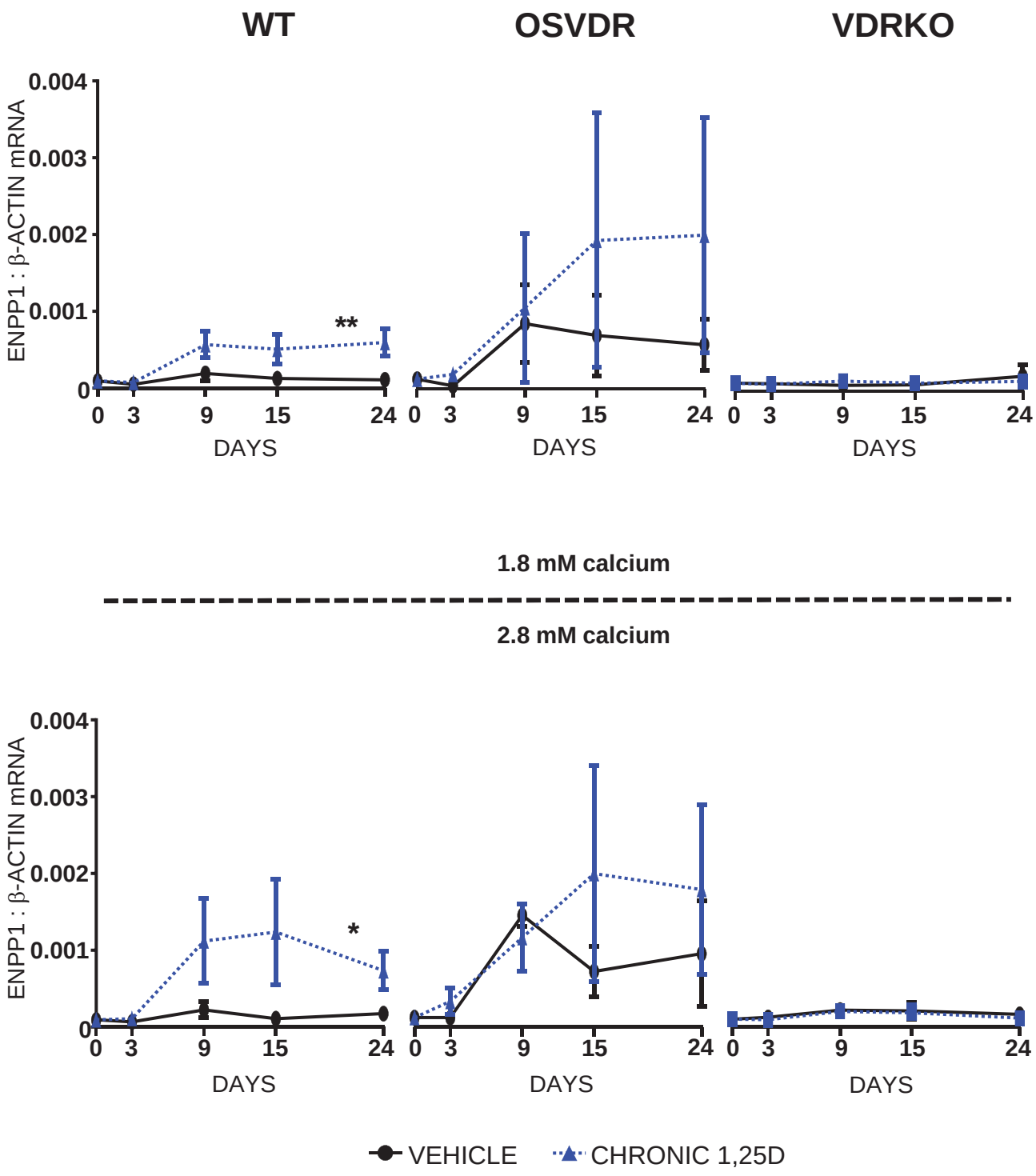

Appendix II. D **mRNA levels of *Enpp1***

The mRNA ratios of *Enpp1* to *β-Actin* by WT (left), OSVDR (middle) and VDRKO (right) cells, with vehicle (solid line) and chronic 1,25D (1nM) (broken line) treatments with 1.8 mM (upper) and 2.8 mM total calcium (lower) presented in culture media. Three independent experiments for gene expression analyses were conducted and the error bars on graphs represent the standard errors of mean data collected from the three experiments (mean±SEM, n = 3; * $p<0.05$, ** $p<0.01$).

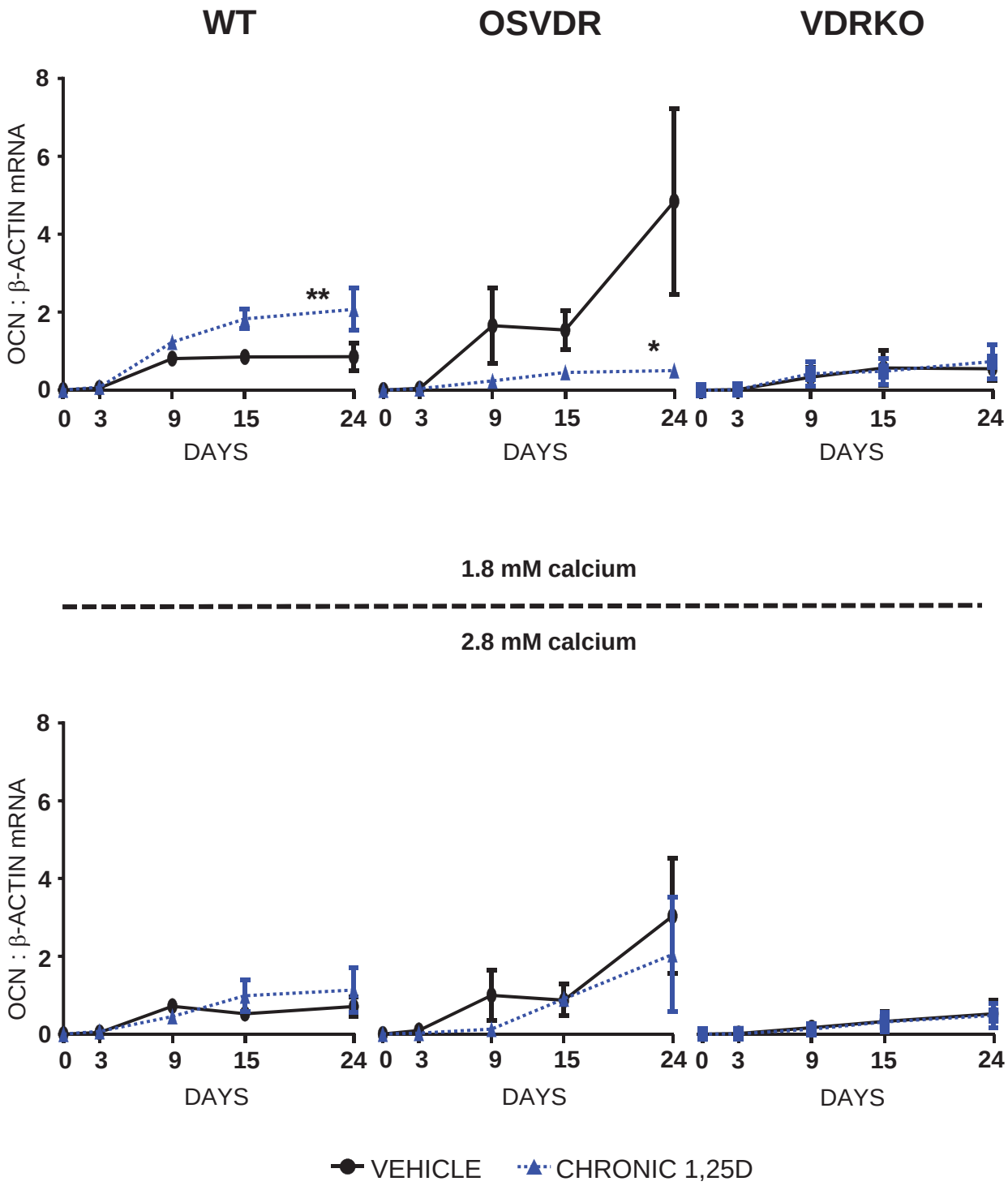

Appendix II. E **mRNA levels of *Ocn***

The mRNA ratios of *Ocn* to *β-Actin* by WT (left), OSVDR (middle) and VDRKO (right) cells, with vehicle (solid line) and chronic 1,25D (1nM) (broken line) treatments with 1.8 mM (upper) and 2.8 mM total calcium (lower) presented in culture media. Three independent experiments for gene expression analyses were conducted and the error bars on graphs represent the standard errors of mean data collected from the three experiments (mean±SEM, n = 3; * $p<0.05$, ** $p<0.01$).

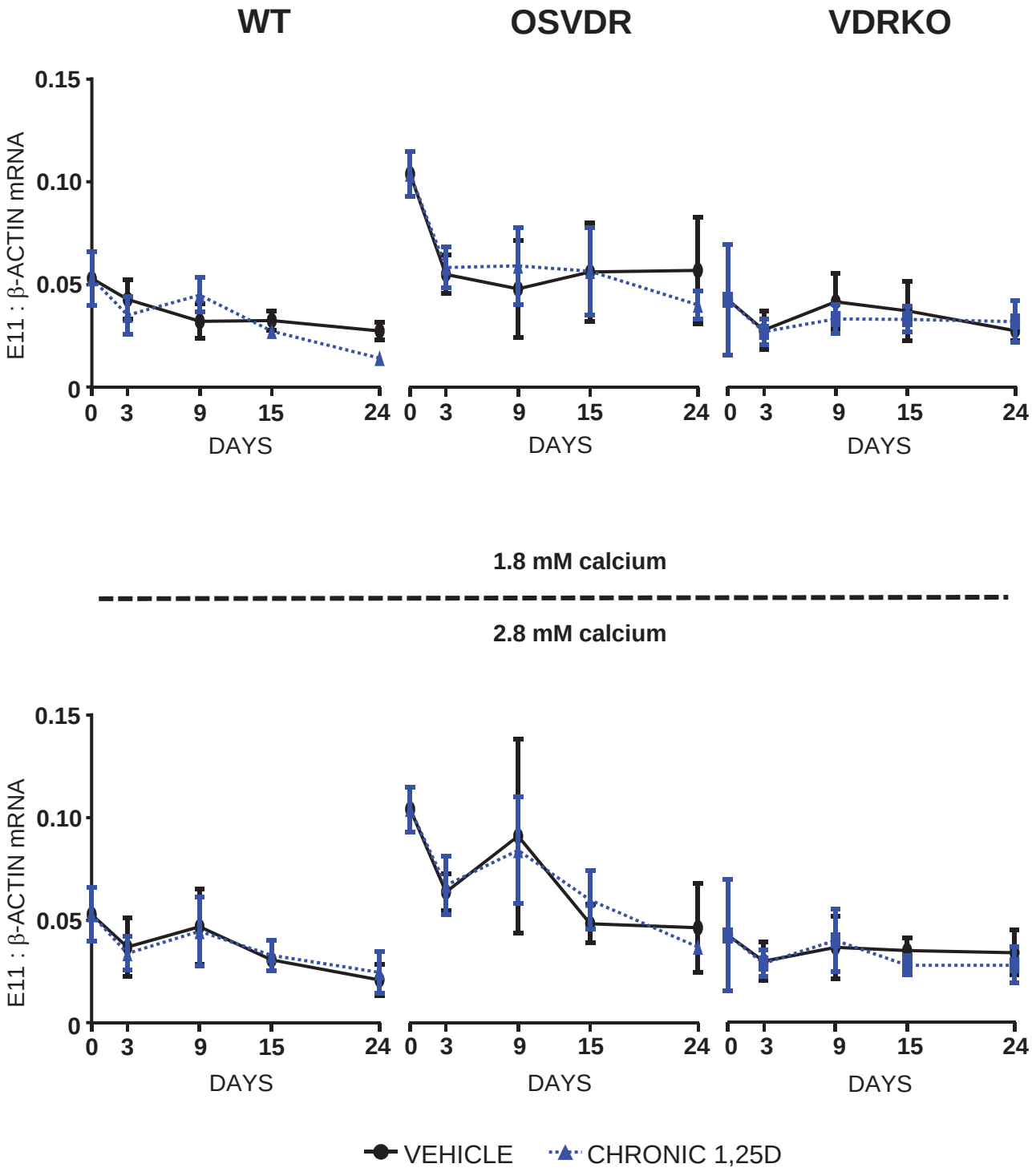

Appendix II. F **mRNA levels of *E11***

The mRNA ratios of *E11* to *β-Actin* by WT (left), OSVDR (middle) and VDRKO (right) cells, with vehicle (solid line) and chronic 1,25D (1nM) (broken line) treatments with 1.8 mM (upper) and 2.8 mM total calcium (lower) presented in culture media. Three independent experiments for gene expression analyses were conducted and the error bars on graphs represent the standard errors of mean data collected from the three experiments (mean±SEM, n = 3).

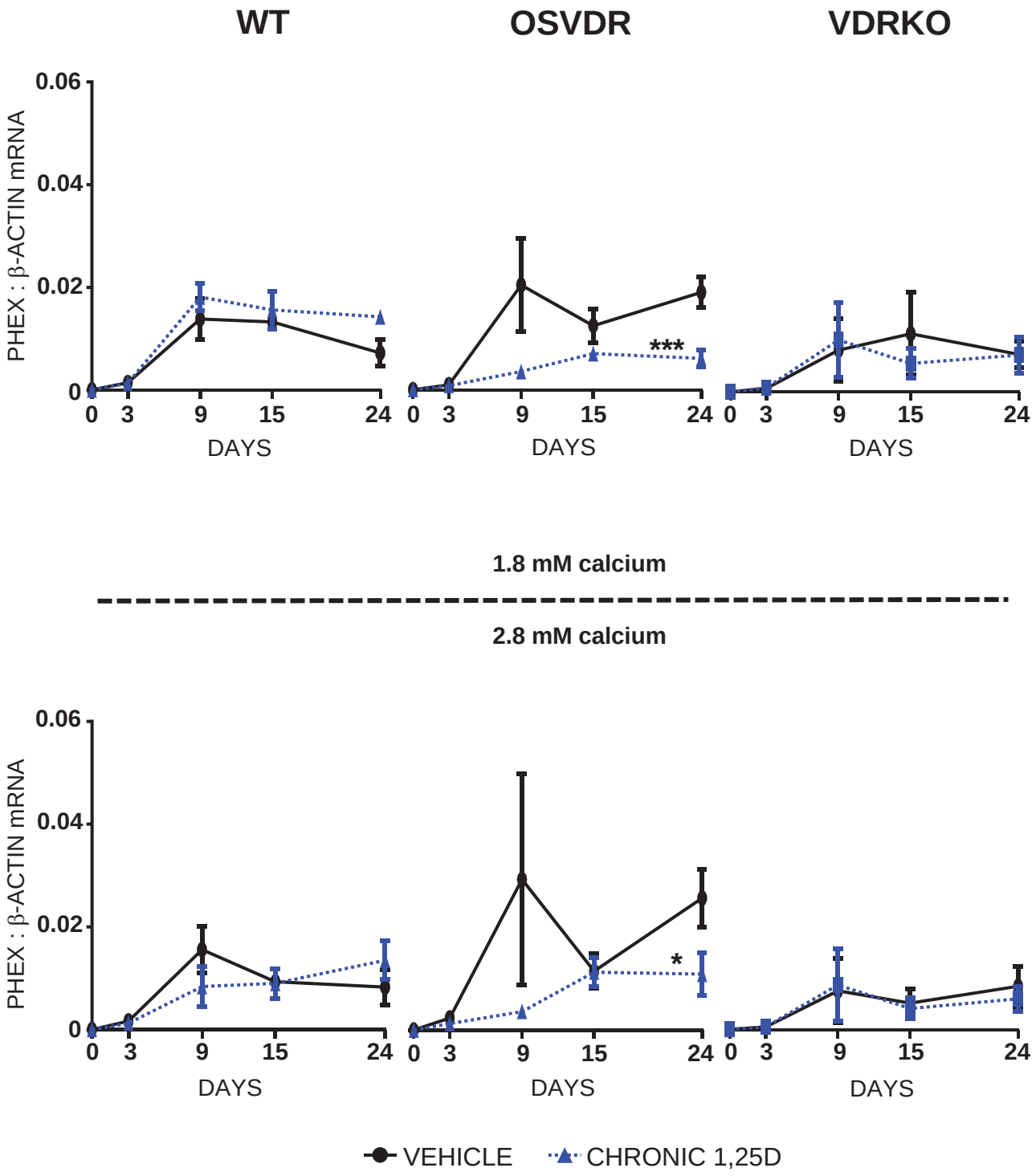

Appendix II. G **mRNA levels of *Phex***

The mRNA ratios of *Phex* to *β-Actin* by WT (left), OSVDR (middle) and VDRKO (right) cells, with vehicle (solid line) and chronic 1,25D (1nM) (broken line) treatments with 1.8 mM (upper) and 2.8 mM total calcium (lower) presented in culture media. Three independent experiments for gene expression analyses were conducted and the error bars on graphs represent the standard errors of mean data collected from the three experiments (mean±SEM, n = 3; * $p<0.05$, *** $p<0.001$).

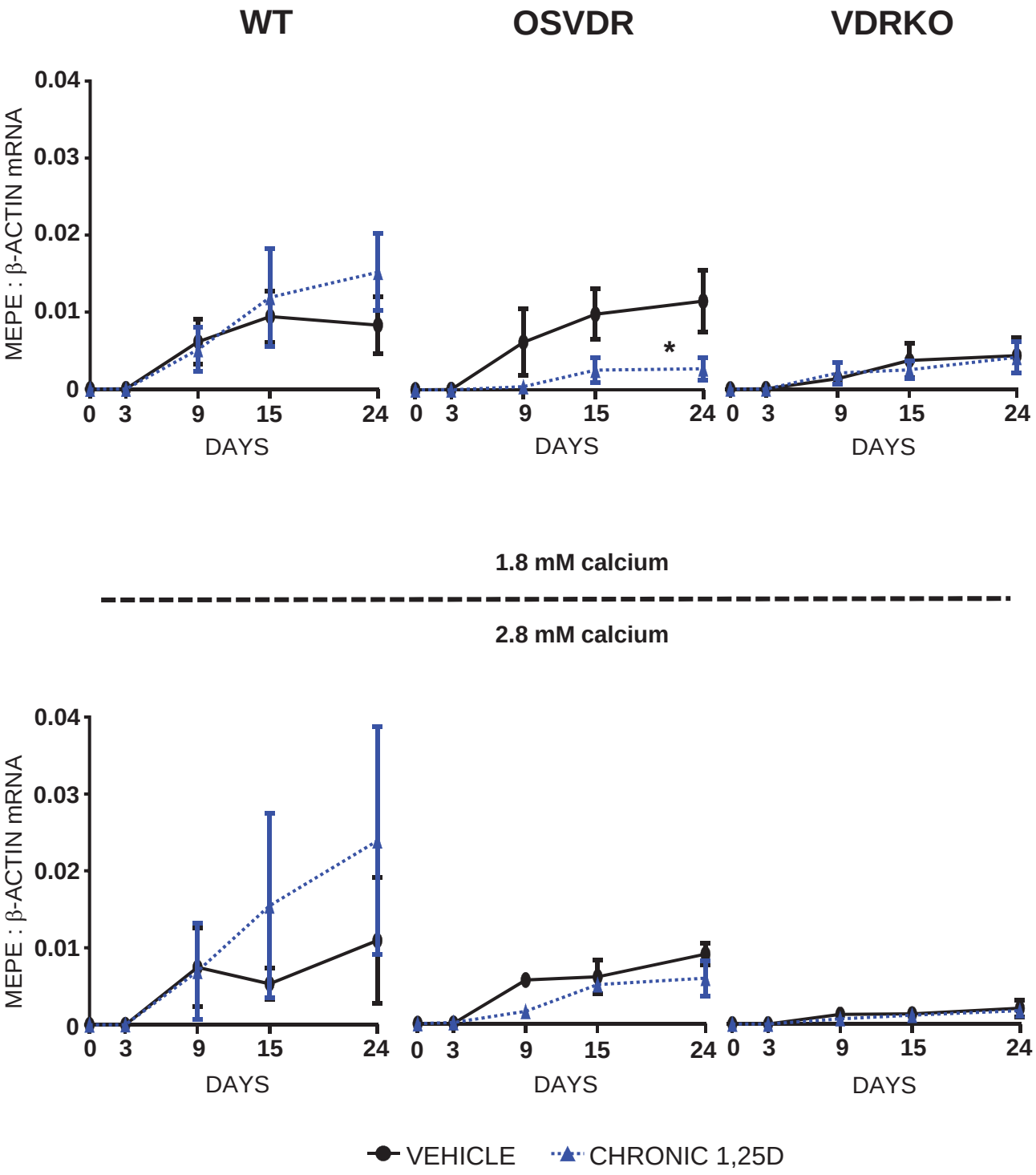

Appendix II. H **mRNA levels of *Mepe***

The mRNA ratios of *Mepe* to *β-Actin* by WT (left), OSVDR (middle) and VDRKO (right) cells, with vehicle (solid line) and chronic 1,25D (1nM) (broken line) treatments with 1.8 mM (upper) and 2.8 mM total calcium (lower) presented in culture media. Three independent experiments for gene expression analyses were conducted and the error bars on graphs represent the standard errors of mean data collected from the three experiments (mean±SEM, n = 3; * $p<0.05$).

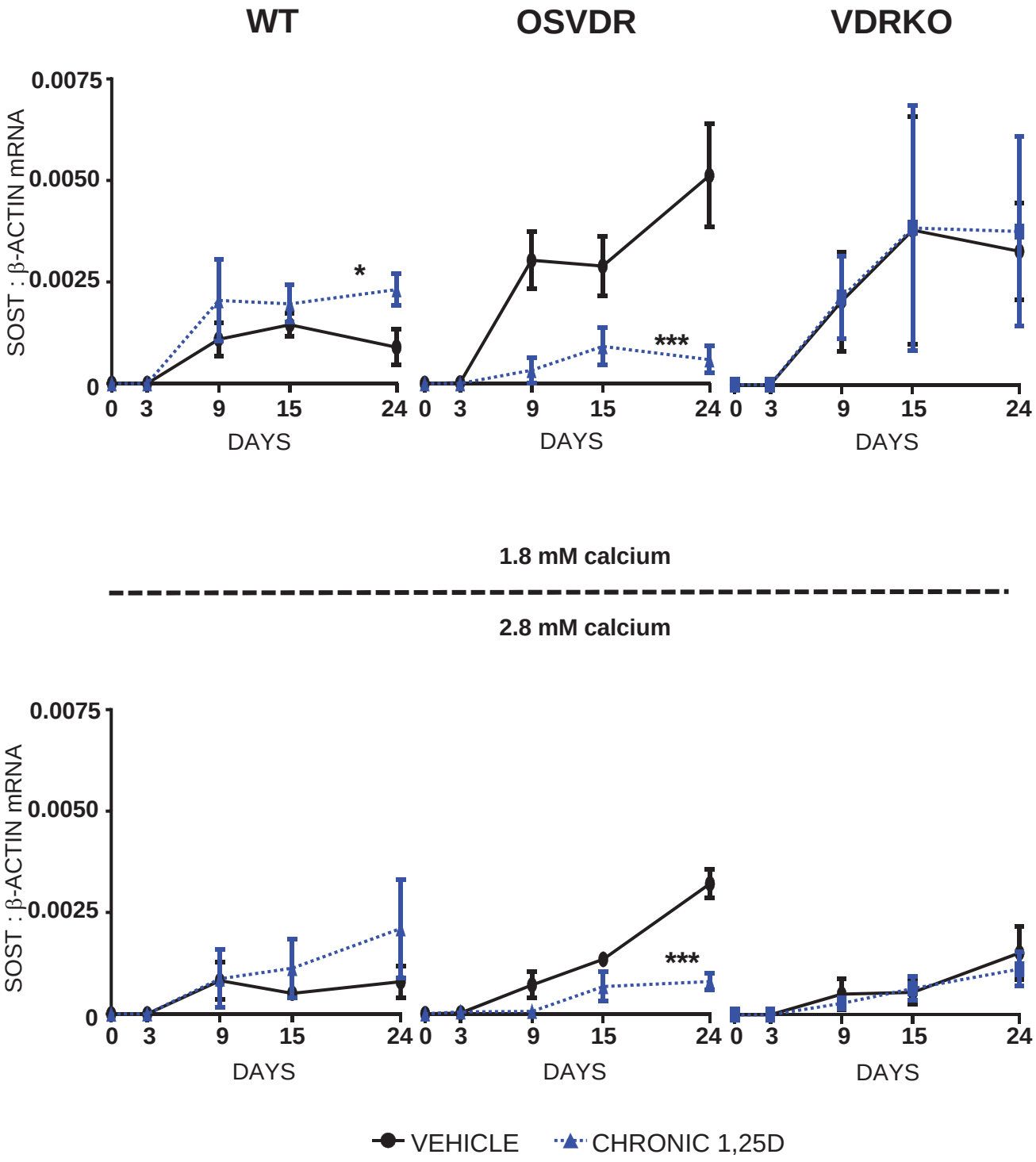

Appendix II. I **mRNA levels of *Sost***

The mRNA ratios of *Sost* to *β-Actin* by WT (left), OSVDR (middle) and VDRKO (right) cells, with vehicle (solid line) and chronic 1,25D (1nM) (broken line) treatments with 1.8 mM (upper) and 2.8 mM total calcium (lower) presented in culture media. Three independent experiments for gene expression analyses were conducted and the error bars on graphs represent the standard errors of mean data collected from the three experiments (mean±SEM, n = 3; * $p<0.05$, *** $p<0.001$).

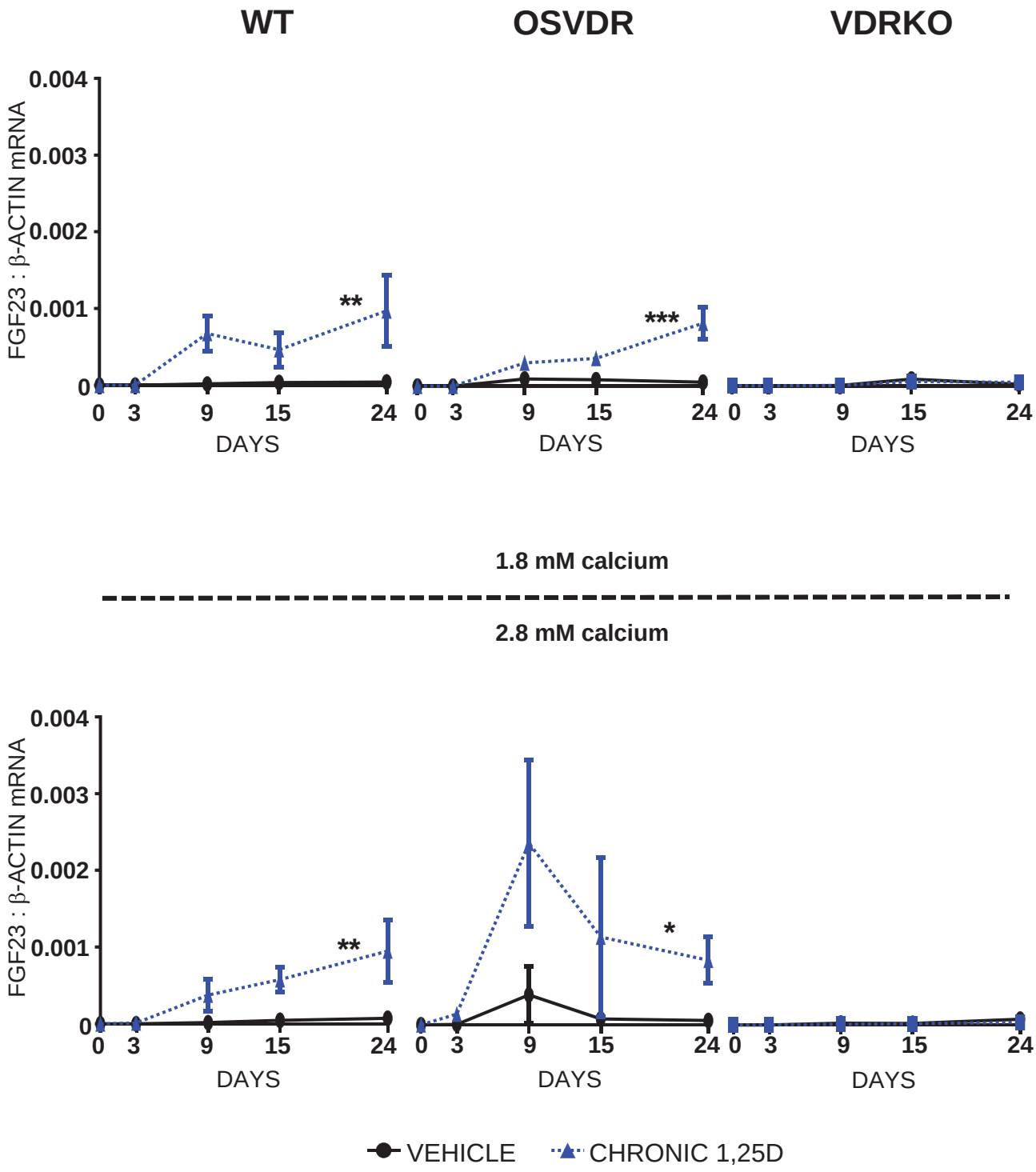

Appendix II. J **mRNA levels of *Fgf23***

The mRNA ratios of *Fgf23* to *β-Actin* by WT (left), OSVDR (middle) and VDRKO (right) cells, with vehicle (solid line) and chronic 1,25D (1nM) (broken line) treatments with 1.8 mM (upper) and 2.8 mM total calcium (lower) presented in culture media. Three independent experiments for gene expression analyses were conducted and the error bars on graphs represent the standard errors of mean data collected from the three experiments (mean±SEM, n = 3; * p<0.05, ** p<0.01, *** p<0.001).

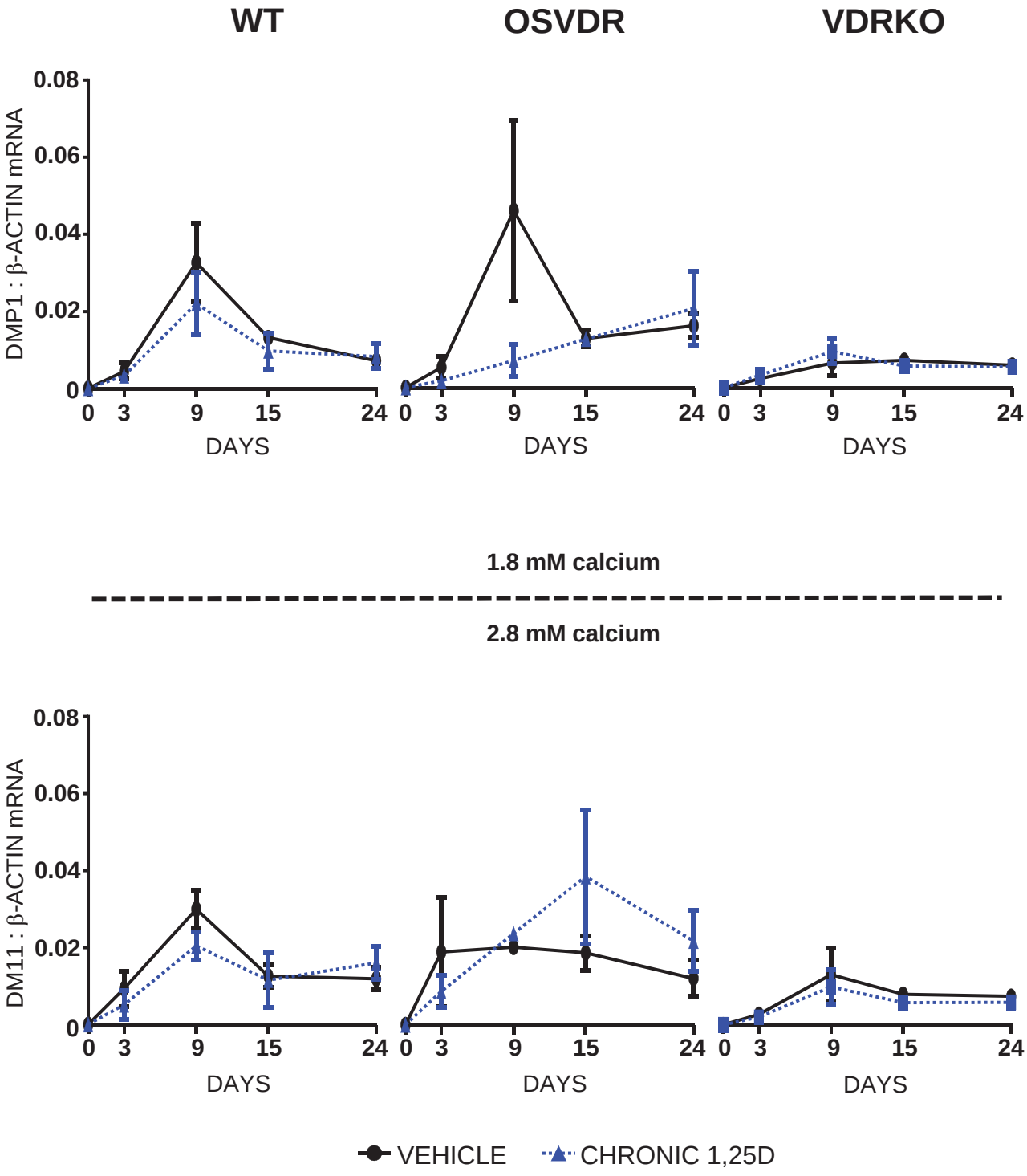

Appendix II. K **mRNA levels of *Dmp1***

The mRNA ratios of *Dmp1* to *β-Actin* by WT (left), OSVDR (middle) and VDRKO (right) cells, with vehicle (solid line) and chronic 1,25D (1nM) (broken line) treatments with 1.8 mM (upper) and 2.8 mM total calcium (lower) presented in culture media. Three independent experiments for gene expression analyses were conducted and the error bars on graphs represent the standard errors of mean data collected from the three experiments (mean±SEM, n = 3).

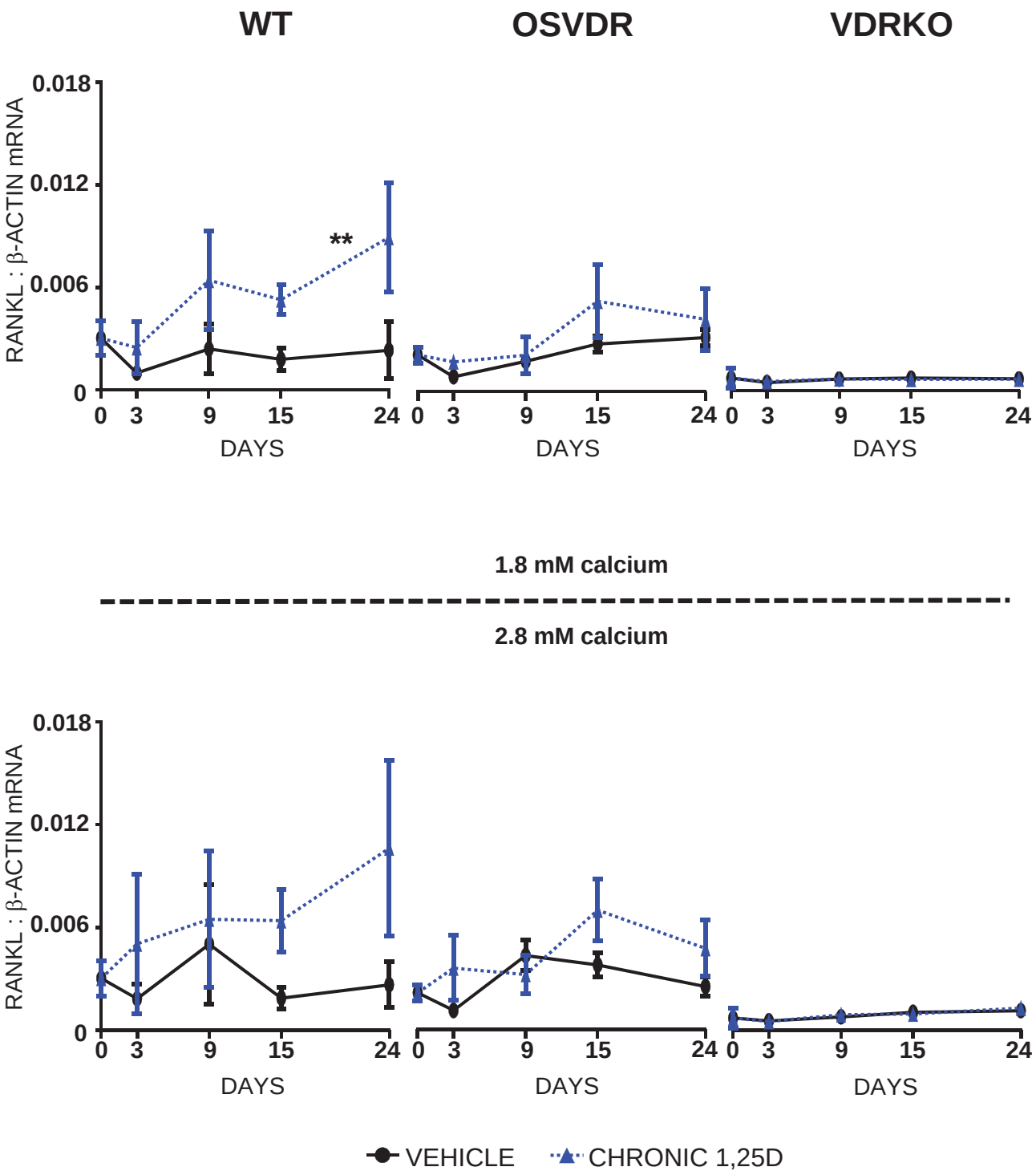

Appendix II. L **mRNA levels of *Rankl***

The mRNA ratios of *Rankl* to *β-Actin* by WT (left), OSVDR (middle) and VDRKO (right) cells, with vehicle (solid line) and chronic 1,25D (1nM) (broken line) treatments with 1.8 mM (upper) and 2.8 mM total calcum (lower) presented in culture media. Three independent experiments for gene expression analyses were conducted and the error bars on graphs represent the standard errors of mean data collected from the three experiments (mean±SEM, n = 3; ** $p<0.01$).

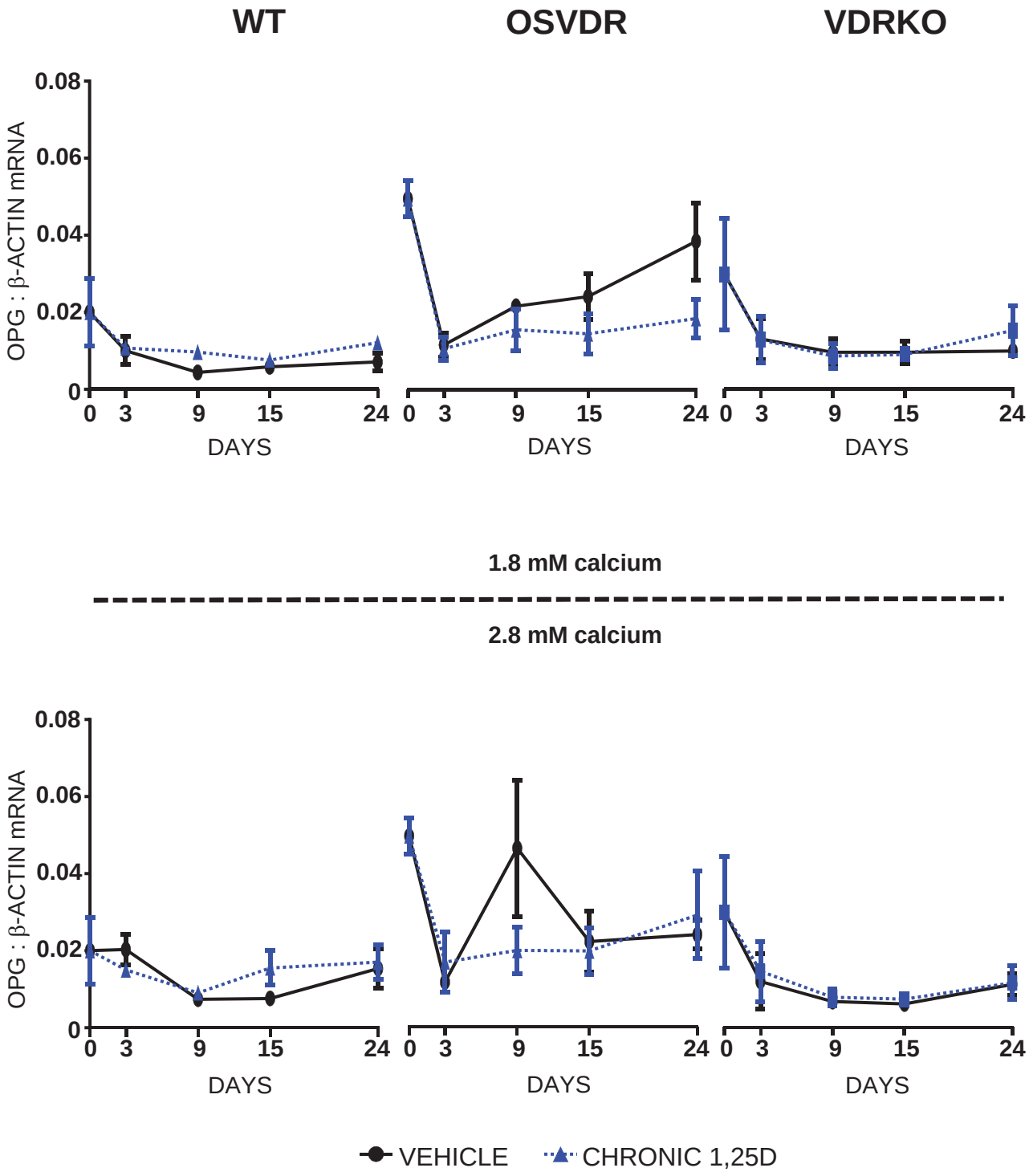

Appendix II. M **mRNA levels of *Opg***

The mRNA ratios of *Opg* to *β-Actin* by WT (left), OSVDR (middle) and VDRKO (right) cells, with vehicle (solid line) and chronic 1,25D (1nM) (broken line) treatments with 1.8 mM (upper) and 2.8 mM total calcium (lower) presented in culture media. Three independent experiments for gene expression analyses were conducted and the error bars on graphs represent the standard errors of mean data collected from the three experiments (mean±SEM, n = 3).

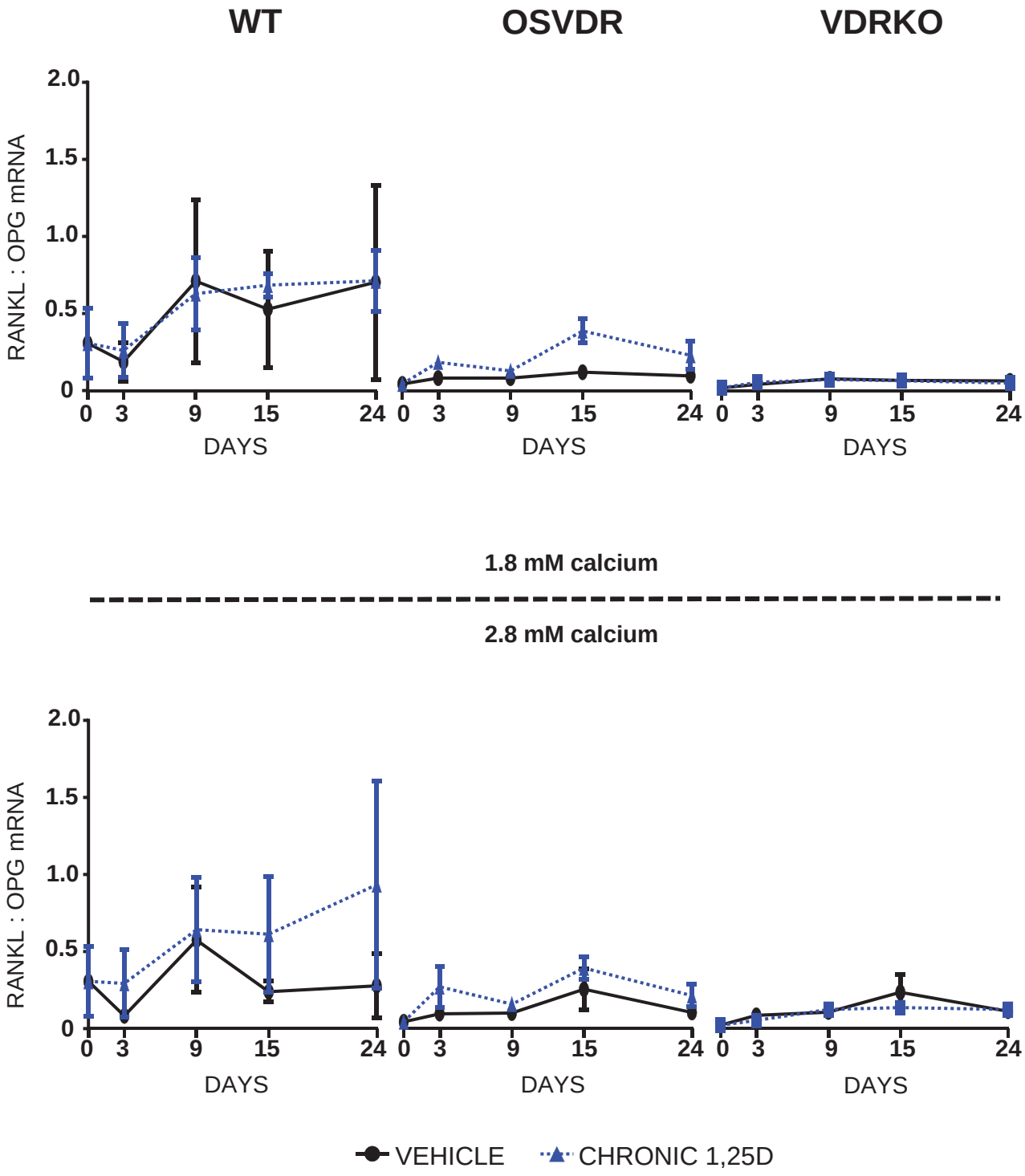

Appendix II. N **mRNA ratios of *Rankl/Opg***

The mRNA ratios of *Rankl/Opg* by WT (left), OSVDR (middle) and VDRKO (right) cells, with vehicle (solid line) and chronic 1,25D (1nM) (broken line) treatments with 1.8 mM (upper) and 2.8 mM total calcium (lower) presented in culture media. Three independent experiments for gene expression analyses were conducted and the error bars on graphs represent the standard errors of mean data collected from the three experiments (mean±SEM, n = 3).

Appendix III

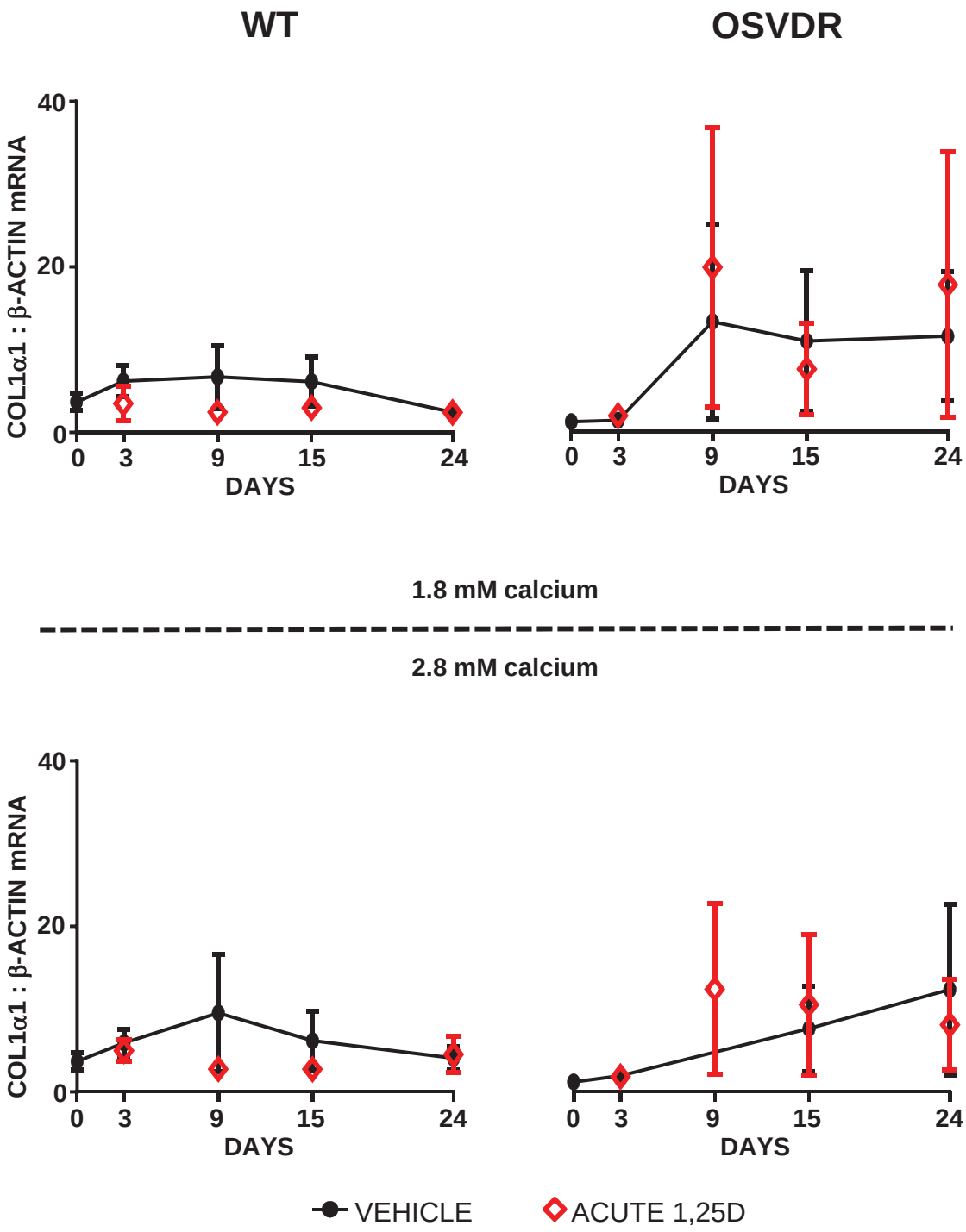

Appendix III. A **mRNA levels of *Col1α1***

The mRNA ratios of *Collα1* to *β-Actin* by WT (left) and OSVDR (right) cells, with vehicle (black lines) and acute 1,25D (1nM) (dots) treatments with 1.8 mM (upper) and 2.8 mM total calcium (lower) presented in culture media. Three independent experiments for gene expression analyses were conducted and the error bars on graphs represent the standard errors of mean data collected from the three experiments (mean±SEM, n = 3).

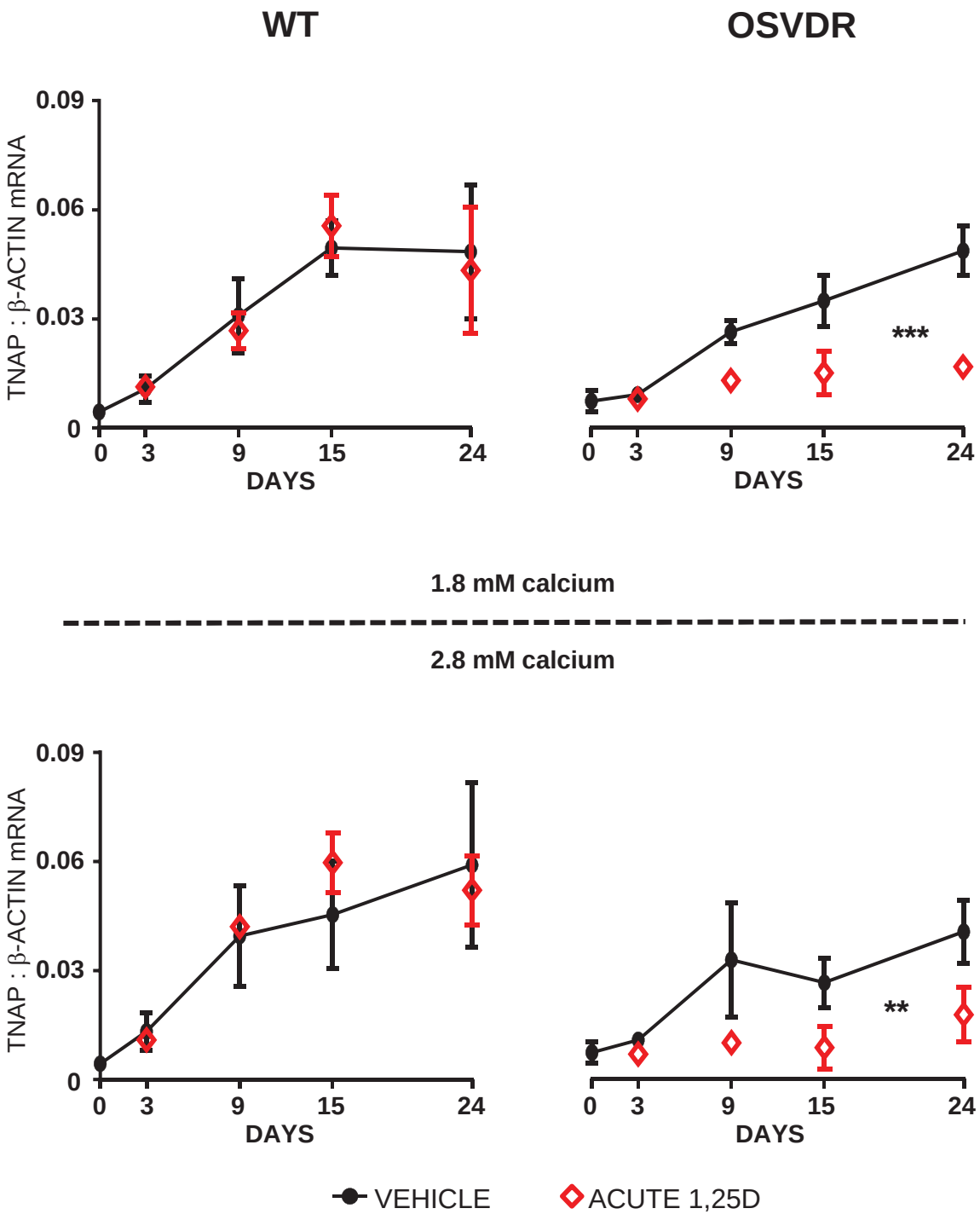

Appendix III. B **mRNA levels of *Tnap***

The mRNA ratios of *Tnap* to *β-Actin* by WT (left) and OSVDR (right) cells, with vehicle (black lines) and acute 1,25D (1nM) (dots) treatments with 1.8 mM (upper) and 2.8 mM total calcium (lower) presented in culture media. Three independent experiments for gene expression analyses were conducted and the error bars on graphs represent the standard errors of mean data collected from the three experiments (mean±SEM, n = 3; ** $p<0.01$, *** $p<0.001$).

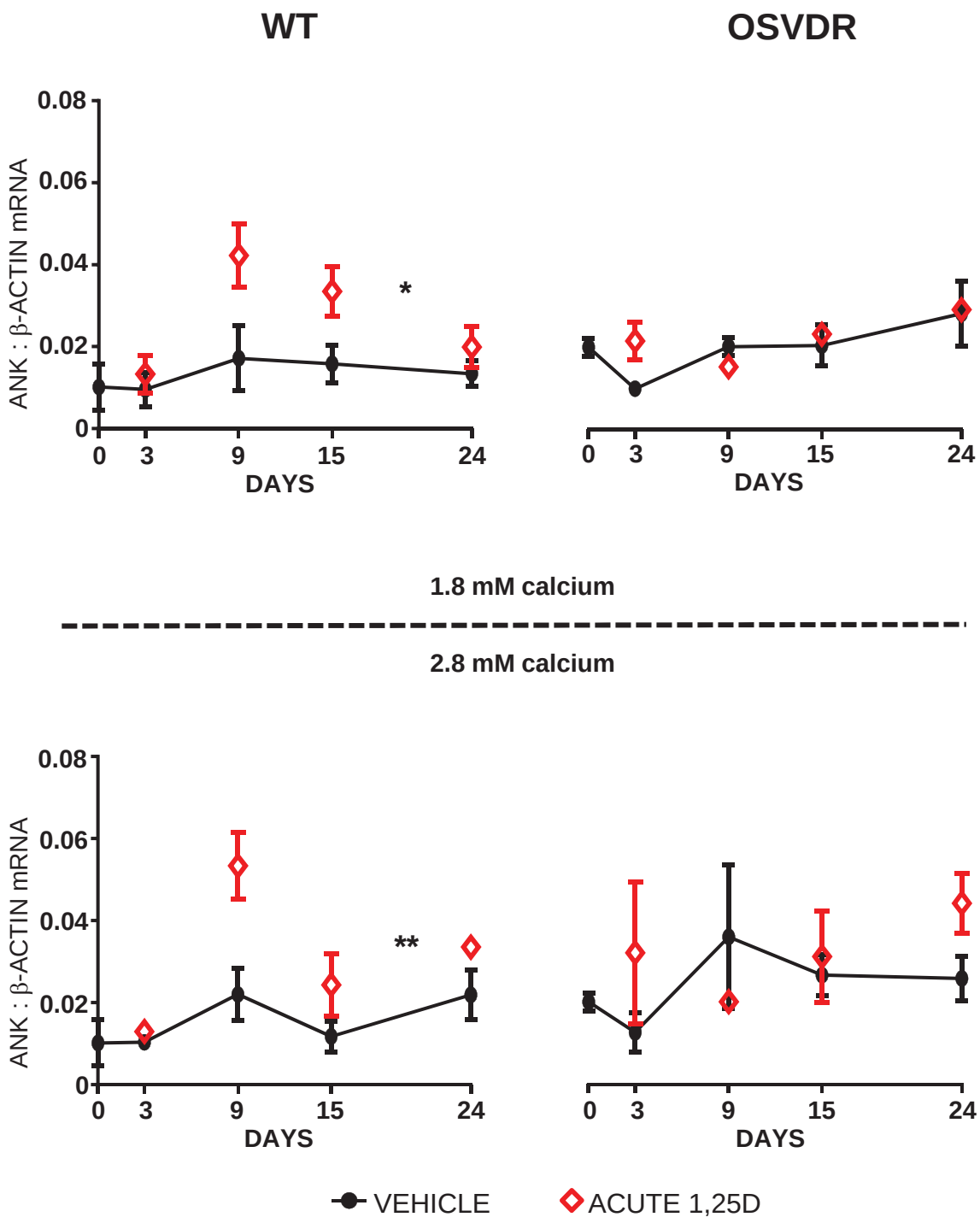

Appendix III. C **mRNA levels of *Ank***

The mRNA ratios of *Ank* to *β-Actin* by WT (left) and OSVDR (right) cells, with vehicle (black lines) and acute 1,25D (1nM) (dots) treatments with 1.8 mM (upper) and 2.8 mM total calcium (lower) presented in culture media. Three independent experiments for gene expression analyses were conducted and the error bars on graphs represent the standard errors of mean data collected from the three experiments (mean±SEM, n = 3; * $p<0.05$, ** $p<0.01$).

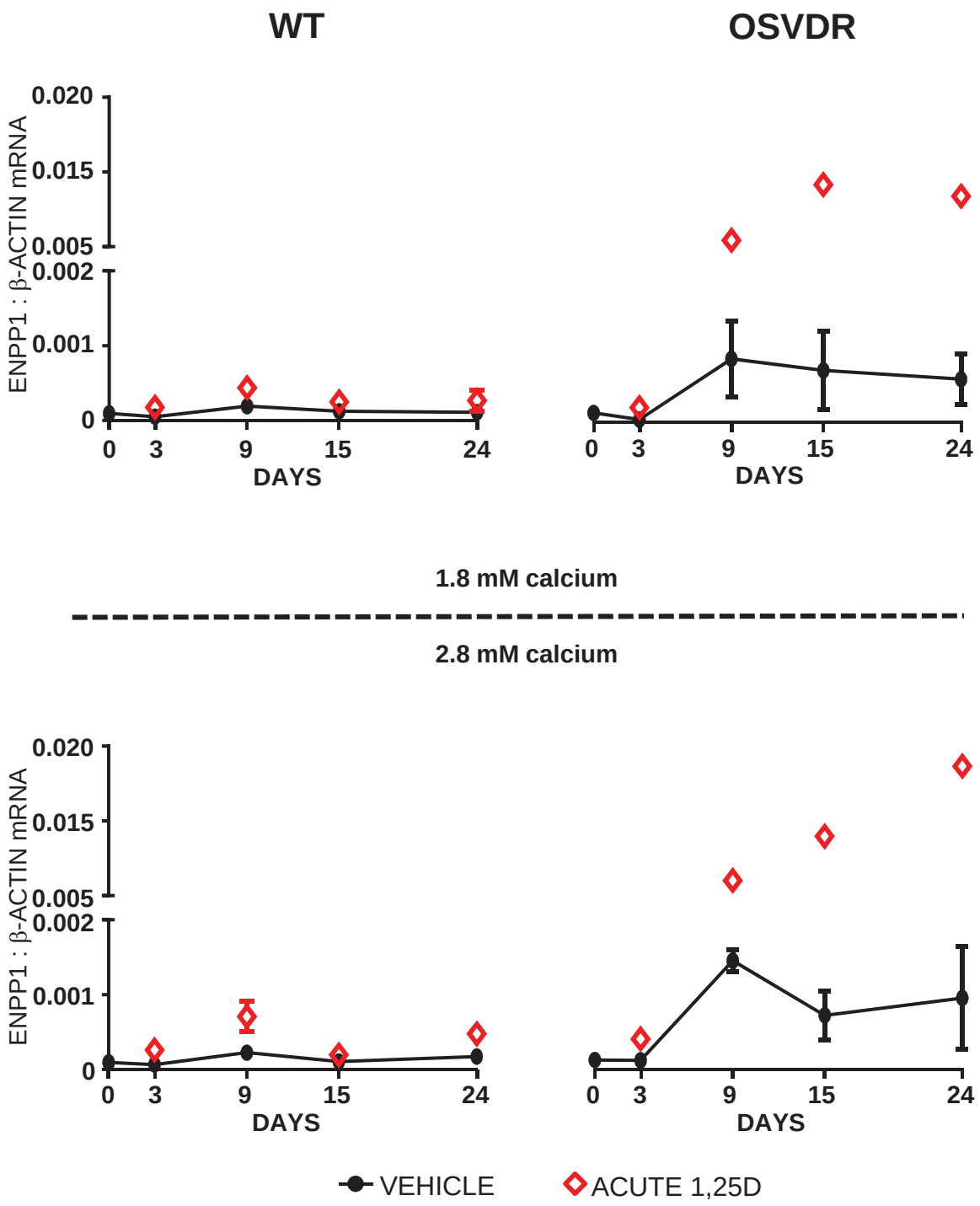

Appendix III. D **mRNA levels of *Enpp1***

The mRNA ratios of *Enpp1* to *β-Actin* by WT (left) and OSVDR (right) cells, with vehicle (black lines) and acute 1,25D (1nM) (dots) treatments with 1.8 mM (upper) and 2.8 mM total calcum (lower) presented in culture media. Three independent experiments for gene expression analyses were conducted and the error bars on graphs represent the standard errors of mean data collected from the three experiments (mean±SEM, n = 1 with OSVDR under acute 1,25D treated group and n = 3 with all other groups).

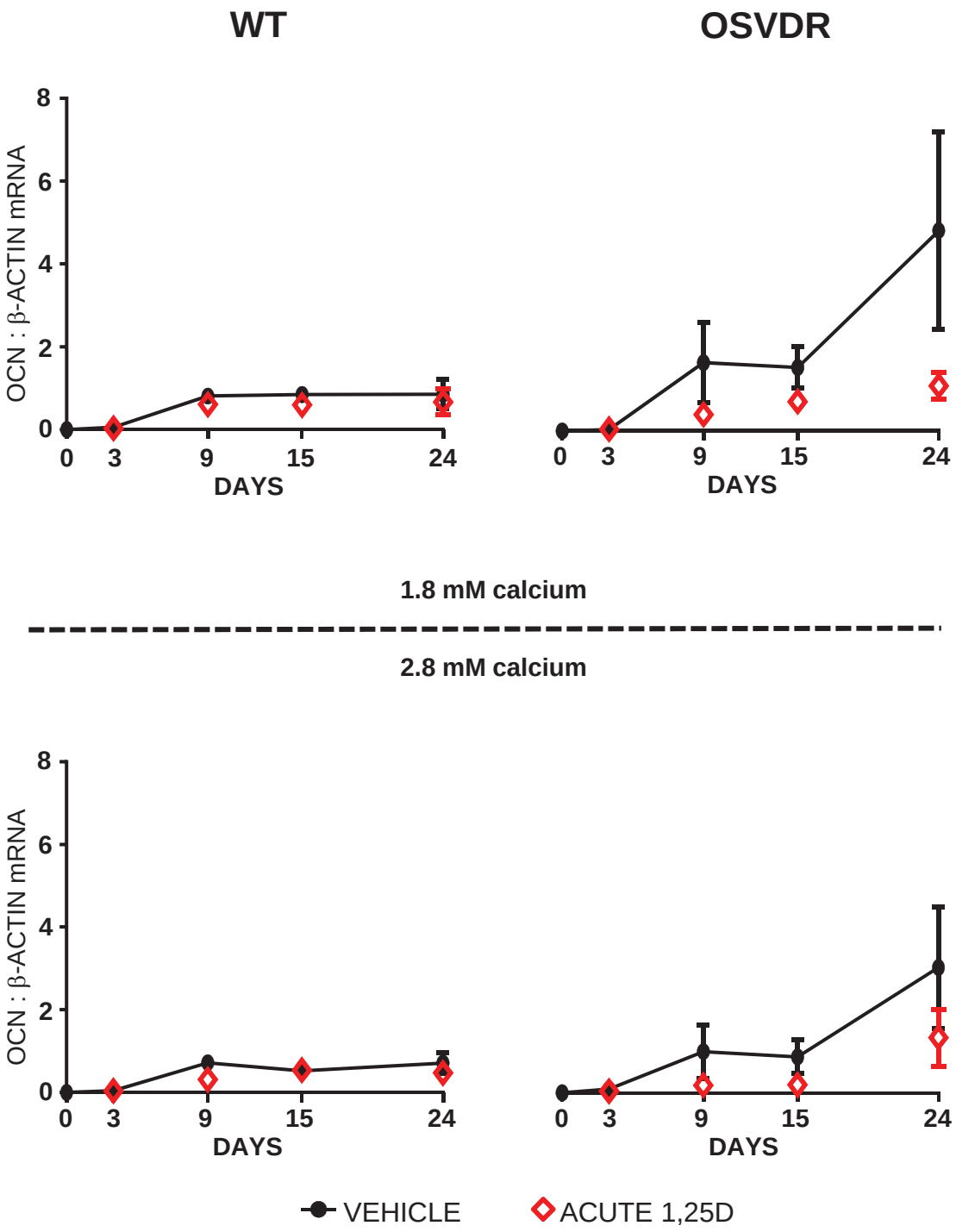

Appendix III. E **mRNA levels of *Ocn***

The mRNA ratios of *Ocn* to *β-Actin* by WT (left) and OSVDR (right) cells, with vehicle (black lines) and acute 1,25D (1nM) (dots) treatments with 1.8 mM (upper) and 2.8 mM total calcium (lower) presented in culture media. Three independent experiments for gene expression analyses were conducted and the error bars on graphs represent the standard errors of mean data collected from the three experiments (mean±SEM, n = 3).

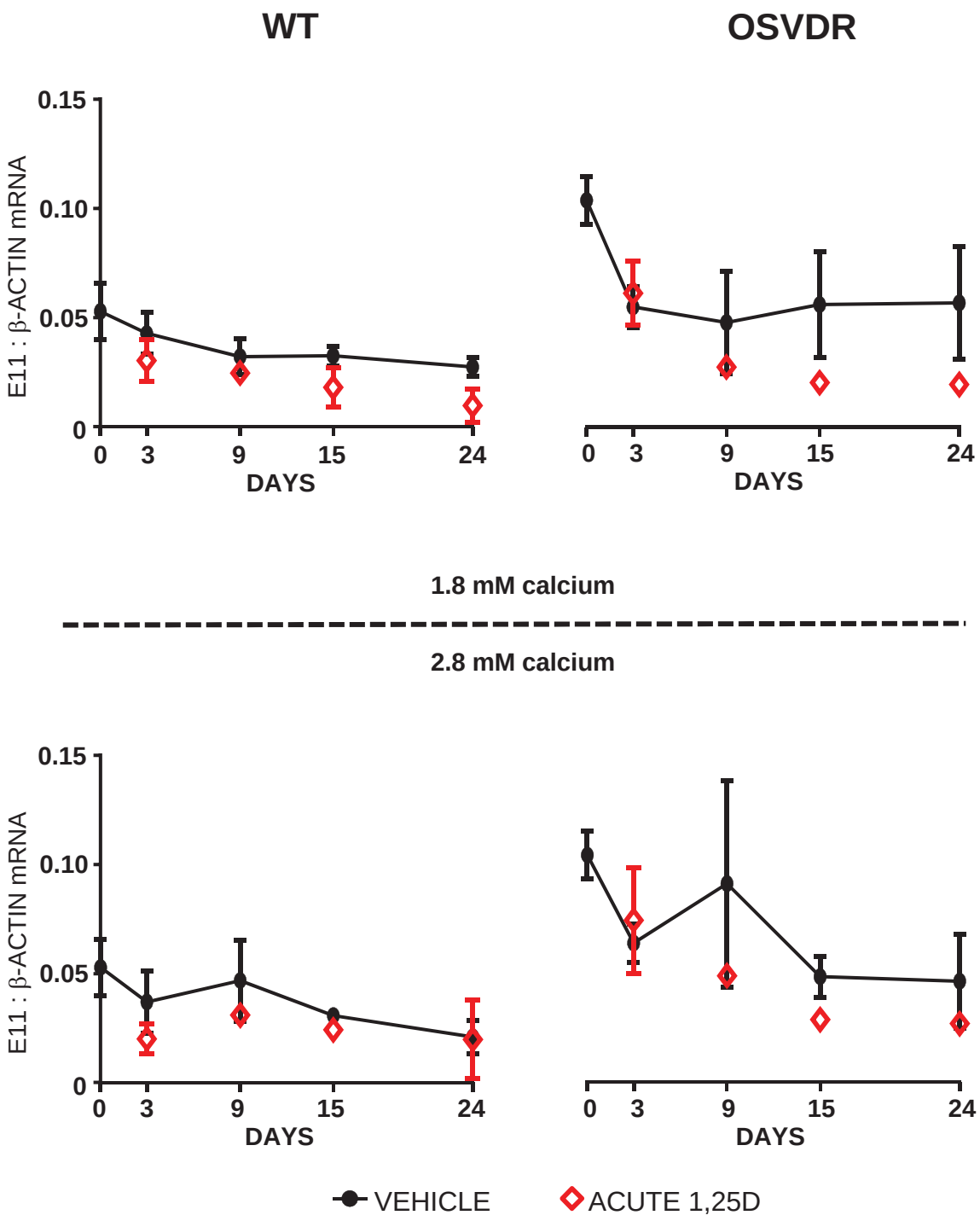

Appendix III. F **mRNA levels of *E11***

The mRNA ratios of *E11* to *β-Actin* by WT (left) and OSVDR (right) cells, with vehicle (black lines) and acute 1,25D (1nM) (dots) treatments with 1.8 mM (upper) and 2.8 mM total calcium (lower) presented in culture media. Three independent experiments for gene expression analyses were conducted and the error bars on graphs represent the standard errors of mean data collected from the three experiments (mean±SEM, n = 3).

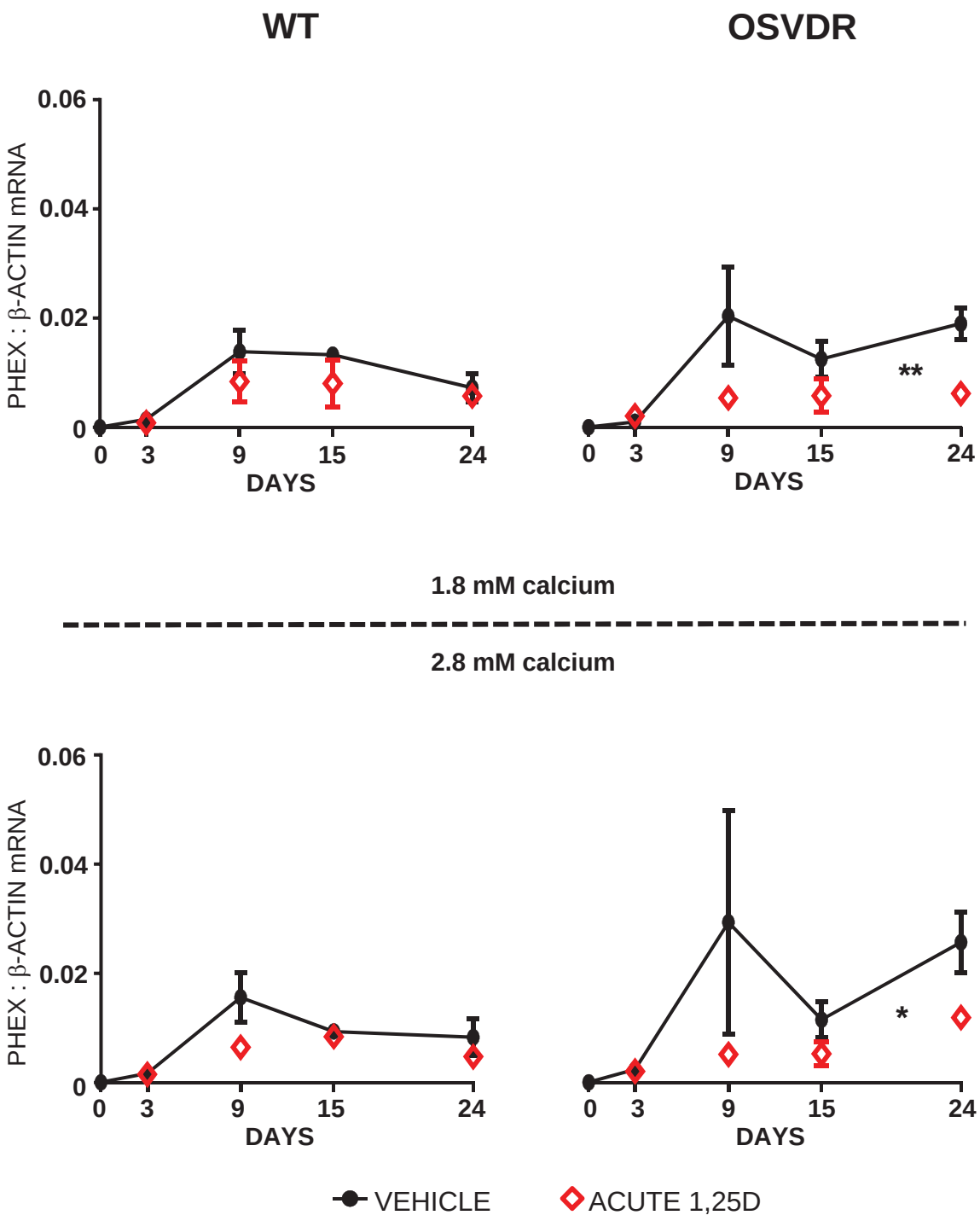

Appendix III. G **mRNA levels of *Phex***

The mRNA ratios of *Phex* to *β-Actin* by WT (left) and OSVDR (right) cells, with vehicle (black lines) and acute 1,25D (1nM) (dots) treatments with 1.8 mM (upper) and 2.8 mM total calcium (lower) presented in culture media. Three independent experiments for gene expression analyses were conducted and the error bars on graphs represent the standard errors of mean data collected from the three experiments (mean±SEM, n = 3; * $p<0.05$, ** $p<0.01$).

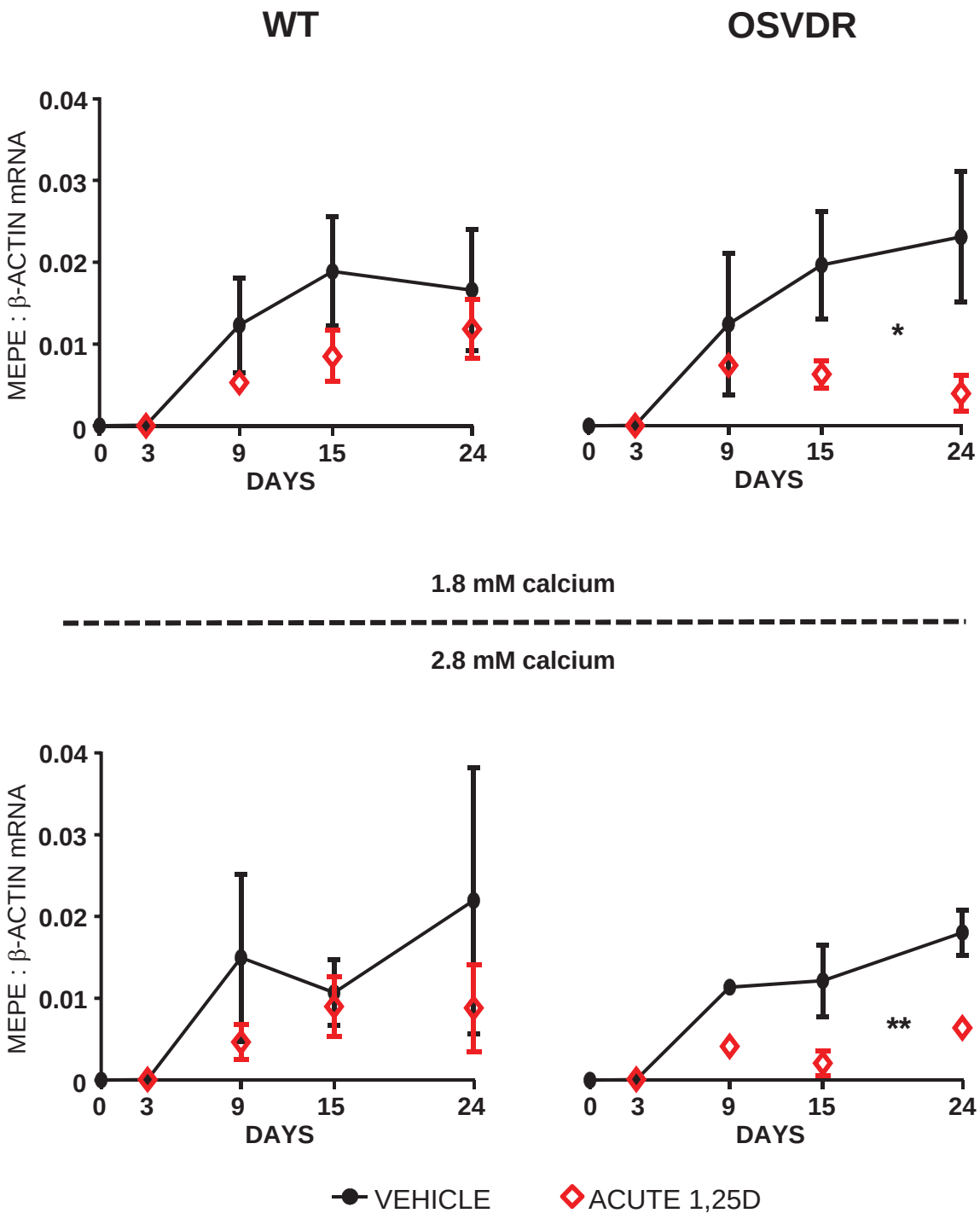

Appendix III. H **mRNA levels of *Mepe***

The mRNA ratios of *Mepe* to *β-Actin* by WT (left) and OSVDR (right) cells, with vehicle (black lines) and acute 1,25D (1nM) (dots) treatments with 1.8 mM (upper) and 2.8 mM total calcium (lower) presented in culture media. Three independent experiments for gene expression analyses were conducted and the error bars on graphs represent the standard errors of mean data collected from the three experiments (mean±SEM, n = 3; * $p<0.05$, ** $p<0.01$).

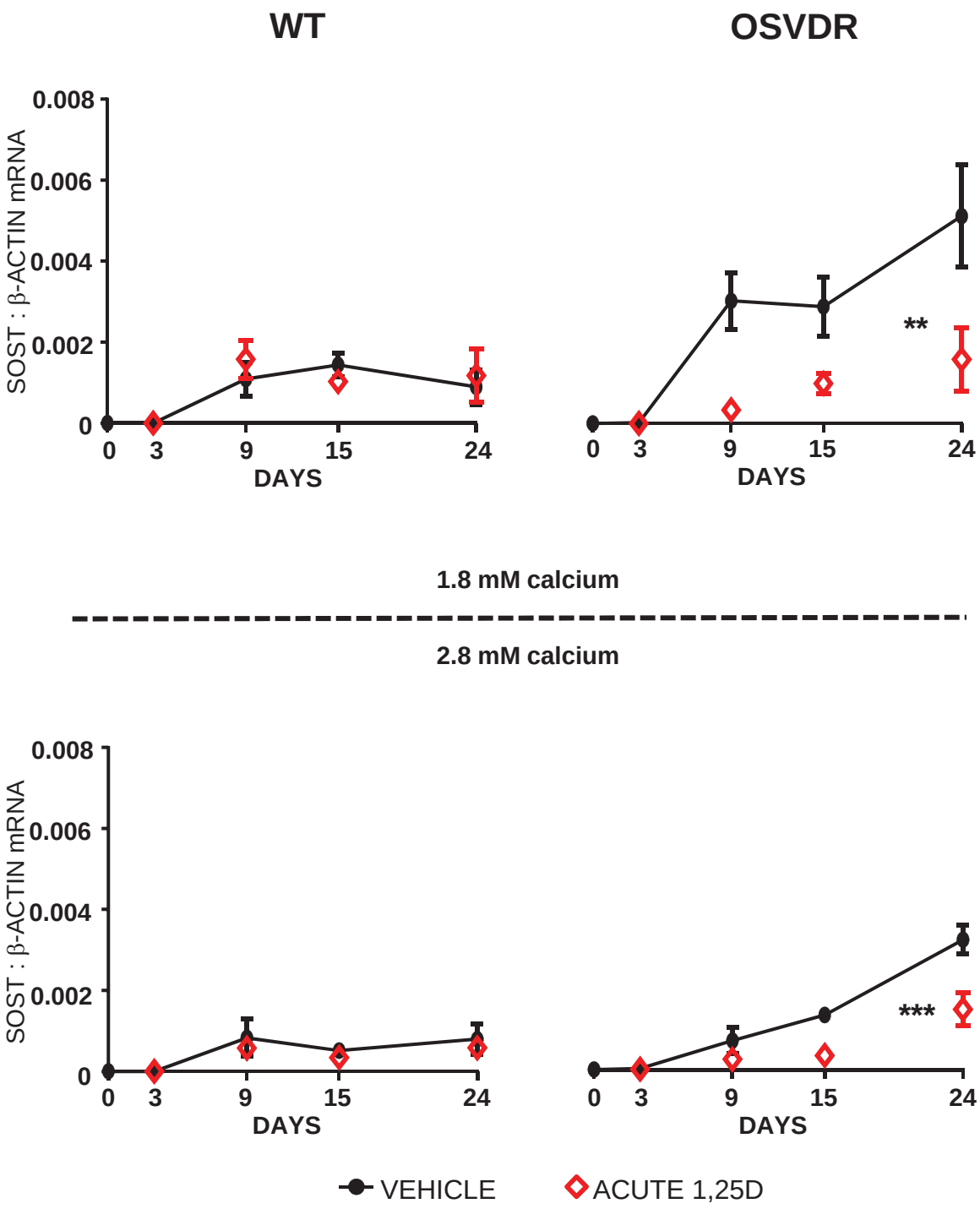

Appendix III. I **mRNA levels of *Sost***

The mRNA ratios of *Sost* to *β-Actin* by WT (left) and OSVDR (right) cells, with vehicle (black lines) and acute 1,25D (1nM) (dots) treatments with 1.8 mM (upper) and 2.8 mM total calcium (lower) presented in culture media. Three independent experiments for gene expression analyses were conducted and the error bars on graphs represent the standard errors of mean data collected from the three experiments (mean±SEM, n = 3; ** $p<0.01$, *** $p<0.001$).

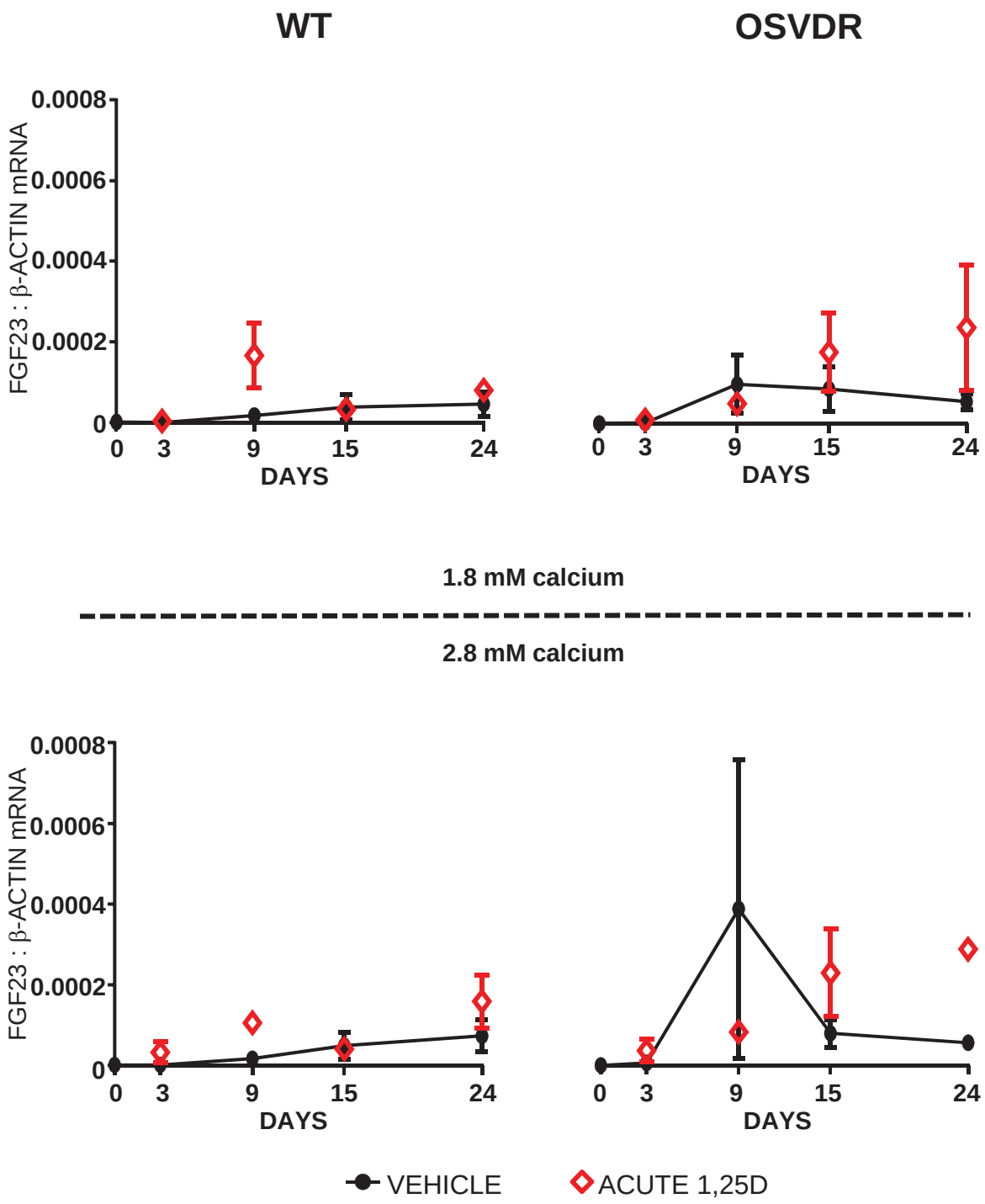

Appendix III. J **mRNA levels of *Fgf23***

The mRNA ratios of *Fgf23* to *β-Actin* by WT (left) and OSVDR (right) cells, with vehicle (black lines) and acute 1,25D (1nM) (dots) treatments with 1.8 mM (upper) and 2.8 mM total calcium (lower) presented in culture media. Three independent experiments for gene expression analyses were conducted and the error bars on graphs represent the standard errors of mean data collected from the three experiments (mean±SEM, n = 3).

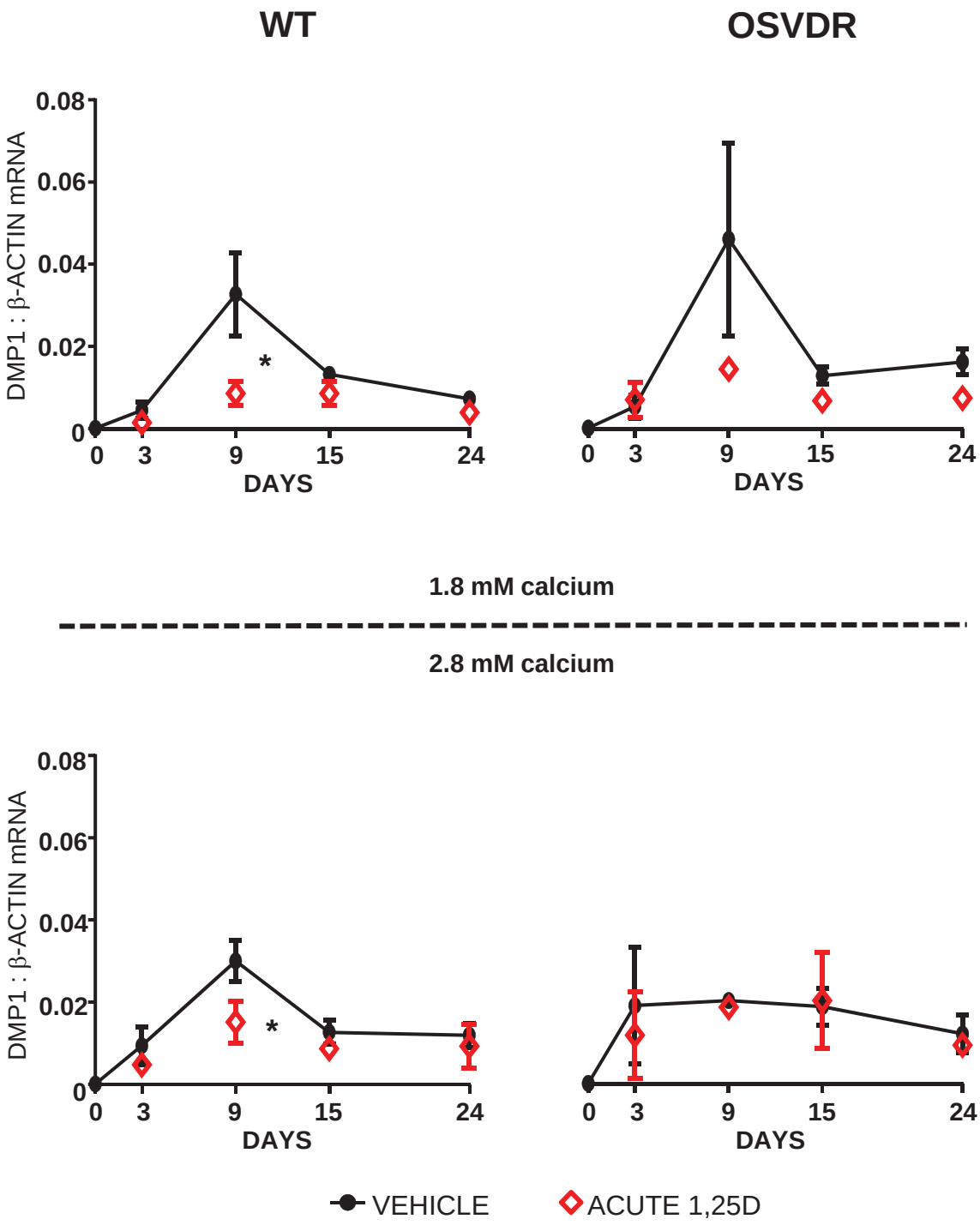

Appendix III. K **mRNA levels of *Dmp1***

The mRNA ratios of *Dmp1* to *β-Actin* by WT (left) and OSVDR (right) cells, with vehicle (black lines) and acute 1,25D (1nM) (dots) treatments with 1.8 mM (upper) and 2.8 mM total calcium (lower) presented in culture media. Three independent experiments for gene expression analyses were conducted and the error bars on graphs represent the standard errors of mean data collected from the three experiments (mean±SEM, n = 3; * $p<0.05$).

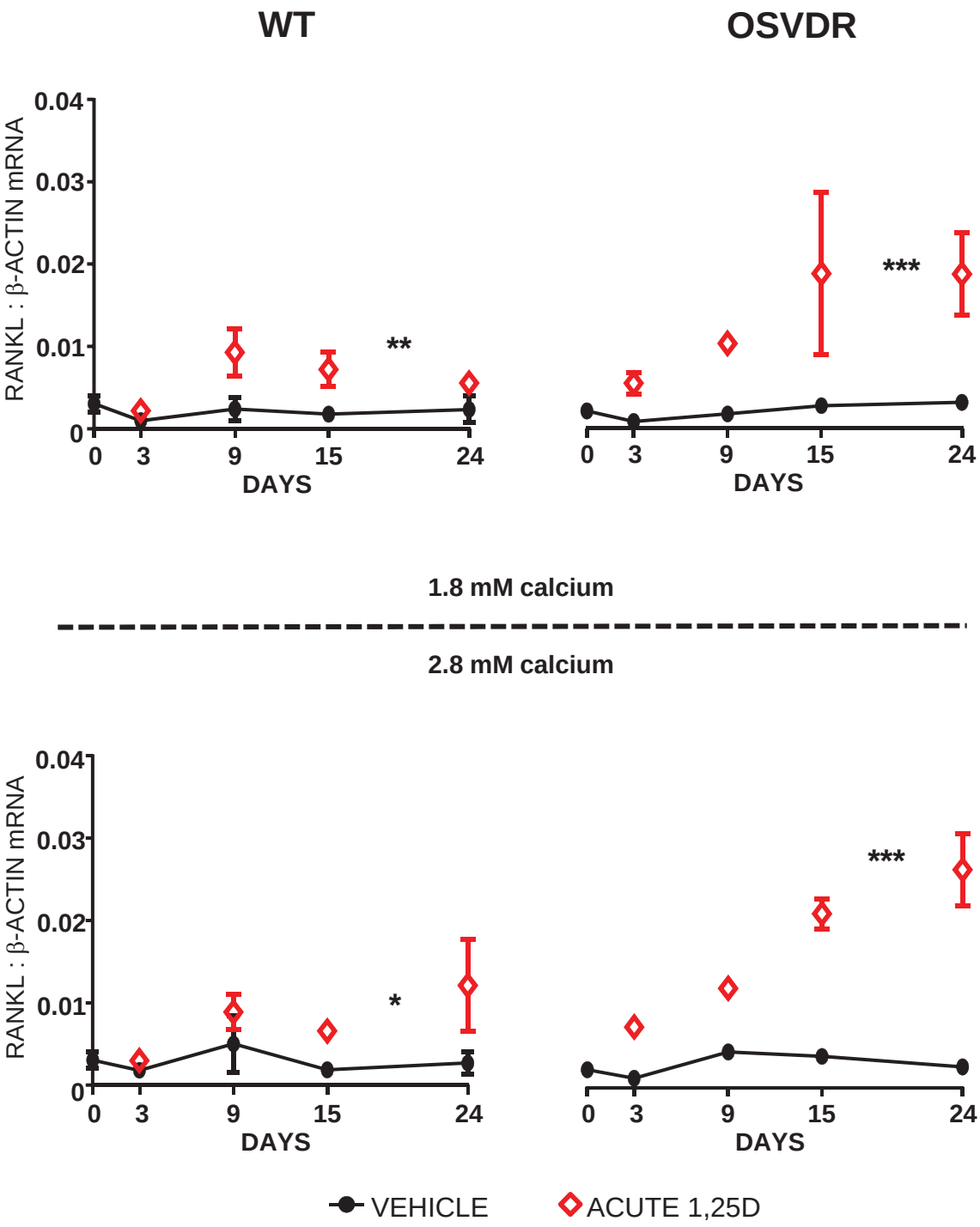

Appendix III. L **mRNA levels of *Rankl***

The mRNA ratios of *Rankl* to *β-Actin* by WT (left) and OSVDR (right) cells, with vehicle (black lines) and acute 1,25D (1nM) (dots) treatments with 1.8 mM (upper) and 2.8 mM total calcium (lower) presented in culture media. Three independent experiments for gene expression analyses were conducted and the error bars on graphs represent the standard errors of mean data collected from the three experiments (mean±SEM, n = 3; * $p<0.05$, ** $p<0.01$, *** $p<0.001$).

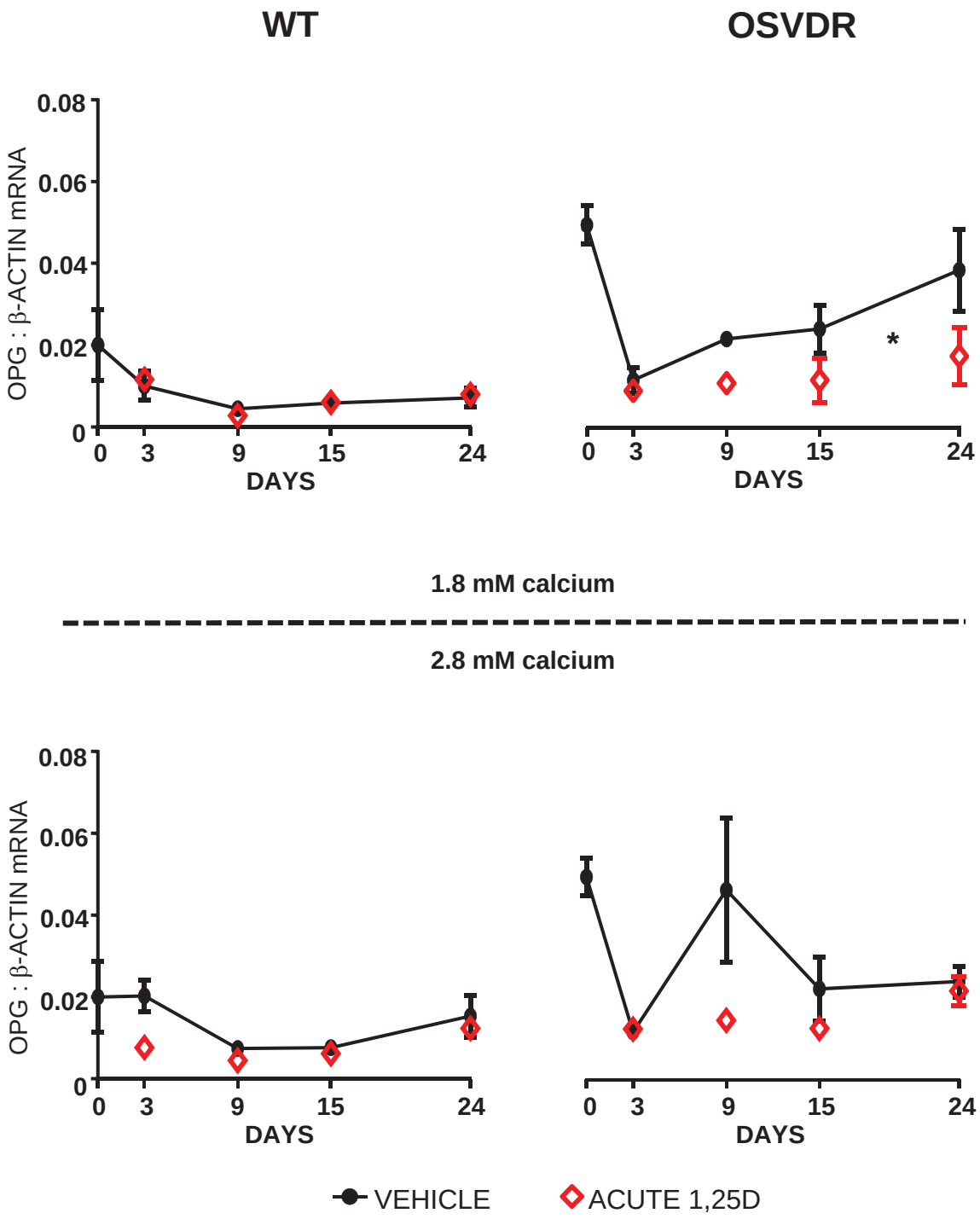

Appendix III. M **mRNA levels of *Opg***

The mRNA ratios of *Opg* to *β-Actin* by WT (left) and OSVDR (right) cells, with vehicle (black lines) and acute 1,25D (1nM) (dots) treatments with 1.8 mM (upper) and 2.8 mM total calcium (lower) presented in culture media. Three independent experiments for gene expression analyses were conducted and the error bars on graphs represent the standard errors of mean data collected from the three experiments (mean±SEM, n = 3; * $p<0.05$).

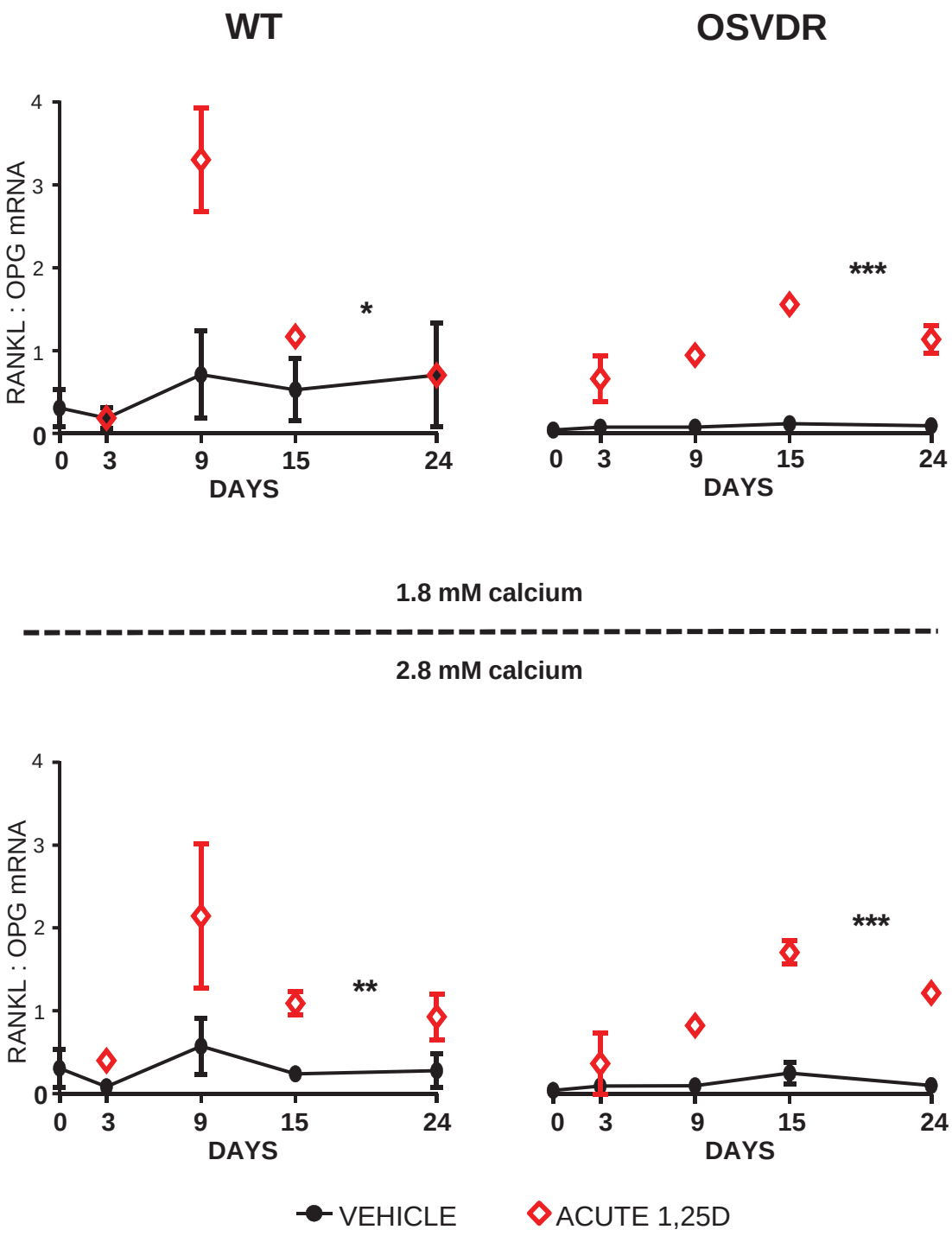

Appendix III. N **mRNA ratios of *Rankl/Opg***

The mRNA ratios of *Rankl/Opg* by WT (left) and OSVDR (right) cells, with vehicle (black lines) and acute 1,25D (1nM) (dots) treatments with 1.8 mM (upper) and 2.8 mM total calcium (lower) presented in culture media. Three independent experiments for gene expression analyses were conducted and the error bars on graphs represent the standard errors of mean data collected from the three experiments (mean±SEM, n = 3; * $p<0.05$, ** $p<0.01$, *** $p<0.001$).